H2020-NMBP-ST-IND-2018-2020-GA 958218

PLUG-AND-USE RENOVATION WITH ADAPTABLE LIGHTWEIGHT SYSTEMS

D4.5

PnU kit prototype property and performance characterisation

Version: 1.1

This project has received funding from the European Union's Horizon 2020 research and innovation programme under grant agreement No 958218

	Name	Date
Prepared by Task leader	NTUA (Io. Atsonios) with input from AMS, DEN, RDR, SPF, CVUT, BGTC	19/12/2022
Reviewed by WP leader	AMS	20/12/2022
Reviewed and edited by	Project coordinator (M. Founti)	21/12/2022
Updated by Task leader to address external reviewer comments	NTUA (Io. Atsonios)	27/11/2023

Distribution list

External		Internal	
European Commission	1x	Consortium partners	1x

Change log

Issue	Date	Pages	Remark / changes	Pages
0.1		10	List of contents established and partner input requested	
0.2		N/A	Contributions from all involved partners received	
0.3	19/12/2022	175	First complete issue by NTUA	All
0.4	20/12/2022	175	Feedback, comments of WP leader incorporated	
1.0	21/12/2022	175	Reviewed, edited and submitted by Project Coordinator	
1.1	27/11/2023	176	Updated by Task leader to address external reviewer comments	17-18

To be cited as:

NTUA (2022): “D4.5 - PnU kit prototype property and performance characterisation” of the HORIZON 2020 project PLURAL. EC Grant Agreement No. 958218, Athens, Greece.

Disclaimer

This project has received funding from the European Union’s Horizon 2020 research and innovation programme under grant agreement No 958218

Table of contents

This project has received funding from the European Union's Horizon 2020 research and innovation programme under grant agreement No 958218

This project has received funding from the European Union's Horizon 2020 research and innovation programme under grant agreement No 958218

13 ANNEX III – ONE THIRD OCTAVE BAND OF SOUND PRESSURE LEVEL AT A DISTANCE 1 M FOR EAHC UNIT 182

This project has received funding from the European Union's Horizon 2020 research and innovation programme under grant agreement No 958218

List of figures

This project has received funding from the European Union's Horizon 2020 research and innovation programme under grant agreement No 958218

This project has received funding from the European Union's Horizon 2020 research and innovation programme under grant agreement No 958218

This project has received funding from the European Union's Horizon 2020 research and innovation programme under grant agreement No 958218

This project has received funding from the European Union's Horizon 2020 research and innovation programme under grant agreement No 958218

This project has received funding from the European Union's Horizon 2020 research and innovation programme under grant agreement No 958218

List of tables

This project has received funding from the European Union's Horizon 2020 research and innovation programme under grant agreement No 958218

This project has received funding from the European Union's Horizon 2020 research and innovation programme under grant agreement No 958218

Terms, definitions and abbreviated terms

AHC	Agencia de l'Habitatge
AHU	Air Handling Unit
AMScope	AMS Control Panel
CVUT	Ceske Vysoke Uceni Technicke V Praze
D	Deliverable
eAHC	Air Handling Unit with Heating & Cooling
EHA	Exhaust air outlet to the outdoor environment– for the eAHC acoustic tests
ETA	Extraction of air from the room– for the eAHC acoustic tests
eWHC	External Wall Heating & Cooling system
F.Q.P.	Factory Quality Procedures
HHW	Heat Harvesting Window
IR	Infrared
NTUA	National Technical University of Athens
ODA	Outdoor air inlet– for the eAHC acoustic tests
PnU	Plug and Use
PV	Photovoltaic
R-value	Thermal resistance
SPF	Institute Fur Solartechnik
SUP	Supply of air to the room – for the eAHC acoustic tests
U-value	Thermal transmittance
VIP	Vacuum Insulation Panel
VOC	Volatile Organic Compounds
VVV	Voula – Vari - Vouliagmeni
WP	Work Package

This project has received funding from the European Union's Horizon 2020 research and innovation programme under grant agreement No 958218

1 Executive summary

Deliverable **D4.5** "***PnU kit prototype property and performance characterisation***" of the PLURAL project is a public deliverable aiming to allow key stakeholders that are interested in the technical performance of the prefabricated Plug and Use kits (PnU kits) to access the results. The public presentation of the PLURAL PnU performance testing campaign is expected to promote the broader acceptance of the hybrid PnU kits of the project that combine active and passive technologies and take into account user needs.

Test results are presented for the three core PLURAL prototypes (the SmartWall, the HybridWall and the ConExWall), the smart windows developed in the project as well as specific components and address their thermal, acoustic, structural, seismic and fire performance taking into account EU and national regulations of the country where the kit will be installed.

The deliverable was initially due in M24 of the project (end Sept.2022) but had to be delayed until M27 due to the late completion of the three PnU kit prototypes (reported in D4.4, submitted in M22). D4.5 presents the results of the task T4.5 PnU kit testing campaign.

The main objective of Task 4.5 is the numerical and experimental testing of PnU kits through the execution of Factory Quality Procedures on manufacture's factories and the laboratory testing in terms of their mechanical, fire, acoustic, thermal and hygrothermal performance. The whole testing campaign aims to identify the real behavior of PnU prototypes that were developed inTask 4.4 and to improve / optimize any possible design drawbacks. After a series of experimental tests, including the execution of F.Q.Ps, seismic experiments, reaction to fire tests, acoustic tests and a short monitoring campaign, along with numerical tests, including, finite element structural analysis, thermal and hygrothermal simulations, the Task 4.5 validates the simulation models and optimizes the behavior of PnUs.

The work reported in this deliverable is directly linked to the work of WP6: Manufacturing & Assembly of PnU kits and their optimization reported in D2.7.

This project has received funding from the European Union's Horizon 2020 research and innovation programme under grant agreement No 958218

2 Introduction

The aim of the D4.5 is the validation of the PnU kits by means of a testing campaign, which is divided into two sections: the execution of Factory Quality Procedures for the prototypes on manufacture's factories and the laboratory, medium and full-scale testing of the mechanical-structural, fire, acoustic, thermal and hygrothermal performance of indicative PnU kits. At the same time, the testing campaign provides comprehensive information for the optimization of the PnUs in terms of their performance under real conditions.

The investigated PnUs are the SmartWall (both the "VVV" type and the "Berlin" type), the /ConExWall that includes the external Heating and Cooling (eWHC) system, the /HybridWall and the included air-handling unit (eAHC) and the Smart Window.

A full description of the desing and components of the PLURAL PnU kits and their components can be found in D2.7: Final stage complete design of PnU kits (CO, M24). Summarizing, the current deliverable reports:

Factory Quality Procedures (F.Q.P.s)

The manufacturers of PnU kits provided all needed testing and inspection procedures on their factories to ensure that the manufactured PnU prototypes comply with the proposed F.Q.P.s. The testing procedures performed during the manufacturing of every PnU prototype are reported herewith, while the FQP guidelines have been described in Deliverable 4.4 "PnU kit prototypes addressing the 3 demo building requirements" (M22). The procedures include dimensional measurements, visual inspection for defects, mechanical and operational tests, thermographic images, etc.

Mechanical-structural performance

Mechanical properties of components, connections, and fixing used for installation are assessed in relation to wind loads and seismic loads. The dynamic behavior of conventional brick masonry walls fitted with SmartWall subjected to triaxial earthquake ground motions is investigated by means of shaking table tests. The investigation of the other PnU kits in terms of seismic loads is not required based on the national/local regulations. However, all PnU kits are investigated in terms of their mechanical performance of their anchoring system based on detailed 3D numerical models and in-situ detection of PnU prototypes.

Fire performance

The fire performance of PnUs is evaluated in terms of "reaction to fire" tests, following the EN 13823:2020 + A1:2022 standard, also known as Single Burning Item (SBI) test, while the systems are classified on the basis of EN 13501-1. Medium-scale compartment fire tests are performed in NTUA facilities to evaluate the performance of key components of the PnU kits in realistic fire conditions The fire tests concerns to SmartWall and Smart Window, since the local/national fire requirements for eWHC/ConnexWall and eAHC/HybridWall are met by assessment of the individual components and their relevant certification (further information is available in D1.3).

Acoustic performance

In this Deliverable, acoustic analysis carried out only for the eAHC/hybridWall PnU kit ptototype, because it is the only PnU that generates noise (due to the air flow), while the other PnU kits either contain commercial and certified to noise elements or their acoustic performance has already been

This project has received funding from the European Union's Horizon 2020 research and innovation programme under grant agreement No 958218

evaluated in the frame of the Task 4.1. Full scale tests of two eAHC prototypes are carried out in CVUT acoustic lab. The focus is given to acoustic noise emissions from the integrated AHU by measuring the noise for the body of the air handling unit and for each eAHC unit inlet and outlet.

Thermal performance

The thermal and hygrothermal performance of basic materials and components of PnU kits is analysed in the corresponding section. However, as the incorporated materials of all PnUs are commercial, all needed thermal properties are available by the manufacturers. The most crucial properties (thermal conductivity, density, etc), which are used in building physics simulations, are provided. The focus is given in the thermal conductivity measurement by means of Guarded Hot Plate method for different thicknesses of a certain insulation.

Building physics

Detailed thermal and hygrothermal simulations for all PnU kits using commercial software are performed to analyze their thermal and moisture performance. The analysis focuses on the thermal characteristics of PnUs by calculating the thermal transmittance (U-value) and the impact of all incorporated thermal bridges indicating the weaknesses and the significant regions for further optimization. The results and the outcomes of this sections are crucial for the simulation Tasks.

Monitoring of thermal performance of PnU prototypes

The SmartWall and Smart Window prototypes, which were installed in NTUA livinglab in the frame of the Task 4.4, are monitored for six months. The monitoring campaign focuses on the investigation of the thermal performance of prototypes by measuring the U-value (and g-value for the windows) and their thermal characteristics. The results are also used for the validation of simulation models used for the building physics analysis and the calculation of thermal bridges.

This project has received funding from the European Union's Horizon 2020 research and innovation programme under grant agreement No 958218

3 Factory Quality Procedures of testing for the prototype commissioning (F.Q.P.)

3.1 Overview of F.Q.Ps for the three PnU kits

Table 1 summarizes the testing steps implemented as part of the F.Q.P.s for the commissioning of each PnU prototype (the SmartWall, the ConnexWall and the HybridWall). The Table highlights that although the steps are common for the three PnU kits, the inspection tests differ and are dedicated to the characteristics of each PnU kit

TABLE 1: SUMMARY OF F.Q.P. STEPS FOR EACH PNU KIT

F.Q.P tests	SmartWall	eWHC / ConnExWall	eAHC / HybridWall
Visual Inspection	• Minor aesthetic defects on SmartWall's panels surface • Defects on coating's applications • Frame & hanging system • Windows and Roller blinds (dimensions & alignment, hinges orientation) • PV system (alignment, installation, damages) • Other aesthetical defects	• Dimension, quality and humidity control of input materials. • Dimensional accuracy of wood frame before and after covering them with Fermacell.	• Detailed design (drawings inspection, space availability) • Provision • Components storage • Production processes • Frame assembly processes • Frame storage • Support preparation • Installation
Mechanical test	• Window and Roller blinds (Hinges, handle, lock, water splash test, air blow test) • Toolbox (AMScope, Active fire protection, access panel) • Fan-coil (fittings, pipework, air pressure test, drainage test)	• Check of parts ready for connecting with another element (drilling, opening parts, spacing and overlapping of Fermacell)	• Windows (movement, handle, lock) • Unit ventilation (connection, air flows, strange function) • PV tiles (connection) • Louvers (movement, handle, lock) • Load and wind anchoring (extraction test)
Low Voltage Electrical tests	• Roller blinds (Switch, Motor, End stops) • Switchboard & main electrical system (Wiring, Circuit breaker, Rail connectors, External sockets, Earthing) • PV panel (wiring, connectors, battery,	Not needed	• PV tiles (check electric current circuit)

This project has received funding from the European Union's Horizon 2020 research and innovation programme under grant agreement No 958218

	inverter) • Fan-coil (wiring, fan-motor, control panel) • AMsope (wiring, earthing)		
Operational tests	• Switchboard testing under operational voltage • Roller blinds • Fan-coil • AMscope • Fully operational test	• Secure fastening of the elements on trucks • Prevent any damage during transportation	• Window • Unit ventilation • PV tiles
IR thermography	• Toolbox and AMSscope • Fan-Coil	Not needed	Not needed

3.2 SmartWall Prototype's testing as per F.Q.P. Guidelines

As described in the Deliverable "D4.4 - PnU kit prototypes addressing the 3 demo building requirements" a series of tests were performed at the completion of the SmartWall porotype to ensure that complies with the F.Q.P. proposed into it and extensively analysed to the Deliverable "D6.1 – Manufacturing Methodology for PLURAL PnU kits".

By interpreting the guidelines provided in the aforementioned deliverables, the tests performed during SmartWall prototype development are summarised at the following paragraphs, in the form of Tables and where possible illustrated also with pictures. Additionally, in the following Tables, apart the remedial actions for each inspection test all the loop back actions between the remedial actions and manufacturing process as imposed by the F.Q.P. are also clearly identified and recorded.

The testing methodology presented in the following paragraphs, encodes all main tests with an ID number and their subcategories with roman type numbering wile provides for each one the remedial action should be adopted with a (or combinations) of Greek numbers.

E.g.: ID V6 (iv) g, f:

- V refers to visual tests category,
- (iv) to the testing element which in this case is: "PV panel system – connectors and wiring to be firmly secured at the connection box"

The proposed remedial actions are corresponding to

- f.: "Reconnect loose wires on the connectors; Replace defective connectors", and
- g.: "If connection box is defaulted then return SmartWall to the workshop as per Q.A.P. procedure".

This encoding method apart the fact that facilitates the workers to understand and execute the required quality tests prior the installation of the SmartWall panels but also ensures that:

- No defective systems (by any means) will be transferred from the manufacturing plant to the installation sites;

This project has received funding from the European Union's Horizon 2020 research and innovation programme under grant agreement No 958218

- Provides the basic information to the working station which is responsible for the defect which has been identified;
- Summarises and categorises defects for statistical reasons, where can be implemented in the revision of the Q.A.P. in order to improve assembly performance, and
- Evaluates the overall workmanship during assembly process by identifying human mistakes or omissions providing useful data to the Q.A.P.

3.2.1 Visual Inspection

Table 2 tabulated and presents all the visual tests performed at the completion of the SmartWall prototype encoding them to inspection tasks with a unique ID and interprets the sequence of works for each remedial action of every inspection task to a list of numbered actions, while Figure 1, Figure 2 and Figure 3 illustrate some of those visual inspection tests and their remedial actions as identified during the visual inspection tests at the completion of the manufacturing of the SmartWall prototype at NTUA's premises.

TABLE 2: SMARTWALL'S SURFACE INSPECTION & DEFECTS REMEDIAL ACTIONS.

ID	Inspection Task	Remedial action
V1	Minor aesthetic defects e.g. scratches, cracks etc., on SmartWall's panels surface	a. Mark the damaged areas with charcoal; b. Clean charcoal with detergent prior any repairs; c. Sand with sand paper all around the damaged area to reveal substrate; d. Re-plaster the sanded area; e. Apply primer (if needed); f. Apply 1st layer of coating; g. Wait at least two (2) hours for 1st layer to dry; h. Apply 2nd layer of coating; i. Re-inspect the damaged area and repeat the above process if necessary.
V2	Defects on coating's application, e.g.: i. poor application; ii. decolourisation; iii. not proper sanding of the plaster on the substrate iv. flaking, bubbling, micro-holes, etc.; v. any other visual defects on coting's application.	Follow the same remedial procedure as per *IDV1* description.

This project has received funding from the European Union's Horizon 2020 research and innovation programme under grant agreement No 958218

V3	Frame & hanging system: i. Dimensional check; ii. Measure Z clip system (anchoring system); iii. Check for poor welding on anchoring system; iv. Any other defect on frame and hanging system e.g. misalignment, damaged frame, loose elements etc.	a. Re-measure frame and hanging system, ensuring compliance with drawing's dimensions; b. Check for frame / elements alignment; c. Return to workshop as per Q.A.P. in case of defects related to any defects related to inspection tasks of *IDV3*.
V4	Windows: i. Window's type & dimensions; ii. Sill dimensions; iii. Window and sill alignment; iv. Hinges orientation, direction and opening; v. Sealant application (window's frame & sill); vi. Window's glazing sealing rubbers; vii. Window's hinges.	a. Check window's type e.g. tilting-inwards openings, as per drawings; b. Re-measure window and sill's dimensions, ensuring compliance with drawing's dimensions; c. Check window's and sill alignment, ensuring proper installation; d. If *a, b* and *c* are do not comply with inspection standards, then return it to the workshop as per Q.A.P. procedure. e. Remove excessive sealant with the aid of a cutter. Restore appearance by re-painting surface if necessary or f. Remove all part of improper fitted sealant and replace it with new. Restore appearance with coating application if necessary. g. Check correct installation of rubber sealants of the window frame (glazing sealant). If not properly fitted return it to workshop as per Q.A.P. procedure. h. Ensure hinges that are fully aligned and securely installed on the window's frame. i. Ensure that are not missing and/or loose screws attached on to it. j. If *g* and *h* do not comply with inspection standards, then return it to the workshop as per Q.A.P. procedure.
V5	Roller blinds: i. External box dimensions & alignment; ii. Roller guides alignment; iii. Switch alignment; iv. Frame's ventilation unit type and alignment; v. Roller end stops alignment; vi. Sealant application (box frame)	a. Re-measure all dimensions, ensuring compliance with drawing's dimensions; b. Check alignment of all roller blinds components to ensure proper installation; c. Drill new holes (if necessary) to realign them and/or replace with new (if necessary); d. Remove excessive sealant with the aid of a cutter. Restore appearance by re-painting surface if necessary, or e. Remove all part of improper fitted sealant and replace it with new. Restore appearance with coating

This project has received funding from the European Union's Horizon 2020 research and innovation programme under grant agreement No 958218

		application if necessary.
V6	PV system: i. External panel type to comply with drawings; ii. Brackets to be securely attached on the pre-existing frame's holes; iii. Panel alignment; iv. Connectors and wiring to be firmly secured at the connector box; v. Damages, scratches, stains or other visible defects on the PV panel glass; vi. Any kind of dirt of the PV panel glass.	a. Check PV panel type e.g. dimensions, power, output voltage etc., as per drawings; b. Ensure secure fitting of the supporting brackets that are firmly attached on the pre-allocated positions of the frame; c. Check spacers on the back side of the PV panel; d. Replace defective screws or brackets or spacers; e. Recoat areas that might be affected by brackets replacement; f. Reconnect loose wires on the connectors; Replace defective connectors; g. If connection box is defaulted then return SmartWall to the workshop as per Q.A.P. procedure. h. Clean glass surface with soft cloth and appropriate detergent; i. If surface is damaged e.g. scratched or cracked or stained, then return SmartWall to the workshop as per Q.A.P. procedure.
V7	Other aesthetical defects: i. defective screws' installation; ii. defective corner beads; iii. misaligned brackets, sockets, switches, AMscope box, etc.; iv. Dirty surfaces; v. Packaging	a. Check for defective / loose screws & corner bead; b. Remove defective screw or bead; c. Replace with new one ensuring proper securing; d. Realign brackets, sockets, switches, AMscope if necessary; e. Drill new holes (if necessary) to realign them and/or replace with new (if necessary); f. For all actions follow same remedial procedure as per *IDV1* to restore SmartWall aesthetics (if necessary); g. Clean with detergent and soft cloth the surface of SmartWall panel. h. Proceed to packaging as per F.Q.P. i. Ensure that cover wrap is intact with no defects, scratches or exposed items of the SmartWall panel j. Ensure identification labelling is attached on to it. k. Ensure that transportation hinges are fully attached

This project has received funding from the European Union's Horizon 2020 research and innovation programme under grant agreement No 958218

FIGURE 1: (LEFT): MEASURING PANEL, (MIDDLE): RE-ALIGNMENT OF POWER SOCKETS, (RIGHT): DIRT REMOVAL FROM WINDOW FRAME AND SILL.

FIGURE 2: (LEFT): RECOATING DAMAGED AREA, (MIDDLE): REPLACING DEFECTIVE SCREWS, (RIGHT): ALIGNMENT FAN-COIL'S CONTROL UNIT.

FIGURE 3: (LEFT): LOCAL REPAIRS ON THE CORNER BEAD, (MIDDLE): SEALANT REPAIRS, (RIGHT): PV RE-ALIGNMENT.

3.2.2 Mechanical Tests

Similar to visual inspection tests, Table 3 presents all the mechanical tests performed at the completion of the SmartWall prototype and Figure 4, Figure 5 and Figure 6 present some of the tests performed at the manufacturing completion of the SmartWall prototype at NTUA's premises.

This project has received funding from the European Union's Horizon 2020 research and innovation programme under grant agreement No 958218

TABLE 3: SMARTWALL'S MECHANICAL TESTING & DEFECTS REMEDIAL ACTIONS

ID	Inspection Task	Remedial action
M8	Window: i. Hinges; ii. Handle; iii. Lock; iv. Ventilation outlet; v. Window's water splash test; vi. Window's air blow test.	a. Test hinges operation as per manufacturer installation tests. b. Open and close window in both directions (opening and tilting) several times (>10) to ensure its smooth operation. c. Open and close several times (>10) the ventilation outlet on both internal and external part. d. Check window lock and handle by locking and unlocking the window several times (>10). e. Apply lubricant as per F.Q.P description to the hinges, locks and handle. f. If any of *a, b, c, & d* do not comply with the quality standards as per Q.A.P. then return SmartWall panel to the workshop. g. Perform water splash test on the window; h. Check for water penetration via window's sealants, gaskets, sill and ventilation unit. i. If water splash test fails then perform window's air blow test to determine the points of leakages; j. Mark points of leakages and return SmartWall panel to the workshop for further remedial actions. k. Clean all window area with smooth cloth and the appropriate detergent after water splash test.
M9	Roller Blinds: i. Shutters; ii. Shutters mechanism (mechanical); iii. Roller's strap; iv. Roller guides; v. End stops.	a. Check shutter's sheets for proper interlocking by raising – lowering them several times (>5). b. Ensure that the mechanical shutter's mechanism is not blocking anywhere. c. Apply the appropriate lubricant to its moving parts as per Q.A.P. d. Check strap's tension (for mechanical operation). Ensure that is not lose or extremely tight. Adjust if necessary. e. Ensure that roller guides are clean and free of dust or other elements can disturb smooth operation of roller shutter. Clean them with compressed air if necessary. f. Ensure end stops are on correct position and securing roller on its correct position. Replace them in necessary; g. If remedial actions failed return to workshop as per Q.A.P.

This project has received funding from the European Union's Horizon 2020 research and innovation programme under grant agreement No 958218

M10	Toolbox: i. AMscope; ii. Active fire protection system; iii. Access panel	a. Ensure toolbox casing is firmly secured on frame. Apply 10Mn force to each bolt if lose. b. Ensure toolbox cover is secured on the box. Apply 7Nm force to its screws. c. Check pressure on active fire protection system; d. If pressure is below 6 bars replace BlazeCut unit. e. Ensure access panel fixing to be securely attached on frame by applying >5Nm force to its screws. f. Open-close access panel cover several times (>5) to ensure proper interlocking. Adjust interlocking spring if necessary. Apply the appropriate lubricant on interlocking mechanism as per Q.A.P. g. If f fails to the inspection standards, then return it to the workshop as per Q.A.P. procedure.
M11	Fan-coil: i. Fittings; ii. Pipework; iii. Air ducts; iv. Air grills; v. Drainage test; vi. Air pressure test.	a. Check all fittings that are securely bolted / griped on the pipework / connecting elements. b. Apply force to bolted fittings 40 Nm to ensure proper bolting. c. Apply force 30Nm to puck-lock fittings to ensure proper installation. d. Leave all valves at open state for air pressure test. e. Ensure pipes are securely attached on the designated locations as per drawings. f. Check gasket on the fan-coil ducts that is correctly fitted. Replace if necessary. g. Check air-grills (inlet – outlet) that are firmly attached on the air ducts. Check their gasket. Replace if necessary. h. Empty 0.5l of water in the fan-coil's drainage tank. Adjust its slope if tank will not empty. Ensure that no leaks occur to its connection with the drainage tube. In such a case replace sealant. i. Perform pressurised air test at 4 bars as per F.Q.P. j. Retain air pressure to the system for 30 minutes. k. Maximum permissible loss 0.1 bar at the end of the air pressure test. l. If air pressure test fails then return the SmartWall panel to the workshop as per Q.A.P.

This project has received funding from the European Union's Horizon 2020 research and innovation programme under grant agreement No 958218

FIGURE 4: (LEFT): WINDOW'S TYPE CHECK, (MIDDLE): WINDOW TILTING AND HINGES TEST, (RIGHT): ROLLER BLINDS STRAP RE-TENSIONING.

FIGURE 5: (LEFT): WINDOW'S WATER SPLASH TEST, (MIDDLE): ACTIVE FIRE PROTECTION SYSTEM TEST, (RIGHT): TOOLBOX CHECK

FIGURE 6: (LEFT): ACCESS PANEL OPERATIONAL TEST, (MIDDLE): TRANSPORTATION HINGES TEST, (RIGHT): PIPEWORK AIR PRESSURE LEAKAGE TEST.

3.2.3 Low Voltage Electrical tests

Table 4 records all the low voltage electrical tests executed at the manufacturing completion of the SmartWall prototype at NTUA's premises, while Figure 7 presents some of these tests.

This project has received funding from the European Union's Horizon 2020 research and innovation programme under grant agreement No 958218

TABLE 4: SMARTWALL'S LOW VOLTAGE TESTING & DEFECTS REMEDIAL ACTIONS.

ID	Inspection Task	Remedial action
E12	Roller blinds: i. Switch; ii. Motor; iii. End stops.	a. Check switches' wiring. If wire is lost or unprotected secure it on the connector. b. With the aid of a multimeter in "*Buzzer*" mode or with a Geiger counter, check for power line continuity and short circuits. If short circuit occurs the multimeter will produce a buzz. c. In such a case, follow the instructions as per Q.A.P. by replacing the defaulted switch. If problem insists, return the SmartWall panel to the workshop for further investigation. d. Ensure blinds motor is well attached on its designated position. e. Repeat process for line continuity as per *paragraph b* for the blind motor testing. f. In *"Resistance (R)"* mode in the multimeter or with a Geiger counter, check motor resistance value which must always be rated as *"infinity"* (∞). Any other resistance value indicates motor malfunction or short circuit to earth. g. Using the multimeter in "*Buzzer*" check power line continuity on end stops on the bottom by pressing the connection spring to close power circuit (*"close" mode*) and a buzz by the multimeter should be heard. By releasing the spring, the circuit is transferred to *"open"* mode and the buzz of the multimeter stops. h. Repeat the same action as per *paragraph g* for the upper end-stops. i. With the multimeter in *"Resistance (R)"* mode or a Geiger counter, check earthing of all the aforementioned elements (Value < 1Ω). j. If any of *d, e, f, g, h* and *j* do not comply with the quality standards as per Q.A.P., then return SmartWall panel to the workshop.

This project has received funding from the European Union's Horizon 2020 research and innovation programme under grant agreement No 958218

E13	Switchboard & main electrical system: i. Wiring; ii. Circuit breaker; iii. Rail connectors; iv. External sockets; v. Earthing.	a. Ensure that all elements are properly and correctly secured in the railing system. b. Ensure that there are no visible scratches, damages, signs of wear are visible on to the wiring. c. Ensure that all wires are correctly fitted and secured on their element's connecting system. Apply force <5Nm to each bolt of the connector. d. Perform same actions for power line continuity as per description of *ID E12(b)* for all elements involved in the switchboard. e. If any of the testing elements fail to comply with follow instructions as per *ID E12(b)* description. f. Perform same action as per *ID E12(i)* description to check earthing. g. Provide external source of 12V power to the switch board (by the battery) and earth *"Neutral"* with *"Earth"* cables to the main circuit breaker switch to develop short circuit. Main circuit breaker relay should be automatically switch off the circuit. h. Similarly follow the same process with the *"Line"* and *"Neutral"* cables. Again, main circuit breaker relay will switch off the circuit. i. If any of *d, e, f, g, h* and *j* do not comply with the quality standards as per Q.A.P., then return SmartWall panel to the workshop.
E14	PV panel system: i. Wiring; ii. Connectors; iii. Panels; iv. Charger; v. Battery; vi. Inverter.	a. Ensure that all elements are properly and correctly secured in the toolbox. b. Ensure that there are no visible scratches, damages, signs of wear are visible on to the wiring. c. If *b* fails to the inspection standards, then return it to the workshop as per Q.A.P. procedure. d. Ensure that all wires are correctly fitted and secured on their element's connecting system. Apply force <5Nm to each bolt of the connector. e. Perform same actions for power line continuity as per description of *ID E12(b)* for all elements involved in the switchboard. f. If any of the testing elements fail to comply with follow instructions as per *ID E12(b)* description. g. Perform same action as per *ID E12(i)* description to check earthing. h. With a multimeter in "*DC Voltage"* mode check voltage of the PV Panel (1.5 - 6.0 V) i. Apply the same action to the battery charger (11.5 -14.5 V) to identify if charger is charging the battery and j. Confirm charging by measuring the battery (11.0 - 13.0 V) k. If any of *e, f, g, h, i* and *j* do not comply with the quality standards as per Q.A.P., then return SmartWall panel to the workshop.

This project has received funding from the European Union's Horizon 2020 research and innovation programme under grant agreement No 958218

E15	Fan-coil: i. Wiring; ii. Fan motor; iii. Control panel; iv. Earthing.	a. Ensure that all elements are properly and correctly secured to their connectors. b. Ensure that there are no visible scratches, damages, signs of wear are visible on to the wiring. c. If *b* fails to the inspection standards, then return it to the workshop as per Q.A.P. procedure. d. Perform same actions for power line continuity as per description of *ID E12(b)* for all elements involved in the switchboard. e. If any of the testing elements fail to comply with follow instructions as per *ID E12(b)* description. f. Perform same action as per *ID E12(i)* description to check earthing. g. If any of *d, e,* and *f* do not comply with the quality standards as per Q.A.P., then return SmartWall panel to the workshop.
E16	AMsope: i. Wiring; ii. Earthing.	a. Perform same actions for power line continuity as per description of *ID E12(b)* for all elements involved in the switchboard. b. If any of the testing elements fail to comply with follow instructions as per *ID E12(b)* description. c. Perform same action as per *ID E12(i)* description to check earthing. d. If any of *a, b,* and *c* do not comply with the quality standards as per Q.A.P., then return SmartWall panel to the workshop.

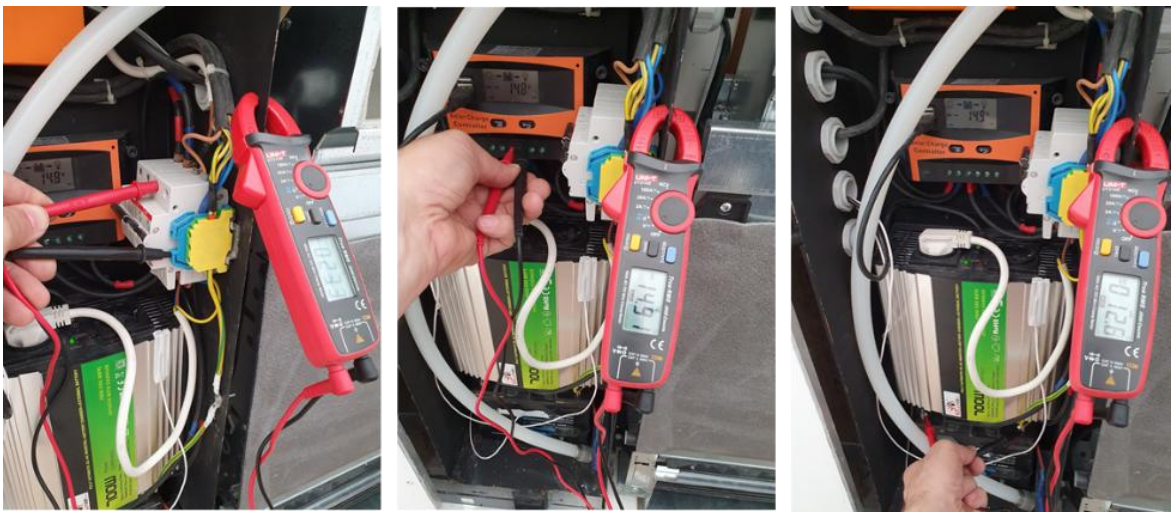

FIGURE 7: (LEFT) LINE CONTINUITY TEST, (MIDDLE): CHARGER INVERTER TEST, (RIGHT): INVERTER VOLTAGE TESTING

This project has received funding from the European Union's Horizon 2020 research and innovation programme under grant agreement No 958218

3.2.4 Operational tests

The following Table 5 presents the operational tests for the SmartWall prototype while in Figure 8 and Figure 9 some of those tests performed are illustrated.

TABLE 5: SMARTWALL'S OPERATIONAL TESTING & DEFECTS REMEDIAL ACTIONS.

ID	Inspection Task	Remedial action
O17	Switchboard testing under operational voltage	a. Switch on the main circuit breaker on the switch board. b. With the aid of a multimeter in "*AC Voltage*" mode measure voltage values on the switch board supply bar (220 – 245 V). c. Earth "*Neutral*" with "*Earth*" cables to the main circuit breaker to develop short circuit. Main circuit breaker relay should be automatically switch off the circuit. d. Similarly follow the same process with the "*Line*" and "*Neutral*" cables. Again, main circuit breaker relay will switch off the circuit. e. Repeat the same actions as per paragraphs *b, c* and *d* for each circuit breaker of the switch board. f. If any of *b, c, d* and *f* do not comply with the quality standards as per Q.A.P., then return SmartWall panel to the workshop. g. Put SmartWall panel on "*Standby*" mode (all circuit breakers on "*ON*" and external power supply connected.
O18	Roller blinds	a. On "*Standby*" mode, follow same testing actions as per mechanical operation testing (*ID M9 a & b)* b. If any of the actions fail, then return SmartWall panel to the workshop.

This project has received funding from the European Union's Horizon 2020 research and innovation programme under grant agreement No 958218

O19	Fan-coil *(Can be tested only if is connected on a HVAC system e.g. heat pump, boiler etc.)*	*Assuming that fan-coil is connected on a heat pump, in controlled conditions (room temperature to 22°C) and SmartWall is on "Standby" mode:* a. Switch to "*ON*" the fan-coil by its control panel. b. Turn on "*Heating*" mode and adjust it to its maximum temperature (30°C). c. Wait for 10 minutes and switch it "*OFF*". d. Repeat same action for two (2) more times. e. During last circle decrease temperature by the control panel to 16°C. Fan-coil should stop its operation. f. Increase again temperature to 30°C. Fan-coil should start its operation again. g. Repeat same actions as per paragraphs *c, d* and *e* by setting the fan-coil on "*Cooling*" mode. *In both operational modes:* h. Check that air blowing is constant and changes its direction according air-grills movement. i. Check for leakages and condensation on the piping system. j. Check for abnormal noises produced by the motor fan. k. Check drainage tank for leakages. l. If any of the above do not comply with the quality standards as per Q.A.P., then return SmartWall panel to the workshop.
O20	AMscope	a. Set SmartWall on "*Standby*" mode. b. Set AMscope's control panel to "*ON*" and wait until software will be loaded (appx. 10 sec). c. Wait for 5 minutes until all sensors will be self-calibrated. d. Check readings on the panel: ➢ Date (present) ➢ Mode (manual or auto) ➢ Room temp (-10 – 60°C) ➢ Room humidity (10 -100%) ➢ Room CO_2 (200 – 10000 ppm) ➢ Room VOC (10 – 100000 ppm) ➢ Room luminance (0 -2000 lux) ➢ Temp sensor on toolbox (0 – 150°C) ➢ Temp sensor on fan-coil (0 – 150°C) ➢ Temperature on battery (0 – 150°C) ➢ Humidity on fan-coil area (10 -100%) ➢ Smoke alarm operation (b mode) e. If any of the above values does not illustrated or is out of the nominal measurement ranges press '*RESET*" button for 5 seconds and wait until the system will reboot. f. If problem persists then return SmartWall panel to the workshop for further actions. g. Set AMscope to "*MANUAL*" mode. h. Press "*BLINDS*" bottom to "*DOWN*" and the roller blinds should move downwards.

This project has received funding from the European Union's Horizon 2020 research and innovation programme under grant agreement No 958218

		i. Press it again and roller blinds should stop their movement. j. Press "*BLINDS*" bottom to "*UP*" and roller blinds should move upwards. k. Press it again and roller blinds should stop their movement. l. Repeat same operation for several times (>3). m. If in any mode blinds movement does not function properly then return it back to the workshop for further actions. n. Repeat sae actions as per *ID O19 a-g* description to check the fan-coil's operation. o. Set AMscope to "*AUTO*" mode p. Plug the micro USB cable to the AMscope panel and connected with a PC loaded with YAT programming terminal software. q. In YAT on the relevant "*Luminance sensor*" set: ➢ BLINDS "*OFF*" > blind rollers should close ➢ BLINDS "*ON*" > blind rollers should open ➢ Luminance to *2000* lux > rollers should close ➢ Luminance to *10* lux > rollers should open ➢ Luminance to *500* lux > rollers should be half open r. In YAT on the "fan-coil mode" set it to "*AUTO*" to allow fan-coil to operate according the reading of its own control panel. s. Repeat same actions as per as per *ID O19 a-g* description to check the fan-coil's operation in auto mode. t. In YAT set "*Vent unit*" to "*AUTO*" mode and change values ➢ on "CO_2" sensor to *800ppm* > ventilation relay will be triggered to "*ON*". Reset sensor. ➢ on "*ROOM HUMIDITY*" sensor value to 65 > ventilation relay will be triggered to "*ON*". Reset sensor. ➢ On "VOC" sensor set value to 3000 > ventilation relay will be triggered to "*ON*". Reset sensor. u. In YAT set "*Vent unit*" to "*MANUAL*" if **no** ventilation unit is attached on the SmartWall panel. v. In YAT set consequently: ➢ "*BATTERY TEMP SENSOR*" to "*60*". Check AMscope control panel for the flashing warning on the battery temperature reading and a warning buzz should be generated. Reset sensor. ➢ Do the same for "*FAN-COIL SENSOR*", "*TOOLBOX SENSOR*" and ➢ "*HUMIDITY FAN-COIL SENSOR*" (setting value to "*80*"). ➢ "*SMOKE SENSOR*" to "*ON*" w. Reset all "*SENSORS*". x. Repeat the same action (apart "*HUMIDITY FAN-COIL SENSOR*") by setting their value to "*70*" and "*SMOKE SENSOR*" to "*ON*". y. Apart the acoustic and visual warning system "*EMERGENCY MODE*" will be triggered to "*ON*". ➢ In 15 seconds from triggering main power supply on SmartWall will cut-off. ➢ In 20 seconds from triggering battery power supply will cut off and system will be isolated. *Under real operational conditions BlazeCurt fire extinguishing system will be*

This project has received funding from the European Union's Horizon 2020 research and innovation programme under grant agreement No 958218

		triggered on 70°C z. Reset all "*SENSORS*". aa. In YAT "*FIRMWARE*" section set Wi-Fi to "*ON*" (command *M552-S1*). bb. Check its status (*M552*) cc. Use *M552 S1 P"my_ SSID*" command to set up the SSID name and password. dd. Check its status with *M587* command. ee. Disconnect YAT and USB cable from the AMscope and turn off its main power supply for 10 seconds. Reconnect main power supply and select either "*AUTO*" or "*MANUAL*" mode in the control panel. System is ready for use. ff. If any of the actions in "*AUTO"* mode fail then: ➢ Perform "*RESET*" as per paragraph *e* description and repeat all actions described on the above. ➢ If "*RESET*" fails then return SmartWall panel to the workshop for further investigation.
O21	Fully operational test	a. Check voltage (220 – 245 V) b. Switch to "*ON*" roller blinds. Measure its current with a multimeter (values between 0.15 – 0.3 A). c. Switch to "*ON*" fan-coil to either "*Heating*" or "*Cooling*" mode and measure current (0.2 – 0.4 A) d. Check current of PV system (0.1 – 0.3 A) e. Let all systems on power and in fully operational mode for one (1) hour and proceed to IR thermography to determine possible overheating or other operational issues.

FIGURE 8: (LEFT) FAN-COIL AIR BLOW TEST, (MIDDLE): AMSCOPE TESTING, (RIGHT) AMSCOPE PROGRAMMING.

This project has received funding from the European Union's Horizon 2020 research and innovation programme under grant agreement No 958218

FIGURE 9: (LEFT) TOOLBOX TESTING, (MIDDLE) SENSOR TESTING, (RIGHT): BLIND ROLLERS TESTING.

3.2.5 IR thermography

IR thermography is a method to indicate the crucial areas of an electrical infrastructure under load as these areas will be appeared as overheated areas in the IR image. This process will protect the PnU by a possible electrical system failure which may be led to a spread of fire and smoke. Besides, the IR thermography can point out liquid leakage issues at piping connections of fan-coil unit.

***Important condition for IR Thermographic Testing**:*

All IR thermographic testing should be executed after the completion of all the operational tests to ensure the safe operation and use of SmartWall panel and under fully operational conditions (all components to be operational during testing).

The IR thermography was obtained according to ISO 10880 and ASTM E 1934. The infrared thermography was performed 2 hours after the sunset for the avoidance of solar radiation and gathering accurate data. The examined equipment was ensured to be under adequate load, and sufficient time was allowed for recently energized equipment to produce stable thermal patterns. All necessary cabinet and enclosure covers were opened or removed immediately before the examination to provide direct views of the equipment.

Figure 10 illustrates an IR image of the Toolbox and fan-coil during the thermography tests. The temperature is higher at the Toolbox area, due to the electricity, however, the temperatures do not exceed 40°C. Also, no overheating areas were presented during the operation of roller blinds, fan-coil (both on heating and cooling mode).

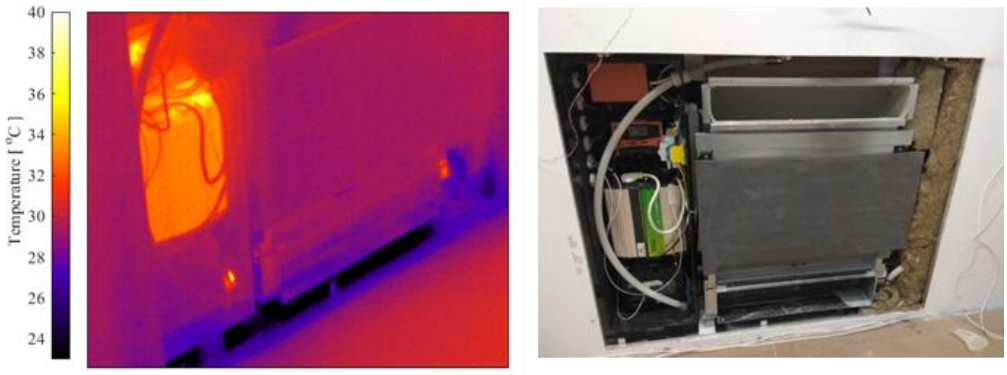

FIGURE 10: IR IMAGE AND PHOTO OF TOOLBOX AND FAN-COIL DURING THERMOGRAPHY TESTS.

This project has received funding from the European Union's Horizon 2020 research and innovation programme under grant agreement No 958218

TABLE 6: SMARTWALL IR THERMOGRAPHIC INSPECTION & DEFECTS REMEDIAL ACTIONS

ID	Inspection Task	Remedial action
I22	Toolbox and AMSscope	a. Check crucial areas for overheating temperature b. Switch to "ON" roller blinds and check for overheating areas. c. Switch to "ON" fan-coil and check for overheating areas. d. Switch to "ON" both roller blinds and fan-coil and check for overheating areas.
I23	Fan-coil	a. Switch to "ON" fan-coil and check crucial areas for overheating areas or water leakage. b. Turn the system at heating mode and check for overheating areas or water leakage. c. Turn the system at cooling mode and check for overheating areas or water leakage.

3.3 eWHC / ConExWall Prototype's testing as per F.Q.P. Guidelines

Since the main part of the ConExWall is a prefabricated façade element from RDR most of the tests are performed within their standard procedure. This includes for example visual inspections and functionality test. The production of façade elements is certified according to ETA-ETAG 007.

The main control point in the pre-production process is the satisfaction of technical requirements of each module, such as U-values, fire resistance, acoustic parameters and precise dimensions. In the production stage is established quality control in six critical points of production, as presented in Figure 11. The description of the FQPs during and after the production process is presented in Table 7 and Table 8, respectively.

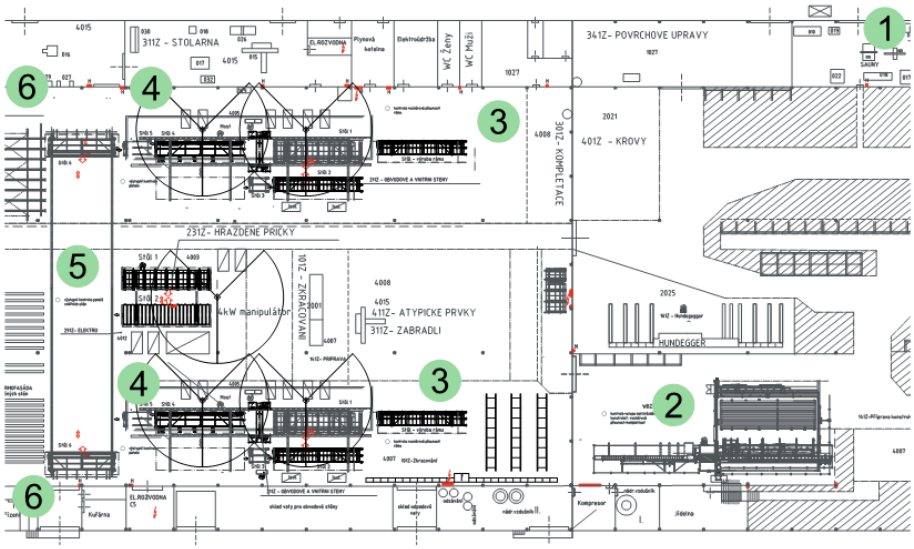

FIGURE 11: QUALITY CONTROL POINTS AT RDR FACILITIES.

This project has received funding from the European Union's Horizon 2020 research and innovation programme under grant agreement No 958218

TABLE 7: DESCRIPTION OF THE FQPS DURING THE PRODUCTION PROCESS

Check point		Related with	Remedial action
1	Checkpoint of input materials (chipboard, Fermacell, construction wood). Overall check of main input materials.	The checkpoint is related with the Central delivery office, and working places in production: a. CNC shortening saw b. CNC formatting saw Holzma c. CNC center Hundegger d. Weinmann woodframe machine	Checking activities: • dimension control • quality control • humidity control
2	Checkpoint of input materials (woodframe constructions, ceiling panels, roof panels). Overall check of misconceptions of part after first processing, in production.	a. Weinmann woodframe machine b. CNC center Hundegger c. CNC formatting saw Holzma	• Check of completeness of prepared materials • Check of dimensional accuracy • Checking the quality and accuracy of machining
3	Checkpoinf of the dimensional accuracy of the woodframe, before first covering by Fermacell.	a. Inside wall production b. Main wall production c. Ceiling and roof elements production	Checking activities: • Outside size control of the frames • Diagonal size control (rectangularity) • Size control of construction holes of windows and doors
4	Checkpoinf of the dimensional accuracy of the woodframe, before first covering by Fermacell.	a. Inside wall production b. Main wall production c. Ceiling and roof elements production	Checking activities: • Outside size control of the frames • Diagonal size control (rectangularity)
5	Output frame control, overall second checkpoint in production of walls after covering them with Fermacell before starting to applying the Thermophasade	a. Inside wall production b. Outside wall production Weinmann	Checking activities: • Outside size control of the frames • Diagonal size control (rectangularity) • Check of the fillings of the construction holes

This project has received funding from the European Union's Horizon 2020 research and innovation programme under grant agreement No 958218

			• Control of the dampfoil overlap
6	Final output frame control, the last check in process of walls production.	a. Inside wall production b. Outside wall production c. Production of ceiling and roof elements	Checking activities: • Panel completeness check • Check of parts ready for connecting with another element (drilling, opening parts, spacing and overlapping of Fermacell) • Check of flatness and thickness of TMF • Electroinstallation check • Control of windows (way of opening, cover, accuracy and perpendicular of spelled) • Check of shielding technology
7	Photodocumentation of dispatched elements, to		Checking activities: • Check possible damage during transport.

TABLE 8: DESCRIPTION OF THE FQPS AFTER THE PRODUCTION PROCESS

Inspection Task	Remedial action
Production output and procedure of overhanding to the construction site	• Check completeness of sets for delivery from depo • Secure fastening of the elements on trucks • Prevent any damage during transportation
Responsibilities on the construction site	• Check precision of modules' assembly and the geometry of finalized assembly (on site).
Guarantee for the finalized construction work	As the production is certified according ETA-TEAG 007, the guarantees are provided in line with the certificate's directives.
Progress made during the project	Practical validation of delivery of the modules for retrofitting, detailed knowledge on production times, and new know how on quality control in large production series.

This project has received funding from the European Union's Horizon 2020 research and innovation programme under grant agreement No 958218

3.4 eAHC / HybridWall Prototype's testing as per F.Q.P. Guidelines

3.4.1 Visual inspection

The next tables detail the results of that F.Q.P. guidelines applied on the prototypes and a series of remedial actions for each task in case mistakes could occur.

The structure of the F.Q.P. follows the same basic manufacturing process that will be developed in Task 6.1 to make easy to establish clear manufacturing strategies organised in sequential "workings stations".

The description of the tables is as follows:

- F.Q.P.: Identifies the manufacturing process for the Panel Unit Kits.
- Inspection task column are the basic F.Q.P. Basic guidelines (based on prototype's production) described in tasks 4.4. This column is also written in different colors, as a resume of the inspection task during the prototyping of the PnU. Each color has the next meaning:
  - Green: describes the inspection task thatwent wall on the prototype manufacturing.
  - Orange: describes the inspection task that went wrong for the prototype.
  - Blue: describes the improvements in case they were need.
- Remedial actions: Describes the remedial actions in case the inspection task went wrong.

3.4.1.1 Phase 1: Detailed design

TABLE 9: DETAILED DESIGN VISUAL INSPECTION TABLE

F.Q.P	Inspection Task	Remedial action
FQP.P1.a	Check there are not interferences between components. TEST & MESUREMENTS: The drawings were done in 3D model, so that is easy to check that there are no interferences. For better results, drawing were revised by a second investigator. IMPROVEMENTS: No need to do at this stage	a. Draw again the components. b. If change implies a modification of the final exterior design / change of budget, send modification to customers / designers to have the approval.
FQP.P1.b	Drawings inspection for mistakes & omission: Make doble check / revision of the hole process (metrics, position,…). From that point every mistake will be real, not digital. TEST & MESUREMENTS: The drawings were done in 3d model, so that is easy to check there are no interferences. For better results, drawings were revised by a second investigator. IMPROVEMENTS: No need at this stage	Follow the same remedial procedure as per FQP.P1.
FQP.P1.c	Check that all the components that require it, have their 3d file.	a. Draw the missed components. b. Ensure these components was

This project has received funding from the European Union's Horizon 2020 research and innovation programme under grant agreement No 958218

	TEST & MESUREMENTS: A double check revision was done. And it seemed to be all ok. When realizing the prototype, a mistake was discovered. The load windows were supposed to be the same for the up and the down position, but in fact they are mirror pieces. IMPROVEMENTS: Since it is easy to confuse different components which have same design but in mirror way, in next productions a special mirror component checking will be done.	already on the project budget. c. If not, and change implies a modification of the final exterior design / change of budget, send modification to customers / designers to have the approval.
FQP.P1.d	Check that the assembly drawings are clear and updated to the latest version. TEST & MESUREMENTS: It was done. IMPROVEMENTS: No need.	a. Use latest version drawing.
FQP.P1.e	Check that the installation drawings are clear and updated to the latest version. TEST & MESUREMENTS: It was done. IMPROVEMENTS: No need.	a. Use latest version drawing.
FQP.P1.f	Check the availability of space at the factory to ensure there will be enough space for the material reception and for the frame's assemblies and storage during the foreseen dates. TEST & MESUREMENTS: It was done. IMPROVEMENTS: No need.	a. Optimize the space b. Modify the dates for the production. c. Work in double shift to unfroze space in the factory.

3.4.1.2 Phase 2: Provision

TABLE 10: PROVISION VISUAL INSPECTION TABLE.

F.Q.P	Inspection Task	Remedial action
FQP.P2.a	Double check the components list before formalizing the order TEST & MESUREMENTS: It was done. IMPROVEMENTS: No need.	a. Add missing information in case it does not exist. Go to Phase 1. b. Go to Phase 1 to discover why this information is missing and if it affects to the budget or the final design.
FQP.P2.b	Check that all the information required has been sent to the providers TEST & MESUREMENTS: It was done. IMPROVEMENTS: No need.	a. Send additional information in case it is required. c. Go to Phase 1 to discover why this information is missing and if it affects to the budget or the final design.
FQP.P2.c	Follow the sending regularly (update the production time if necessary) TEST & MESUREMENTS: It was done. IMPROVEMENTS: No need.	a. In delay case check if it affects to the critical way. b. Ask to provider not to be delayed. c. Try to find another provider. d. Go to Phase 1 to check if this modification can be solved with Study if work in double shift or need approval from customer to change delivery day.
FQP.P2.d	Received components validation (Material, Element	a. In case of mistake ask provider to do it again. b. Study how affects this delay as per FQP.P2.c

This project has received funding from the European Union's Horizon 2020 research and innovation programme under grant agreement No 958218

	codification/Labelling, Weight, Dimensions, Certifications). TEST & MESUREMENTS: It was done. IMPROVEMENTS: No need.	remedial actions.

3.4.1.3 Phase 3: Components storage

TABLE 11: COMPONENTS STORAGE VISUAL INSPECTION TABLE.

F.Q.P	Inspection Task	Remedial action
FQP.P3.a	Check that the components are stored by functionalities TEST & MESUREMENTS: It was done. IMPROVEMENTS: No need.	a. Order the components by functionalities. b. Investigate why it was not done this way (some mistakes have been done in the previous phases).
FQP.P3.b	Check the stock of attaching elements. TEST & MESUREMENTS: It was done. IMPROVEMENTS: No need.	a. Go to Phase 1 to start a process to get a provision for these components. b. Investigate why it was not done this way (some mistakes have been done in the previous phases)
FQP.P3.c	Check the storage area conditions. TEST & MESUREMENTS: It was done. IMPROVEMENTS: No need.	a. Improve conditions. b. Investigate why conditions were not ok and establish protocols to arrange it.
FQP.P3.d	Visual inspection for all components for damages, scratches any other possible visually observed defects. TEST & MESUREMENTS: It was done. IMPROVEMENTS: No need.	a. Go to Phase 1 to start a process to get a provision for these components as per FQP. P2.c . b. Investigate how damages has appear in the components (some mistakes have been done in the previous phases) and establish protocols to arrange it.

3.4.1.4 Phase 4: Production Processes

TABLE 12: PRODUCTION PROCESS VISUAL INSPECTION TABLE.

F.Q.P	Inspection Task	Remedial action
FQP.P4.a	Check for good cleaning conditions of stored materials prior any intervention TEST & MESUREMENTS: It was done. IMPROVEMENTS: No need.	a. Clean components.
FQP.P4.b	Cut on size dimensional & quality check TEST & MESUREMENTS: It was done. The cutting of the isolation dimensions was more difficult than expected. The final dimensions were larger than needed. It was decided to use it as well, to check if larger dimensions also were able to be	a. Start again the cutting process. b. Investigate how mistake has happened to improve the manufacturing process at this stage.

This project has received funding from the European Union's Horizon 2020 research and innovation programme under grant agreement No 958218

	installed within the system. It was confirmed that it is possible to use larger size insulation, but did not produce any benefits. IMPROVEMENTS: New table for cutting isolation will be arranged, with a new tool to make easy its measurement and later cutting in 90º orientations.	
FQP.P4.c	Visual inspection for all installed components for damages, scratches any other possible visually observed defects TEST & MESUREMENTS: It was done. No components were damaged, with the exception of the larger dimensions of the isolation explained in point before. IMPROVEMENTS: Need. Explained in point before.	a. Follow the same remedial procedure as per FQP.P4.b.

3.4.1.5 Phase 5: Frame Assembly Processes

TABLE 13: FRAME ASSEMBLY PROCESS (VISUAL INSPECTION - TABLE I)

F.Q.P	Inspection Task	Remedial action
Place Lines	Check that the length of the lines is correct. TEST & MESUREMENTS: It was done. IMPROVEMENTS: No need.	
Install Hinges FQP.P5.a	Check the screws are firmly installed TEST & MESUREMENTS: It was done. IMPROVEMENTS: No need.	a. Install again b. Update storage number of rivets and screws.
Install Wind bridges FQP.P5.b	Check the screws are firmly installed TEST & MESUREMENTS: It was done. IMPROVEMENTS: No need. Check that distances between lines are the same as the frame plan TEST & MESUREMENTS: It was done. IMPROVEMENTS: No need.	a. Install again b. Update storage number of rivets and screws. c. In case distances are not ok find the correct component to be installed by checking it is identification number. d. In case does not exist go to phase 1. e. Investigate how mistake has happened to improve the manufacturing process at this stage.
Sort and place connectors FQP.P5.c	Check that the disposition of the connectors with the frame plan. Check that distances between lines are the same as the frame plan TEST & MESUREMENTS: It was done.	a. Install again b. In case distances are not ok find the correct connector to be installed by checking it is identification number.

This project has received funding from the European Union's Horizon 2020 research and innovation programme under grant agreement No 958218

	Interferences with the load window down were discovered, due to the mistake of having mirror components design (see point FQP.P1.c) IMPROVEMENTS: Need. Apply correction action in DQP.P1.c)	c. In case does not exist go to phase 1. d. Investigate how mistake has happened to improve the manufacturing process at this stage.
Attach connectors FQP.P5.d	Every union between line and connector must touch to ensure the union is finish. TEST & MESUREMENTS: It was done. Interferences with the load window down were discovered, due to the mistake of having mirror components design (see point FQP.P1.c) IMPROVEMENTS: Need. Apply correction action in DQP.P1.c)	a. In case connector cannot be installed due to some interference go to phase 1 to modify the component that causes the interference. b. Investigate how mistake has happened to improve the manufacturing process at this stage.
Install load guides FQP.P5.e	Check the screws are firmly installed TEST & MESUREMENTS: It was done. IMPROVEMENTS: No need. Check the load guide is well oriented to the back façade TEST & MESUREMENTS: It was done. IMPROVEMENTS: No need.	a. Follow the same remedial procedure as per FQP.P5.b
Install load windows FQP.P5. f	Check the screws are firmly installed TEST & MESUREMENTS: It was done. IMPROVEMENTS: No need. Check the load window is well oriented to the back façade TEST & MESUREMENTS: It was done. Same problem as described in FSP.P1.c) were found. IMPROVEMENTS: Need. Apply correction action in DQP.P1.c)	a. Follow the same remedial procedure as per FQP.P5.b
Install insulation knives FQP.P5. g	Check the screws are firmly installed TEST & MESUREMENTS: It was done. IMPROVEMENTS: No need. Check the knives situation is the same as the frame plan TEST & MESUREMENTS: It was done. IMPROVEMENTS: No need.	a. Follow the same remedial procedure as per FQP.P5.b
Install insulation layer FQP.P5. h	Check that the perimeter of the isolation fits with the perimeter of the lines like is drawn in the frame plane. TEST & MESUREMENTS: It was done. The effects of the problems described in FQP.P4.b were seen in here. The perimeter of the isolation layer was too larger from the frame dimensions.	a. Follow the same remedial procedure as per FQP.P5.b

This project has received funding from the European Union's Horizon 2020 research and innovation programme under grant agreement No 958218

	IMPROVEMENTS: Need. Described in FQP.P4.b	

TABLE 14: FRAME ASSEMBLY (VISUAL INSPECTION - TABLE II).

F.Q.P	Inspection Task	Remedial action
Frame rotation FQP.P5. i	Check the strap is well fixed. TEST & MESUREMENTS: It was done. IMPROVEMENTS: No need. Take out the easels before moving the frame. TEST & MESUREMENTS: It was done. IMPROVEMENTS: No need. Before removing the strap, check that the frame is well attached to the vertical installation support. TEST & MESUREMENTS: It was done. IMPROVEMENTS: No need.	a. Do again the process with the correct protocol.
Install window temporal anchors FQP.P5. j	Check the number and positions of the installed anchors with the frame plan. TEST & MESUREMENTS: It was done. This operation was not acceptable. The window frame was too weak to keep their geometry with no deformations. It was supposed that the attachment of the window in its interior would fix the problem, but it did not. At this point was stated to see that the windows frame would not work. IMPROVEMENTS: No need. A new strategy for installing the window was decided to be done. It was defined to finish the mockup anyway to complete the installation of the full prototype. New design has been done and will be tested and beginning of October. **(See attached plans for new mock design)** Check that the screw over the nut has at least 2 mm left. TEST & MESUREMENTS: It was done. IMPROVEMENTS: No need.	a. Follow the same remedial procedure as per FQP.P5.b
Install window assembly C (Assembly described in table C)	Check the nuts of al the temporal Anchors are installed. No torque is required but there no must be space between the nut and the window frame anchoring point of connection to the	a. Follow the same remedial procedure as per FQP.P5.b

This project has received funding from the European Union's Horizon 2020 research and innovation programme under grant agreement No 958218

FQP.P5. k	temporal anchor. TEST & MESUREMENTS: It was done. As described in point before it was a fail operation. Window could be inserted in the windows frame but the fitting between both were bad an nonacceptable. IMPROVEMENTS: Need. As described in point before. Check the position of the window is the closest to the lines to reduce the thickness of the frame during its factory storage and later transportation. TEST & MESUREMENTS: It was done. In spite the bad assembly / fitting between windows and windows frame, the position of the window using the temporal anchors worked as expected. IMPROVEMENTS: No need.	
Install the louver rail and wheels in the window loads top and down area FQP.P5. l	Check all required attachment points are placed. TEST & MESUREMENTS: It was done. IMPROVEMENTS: No need. No torque is required but there no must be space between the nut and the window load line anchoring points of connection to the temporal anchor. TEST & MESUREMENTS: It was done. IMPROVEMENTS: No need.	a. Follow the same remedial procedure as per FQP.P5.b
Install Plural lov 1480 lines (assembly D) + louver rail and wheels FQP.P5. m	Check all required attachment points are installed. TEST & MESUREMENTS: It was done. IMPROVEMENTS: No need. Check that the nuts between the lover rail and the 1480 down had been placed. TEST & MESUREMENTS: It was done. IMPROVEMENTS: No need. Check the wheels move easily with no interruptions. TEST & MESUREMENTS: It was done. Critical. The movement of the Lov 1480 tiles had bad feeling. In fact it was done just to present the system to get more and real information about all the Louvers movement new system. IMPROVEMENTS: Need. New definition of the movements' requirements which	a. Follow the same remedial procedure as per FQP.P5.b

This project has received funding from the European Union's Horizon 2020 research and innovation programme under grant agreement No 958218

	implies to eliminate the down louver rail, and which modified the system to move the louvers. New design has been developed and will be tested in a new renovation mockup.	
Install UV temporal anchor FQP.P5.m	Check the screws are firmly installed TEST & MESUREMENTS: It was done. IMPROVEMENTS: No need.	a. Follow the same remedial procedure as per FQP.P5.b
Install UV FQP.P5. n	Check the screws are firmly installed. TEST & MESUREMENTS: It was done. IMPROVEMENTS: No need.	a. Follow the same remedial procedure as per FQP.P5.b
Install PV anchors to the Lines FQP.P5. o	Check that there is no space between the nut cartela and the lines point of connection. TEST & MESUREMENTS: It was done. IMPROVEMENTS: No need.	a. Follow the same remedial procedure as per FQP.P5.b
Install PV tiles FQP.P5. p	Check all the PV tiles of the frame plane has been installed TEST & MESUREMENTS: It was done. IMPROVEMENTS: No need. Check the special washer has been well installed. TEST & MESUREMENTS: It was done. IMPROVEMENTS: No need. Check that there is no space between the nut cartela and the PV tiles point of connection. TEST & MESUREMENTS: It was done. IMPROVEMENTS: No need.	a. Follow the same remedial procedure as per FQP.P5.b
Connect PV tiles FQP.P5.q	Check that all the connections of the frame plane has been connected. TEST & MESUREMENTS: It was done. IMPROVEMENTS: No need.	a. Follow the same remedial procedure as per FQP.P5.b
Install final tiles cladding FQP.P5. r	Check that the disposition and colors of the tiles frames is the same detailed on the frame plane. TEST & MESUREMENTS: It was done. IMPROVEMENTS: No need. Check all pieces are horizontal aligned, which means all of them have been inserted correctly to the connectors. TEST & MESUREMENTS: It was done. IMPROVEMENTS: No need.	a. Follow the same remedial procedure as per FQP.P5.b

This project has received funding from the European Union's Horizon 2020 research and innovation programme under grant agreement No 958218

3.4.1.6 Phase 6: Frame storage

Due to the amount of necessary FQP during the assemblies of the frames, it has been decided to present them sorted for each task and follows the Frame Assembly diagram presented at section 4.3 of this deliverable.

TABLE 15: FRAME STORAGE VISUAL INSPECTION TABLE

F.Q.P	Inspection Task	Remedial action
FQP.P6.a	Check that the exo-palleted frame is firmly attached to the transportation pallet. TEST & MESUREMENTS: It was done. IMPROVEMENTS: No need.	a. Do again the process with the correct protocol.
FQP.P6.b	Visual inspection for all components for damages, scratches any other possible visually observed defects. TEST & MESUREMENTS: It was done. IMPROVEMENTS: No need.	a. Go to phase 1 to define a new frame manufacturing process. b. Investigate how mistake has happened to improve the manufacturing process at this stage.
FQP.P6.c	Check that the order of the frames store corresponds to the installation plan. TEST & MESUREMENTS: It was done. IMPROVEMENTS: No need.	a. Do again the process with the correct protocol.

3.4.1.7 Phase 7: Support preparation

TABLE 16: SUPPORT PREPARATION VISUAL INSPECTION TABLE.

F.Q.P	Inspection Task	Remedial action
FQP.P7.a	Check the real position of the holes to see if they have been done under the tolerances. TEST & MESUREMENTS: It was done. IMPROVEMENTS: No need.	a. Do again the process with the correct protocol.
FQP.P7.b	Check the screws are firmly installed. TEST & MESUREMENTS: It was done. IMPROVEMENTS: No need.	a. Do again the process with the correct protocol. b. In case not possible go to Phase 1 to define new anchoring solution.

3.4.1.8 Phase 8: Installation

TABLE 17: INSTALLATION VISUAL INSPECTION TABLE.

F.Q.P	Inspection Task	Remedial action

This project has received funding from the European Union's Horizon 2020 research and innovation programme under grant agreement No 958218

FQP.P8.a Frame / sequence generation	Check the pallet and frames in relation of the installing frame plane. TEST & MESUREMENTS: It was done. IMPROVEMENTS: No need. Check that the screws are firmly installed. Every hinge has 3 rivets, and every line has a hinge, all of them must be perfectly linked. TEST & MESUREMENTS: It was done. IMPROVEMENTS: No need. While the sequence is being generated check that the joins between the insulation of the frames fits. TEST & MESUREMENTS: It was done. IMPROVEMENTS: No need.	a. Follow the same remedial procedure as per FQP.P5.b
FQP.P8.b Attach sequence to load anchors	Move the sequence slowly to prevent crashes against the façade or the scaffold lift. TEST & MESUREMENTS: It was done. IMPROVEMENTS: No need. Check the screws are firmly installed. TEST & MESUREMENTS: It was done. IMPROVEMENTS: No need.	a. Follow the same remedial procedure as per FQP.P5.b
FQP.P8.c Wind anchors installing	Check that the position of the anchors corresponds with the detailed project. TEST & MESUREMENTS: It was done. IMPROVEMENTS: No need. Check the final separation between façade and line is correct or under tolerances. TEST & MESUREMENTS: It was done. IMPROVEMENTS: No need.	a. Follow the same remedial procedure as per FQP.P7a and FQP.P7b
FQP.P8.d Window installation	Check the level of the window is perfect and works ok. TEST & MESUREMENTS: It was done. IMPROVEMENTS: No need. Temporal anchor are removed. TEST & MESUREMENTS: It was done. IMPROVEMENTS: No need. Check the insulation is covering all spaces without leaving thermal bridges. TEST & MESUREMENTS: It was done. The window frame did not work, and after installation, gaps and thermal bridges appear. IMPROVEMENTS: Need. Redefining this operation. Work done in new details	a. Do again the process with the correct protocol.

This project has received funding from the European Union's Horizon 2020 research and innovation programme under grant agreement No 958218

	done	
FQP.P8.e Installation of window perimetral finishes	Check there is space to have access to Unit Ventilation Filters TEST & MESUREMENTS: It was done. IMPROVEMENTS: No need. Check all pieces fits with the window frame attachment holes TEST & MESUREMENTS: It was done. In spite all window peripheral components were successfully installed, a problem occurred with the resistance and sound feeling of the component nº 35 PLURAL WFI 1470.150 DOWN. Besides it was found that the designed system had no tolerances in case that initial façade measurements had small mistakes. IMPROVEMENTS: Need. Even because the window frame has been eliminating all the perimetral finishing needs a new attachment system. This new design also must resolve to do a reinforcement design for 35 PLURAL WFI 1470.150 DOWN. This new design has been done in the new update mock up design.	a. Do again the process with the correct protocol.
FQP.P8.f Unit ventilation installation	Check the insulation is covering all spaces without leaving thermal bridges. TEST & MESUREMENTS: It was done. IMPROVEMENTS: No need. Check filters can be removed. TEST & MESUREMENTS: It was done. IMPROVEMENTS: No need. Connect the unit ventilation and check it works and don't produce noise due to possible contacts the Denvelops system TEST & MESUREMENTS: Not possible to do because the received UV was a dummy only to check dimensions. IMPROVEMENTS: Will be defined when real connection will be able to be done.	a. Do again the process with the correct protocol.
FQP.P8.g Installation PV tiles	Check the installation plan TEST & MESUREMENTS: It was done. IMPROVEMENTS: No need. Do an electrical test to see everything is connected. TEST & MESUREMENTS: It was done. Critical	a. Do again the process with the correct protocol.

This project has received funding from the European Union's Horizon 2020 research and innovation programme under grant agreement No 958218

	IMPROVEMENTS: No need.	
FQP.P8.h Insulation fitting	Check the joins of the insulation between panels are aligned and has good fitting. TEST & MESUREMENTS: It was done. The first result was not ok. The developed process to finish the isolation installation showed that the contact between the surfaces of the wall and the isolation was not 100% contacting. Trying to solve the problem a new process was discovered by using the same isolation knifes. IMPROVEMENTS: No need. Modify the description process for the installation of the isolation Hybrid wall layer.	a. Do again the process with the correct protocol.

3.4.2 Mechanical tests

Mechanical tests present the work and actions that complements the visual inspection in deeply way in order to achieve at better quality standards. Mechanical tests could had been described in the previous section, as they were performed at the same time, however, it is interesting to describe them in a separated section, to give better detailed description and clear understanding. To describe it has been used again, the same structure of sections and codification of the visual inspection tables.

3.4.2.1 Phase 1: Detailed design

In Detailed design phase there are no mechanical tests required.

3.4.2.2 Phase 2: Provision

In Provision phase there are no mechanical tests required.

3.4.2.3 Phase 3: Components storage

In the Components storage phase, there are some mechanical tests to be done. They are related to check, in a statistic way, the quality of the components that arrive to the factory for them storage.

TABLE 18: COMPONENTS STORAGE MECHANICAL TEST TABLE.

F.Q.P	Inspection Task	Remedial action
FQP.P3.d	**WINDOW:** 100% of units must be inspected. **Inspection task:** • Doors movement. • Handle • Lock	WINDOWS: a. Evaluate the type of malfunction. b. Contact to provider to find out solution. Decide if it can be repaired in Denvelops or must be sent again to the provider.

This project has received funding from the European Union's Horizon 2020 research and innovation programme under grant agreement No 958218

	UNIT VENTILATION: 100% of units must be inspected. **Inspection task:** • Connect them and switch on. • Check for strange function • Check air flows	UNIT VENTILATION a. Evaluate the type of malfunction. b. Contact to provider to find out solution. Decide if it can be repaired in Denvelops or must be sent again to the provider.
	PHOTOVOLTAIC TILES: 10% of units must be inspected. **Inspection task:** • Connect them and check electric current circuit can be closed and makes energy under the sun.	PHOTOVOLTAICS TILES a. Evaluate the type of malfunction. b. Contact to provider to find out solution. Decide if it can be repaired in Denvelops or must be sent again to the provider.

3.4.2.4 Phase 4: Production Processes

TABLE 19: COMPONENTS STORAGE MECHANICAL TEST TABLE.

Processes F.Q.P	Inspection Task	Remedial action
FQP.P5. l FQP.P5. m	**LOUVERS:** 100% of units must be inspected. **Inspection task:** • Louvers movement. • Handle • Lock	LOUVERS: a. Evaluate the type of malfunction. b. repair it. c. In case of need some components replacement go to Phase 2.

3.4.2.5 Phase 6: Frame storage

In Provision phase there are no mechanical test required.

3.4.2.6 Phase 7: Support preparation

TABLE 20: COMPONENTS STORAGE MECHANICAL TEST TABLE.

Processes F.Q.P	Inspection Task	Remedial action
FQP.P7.b	**LOAD AND WIND ANCHORS:** 1 UT units must be inspected: **Inspection task:** • Load extraction test	LOAD AND WIND ANCHORS: a. Evaluate the type of malfunction. b. Repeat test with another screw type c. Redesign anchors with more anchoring screws to reduce the load demand for each screw.

This project has received funding from the European Union's Horizon 2020 research and innovation programme under grant agreement No 958218

3.4.2.7 Phase 8: Installation

TABLE 21: COMPONENTS STORAGE MECHANICAL TEST TABLE

Processes F.Q.P	Inspection Task	Remedial action
FQP.P8.d Window installation	**WINDOW:** 100% of units must be inspected. **Inspection task:** • Doors movement. • Handle • Lock	WINDOWS: b. Evaluate the type of malfunction. c. Contact to provider to find out solution. Decide if it can be repaired in Denvelops or must be send again to the provider.
FQP.P8.f Unit ventilation installation	**UNIT VENTILATION:** 100% of units must be inspected. **Inspection task:** • Connect them and switch on. • Check for strange function Check air flows	UNIT VENTILATION a. Evaluate the type of malfunction. b. Contact to provider to find out solution. Decide if it can be repaired in Denvelops or must be send again to the provider.
FQP.P8.g Installation PV tiles	**PHOTOVOLTAIC TILES:** 10% of units must be inspected. **Inspection task:** • Connect them and check electric current circuit can be closed and makes energy at the final stage of the system.	PHOTOVOLTAICS TILES a. Evaluate the type of malfunction. b. Contact to provider to find out solution. Decide if it can be repaired in Denvelops or must be sent again to the provider.

3.4.3 IR thermography

Due to the characteristics developed for the eAHC/HybridWall, it was decided that the thermal test would not be done at the prototype stage for the following reasons:

- The solution has been thought in terms of layers, with the main innovation that no peripheral steel frame is required. One of the advantages of this design is that it avoids in a clear and objective way thermal bridges.
- Instead of doing a real thermography, it was proposed to do a simulation study. This simulation was specially focused on the thermal bridges that the Ventilation Unit (eAHC) can produce
- The developed prototype was not installed in a closed room satisfying the requirements of thermography test As alternative was proposed; to do a real thermography test once the PnU will be installed on the real demo site.

This project has received funding from the European Union's Horizon 2020 research and innovation programme under grant agreement No 958218

4 Mechanical Performance

4.1 SmartWall

A real-scale steel frame structure with brick masonry infill wall fitted with Core System 1 ("SmartWall") was experimentally investigated by means of shaking table tests, allowing for proper validation of the structural response under different earthquake tests. The SmartWall was assumed to behave as a non-structural component, while the brick wall was its supporting structure. The SmartWall was fixed to the brick wall using Z-shape steel plates (hanging brackets) at three positions through its height. Additionally, it was anchored to the brick wall with two chemical anchors at the top, to ensure no vertical and in-plane movements of the module independent of the infill wall during earthquake. Thus, the SmartWall is considered acceleration-sensitive non-structural component and damage could occur from inertial forces. The Floor Response Spectrum (FRS) method is used for the analysis of SmartWall. The FRS was calculated for PGA equal to 0.36g and EC8 soil category B[1] for the two horizontal directions, resulting in a 0.86g peak floor acceleration. The vertical component spectrum was set equal to 0.80 of the horizontal ones. Compatible floor acceleration time histories were generated and used as the input motion. The characteristic periods of the FRS were chosen to cover floor spectra for buildings with 1 to 10 stories and the non-structural component assumed to be located at the upper floor (roof). This spectrum was considered as the Required Floor Response Spectrum (RFRS) for the present study. Peak ground acceleration (PGA) of 0.36g (highest seismic zone for Greece) and soil category B according to EC8 were chosen. The acceleration time histories used as base motion were modified from the Landers earthquake that occurred on June 28, 1992 near the town Landers of California, in order to be compatible with the RFRS.

The specimen was subjected to triaxial ground motion time history with base acceleration increased stepwise corresponding to the different limit states, in order to investigate the response of SmartWall. Prior and after the execution of the shaking table tests, the dynamic properties of the specimen were measured through logarithmic sine sweep excitation along the X, Y and Z main axes.

The following testing programme was executed:

- Step 1: Preliminary sine sweep tests in order to determine the natural frequencies and damping characteristics of the specimen (SmartWall and its supporting structure).
- Step 2: Calculation of Required Floor Response Spectrum (RFRS) for experimental study. Generation of acceleration time histories along X, Y and Z directions to match the RFRS.
- Step 3: A series of triaxial ground motion time histories with increased base acceleration corresponding to different limit states to examine the behaviour of the specimen to floor motions.
- Step 4: Repetition of Step 1 to assess the dynamic characteristics of the specimen after earthquake excitations.

[1] CEN, EN 1998-1 (2004) (English): Eurocode 8: Design of structures for earthquake resistance – Part 1: General rules, seismic actions and rules for buildings, EC8.

This project has received funding from the European Union's Horizon 2020 research and innovation programme under grant agreement No 958218

The specimen was tested at the Laboratory for Earthquake Engineering (LEE) of the National University of Athens (NTUA), using the shaking table facility. The main experimental results are presented in this report.

4.1.1 Specimen

The specimen was a full-scale one-story steel 3D frame, with one bay of 1.97m span along X direction and one bay of 3.30m span along Y direction (Figure 12). The storey height was equal to 3.20m. The floor plan and elevations are shown in Figure 12 (middle and right). The column and beam cross sections were RHS 120.120.5. Bolted connection was used for beams to columns joints (Figure 13a) along X direction, while in Y directions the members were welded (Figure 13b). Steel X braces of L60.60.6 cross section (Figure 13c) with mid-connection, were also added to the three external frames, while a brick masonry wall was constructed in the front X-Z frame. The infilled wall was fitted with Core System 1 ("SmartWall").

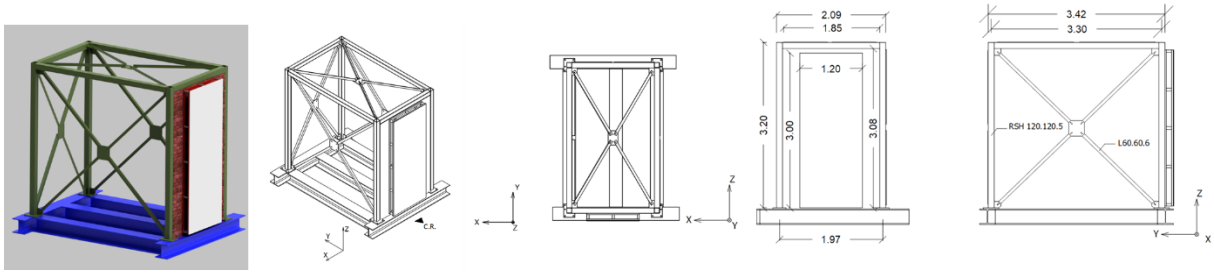

FIGURE 12: STEEL FRAME - INFILLED WALL FITTED WITH SMARTWALL AND PLAN VIEW OF SPECIMEN AND ELEVATIONS Z-X AND Z-Y.

FIGURE 13: A) BEAM TO COLUMN BOLTED CONNECTION; B): WELDED BEAM TO COLUMN JOINTS AND C) MID-HEIGHT CONNECTION OF X-BRACES.

The masonry infill wall was constructed with 12-hole brick clay units with dimensions 9x12x19cm^3 and mortar with compressive strength of 5MPa. The compressive strength of bricks was estimated at 5.5MPa. The infill wall had a height of 3.08m, length of 1.85 and thickness of 0.12m. The mortar joint thickness was approximately 10mm. The wall was reinforced every three layers. The bed joint reinforcement consisted of steel wires which were anchored to the surrounding steel columns. Special care was taken during the construction of the last layer of the wall in order to avoid any detachment between wall and bounding steel beam of frame (Figure 14).

This project has received funding from the European Union's Horizon 2020 research and innovation programme under grant agreement No 958218

FIGURE 14: BRICK WALL

The dimensions of the panel of the SmartWall were 1.20m (length) x 0.130m (width), while its height was 3.00m. The two steel frames of the SmartWall are made of hollow structural steel members (50 x 30 x 1.8 mm), connected using antivibration mounts.

The SmartWall was anchored to the brick wall using two chemical anchors, as shown in Figure 15 and Figure 16. Additionally, the SmartWall was attached to the wall at three positions along the module's height using Z-shape plates with dimensions 1200 x 80 x 5 mm (Figure 17). At each position, one z-shape plate was fixed on the brick wall using four chemical anchors, while another one was welded to the inner SmartWall steel frame (Figure 15 and Figure 17). The SmartWall placed onto the steel base with four supports (hollow section of 50 x 30 x 2 mm).

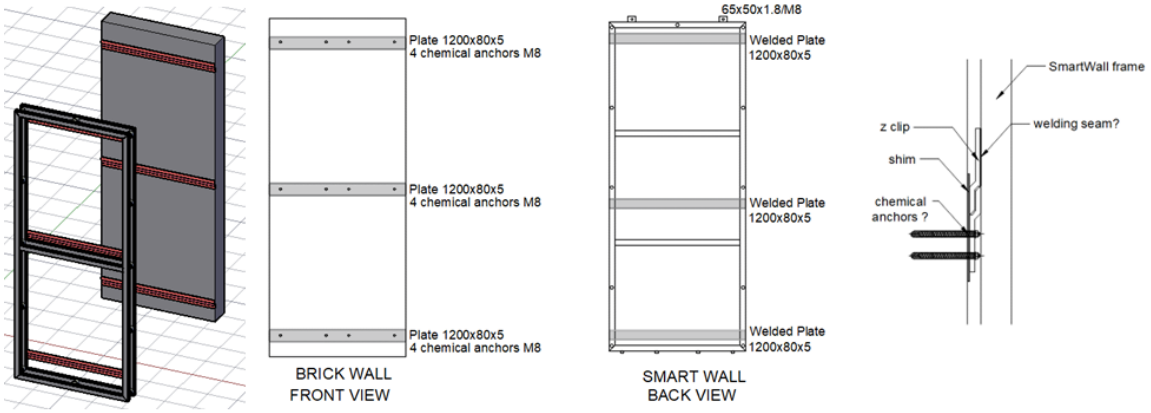

FIGURE 15: CONNECTION BETWEEN SMARTWALL AND INFILL WALL: 3D MODEL, DRAWINGS AND DETAIL.

FIGURE 16: FIXING SMARTWALL TO BRICK WALL- TOP ANCHORS.

This project has received funding from the European Union's Horizon 2020 research and innovation programme under grant agreement No 958218

FIGURE 17: FIXING SMARTWALL TO BRICK WALL- Z CLIPS.

4.1.2 Experimental and Instrumentation set-up

The experimental setup is shown in Figure 18. The specimen was mounted (base of columns) on a steel adaptor base that was installed onto the shaking table, using an adapter plate and six M20 8.8 bolts. The steel base was securely fixed to the shaking table with M30 bolts. The orientation of the specimen with respect to the main axes of the shaking table is also shown in Figure 12.

FIGURE 18: EXPERIMENTAL SET-UP

The instrumentation used in the shaking table experiments was organised to measure the accelerations along X, Y and Z directions at different positions along the heigh of brick wall and SmartWall. The instrumentation set-up is depicted in Figure 19. Accelerometers A1 and A3 were placed at the outer frame of SmartWall at the middle and at the end level of wall respectively. Accelerometers A2 and A4, were placed at the inner frame of SmartWall, at the same heights as A1 and A3. Accelerometers A5 to A7 were measured the acceleration on the brick wall. The accelerations and displacements of the shaking table were also recorded during each test. Photographs with the sensor positions are presented in Annex I.

This project has received funding from the European Union's Horizon 2020 research and innovation programme under grant agreement No 958218

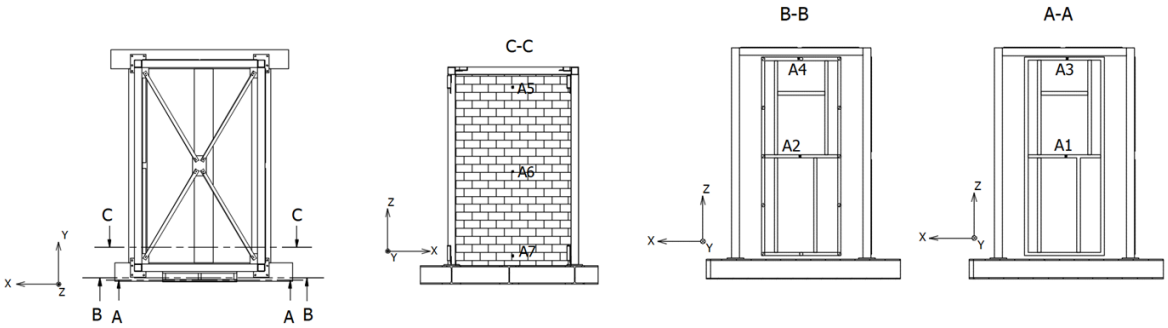

FIGURE 19: INSTRUMENTATION SET-UP: ACCELEROMETERS

4.1.3 Floor Response Spectrum

The Floor Response Spectrum (FRS) for damping ζ=5% is defined according to the following equations in the time domain[2]:

$$S_{\mathrm{Fa}} = a \cdot S \cdot g \cdot (1 + \mathrm{z/H}) \cdot \left[\frac{\alpha_p}{1 + (\alpha_p - 1) \cdot (1 - \mathrm{T}/\alpha \cdot T_1)^2}\right] \geq \mathrm{a} \cdot S \cdot \mathrm{g} \qquad \mathrm{T} < \alpha \cdot T_1$$

$$S_{\mathrm{Fa}} = a \cdot S \cdot g \cdot (1 + \mathrm{z/H}) \cdot \alpha_p \qquad \alpha \cdot T_1 \leq T < b \cdot T_1$$

$$S_{\mathrm{Fa}} = a \cdot S \cdot g \cdot (1 + \mathrm{z/H}) \cdot \left[\frac{\alpha_p}{1 + (\alpha_p - 1) \cdot (1 - \mathrm{T}/\mathrm{b} \cdot T_1)^2}\right] \geq \mathrm{a} \cdot S \cdot \mathrm{g} \qquad \mathrm{T} > b \cdot T_1$$

where a is the ratio between the PGA on soil category A and the gravity acceleration; S is the soil amplification factor; T_1 is the fundamental period of structure and z/H is the relative structural height at which the non-structural component is placed and T is the non-structural component period. The coefficients α, b and α_p are given in Table 22. For the aims of the PLURAL project, the SmartWall is assumed to be installed in a residential reinforced concrete building of up to 10-story height. The fundamental frequency of this kind of building is estimated using the following empirical formula, which is derived from ambient vibration measurements on undamaged reinforced concrete buildings in Greece (apartments with constant stiffness)[3]:

$$\mathrm{T\ (sec)} = 0.032 \cdot N + 0.145$$

where N is the number of stories. The estimated fundamental periods for 1-, 2-, 3-, 5- and 10-story buildings are given in Table 23.

TABLE 22: VALUES FOR PARAMETERS A, B, A_p.

Number of stories	α	b	α_p
T1<0.5sec	0.8	1.4	5.0
0.5sec<T1<1.0sec	0.3	1.2	4.0
T1>1.0sec	0.3	1.0	2.5

[2] C. Petrone, G. Magliulo, G. Manfredi, "Seismic demand on light acceleration-sensitive non-structural components in European reinforced concrete buildings", Earthquake Engineering and Structural Dynamics, 44:1203–1217, 2015.
[3] P. Carydis, H. Mouzakis, "Small Amplitude Vibration measurements of buildings undamaged, and Repaired after earthquake", Earthquake Spectra 2(3), 1986.

This project has received funding from the European Union's Horizon 2020 research and innovation programme under grant agreement No 958218

TABLE 23: FUNDAMENTAL FREQUENCIES OF RESIDENTIAL BUILDINGS

Number of stories	Fundamental period (sec)
1	0.08
2	0.209
3	0.241
5	0.305
10	0.465
1	0.08

For the present study, the parameter a was chosen as 0.36 (PGA/g), corresponding to the highest seismic zone in Greece, soil category B was considered with amplification factor S=1.20 and z/H equals 1.0. The coefficients α, b and αp were taken from Table 1 for fundamental period T less than 0.5sec.

The defined FRS for the above-mentioned parameters is shown in Figure 20a for 1-, 2-, 3-, 5- and 10-story buildings, while in Figure 20b, the envelope of all spectra is depicted. The envelope spectrum is used as the Required Floor Response Spectrum (RFRS) for seismic triaxial tests, in order to take into account that the SmartWall will be placed at the top (z/H=1) of buildings with 1 up to 10 stories. It is pointed out that soil category A and C are also covered by the defined FRS of Figure 18 for the same and lower levels of PGA, as the amplification factor is 1.0 and 1.15 for soil category A and C respectively. In vertical direction Z, the FRS is assumed equal to 80% of the FRS of horizontal directions (Figure 20c).

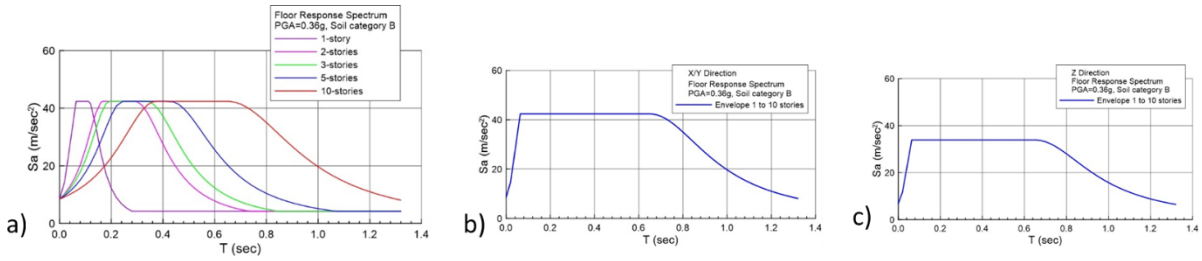

FIGURE 20: A) FLOOR RESPONSE SPECTRUM, B) FLOOR RESPONSE SPECTRUM IN X AND Y DIRECTION-ENVELOPE AND C) FLOOR RESPONSE SPECTRUM IN Z DIRECTION-ENVELOPE

4.1.4 Base motion

Three different acceleration time histories in X, Y and Z main axes, were generated to match the Required Floor Response Spectrum along X, Y and Z directions as defined in section 4.1.3. These acceleration time histories were modified from the Landers earthquake that occurred on June 28, 1992 near the town Landers of California, in order to be compatible with the FRS. The time histories were filtered with a high pass filter of 2Hz, to meet the stroke limitation of 100mm of the shaking table; consequently, spectrum matching was executed from 0 to 0.5 sec, in terms of periods (2.0Hz in frequency domain). As shown previously, this period covers the fundamental periods of residential reinforced concrete buildings up to 10 stories. The software SeismoSignal[4] and

[4] SeismoSignal "Earthquake Software for Signal Processing of Strong-Motion data", SeismoSoft.

This project has received funding from the European Union's Horizon 2020 research and innovation programme under grant agreement No 958218

SeismoMatch[5] were used. In Figure 21, the generated acceleration time history and the corresponding FRS are presented for X, Y and Z directions. The 90% and 150% of Required Floor Response Spectrum are also shown.

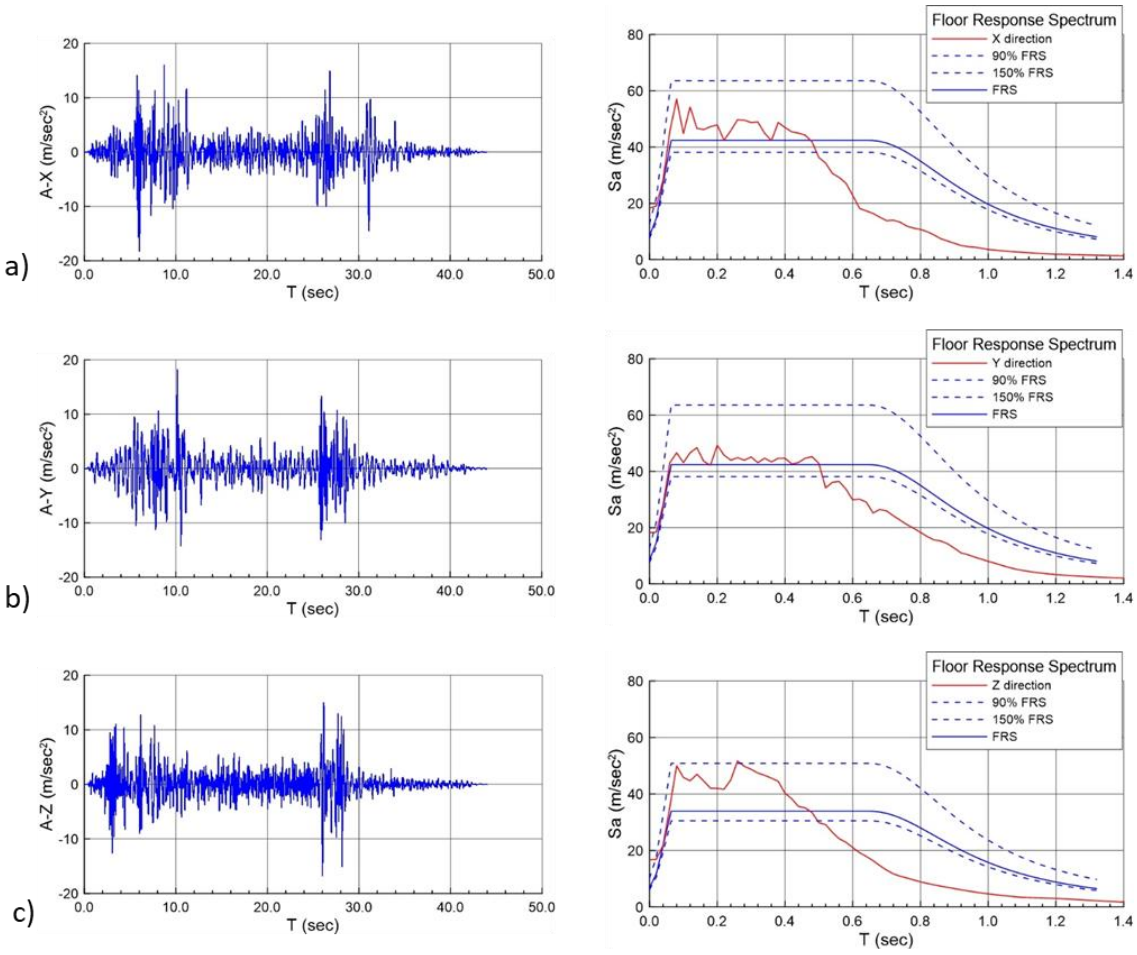

FIGURE 21: GENERATED ACCELERATION TIME HISTORY AND CORRESPONDING FLOOR RESPONSE SPECTRUM: A) X-DIRECTION, B) Y-DIRECTION AND C) Z-DIRECTION.

4.1.5 Experimental data

4.1.5.1 Test procedure

The specimen was tested on the shaking table under triaxial excitation in both horizontal X and Y and vertical Z directions. Five seismic tests were performed, with the base acceleration increased stepwise corresponding the different limit state earthquakes. Before and after the execution of all seismic tests, the dynamic properties of the specimen were measured through logarithmic sine sweep excitation along X, Y and Z main axes. The testing programme is shown in Table 24.

[5] SeismoMatch "Earthquake Software for Response Spectrum Matching", SeismoSoft.

This project has received funding from the European Union's Horizon 2020 research and innovation programme under grant agreement No 958218

TABLE 24: TESTING PROGRAMME

Test No	Direction	Excitation	Acceleration on table (g)
1	X	Sine sweep	0.05
2	Y	Sine sweep	0.05
3	Z	Sine sweep	0.05
4	XY/Z	Triaxial earthquake	0.82/0.66
5	XY/Z	Triaxial earthquake	1.03/0.82
6	XY/Z	Triaxial earthquake	1.23/0.98
7	XY/Z	Triaxial earthquake	1.55/1.24
8	XY/Z	Triaxial earthquake	1.84/1.47
9	X	Sine sweep	0.05
10	Y	Sine sweep	0.05
11	Z	Sine sweep	0.05

4.1.5.2 Dynamic characteristics- prior shaking table tests

Logarithmic sine sweep was performed prior to triaxial tests in order to determine the dynamic characteristics (natural frequencies and damping) of the specimen. These tests were performed separately along X, Y and Z directions. The frequency range was from 0.5 Hz to 35 Hz, at a rate of one octave per minute. Thus, the excitation frequency, f (in Hz), versus time, t (in sec), follows the expression:

$$f\,(Hz) = 0.50 \times 2^{t/60}$$

The amplitude of the excitation was small, equal to 0.50 m/sec^2 (0.05 g), in order to prevent the occurrence of any damage. The frequencies were determined from the recorded accelerations at points A1 to A6. The damping was calculated using the half power bandwidth method. In Table 25, the natural frequencies and the damping coefficients, prior shaking table tests of the specimen are given.

This project has received funding from the European Union's Horizon 2020 research and innovation programme under grant agreement No 958218

TABLE 25: DYNAMIC PROPERTIES PRIOR SHAKING TABLE TESTS

Position	Direction	Fundamental frequency [Hz]	Period [sec]	Damping ratio [%]
A1 SmartWall Outer frame	X Y Z	11.38 14.21/17.72/20.41 -	0.088 0.070/0.056/0.049 -	3.19 2.34/1.10/2.02 -
A2 SmartWall Inner frame	X Y Z	28.22 14.16/17.68/20.51 -	0.035 0.071/0.057/0.049 -	3.19 2.34/1.10/2.02 -
A3 SmartWall Outer frame	X Y Z	11.43 14.21, 17.72, 20.41 29.93	0.087 0.070/0.056/0.050 0.033	3.19 2.34/1.10/2.02 2.31
A4 SmartWall Inner frame	X Y Z	28.23 14.06/17.67/20.51 -	0.035 0.071/0.057/0.049 -	7.21 2.34/1.10/2.02 -
A5 Brick wall	X Y Z	28.23 14.06/17.67/20.51 -	0.035 0.071/0.057/0.049 -	7.21 2.34/1.10/2.02 -
A6 Brick wall	X Y Z	28.08 14.06/17.67/20.51 -	0.036 0.071/0.057/0.049 -	7.21 2.34/1.10/2.02 -

The Transfer functions (TRF) between base and recorded acceleration at points A1 to A6 are shown in Figure 22 and Figure 23, for sine sweep tests in X and Y direction. The fundamental frequency of the SmartWall and the brick wall was calculated as 11.38Hz and 28.28Hz, respectively, for sine sweep in X direction, while the corresponding damping ratio was estimated 3.19% for SmartWall and 7.21% for brick wall. In Y direction, three frequencies were found for the SmartWall, 14.21Hz, 17.72Hz and 20.41Hz. The first frequency corresponds to the steel frames with antivibration mounts, the second one to the connection between brick wall and SmartWall (also found using accelerometers on brick wall) and the third to the frame of the SmartWall. The damping ratio in Y direction ranges from 1% to 2.4%. In Z direction, the fundamental frequency of the SmartWall was 29.93Hz with damping ratio of 2.31%. No frequency up to 35Hz was found for the brick wall in Z direction.

This project has received funding from the European Union's Horizon 2020 research and innovation programme under grant agreement No 958218

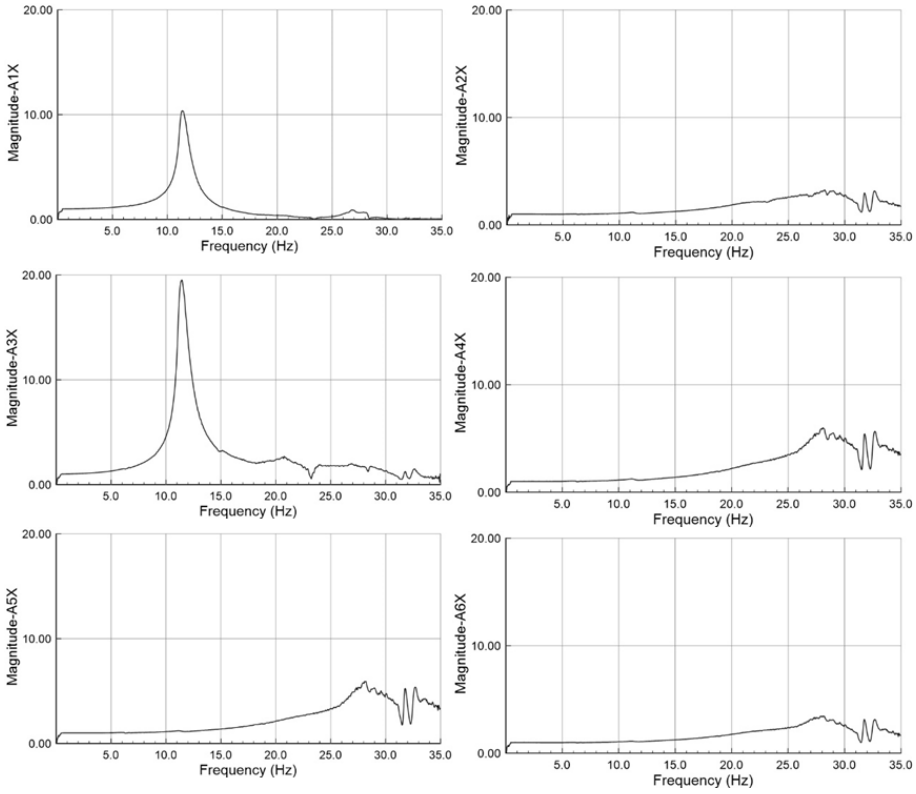

FIGURE 22: SINE SWEEP IN X DIRECTION PRIOR SEISMIC TESTS: TRANSFER FUNCTION AT MEASUREMENT POINTS A1 TO A6

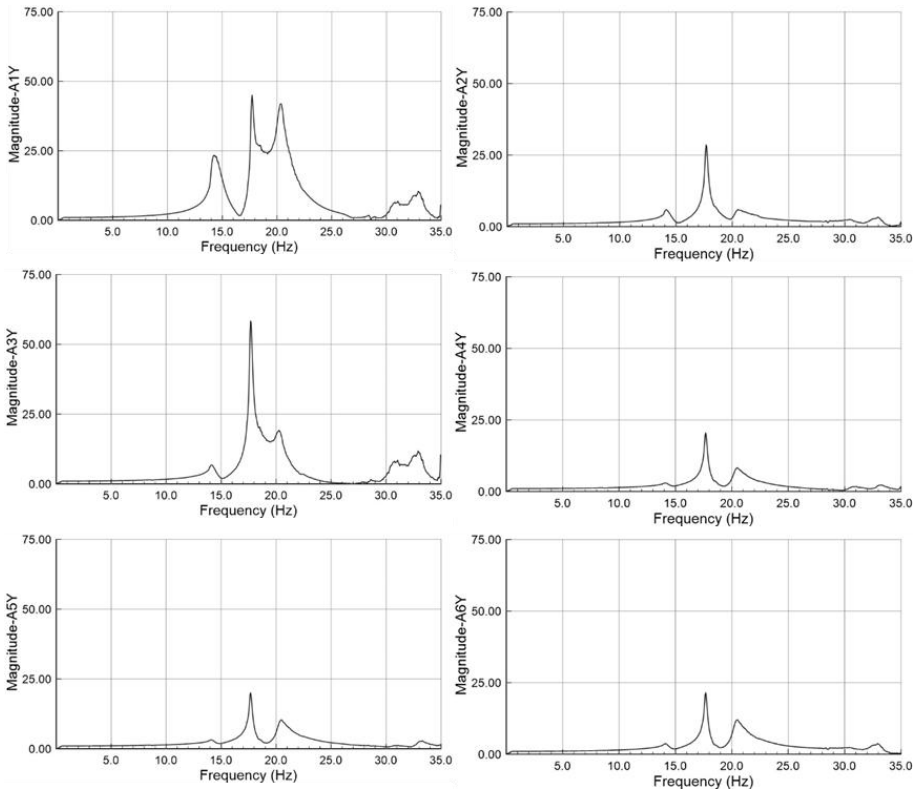

FIGURE 23: SINE SWEEP IN Y DIRECTION PRIOR SEISMIC TESTS: TRANSFER FUNCTION AT MEASUREMENT POINTS A1 TO A6

This project has received funding from the European Union's Horizon 2020 research and innovation programme under grant agreement No 958218

4.1.5.3 Triaxial time histories tests

A series of triaxial earthquake test in X, Y and Z global axes using the generated time histories was performed. The 100% of base motion corresponds to peak floor acceleration of 1.84g resulting from PGA equal to 0.36g and soil category B. The tests were run under acceleration control. The achieved shaking table accelerations along the main X, Y and Z directions are given in Table 26.

TABLE 26: TESTING PROGRAMME

Test No	Pga [g]	Scale [%]	Peak Floor Acceleration [g] (on shaking table)	
			Theoretical X-Y/Z	Achieved X/Y/Z
4	0.19	44	0.82/0.66	0.737/0.751/0.922
5	0.24	56	1.03/0.82	0.935/1.022/1.05
6	0.29	67	1.23/0.98	1.187/1.23/1.351
7	0.36	84	1.55/1.24	1.443/1.482/1.713
8	0.43	100	1.84/1.47	1.841/1.663/1.797

4.1.6 Results and conclusion

The detailed analysis of experimental data is presented in Annex I (section 11.2). From the experiments carried out on the full-scale, steel frame specimen with brick masonry infill wall fitted with Core System 1 ("SmartWall"), the following main conclusions can be derived:

- No visible damage was observed in steel members, brick wall and SmartWall during triaxial shaking table tests.
- For the SmartWall, frequencies and corresponding damping ratios were close to the dynamic characteristics before testing in both horizontal and vertical direction.
- For the brick wall, a reduction of frequency and an increase of damping ratio was found in X direction. This may be attributed to very light not visible damages, such as sliding along bed and head mortar joints, as well as sliding between the brick wall and surrounding steel frame.
- The design of steel frame infilled with brick masonry was found to be adequately stiff for the investigation of the seismic response of a non-structural acceleration-sensitive component, as the floor response spectrum was reproduced by the shaking table without any significant amplification.
- The selected method of fixing the SmartWall onto the brick wall with Z-shape plates was found adequate for the tested level of base motion.
- The two chemical anchors used at the top of the SmartWall could withstand the imposed inertial forces for the tested level of base acceleration.
- During the design process, additional checks related to the strength capacity of brick wall should be carried out in order to ensure that the brick wall is able to withstand the imposed inertial forces.
- For the verification test of an acceleration-sensitive non-structural component, the comparison between Test Response Spectrum and Required Floor Response Spectrum

This project has received funding from the European Union's Horizon 2020 research and innovation programme under grant agreement No 958218

could be done up to 1.4 times the highest period of non-structural component. Periods higher than this value do not affect the response of the component, when its response is linear or when slight inelastic behaviour could be exhibited. This recommendation is also proposed in other standards (as for example IEEE693), where the seismic design of equipment is examined.

4.2 eWHC / ConExWall

According to Eurocode 8: "Actions of structures for earthquake resistance - Part 1: General rules, seismic actions and rules for buildings", the Czech Republic is divided according to the map of seismic areas, depicted in Figure 24. A reference peak acceleration value a_{gR} is defined for individual areas. According to ČSN EN 1998-1, the significance of seismicity for a specific object is evaluated depending on:

- the reference peak acceleration value a_{gR}
- the ground type
- the building importance class

For the Kasava demo, the reference peak acceleration value is a_{gR} = 0.05g, the groun type is A, S=1,0 and the building importance is class II., γ_I= 1.0 These parameters indicates that there is very low seismicity at the Kasava demo ($a_{gR} \times S \times \gamma \leq 0{,}05$).

Thus, according to ČSN EN 1998-1, it is not necessary to assess the building in terms of seismic resistance. In the territory of the Czech Republic, most zones are rated as "very low seismicity". Another large zone is defined as low seismicity, where it is only necessary to observe the design rules according to ČSN EN 1998-1.

FIGURE 24: MAP OF SEISMIC AREAS OF CZECH REPUBLIC.

This project has received funding from the European Union's Horizon 2020 research and innovation programme under grant agreement No 958218

4.2.1 Design of anchoring system for the Kasava demo

The mechanical properties of connections and fixing for installation of eWHC PnU kit (ConnExWall) is assessed in relation to self-weight, wind and snow loads. It is proposed to anchor the ConnExWall panels on the existing load bearing walls using point steel anchors. Each anchor consists of a steel element and chemical anchors for masonry or concrete. The following basic parameters need to be taken into account for the design of panel anchors:

- Material of the main construction of panels and joints
- The material of the existing structure of the building into which it will be anchored

The ConExWall panels that are planned to be installed in Kasava demo building are designed as large-format wood-based panels. So, pressed structural joints of timber panel elements are statically more advantageous, while tensile joints are less advantageous.

An on-site survey was conducted on M18, revealing that the load-bearing walls of the building are made of solid ceramic bricks, while there are sandwich walls in the underground- inside solid bricks and outside stones. A total of 8 probes were installed as part of these works (Figure 25). Of this number, there were 3 probes for the purpose of determining the material characteristics of masonry (drilling holes in masonry 1.PP – SZ.01 to SZ.03, see Figure 26). The inner part is made of ceramic solid bricks on lime cement mortar, with total thickness 150-300mm. The outer part is faced with hack-lite stone masonry (sandstone).

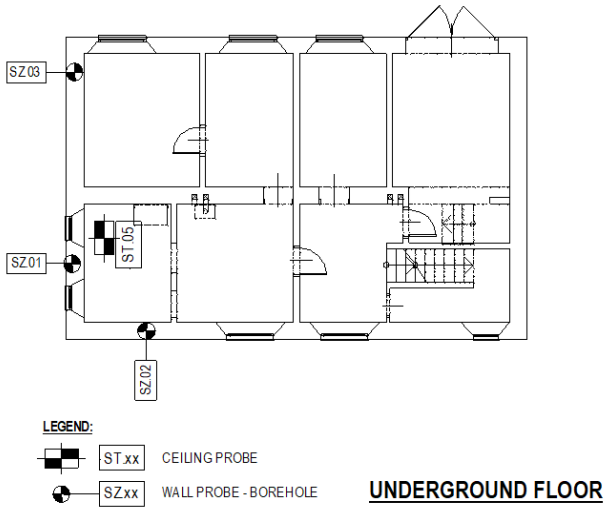

FIGURE 25: POSITIONS OF INDIVIDUAL PROBES UNDERGROUND FLOOR.

This project has received funding from the European Union's Horizon 2020 research and innovation programme under grant agreement No 958218

FIGURE 26: PROBES SZ.01, SZ.02, SZ.03

The analysis of elements follows the European Standards - Eurocodes and Czech adjustment ČSN EN. The requirements for mechanical resistance and stability must be met:

- existing structures of the building
- anchoring of panels
- panel construction

The general rules and the methodology used stay within standard of the Eurocodes (Basis of structural design and Czech adjustment ČSN EN (incl. National Annexes – ČSN EN 1990 NA, ed.A, 02/2021) dividing the loads into: permanent, variable and accidental loads. The expected load derived from

- self-weight of the panel
- wind load
- snow load (irrelevant for this case)
- Pre-stress axial load

The steel part of the anchor depends on the geometry of the panel. The size is chosen so that the panel can be supported and the steel part of the anchor is designed from a static point of view with a large margin. A critical part of the construction of the facade system is anchoring to the brick wall. The anchor must be able to withstand vertical V_{Sd} = 3.645 kN and horizontal loads (tension), N_{Sd} = 3.316 kN.

This project has received funding from the European Union's Horizon 2020 research and innovation programme under grant agreement No 958218

Figure 27 illustrates a scheme of the anchoring system that is designed for the installation ConnExWall on the Kasava demo building. The detailed calculations are presented in Annex II (see section 12).

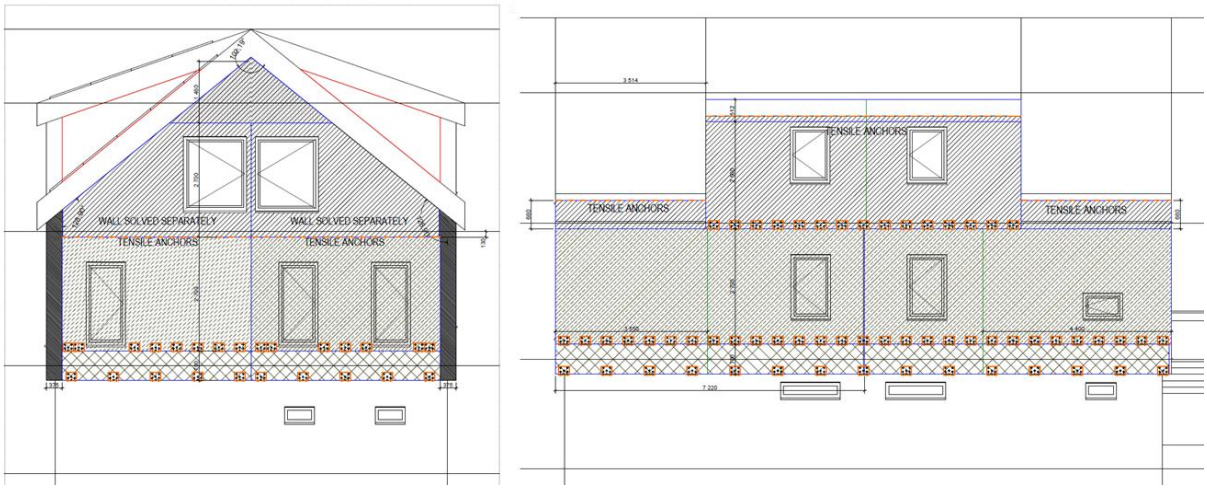

FIGURE 27: SCHEME OF THE ANCHORS. ELEVATIONS

4.2.2 Detection of possible deformation of ConExWall prototype during its installation in laboratory wall

A new part, however, is the anchoring system and the resulting horizontal forces on the façade elements. In order to detect possible deformation of the façade element while applying force to the module, two wires were tensioned like shown in Figure 28. One was stretched horizontally just below the window, the second vertically to the right of the window. Four measuring points were defined for each wire, at which the distance between the wire and the facade element was measured. Then all ten nuts (five on the top and five on the bottom) of the anchoring systems were tightened evenly piece by piece to push the element closer to the wall while measuring the wire distance at the defined points like seen in Figure 29. This was done until the flexible layer was compressed by 2 cm (from 5 cm to 3 cm width). The test was successful and no deformation of the facade could be detected (measurement resolution approx. 0.5 mm).

This project has received funding from the European Union's Horizon 2020 research and innovation programme under grant agreement No 958218

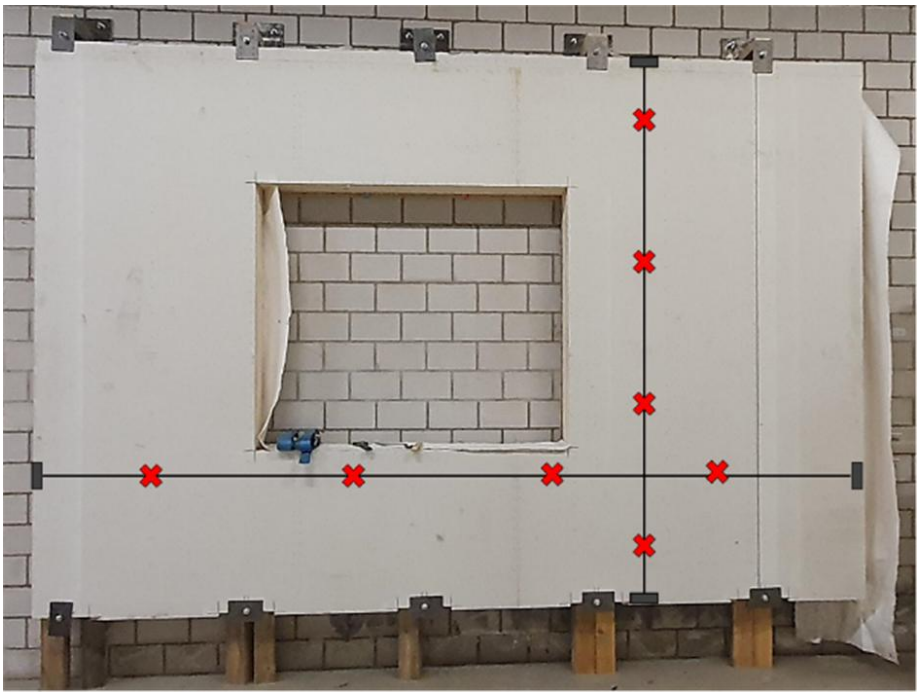

FIGURE 28: FAÇADE ELEMENT WITH SCHEMATIC WIRES ATTACHED. THE RED CROSSES INDICATE THE MEASURING POINTS, WHERE THE DISTANCE BETWEEN THE WIRE AND THE ELEMENT WERE DETERMINED. THE FLEXIBLE LAYER GETS COMPRESSED WHEN THE FIVE NUTS ON THE BOTTOM AND THE FIVE NUTS ON THE TOP ARE TIGHTENED, AND THEREFORE PUSH THE ELEMENT CLOSER TO THE WALL.

FIGURE 29: THE DISTANCE BETWEEN THE FAÇADE ELEMENT WAS MEASURED WITH A CARPENTER ANGLE TO INCREASE THE ACCURACY OF THE MEASURED POINTS. THE MEASUREMENT IS NECESSARY AS THE FLEXIBLE LAYER ON THE RIGHT GETS COMPRESSED WHEN THE MODULE IS INSTALLED. THIS RESULTS IN A HIGH FORCE ON THE COMPLETE MODULE THAT MAY CAN DEFORM IT.

Another test carried out with the façade element was the behaviour observation when there is an obstacle between the wall and the module. The obstacle seen in Figure 30 is a 2.5 cm thick board. Such big unevenness is usually removed on-site. Anyway, the test was done to get a general idea what happens when the PnU-Kit is mounted to an uneven wall.

This project has received funding from the European Union's Horizon 2020 research and innovation programme under grant agreement No 958218

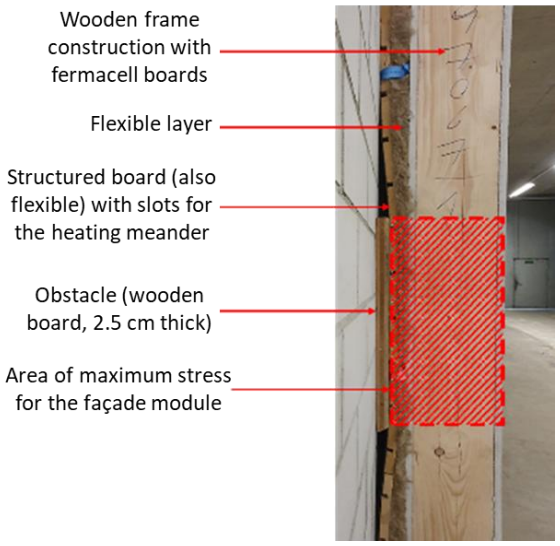

FIGURE 30: SIDE VIEW ON THE FAÇADE ELEMENT. AN OBSTACLE IS PUT BETWEEN WALL AND MODULE TO SEE ITS BEHAVIOR AND THE WORKING PRINCIPLE OF THE FLEXIBLE LAYER

Figure 30 shows the working principle of the flexible layer. The obstacle leads to a compression of 3.5 cm (from 5 cm to 1.5 cm). Thus, the stress on the module in this area is the highest. This could also be measured as the deformation of the module in the horizontal axis is 3 mm in this area (height of the module is 2.7 m). Due to the forces generated by the spring-like behaviour or of the flexible layer, the structured board with the included heating meander gets pushed back against the wall shortly below and above the obstacle as desired.

4.3 eAHC / HybridWall

A detailed analysis of the HybridWall PnU kits for the Terrassa demo building has been carried out. The calculations have been done using all the available data about the systems components, coming from:

- Standard calculations methods for structures as described in the mind Eurocodes and Spanish adjustment “Documento Básico de Seguridad Estructural” (CTE).
- Studies and calculation of components forces by using a finites elements simulations program.
- Recommendations and new criteria described in the new ETA certification. A process is now (December 2022) in the final stages.

For the certification, all required mechanical test on the system components were defined in order to confirm and calibrate that the standard calculations are reliable and don’t exceed from the limits of the real characteristics of the system. It should be clarified that final testing reports has not been completed. However, it has been consortium agreed that this task reporting will be attached to the task 6.2 (Assembly of the panel unit kits) since in this task another calculation revision will be done to define the Detailed Project Design.

The next sections describe the main calculations that were carried out for the analysis of mechanical performance and anchoring system of HybridWall, required for the Terrassa demo building.

This project has received funding from the European Union’s Horizon 2020 research and innovation programme under grant agreement No 958218

However, there is no requirement of seismic tests in accordance with the applicable Spanish regulations:

- NSCE-02: Norma de Construcción Sismorresistente (Seismic Resistance Construction Standard)
- CTE DB-SE: Código Técnico de la Edificación – Documento Básico de Seguridad Estructural (Building Technical Code – Basic Document of Structural Safety)

eAHC-HybridWall is considered, according to NSCE-02, as an add-on constructive element and, therefore, not part of the building structure. For such cladding systems, only the mechanical resistance of the connections between the add-on element and the building structure must be verified in front of the seismic actions.

Metallic anchoring is required and its fitness for use is justified by design, in accordance with the calculation procedures given in NSCE-02 and Eurocode 8, taking a seismic acceleration of 0.4g (as established for the area of Terrassa in accordance with NSCE02). Therefore, the technical justification is carried out by an adequate design of the anchors in relation to their mechanical resistance, considering the mode and vibrational frequency of the installed eAHC/HybridWall, and it is not necessary to carry out any additional test to characterize the system performance.

4.3.1 Methodology

The mechanical performance and anchoring system analysis is in accordance with Eurocodes and Spanish adjustment "Documento Básico de Seguridad Estructural" (CTE). The structure is a main facade. The loads consider rule it divides in: Permanents loads, variable loads and accidental loads. Specific weights of DB SE-AE "Seguridad Estructural - Acciones en la Edificación" (Eurocode 0) for permanent and variable loads are assumed. The accidental loads have not been taken into account, because the mesh is designed with left free degree. The mesh is calculated based on the following equation:

$$\sum_{j\geq 1} \gamma_{G,j} \cdot G_{k,j} + \gamma_{Q,1} \cdot Q_{k,1}$$

where $G_{k,j}$ is the characteristic value of the permanent action, $Q_{k,1}$ is the characteristic value of variable action and γ is the partial security factor, which is obtained from Table 27. The worst efforts from the combination of different hypothesis for sizing are considered.

TABLE 27: SECURITY FORCES FACTORS

Type of verification	Load type	Persistent or transient situation	
		Unfavorable	Favorable
Resistance	Permanent	1.35	0.80
	Variable	1.50	0
		Non stabilizing	Stabilizing
Stability	Permanent	1.1	0.9
	Variable	1.5	0

This project has received funding from the European Union's Horizon 2020 research and innovation programme under grant agreement No 958218

4.3.2 Actions to consider

The adapted actions will adjust to the prescribed in the DB SE-AE rule, are detailed below:

Self-weights

Stainless steel 79 kN/m³

Wind pressure

The wind load, q_e , is expressed by the equation:

$$q_e = q_b \cdot c_e \cdot c_p$$

where q_s is the wind dynamic pressure, c_e the exposure's factor and c_p the pressure's factor.

There are investigated two possible wind pressures:

- the middle of the mesh ($q_{e,m}$), applying the values of c_e=1.9 and c_p=0.8,
- the side of the mesh ($q_{e,s}$). applying the values of c_e=1.9 and c_p=1.2.

The level of wind pressure apply for the mesh will be:

$$q_{e,s} = 0{,}53\text{k}Pa \cdot 1{,}9 \cdot 1{,}2 = 1{,}20kPa$$

$$q_{e,m} = 0{,}53\text{k}Pa \cdot 1{,}9 \cdot 0{,}8 = 0{,}80kPa$$

4.3.3 Calculation bases

For the design of steel structures, the rules described in the Eurocode 3 and the DB-SE-EA are taken into account.

Design resistance

For Steel structures the following equation is applied:

$$f_{yd} = {f_y}/{\gamma_M}$$

where f_y is the characteristic value of the particular resistance determined with characteristic or nominal values for material properties and dimensions, and γ_M is the global partial factor for the particular resistance.

Tension

When the section is subjected to an axial force, $N_{t,Rd}$, it should be less than design plastic resistance, $N_{pl,Rd}$:

$$N_{t,Rd} \leq N_{Pl,Rd} = A \cdot f_{yd}$$

Shear

The design value of the shear force, V_{Ed}, at each cross section shall satisfy:

$$V_{pl,Rd} = A_v \cdot \frac{f_{yd}}{\sqrt{3}}$$

where A_v is the shear area.

This project has received funding from the European Union's Horizon 2020 research and innovation programme under grant agreement No 958218

Bending and axial force

For sections subjected to the combination of N_{Ed}, $M_{y,Ed}$ and $M_{z,Ed}$, the following criteria should be met:

$$\frac{N_{Ed}}{N_{Rd}} + \frac{M_{y,Ed}}{M_{y,Rdy}} + \frac{M_{zEd}}{M_{y,Rdz}} \leq 1$$

where N_{Rd}, $M_{y,Rd}$, and $M_{z,Rd,}$ are the design values of the resistance depending on the cross sectional classification, elastic or plastic resistance.

Buckling resistance

A laterally unrestrained member subject to major axis bending should be verified against lateral-torsional buckling as follow:

$$\frac{M_{Ed}}{M_{b,Rd}} \leq 1$$

where M_{Ed} is the design value of moment and $M_{b,Rd}$ is the design buckling resistance moment.

4.3.4 Materials

Table 28 presents the material characteristics that are taken into account.

TABLE 28: MATERIAL CHARACTERISTICS

Component	Material
Connector	Stainless steel AISI 316
Line	Stainless steel AISI 304
Primary profile	Stainless steel AISI 304

4.3.5 Case study

The worst structural situation appearing in the facade textile is investigated. This situation is appeared when the length of adjacent sequences is 1.6m and 1.55m (Frames E3.x and E4.x in Figure 31).

This project has received funding from the European Union's Horizon 2020 research and innovation programme under grant agreement No 958218

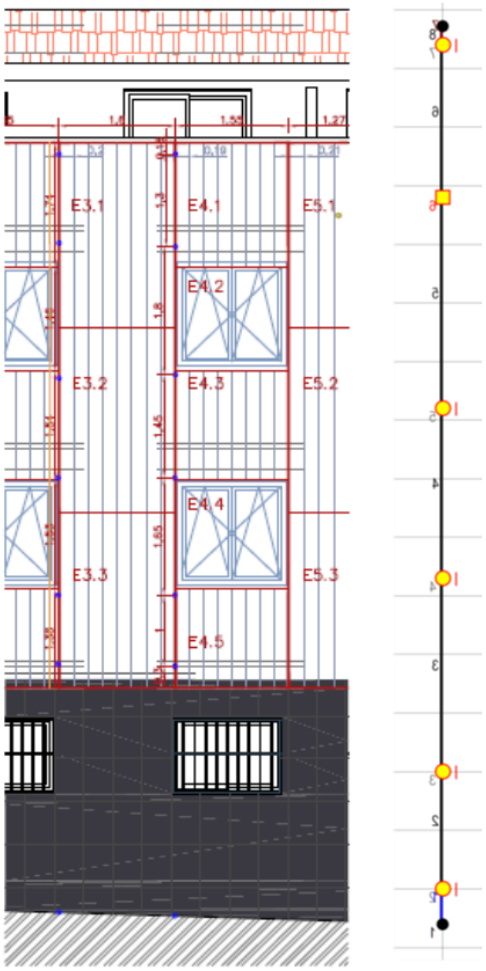

FIGURE 31: SCHEME OF ANCHORING VERSUS LINE PLACEMENT

4.3.6 COMPONENTS' JUSTIFICATION

Connectors

The study of internal forces has been carried out with a finite element simulation. The pressure of wind applied is $q_{e,s}$ and the results are presented in Table 29.

TABLE 29: APPLIED FORCES OVER CONNECTORS

	Strength
Magnitude	54 N
Vector X	0 N
Vector Y	0 N
Vector Z	27 (2) N

Figure 32 presents the applied forces and support point to the connector, while Figure 33 illustrates the Von Mises strengths.

This project has received funding from the European Union's Horizon 2020 research and innovation programme under grant agreement No 958218

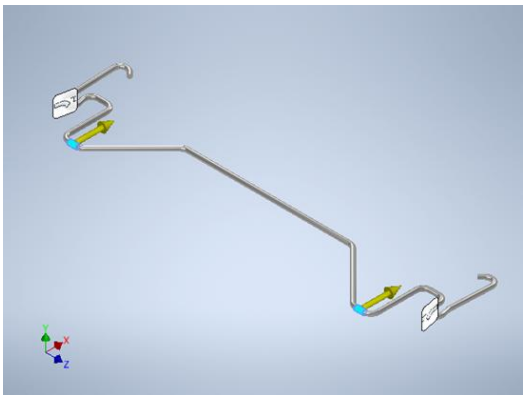

FIGURE 32: DIAGRAM OF APPLIED FORCES AND SUPPORT POINTS TO THE CONNECTORS

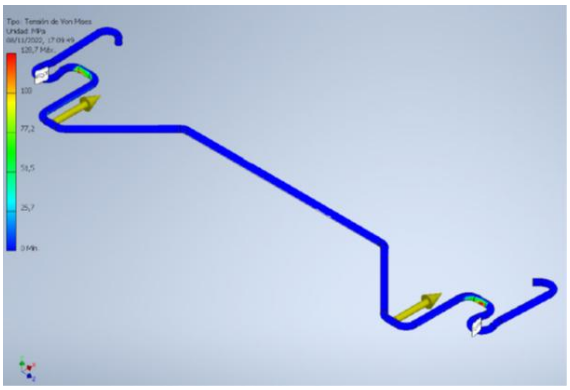

FIGURE 33: VON MISES STRENGTH STUDY FOR THE CONNECTOR

4.3.7 Lines

For the line analysis, the pressure of wind $q_{e,m}$ was considered, as the worst situation is happened in sequences E3.x and E4.x. The calculation parameters, the node data and the results are presented in Figure 34.

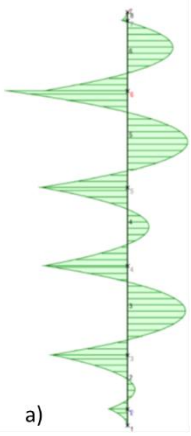

a)

b)

Node	Coord. X m	Coord. Y m	Type
1	0.00	3.20	Free Node
2	0.00	3.50	Moves on Y axis and spin
3	0.00	4.43	Moves on Y axis and spin
4	0.00	6.26	Moves on Y axis and spin
5	0.00	7.5	Moves on Y axis and spin
6	0.00	9.40	Fixed, Attached
7	0.00	10.70	Moves on Y axis and spin
8	0.00	10.86	Free Node

c)

Cross calculation parameters:

h=50,0 mm A_{wf}= 150 mm² I= 31.250 mm⁴

b=3,0 mm $W_{el,Rd}$= 1.250 mm³ $W_{pl,Rd}$= 1.875 mm³

Internal forces and ultimate resistance:

N_{Ed}= 1.160 N $M_{y,Ed}$= 0,336 kNm $V_{y,Ed}$= 984 N $M_{b,Rd}$=0,429 kNm

$N_{Pl,Rd}$= 34.286 N $M_{pl,Rd}$= 0,429 kNm $V_{pl,Rd}$= 19.795 N

Verification

Cross Section control:

$$\frac{N_{Ed}}{N_{pl,Rd}} = 0{,}02 \leq 1$$

$$\frac{N_{Ed}}{N_{pl,Rd}} + \frac{M_{y,Ed}}{M_{pl,Rd}} + \frac{M_{z,Ed}}{M_{pl,Rd}} = 0{,}82 \leq 1$$

$$\frac{V_{y,Ed}}{V_{pl,Rd}} = 0{,}05 \leq 1$$

Buckling:

$$\frac{M_{Ed}}{M_{b,Rd}} = 0{,}78 \leq 1$$

FIGURE 34:LINE ANALYSIS: A) DIAGRAM OF INTERNAL FORCES ALONG THE LINE, B) NODE DATA UBICATION ALONG THE LINE AND C) PARAMETERS AND CROSS SECTION CHECK.

Load Line

The calculation parameters, the node data and the results of load line analysis are presented in Figure 35.

This project has received funding from the European Union's Horizon 2020 research and innovation programme under grant agreement No 958218

a)

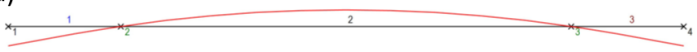

b)

Node	Coord. X m	Coord. Y m	Type
1	0.00	0.00	Free node
2	0.40	0.00	Only spin: joint
3	1.20	0.00	Only spin: joint
4	1.60	0.00	Free node

c)

Cross calculation parameters:

L profile

h=45,0 mm A= 430,0 mm² I= 12,42 cm⁴

b=5,0mm $W_{el.Rd}$= 2,43 cm³ $W_{pl.Rd}$= 2,79 cm³

Internal forces and ultimate resistance:

N_{Ed}= 0 N $M_{y.Ed}$= 0,151 kNm V_{Ed}= 1.207 N

$N_{Pl.Rd}$= 98.286 N $M_{pl.Rdy}$= 0,64 kNm $V_{pl.Rd}$= 56.745 N

$M_{z.Ed}$= 0,457 kNm

$M_{pl.Rdz}$= 0,64 kNm

Verification

Cross Section control:

$$\frac{N_{Ed}}{N_{pl.Rd}} = 0{,}00 \leq 1$$

$$\frac{N_{Ed}}{N_{pl.Rd}} + \frac{M_{y.Ed}}{M_{pl.Rdy}} + \frac{M_{z.Ed}}{M_{pl.Rdz}} = 0{,}86 \leq 1$$

$$\frac{V_{y.Ed}}{V_{pl.Rd}} = 0{,}02 \leq 1$$

FIGURE 35: LINE LOAD: A) DIAGRAM OF INTERNAL FORCES ALONG THE LINE, B) NODE DATA UBICATION ALONG THE LINE AND C) PARAMETERS AND CROSS SECTION CHECK.

Wind anchor

The wind anchor is the part of mesh who apply the wind strength to the façade and it consists of two parts, as depicted in Figure 36.

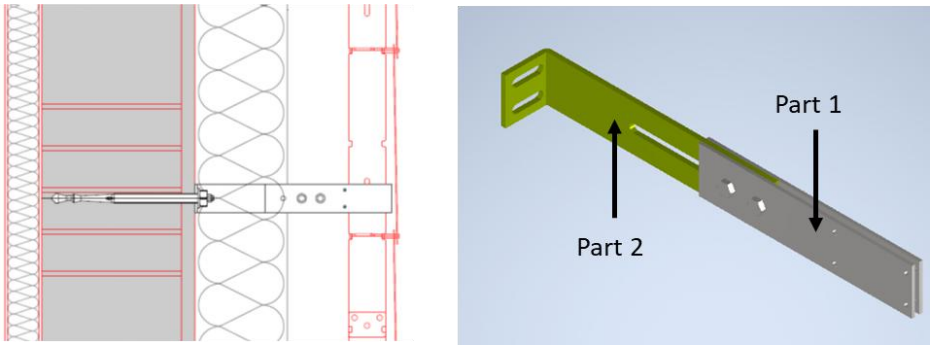

FIGURE 36: SCHEME AND POSITION WAY OF THE WIND ANCHOR ON THE WALL

The study of this the wind anchor has been carried out by means of finite element simulation. The applied forces and the results for the part 1 and part 2 are depicted in Figure 37 and Figure 38, respectively. The maximum wind force applied to the wall happens in the node 5 in the sequences E3.x and E4.x and it's 3.046 N perpendicular to façade.

a)

	Strength
Magnitude	3.046 N
Vector X	0 N
Vector Y	3.046 (4x762) N
Vector Z	0 N

b)

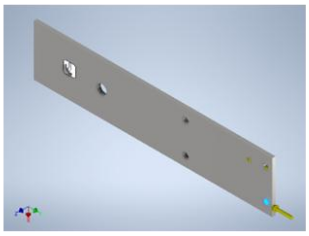

c)

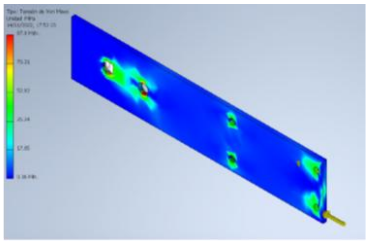

FIGURE 37: WIND ANCHOR - PART 1: A) APPLIED FORCES, B) DIAGRAM OF APPLIED FORCES AND SUPPORT POINTS AND C) VON MISES STRENGTH STUDY.

This project has received funding from the European Union's Horizon 2020 research and innovation programme under grant agreement No 958218

a)

	Strengh
Magnitude	-3.046 N
Vector X	-3.046 N
Vector Y	0 N
Vector Z	0 N

b) 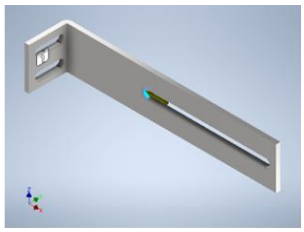

c) 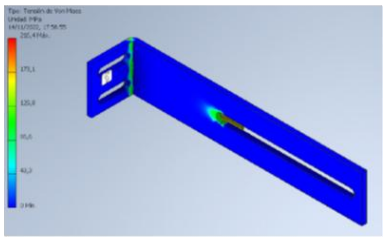

FIGURE 38: WIND ANCHOR - PART 2: A) APPLIED FORCES, B) DIAGRAM OF APPLIED FORCES AND SUPPORT POINTS AND C) VON MISES STRENGTH STUDY.

Load anchor

The study of internal forces has been carried out by means of finite element simulation. Figure 39 presents the applied forces and the results of the load anchor component. The maximum force applied in the load is 1.334N perpendicular to façade and 1.512N parallel to façade.

Force 1

Force 2

a)

	Strengh
Magnitude	1.334 N
Vector X	0 N
Vector Y	-1.334 N
Vector Z	0 N

	Strengh
Magnitude	1.512 N
Vector X	1.512 N
Vector Y	0 N
Vector Z	0 N

b) 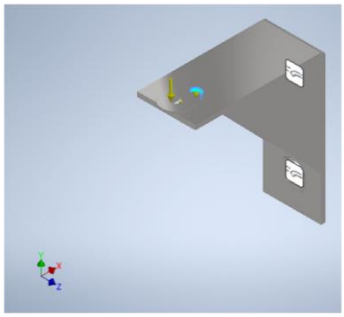

c) 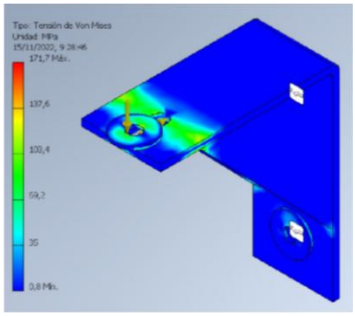

FIGURE 39: LOAD ANCHOR: A) APPLIED FORCES, B) DIAGRAM OF APPLIED FORCES AND SUPPORT POINTS AND C) VON MISES STRENGTH STUDY

This project has received funding from the European Union's Horizon 2020 research and innovation programme under grant agreement No 958218

5 Fire performance

The fire performance of the specimens were assessed by performing standard "Reaction to Fire" tests, following the EN 13823: 2020 + A1 : 2022[6] standard, also known as Single Burning Item (SBI) test. This test requires either a corner specimen or two specimens to be joined as a corner. Table 30 shows the external dimensions of the tested specimens.

TABLE 30: SPECIMEN DIMENSIONS

Specimen	Height	Weight
Short Wing	1500	500
Long Wing	1500	1000

During the first part of the test procedure, an auxiliary burner is ignited in order to calculate precisely the fire power level and smoke production of the burner itself. After that, the auxiliary burner is turned off and the main burner is ignited. The main burner is located at the internal corner of the specimen, providing a steady fire power level of 30 kW. The duration of the test is 20 minutes and during this period the combustion gas products (used to calculate the heat release rate), the smoke production and the potential creation of burning droplets are measured. Based on the heat release rate, two main parameters are calculated, the fire growth rate (FIGRA) and the total heat release, 600 s after the fire test initiation (THR_{600s}). Equations 6.1 and 6.2 are used to estimate the aforementioned parameters. In addition, two smoke production parameters are calculated, i.e. the smoke growth rate (SMOGRA) and the total smoke production, 600 s after the fire test initiation (TSP_{600s}); Equations 6.3 and 6.4 are used in this case.

$$FIGRA = 1000 \times max\left(\frac{HRR_{av}(t)}{t}\right) \tag{6.1}$$

$$THR_{600s} = \frac{\sum_{0}^{600}\left(max\left[HRR(t),0\right]\right)}{1000} \tag{6.2}$$

$$SMOGRA = 10000 \times max\left(\frac{SPR_{av}(t)}{t}\right) \tag{6.3}$$

$$TSP_{600s} = \sum_{0}^{600}\left(max\left[SPR(t),0\right]\right) \tag{6.4}$$

The criteria for the "reaction to fire" classification, according to the EN 13501-1: 2019 standard "Fire classification of construction products and building elements – Part 1: Classification using data from reaction to fire tests", are presented in Table 31.

[6] EN 13823:2020+A1:2022 - Reaction to fire tests for building products – Building products excluding floorings exposed to the thermal attack by a single burning item

This project has received funding from the European Union's Horizon 2020 research and innovation programme under grant agreement No 958218

TABLE 31: EN 13501-1 CLASSIFICATION CRITERIA.

Parameter	A2/B	C	D	E	s1	s2	s3	d0	d1	d2
FIGRA	<120	<250	<750	>750	-	-	-	-	-	-
THR600s	<7.5	<15	>15	>15	-	-	-	-	-	-
SMOGRA	-	-	-	-	<30	<180	>180	-	-	-
TSP	-	-	-	-	<50	<200	>200	-	-	-
d < 10s	-	-	-	-	-	-	-	0	>0	>0
d > 10s	-	-	-	-	-	-	-	0	0	>0

In the frame of the performed tests, a number of additional thermocouples (Type K, 1.5 mm diameter) were added to the specimens, in order to achieve a better understanding of their fire behaviour.

5.1 SmartWall

Two different SmartWall types were examined. The first one (Type A), serving as a “blank type”, was a simple configuration, constructed by the metal frame, gypsum plasterboards and rockwool (Figure 40). The second type (Type C) corresponded to a SmartWall module, with the addition of a Toolbox and a fan-coil unit (Figure 41).

FIGURE 40: SMARTWALL WITHOUT FAN COIL AND BATTERY, EXPOSED SIDE (LEFT) AND UNEXPOSED SIDE (RIGHT).

This project has received funding from the European Union’s Horizon 2020 research and innovation programme under grant agreement No 958218

FIGURE 41: SMARTWALL WITH FAN COIL AND BATTERY, EXPOSED SIDE (LEFT) AND UNEXPOSED SIDE (RIGHT).

The extra thermocouples were added at the gypsum plasterboard at the unexposed side, at heights of 100 mm, 400 mm (battery height for the second SmartWall) and 800 mm and at the metal frame at the height of 400 mm. In the SmartWall with the fan coil, an extra thermocouple was added at the geometric center of the fan coil unit. The results of the EN 13823 tests are presented in Table 32.

TABLE 32: EN 13823 RESULTS FOR THE SMARTWALL TYPES.

Parameter	Blank type of SmartWall	SmartWall with fan-coil and Toolbox
FIGRA	0.00	0.00
THR600s	0.79	0.44
SMOGRA	0.00	0.00
TSP	43.34	44.85
d < 10s	No	No
d > 10s	No	No

Based on these test results, according to the EN 13501-1 standard, both specimens are classified as “B-s1, d0”. Figure 42 depicts the temporal variation of the temperature at the aforementioned measuring locations.

This project has received funding from the European Union’s Horizon 2020 research and innovation programme under grant agreement No 958218

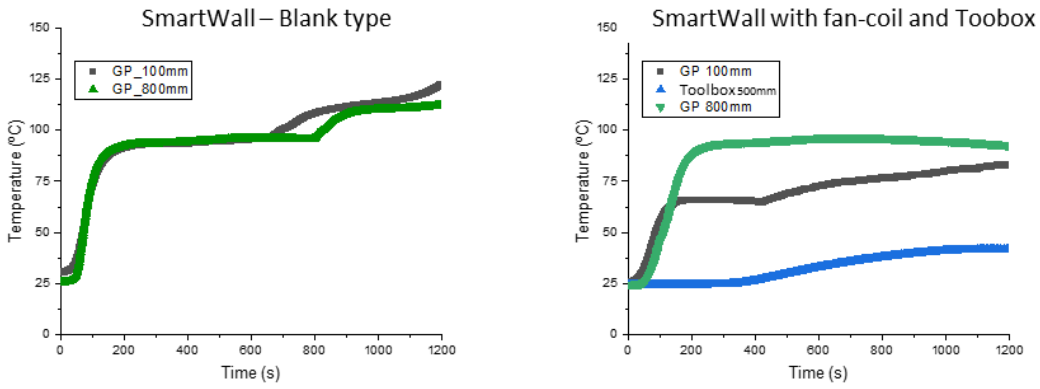

FIGURE 42: TEMPERATURES AT THE SMARTWALL WITHOUT (LEFT) AND WITH (RIGHT) FAN-COIL AND TOOLBOX.

In both test cases, the temperature in the back of the specimen did not exceed 100°C. There was no major difference in the fire performance of the two specimens, judging by both the EN 13823 results and the additional thermocouples. As a result, the existence of the fan-coil unit and the battery does not seem to have a significant effect the fire performance of the specimen (the rise of the temperature at the height of 400 mm was due to a crack in the gypsum plasterboard). Figure 42 depicts both specimens after the test.

FIGURE 43: SMARTWALL WITHOUT (LEFT) AND WITH FAN-COIL AND BATTERY (RIGHT) AFTER THE TEST.

This project has received funding from the European Union's Horizon 2020 research and innovation programme under grant agreement No 958218

5.2 Smart Window

The smart window configuration was also tested, aiming to determine the "reaction to fire" performance. The tested system had three layers of glass and the ventilation system. The specimen's height was 1400 mm and its length was 850 mm. The rest of the long wing, in order to reach the "full" specimen dimensions of 1500 mm x 1000 mm, was made of Calcium Silicate panels. The short wing was also constructed from Calcium Silicate panels (Figure 6.5, left). This specimen was prepared following the configuration suggested in EN 14351-1 : 2006 + A1 : 2010[7].

FIGURE 44: SMART WINDOW CONFIGURATION BEFORE (LEFT) AND DURING (RIGHT) THE FIRE TEST.

Once more, 6 additional thermocouples were added; 2 in the lower vent (in the middle of the vent, one in the unexposed side and one at exposed side), 3 in the upper vent (in the middle of the vent, one in the unexposed side, one in the centre of the Smart window and one at exposed side) and 1 in the frame (at the unexposed side, at 400 mm height). Figure 44 (right) shows the smart window after 10 minutes of fire exposure. The results of the EN 13823 fire test are presented in Table 33.

[7] EN 14351-1:2006+ A1:2010. Windows and doors -Product standard, performance characteristics - Part 1: Windows and external pedestrian doorsets without resistance to fire and/or smoke leakage characteristics.

This project has received funding from the European Union's Horizon 2020 research and innovation programme under grant agreement No 958218

TABLE 33: EN 13823 FIRE TEST RESULTS FOR THE SMART WINDOW.

Parameter	Smart window
FIGRA	177.15
THR600s	10.82
SMOGRA	116.87
TSP	891.99
d < 10s	No
d > 10s	No

The test had to be terminated earlier than the standard duration because of extreme rise of the temperature in the exhaust gas duct; therefore, a proper "reaction to fire" classification could not be completed. However, if the test was completed, the classification is estimated to be C-s3,d0, based on the results presented in Table 33. Figure 45 depicts the temporal evolution of the temperature at the aforementioned thermocouple locations.

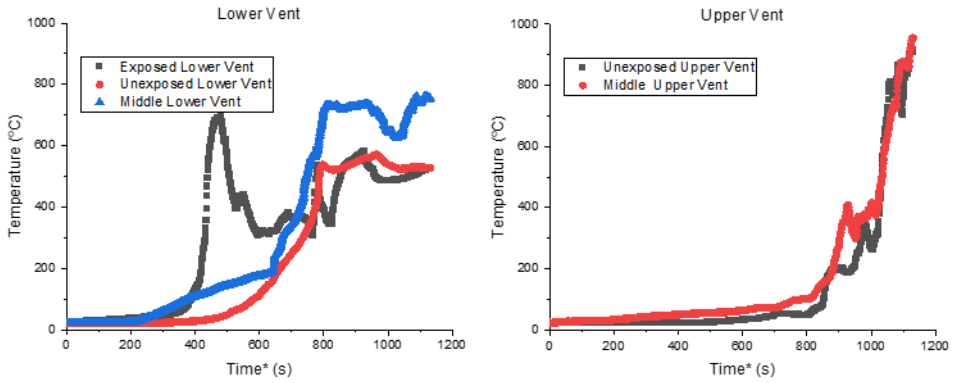

FIGURE 45: LOWER (LEFT) AND UPPER (RIGHT) VENT TEMPERATURES

There was a radical rise in the temperature of the specimen, especially after the 900 s mark; the temperature in the upper vent reached a peak temperature of 950°C. Also, the specimen collapsed before the test was finished. Figure 46 shows the smart window after it was extinguished. The use of standard, non fire-retardant treated plastic window frame is the main reason for the observed collapse of the specimen, as well as for the very high temperatures measured in the frame. The use of a fire-treated material in the frame is expected to significantly improve the overall fire behaviour of the unit.

This project has received funding from the European Union's Horizon 2020 research and innovation programme under grant agreement No 958218

FIGURE 46: SMART WINDOW AFTER THE END OF THE TEST.

5.3 eWHC/ConExWall

eWHC-ConExWall doesn´t includes materials that require fire tests (e.g. gipsumboards, insulation) or materials not classified in fire codes (e.g. wood). All structures can be individually calculated on each specific project. eWHC/ConExWall is installed in 3 different ways:

- Basic type is installation as external insulation complex on external wall. In this case external walls are constructed from non-flammable materials – typical concrete, bricks, stones. Fire regulations require load-bearing structure from materials with certain fire resistance. eWHC/ConExWall is not load-bearing structure in this case. eWHC-ConExWall has only influence on fire risk area which limit neighboring buildings. Dimension of fire risk area is various, it depends on specific layer composition, surface layer (e.g. plaster, wood cladding) and windows dimensions. Dimension of fire risk area is individually calculated according to fire protection codes for each specific case.
- Installation eWHC/ConExWall as loadbearing external walls in last storey requires specific fire resistance. Fire resistance is achieved by using gipsboard / gipsfiberboard plates from interior with existing fire tests (e.g. Fermacell, Knauf ..). Influence on fire risk area is individually calculated as in first case.
- Installation eWHC/ConExWall as roofs requires specific fire resistance. Fire resistance is achieved by using gipsboard / gipsfiberboard plates from interior with existing fire tests (e.g. Fermacell, Knauf ..)

This project has received funding from the European Union's Horizon 2020 research and innovation programme under grant agreement No 958218

5.4 eAHC / HybridWall

The applicable Spanish regulation CTE DB-SI Código Técnico de la Edificación – Documento Básico de Seguridad en caso de incendio (Building Technical Code – Basic Document of Safety in case of fire) establishes requirements on reaction to fire and resistance to fire for external walls.

As for reaction to fire, the applicable requirement (class D-s3,d0 for façades up to 10 m height) is met by assessment of the individual eAHC/HybridWall integrated components and their relevant certification (metallic cladding elements and substructure, mineral wool insulation, etc). Information on the relevant certifications of the integrated components, where reaction to fire performance is declared, can be consulted in D1.3, Table 5. Therefore, it is not necessary to carry out any additional test according to EN 13501-1.

As for resistance to fire, the applicable requirement (EI 60 for the external wall as a whole) is already met by the previously existing external wall. The addition of the eAHC/HybridWall does not adversely affect the performance, except for the penetration of the ventilation pipework. In such points, the resistance to fire of the existing external wall is reinstated by the installation of an intumescent fire sealing collar. The resistance to fire performance of the intumescent collar is addressed by its own product certification or, at least, by the relevant test according to EN 1366-3 and classification according to EN 13501-2. Information on the relevant certification of the fire penetration seal, where resistance to fire performance is declared, can be consulted in D1.3, table 5. Therefore, it is not necessary to carry out any additional test of the eAHC-HybridWall system or their components.

Finally, the CTE DB-SI does not establish any requirement on large-scale testing for façade elements.

This project has received funding from the European Union's Horizon 2020 research and innovation programme under grant agreement No 958218

6 Acoustic performance

The acoustic analysis is carried out only for the eAHC/HybridWall PnU kit, because it is the only PnU that create noise due to the air flow and other moving elements (fans). The SmartWall contains commercial and certified fan-coils that are designed for residential buildings satisfying all requirements concerning the acoustic performance. Besides, the acoustic analysis of SmartWall, including acoustic tests, has been done in the frame of Task 4.1 and the relative information is available in Deliverable D4.1. The eWHC/ConnExWall consists of heating pipes as an active layer embodied in the facade system. The elements of ConnExWall do not create noise, so the acoustic performance analysis of eWHC has not make sense.

This chapter describes the acoustic testing of two eAHC unit prototypes. The first prototype was in the basic configuration, the second prototype was equipped with a silencer box to reduce the noise generated to the room. Consequently, the full-scale laboratory test was performed with the final prototype.

The noise was measured independently for the body of the air handling unit and for each eAHC unit inlet and outlet, i.e., outlet of supply air to the room – SUP, inlet of extraction air from the room ETA, outlet of exhaust air to the outdoor environment – EHA and inlet of outdoor air to the unit – ODA (see Figure 47). The principle of this division of the complex source of noise into sub-sources was carried out in order to evaluate the individual parts of the air handling unit in detail.

The silencer box was developed in order to achieve an attenuation of 10 dB (A-weighted) at the ETA inlet of the air handling unit, which was necessary to achieve sufficiently low A-weighted sound pressure levels. The sound pressure levels of the eAHC unit were required to be 2 dB lower that the noise limits for the living area, defined by the Deliverable D4.2 ($L_{pAMAX,\ Night}$ = 25 dB for the night and $L_{pAMAX,Day}$ = 35 dB for the day).

The SUP outlet (supply of air to the room) was sufficiently silent without the installation of the silencer box, thanks to the design of the eAHC unit. However, the final assembly of the eAHC unit was equipped with two silencer boxes at the inlet and outlet facing the living area (ETA unit inlet and SUP unit outlet). This ensured better acoustic comfort to the occupants. This configuration was tested in the full-scale model.

This project has received funding from the European Union's Horizon 2020 research and innovation programme under grant agreement No 958218

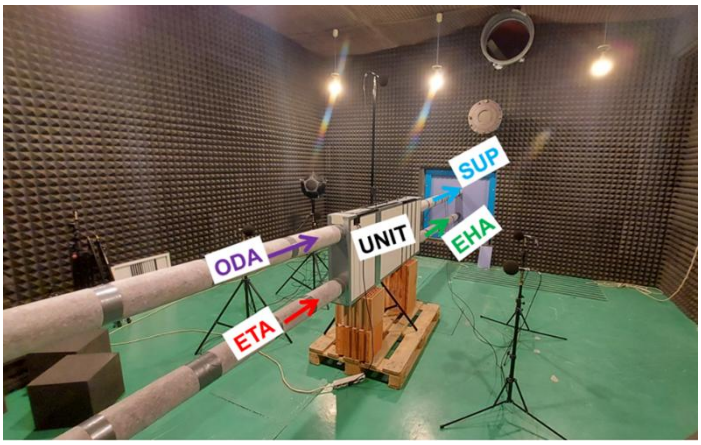

FIGURE 47: NOISE MEASUREMENT IN THE ANECHOIC ACOUSTIC LABORATORY – NOISE FROM THE AIR HANDLING UNIT BODY. SUP – SUPPLY OF AIR TO THE ROOM; ETA – EXTRACTION OF AIR FROM THE ROOM; EHA – EXHAUST AIR OUTLET TO THE OUTDOOR ENVIRONMENT, ODA – OUTDOOR AIR INLET

6.1 Description of the acoustic tests

The measurements were performed in two laboratories – Anechoic acoustic laboratory for evaluation of the sub-sources (SUP, ETA, EHA, ODA and body of the unit) and Building acoustic laboratory with two separated rooms, for the full-scale test.

6.1.1 Anechoic acoustic laboratory

The dimensions of the Anechoic acoustic laboratory were 5.5 x 5.5 x 3.5 m (width x depth x height). Walls and ceiling of the laboratory were covered with high absorptive material Polyson, the floor was made of concrete (i.e., reflective surface). The sound absorption of the laboratory is presented in Table 34. The high sound absorption allows measurement of sound pressure levels for direct sound waves at the distance of 1 m from the sound source, i.e. in the free acoustic field.

TABLE 34: THE SOUND ABSORPTION OF THE ANECHOIC ACOUSTIC LABORATORY ACCORDING TO EYRING.

f [Hz]	20	25	31.5	40	50	63	80	100	125	160	200	250	315	400	500	630
α_{mE}	0.03	0.04	0.04	0.07	0.21	0.26	0.31	0.37	0.42	0.42	0.43	0.44	0.44	0.43	0.43	0.45
f [Hz]	800	1000	1250	1600	2000	2500	3150	4000	5000	6300	8000	10000	12500	16000	20000	-
α_{mE}	0.45	0.45	0.45	0.45	0.45	0.45	0.45	0.45	0.45	0.45	0.45	0.45	0.41	0.41	0.41	-

6.1.2 Building acoustic laboratory

The Building acoustic laboratory for wall airborne sound absorption measurement consists complies with the requirements of EN ISO 10140-5. The walls of the test rooms are made of reinforced concrete with the thickness of 250 mm. In order to suppress lateral sound transmission through the

This project has received funding from the European Union's Horizon 2020 research and innovation programme under grant agreement No 958218

building structures of the laboratory, the test rooms are separated from each other by two elastic joints. The test rooms have the following parameters:

Test room 1 (Receiving room)

- Room dimensions: approx. 3.93 x 5.2 x 3.18 m (w x d x h)
- Room volume: approx. 65 m^3
- 6 diffusion elements (2 volume and 4 plate diffusers), 6 absorbers

Test room 2 (Source room)

- Room dimensions: approx. 4.3 x 5.0 x 3.49 m (w x d x h)
- Room volume: approx. 75 m3
- 6 diffusion elements (2 volume and 4 plate diffusers), 7 absorbers

Dimensions of the test opening: 2.4 x 4.2 m (area 10.08 m^2)

Reverberation time T20 (s) of the Receiving room:

TABLE 35: REVERBERATION TIME T20 (S) OF THE RECEIVING ROOM:

Frequency [Hz]	50	63	80	100	125	160	200	250	315	400	500
T20 (s)	1.1	1.13	1.63	1.83	1.68	1.87	1.72	1.76	1.73	1.79	1.71
Frequency [Hz]	630	800	1000	1250	1600	2000	2500	3150	4000	5000	-
T20 (s)	1.57	1.51	1.54	1.49	1.43	1.42	1.36	1.29	1.13	1.01	-

6.1.3 Noise generated from the inlets and outlets of the eAHC unit emitted to the duct system

Noise measurements were performed in the Anechoic laboratory for each inlet and outlet of the air handling unit separately. During the measurement, the tested inlet or outlet was facing the Anechoic acoustic laboratory, see Figure 48 (left). The unit was placed in the adjacent room and connected to the diffuser by a straight acoustically insulated duct penetrating the wall through the acoustic window. The duct was 3 m long. see Figure 48 (right).

The terminal inlet/outlet was at the height of 1.2 m above the floor. The results of the measurement represent the logarithmic average from five measurement points at the distance of 1 m from the outlet/inlet (in the free acoustic field). The correction to the background noise was done.

This project has received funding from the European Union's Horizon 2020 research and innovation programme under grant agreement No 958218

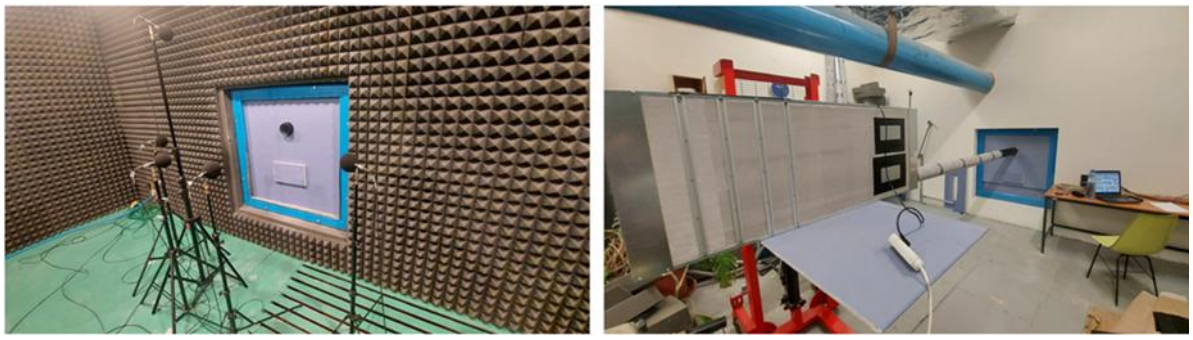

FIGURE 48: NOISE MEASUREMENT IN THE ANECHOIC ACOUSTIC LABORATORY – NOISE FROM THE UNIT OUTLETS AND INLETS; TERMINAL INLET/OUTLET IN ACOUSTIC WINDOW (ON LEFT), AIR HANDLING UNIT IN THE ADJACENT ROOM (ON RIGHT).

6.1.4 Noise generated from the eAHC unit to the surrounding

The air handling unit was placed in the middle of the Anechoic acoustic laboratory, see Figure 47. It was elevated from the floor and installed on the vibration isolation. The unit inlets and outlets were connected to a straight acoustically insulated duct leading outside the laboratory through the acoustic windows on both sides of the room. The sound pressure level was measured at five points at the distance of 1 m from the surface of the unit (in the free acoustic field). The correction to the background noise was applied. The results of the measurements represent the logarithmic average from the five measurement points.

6.1.5 Noise generated from the eAHC during the full-scale model measurement

The measurements were carried out in the building acoustic laboratory of the University Centre for Energy Efficient Buildings (UCEEB) CTU in Prague. The laboratory consists of two test rooms – the so-called Source room and the Receiving room. The rooms are divided by a frame for installation of the tested element (usually a wall).

In the current measurement, the rooms were divided by a wall from Calcium Silicate (sand-lime) bricks, i.e., by a double construction with a sound attenuation of Rw = 42 dB(A), with a plastic double-glazed window. The eAHC unit was mounted on the dividing wall facing the Source room. It was anchored by 4 simple rubber insulators to prevent transfer of vibration from the unit to the wall, see Figure 50. The insulators had dimensions of 30x30 mm and M8x25 inner threaded rod. They were attached to the corners of the eAHC metal body casing and hanged on the C-rails on the wall. The unit was equipped with the developed PASSAGE silencer box at the SUP and the CUBE silencer box at the ETA (see section 6.3)

Measurements were done for 3 volume flow rates of air. The noise was measured at 3 microphone positions for each flow rate. The integration time of each measurement was 30 s. Additionally, an air-tightness measurement was performed, when the unit was switched-off and the measured values were compared with the results for the case of dividing wall without the unit.

This project has received funding from the European Union's Horizon 2020 research and innovation programme under grant agreement No 958218

FIGURE 49: EAHC UNIT INSTALLATION DURING THE FULL-SCALE MODEL MEASUREMENT.

FIGURE 50: DETAIL OF SUPPLY AIR CONNECTION THROUGH THE WALL.

FIGURE 51: DETAIL OF THE SUPPLY AIR OUTLET TO THE OPPOSITE SIDE OF THE DIVIDING WALL (FACING THE RECEIVING ROOM)

6.2 Tested prototypes of eAHC unit

The following unit prototypes were tested:

- PROTOTYPE 1 – first version; served for evaluation of the first design and for first performance tests. The body was made of combination of XPS and EPS components.
- PROTOTYPE 2 – second version with upgraded body; mostly made of XPS and plastic boards on outer shell to increase overall rigidity of the unit body. Internal air channels were modified to decrease air velocity and pressure losses.
- PROTOTYPE 2 with silencer box – external silencer boxes were applied to ensure low noise to the indoor environment.

This project has received funding from the European Union's Horizon 2020 research and innovation programme under grant agreement No 958218

6.3 Development of the Silencer box to reduce noise emitted to the duct system

On the basis of the acoustic measurements, a high noise emitted from the eAHC unit inlet (ETA fan intake) was identified. To target this issue, a silencer box was developed and installed to the ETA inlet (extraction of air from the room). Also, it was verified that the noise from the eAHC unit outlets (SUP and EHA) is reduced by the unit design (air channels, filters, heat exchangers, …) and there is no silencer necessary.

The developed silencer had to fit into the limited available dimensions, with the casing of 345 x 360 140 mm (width x depth x height). It had to provide a change of air flow direction in order to improve the noise damping, compared to the straight air flow direction. An absorptive silencer filled by a porous material (foam) was used. It transforms acoustic kinetic energy to the thermal energy, while the thermal energy generated by the oscillation of the particles is transferred away by the porous material. However, absorption is effective only for the middle and high frequencies of noise. Therefore, resonance and reflection had to be combined with the acoustic energy absorption phenomena, in order to attenuate noise with low frequencies. Required attenuation of the silencer for ETA side was 10 dB (A-weighted).

The following types of the silencer were manufactured and compared for the case of the eAHC unit, see also Figure 52:

- EMPTY BOX – empty silencer case (maximum dimensions limiting the size of the silencer are indicated in the figure);
- CUBE – simple solution with a block of foam positioned to the corner of the silence, with limited reflection ability;
- PASSAGE – separated foam block with air passage; absorptive passage ensures smaller pressure losses (see Figure 53), but also smaller attenuation effect for lower frequencies (see Figure 54);
- CUBE_Daig_PLT – similar to the CUBE case, with foam block separated by 0.8 mm thick metal plate; this type of silencer has higher effect of attenuation by reflection (see Figure 54), but also high pressure losses (see Figure 53).

Sound absorption index of the foam used to fill the silencers is presented in Figure 55.

This project has received funding from the European Union's Horizon 2020 research and innovation programme under grant agreement No 958218

FIGURE 52: THE TYPES OF SILENCERS FOR EAHC UNIT.

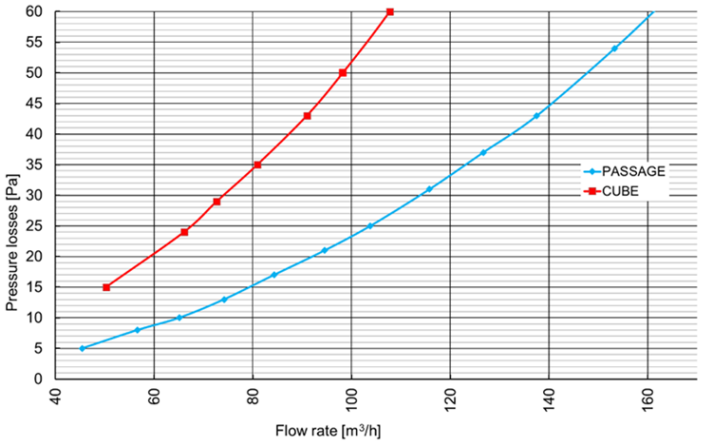

FIGURE 53: DEPENDENCE OF PRESSURE LOSSES ON FLOW RATE OF DIFFERENT SILENCER BOXES

This project has received funding from the European Union's Horizon 2020 research and innovation programme under grant agreement No 958218

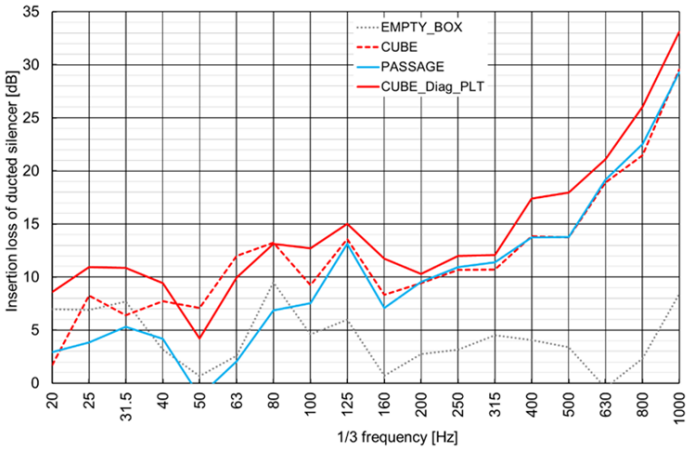

FIGURE 54: INSERTION LOSS OF DIFFERENT SILENCER BOXES IN THE FREQUENCY RANGE 20-1000 HZ.

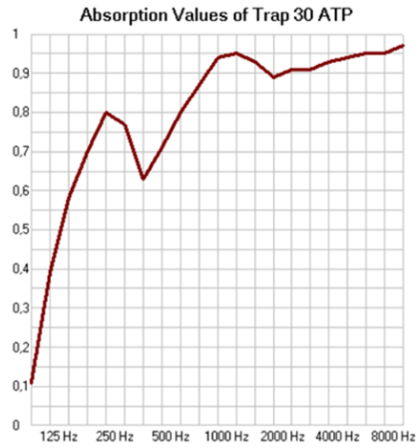

FIGURE 55: SOUND ABSORPTION INDEX OF THE FOAM FILLING OF THE SILENCERS.

6.4 Noise results of the tested prototypes of eAHC units

The comparison of acoustic properties of PROTOTYPES 1 and 2 of the eAHC unit are presented in the Figure 56. One-third octave bands of the sound pressure level are presented in ANNEX III - 13.1. Hearing threshold level is presented in one-third octave band figures, representing the limit of human ear perception. If the tonal component is lower than the hearing threshold limit, it is not evaluated as a tonal component at the acoustic spectrum presented in Figure 56. The tonal components indicate negative effects of sound spectrum. They relate to the revolution frequency of the fan and number of fan blades.

The most significant source of noise for the eAHC unit was the intake ETA, which is emitting noise into the indoor environment (in the room). From the measurements of the PROTOTYPE 1 and 2, as presented in Figure 56, it was evident that the noise generated from ETA to the ventilated room had to be reduced by approx. 10 dB (A-weighted). Therefore, the silencer box was developed and applied.

The inlet SUP generates indoor noise around L_{pA}=31.3 dB for maximum flow rate, meeting the required limits. It was not necessary to reduce the SUP emitted noise. However, it is generally recommended to install a damping element between the unit and the end terminal diffuser to the protected room. The ODA inlet EHA outlet facing the outdoor environment generated low sound pressure levels L_{pA}=43.7 dB and 30.8 dB, respectively. The limits are 50 dB for the day and 40 dB for the night in the protected outdoor area, according to the Deliverable D4.2.

The effect of the silencer box attenuation is presented in Figure 57 for the PROTOTYPE 2. One-third octave band of sound pressure level for silencer box installed on the ETA inlet are presented in ANNEX III 13.2, for the fixed voltage of the fan (i.e., constant revolution speed of the fan, while the silencer pressure loss decreases the flow rate, see Figure 58).

This project has received funding from the European Union's Horizon 2020 research and innovation programme under grant agreement No 958218

	Voltage [V]		Flow rate [m³/hod]		L_{pA} = Sound pressure level corrected by A filter at a distance 1 m [dB] TN = tonal component at 1/3 frequency spectrum [Hz]									
					UNIT		ODA (outdoor air)		SUP (supply air		ETA (extract air)		EHA (exhaust air)	
	Supply	Extract	Supply	Extract	TN	L_{pA}	TN	L_{pA}	TN	L_{pA}	TN	L_{pA}	TN	L_{pA}
PROTOTYPE_1	-	-	-	-	-	-	-	-	-	-	-	-	-	-
PROTOTYPE_2	3.07	3.23	30	30	-	18.0	-	23.1	-	14.5	-	26.3	-	12.9
PROTOTYPE_1	4.7	4.7	50	50	-	33.0	-	31.2	200 Hz	14.6	-	32.0	-	14.6
PROTOTYPE_2	4.4	4.58	50	50	-	23.8	-	30.4	-	19.1	-	33.4	630 Hz	17.5
PROTOTYPE_1	6.5	6.5	75	75	-	41.2	-	38.7	40 Hz, 200 Hz	25.3	-	41.1	-	21.4
PROTOTYPE_2	5.98	6.36	75	75	-	30.6	-	37.7	-	25.1	2.5 kHz	40.9	630 Hz	23.9
PROTOTYPE_1	7.6	7.6	100	100	50 Hz	45.3	50 Hz, 10 kHz	43.4	50 Hz, 200 Hz	29.1	50 Hz	45.0	-	24.5
PROTOTYPE_2	7.33	8.25	100	100	-	36.4	50 Hz	43.7	50 Hz	31.3	50 Hz, 2.5 kHz 12.5 kHz	48.6	630 Hz	30.8
SILENCERS					-		NOT NECESSARY		NOT NECESSARY		NECESSARY -10 dB		NOT NECESSARY	

FIGURE 56: COMPARISON OF ACOUSTIC PROPERTIES OF PROTOTYPE 1 AND 2.

Voltage [V]		Flow rate [m³/hod] WITHOUT Silent box		REDUCED Flow rate [m³/hod] WITH Silent box CUBE_Diag_PLT for ETA, and EMPTY BOX for SUP		L_{pA} = Sound pressure level corrected by A filter at a distance 1 m [dB] TN = tonal component at 1/3 frequency spectrum [Hz]									
						ETA		EMPTY BOX		CUBE		PASSAGE		CUBE_Diag_PLT	
Supply	Extract	Supply	Extract	Supply	Extract	TN	L_{pA}	TN	L_{pA}	TN	L_{pA}	TN	L_{pA}	TN	L_{pA}
3.07	3.23	30	30	27	21	-	26.3	-	23.9	-	15.8	-	16.2	-	14.9
4.4	4.58	50	50	48	36	-	33.4	-	30.5	-	21.0	-	21.2	-	19.8
5.98	6.36	75	75	71	52	-	40.9	2.5 k Hz	37.9	-	27.9	-	28.5	-	26.8
7.33	8.25	100	100	96	71	50 Hz, 2.5 kHz	48.6	50 Hz, 2.5 k Hz	45.4	-	34.6	50 Hz	34.7	-	32.2

FIGURE 57: EVALUATION OF THE EFFECT OF SILENT BOX ATTENUATION FOR PROTOTYPE_2 FOR ETA DIFFUSER.

6.5 Noise results of the full-scale model for the final prototypes of eAHC unit

The following Figure 58 summarizes the results of the Full-scale model measurements in the Building acoustic laboratory. The full-scale model was used to measure the emitted sound pressure level during the real operation of the unit (unit equipped with the silencer boxes, with the real mounting on the façade). For the tested volume flow rates, values from 23.3 to 43.4 dB(A) were measured. The values are about 2.5 dB(A) higher than the ones measured on the sample unit in the Anechoic acoustic laboratory (free acoustic field, direct acoustic field only). Such difference between both experiments is acceptable. This small difference defines, that mounting of the unit does not deteriorate the acoustic comfort in the indoor environment. The structural noise propagation caused by transfer of the unit vibrations through the anchorage to the solid façade was negligible.

This project has received funding from the European Union's Horizon 2020 research and innovation programme under grant agreement No 958218

The night operation of the eAHC unit is possible with the maximum volume flow rate of 35 m^3/hod. In this operation mode the unit generates sound pressure level below 25 dB, meeting the night noise limits L_{AMAX} = 25 dB.

Voltage [V]		Flow rate [m³/hod]		Sound pressure level corrected by A filter at a distance 1 m [dB]			
				INTERIOR (Summary SUP and ETA + structural noise from mounting the unit on the facade)	Acoustic laboratory (free filed, only direct acoustic field) – sources measured separately, without negative effect from structural mounting of the unit on the facade		
Supply	Extract	Supply	Extract		SUP	ETA	Summary
4.1	4.62	35	35	**23.3**	14.5	19.8	**20.9**
7.05	7.73	75	75	**35.3**	25.1	32.2	**33.0**
10	10	115	100	**43.4**	-	-	

FIGURE 58: RESULTS OF THE FULL-SCALE MODEL MEASUREMENT, COMPARISON OF THE REAL AND LABORATORY ACOUSTIC MEASUREMENT

The sound insulation of the construction (dividing wall) with and without the unit was R'_w = 43 dB and 39 dB, respectively. The sound insulation of the facade affected by the openings for the unit inlet duct (ETA) and outlet duct (SUP) was decreased by approx. 4 dB. This has to be taken into account during the design of the building envelope acoustic protection.

This project has received funding from the European Union's Horizon 2020 research and innovation programme under grant agreement No 958218

7 Thermal performance – Material level analysis

7.1 SmartWall

7.1.1 SmartWall version for the Voula (VVV) demo site

All materials of the SmartWall PnU kit are commercial materials and their thermal properties are available by the manufacturers. The only material that required further investigation was the thermal resistance of the mineral wool with aluminium foil which is located between the existing wall and the SmartWall. This material was investigated because its behavior was not obvious after its the pressurization between the SmartWall and the existing wall. The nominal thickness of this layer is 5 cm, however, due to the installation of SmartWall the layer is pressed for 1.5-2.5 cm. The thermal resistance of this layer is investigated by means of the Guarded Hot Plate method for different pressurised thicknesses: 50 mm (nominal, not pressure), 40 mm, 30 mm, 20 mm and 10 mm.

FIGURE 59: THE GUARDED HOT PLATE APPARATUS

FIGURE 60: MINERAL WOOL WITH ALUMINUM FOIL.

This project has received funding from the European Union's Horizon 2020 research and innovation programme under grant agreement No 958218

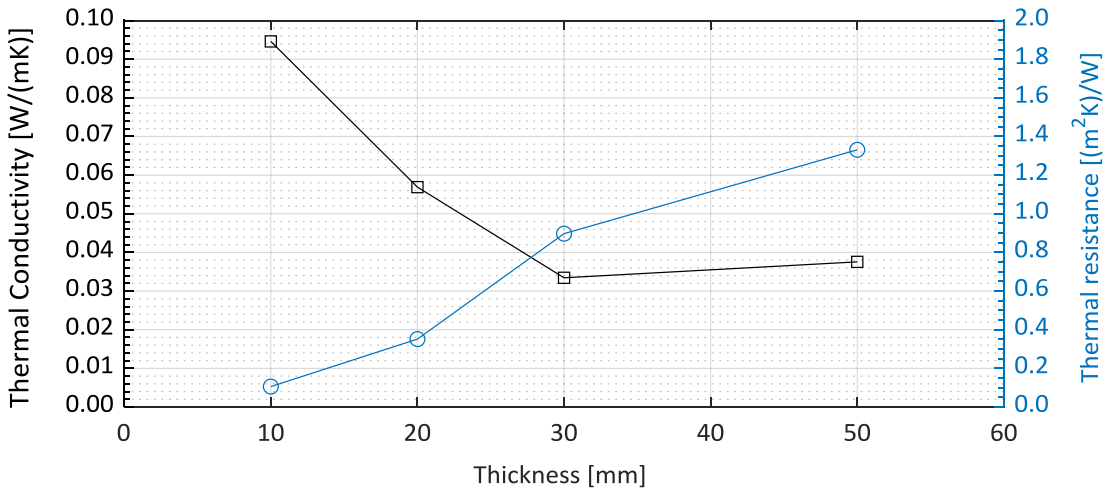

FIGURE 61: THERMAL CONDUCTIVITY AND THERMAL RESISTANCE OF A 50 MM THICK OF MINERAL WOOL UNDER DIFFERENT PRESSURISED THICKNESSES.

The measurements indicated that the pressurised layer of the mineral wool decreases its thermal resistance by 33%. The mean pressurised thickness of this layer is assumed 30mm. For modelling purposes (thermal performance at PnU level and whole building simulation in WP7), this layer is assumed to be 30mm thick mineral wool with thermal conductivity equal to 0.033 W/(mK).

The thermal properties of all incorporated materials for the four types of SmartWall (blank type, SmartWall with window, SmartWall with fan-coil and SmartWall with window and fan-coil) are provided in Table 36.

TABLE 36: THERMAL PROPERTIES OF SMARTWALL (VVV VERSION) MATERIALS.

Material	Thickness [mm]	Thermal Conductivity [W/(m·K)]	Density [kg/m^3]	Specific Heat Capacity [J/(kg·K)]
Steel		60.5	7854	434
Air cavity		0.167[a]	1.1	1000
Gypsum board	12.5	0.20	680	980
Mineral Wool	160	0.035	28	1030
Mineral Wool with aluminium foil	30	0.033	50	1450
Marble sill	10	3.05	2657	508
Vacuum Insulation Panel (VIP)	20	0.0075[b]	195	800

[a] the air can be modelled as solid, taking into account the conduction, convection and radiation heat transfer, according to ISO 6946.
[b] taking into account the edge effect

This project has received funding from the European Union's Horizon 2020 research and innovation programme under grant agreement No 958218

7.1.2 SmartWall version for the Berlin demo site

The Berlin version of the SmartWall is constructed by eco-friendly materials (materials with low embodied energy), replacing the metal skeleton by a timber frame, the cement or gypsum boards by oriented strand board (OSB) and the mineral wool by wood-fibre insulation. Also, in this type of SmartWall, all materials are commercial and their thermal properties are available by the manufacturers.

TABLE 37: THERMAL PROPERTIES OF SMARTWALL (BERLIN VERSION) MATERIALS.

Material layer	Thickness [mm]	Thermal conductivity [W/(m·K)]	Density [kg/m^3]	Specific heat capacity [J/(kg·K)]
Timber frame and studs		0.13	650	1200
Weather board larch (internal surface)	20	0.13	570	2100
Air Cavity	40	0.22 [a]	1.1	1000
Wood fibre board	60	0.048	270	2100
Wood fibre blow-in insulation	240	0.038	30	2100
Vacuum Insulation Panel (VIP)	20	0.0075 [b]	145	1450
Oriented strand board (OSB)	22	0.13	650	2100
Soft wood fibre insulation	60	0.036	60	2100

[a] air can be modelled as solid, taking into account the conduction, convection and radiation heat transfer, according to ISO 6946.
[b] taking into account the edge effect

7.2 eWHC/ConExWall

All materials of eWHC/ConExWall PnU kit are commercial materials and their thermal properties are available by the manufacturers. The thermal properties of the incorporated materials are presented in Table 38.

TABLE 38: THERMAL PROPERTIES OF EWHC MATERIALS.

Material layer	Thickness [mm]	Thermal conductivity [W/(m·K)]	Density [kg/m^3]	Specific heat capacity [J/(kg·K)]
Soft heating board - STEICObase	20	0.047	220	1600
Flexible layer - ISOVER Akustic TP 1	60	0.039	30	800
Gypsum Fibreboard	15	0.32	1150	1100
Insulation - ISOVER Akustic TP 1	180 / 120	0.05	85	1040
Wooden frame - spruce		0.13	450	2300
Insulation - STEICOprotect H	50	0.038	50	2100
Non-ventilated layer in wooden frame	40	0.278	1.1	1000
Wooden cladding - Profilholz	20	0.14	450	1600
Box of ventilation units & L-profiles - Steel	2	20	850	1000
Air inside the ventilation units		0.15 [a]	1.1	1000

[a] The air layer was considered as unventilated layer with thermal resistance equal to 0.18 (m^{2}K)/W, according to ISO 6946.

This project has received funding from the European Union's Horizon 2020 research and innovation programme under grant agreement No 958218

7.3 eAHC/ HybridWall

All materials of eAHC/HybridWall PnU kit are commercial materials and their thermal properties are available by the manufacturers. The thermal properties of the incorporated materials are presented in Table 39.

TABLE 39: THERMAL PROPERTIES OF EAHC MATERIALS.

Material layer	Thickness [mm]	Thermal conductivity [W/(m·K)]	Density [kg/m^3]	Specific heat capacity [J/(kg·K)]
Masonry	80	0.30	900	960
Insulation	50	0.04	20	1270
Enclosed air.	50	0.29	1	1010
Masonry	150	0.32	900	960
Mineral fibres	140	0.04	50	880

7.4 Smart Windows

There are two types of Smart Windows that are used in PLURAL solutions:

- Basic Window: the triple pane window with integrated ventilation system attached on frame which is installed in the SmartWall prototype. This is a certified product of BGTC and it is going to be installed at the real demo buildings (VVV, Terrassa, Kasava).
- Heat Harvesting Window (HHW): an alternative solution of BGTC upgraded within the PLURAL project with integrated heat recovery ventilation system.

The frame material which is investigated in the frame of Task 4.5 is PVC. The thermal and optical properties of the glazing systems were calculated using the Optics6 and WINDOW 7.8 software from Lawrence Berkeley National Laboratory (LBNL). The calculations were made according to European standards EN 673[8] and EN 410[9]. The configurations and calculation results are summarized in Table 40 and Table 41.

[8] EN 673:2011 – Glass in building – Determination of thermal transmittance (U value) – Calculation method
[9] EN 410:2011 – Glass in building – Determination of luminous and solar characteristics of glazing

This project has received funding from the European Union's Horizon 2020 research and innovation programme under grant agreement No 958218

TABLE 40: CONFIGURATIONS OF BASIC AND HEAT HARVESTING GLAZING.

	Basic Window	Heat Harvesting Window
Layer 1	GT SUPERSELEKT 60/27 T on GT EUROFLOAT 6 mm	PLANITHERM XN on PLANICLEAR 4 mm
Gap 1	16 mm Argon (90%)	18 mm Argon (90%)
Layer 2	GT EUROWHITE NG 6 mm	PLANICLEAR 4 mm
Gap 2	12 mm Air (100%)	18 mm Argon (90%)
Layer 3	AGC Planibel G on GT EUROFLOAT 4 mm	PLANITHERM XN on PLANICLEAR 4 mm

TABLE 41: THERMAL AND OPTICAL PROPERTIES OF BASIC AND HEAT HARVESTING GLAZING.

	Basic Window	Heat Harvesting Window
U-value [W/(m^{2}K)]	0.58	0.75
g-value [-]	0.53	0.25
T_{vis} [-]	0.74	0.51

This project has received funding from the European Union's Horizon 2020 research and innovation programme under grant agreement No 958218

8 Building physics – Thermal and hygrothermal performance – PnU level

8.1 Methodology

The thermal performance analysis of the PnU kits was carried out following the ISO 10211:2007, which is a steady state approach aiming to calculate the equivalent thermal transmittance (U-value) or equivalent thermal resistance (R-value) taking into account all thermal bridges. The presence of the metal or wooden frame, the anchoring system, the window or the incorporated heating system create non-negligible thermal bridges.

The equivalent U-value, U_{eq}, taking into account the impact of thermal of thermal bridges is calculated by the equation:

$$U_{eq} = U_{clear} + \frac{\sum_k (\Psi_k \cdot l_k)}{A} + \frac{\sum_n \chi_n}{A}$$

Where U_{clear} is the thermal transmittance without the effect of thermal bridges, calculated according to ISO 6946 standard, Ψ_k expressed in [W/(m·K)] is the linear thermal transmittance of the linear thermal bridges, l_k [m] is the length over the which the Ψ_k value applies, χ_n expressed in [W/K] is the point thermal transmittance of the point thermal bridges and A [m^2] is the total surface of the PnU kit.

The U_{clear} is calculated based on the ISO 6946 and the material properties provided in material level analysis, section 7.

$$U_{clear} = \frac{1}{R_{si} + \sum_{i=1}^{N} \frac{d_i}{k_i} + R_{se}}$$

Where d_i is the thickness of layer i, k_i is the thermal conductivity of the material of layer *I*, N is the number of layers, R_i and R_e are the internal and external surface thermal resistances, respectively. Typical values for the surface thermal resistances of a wall are 0.13 (m^2K)/W for the internal surface and 0.04 (m^2K)/W for the external surface, according to ISO 6946 standard.

The air cavity layers of PnUs are considered as equivalent solid layer with thermal resistance depended on layer thickness, according to ISO 6946. This thermal resistance takes into account both the convention and radiation the heat transfer into the layer.

For the calculation of the equivalent thermal transmittance/resistance of each PnU, each type of PnU is simulated by means of the commercial CFD package (COMSOL and ANSYS) in steady state conditions. The boundary conditions are summarized in Table 42.

TABLE 42: BOUNDARY CONDITIONS.

Boundary Condition	SmartWall - VVV	SmartWall - Berlin	eWHC	eAHC
Outdoor temperature	0°C	-10°C	-15°C	2°C
Indoor temperature	20°C	20°C	20°C	22°C
External heat transfer coefficient, h_{out}	25 W/(m^2K)			
Internal heat transfer coefficient for walls, h_{in}	7.69 W/(m^2K)			

This project has received funding from the European Union's Horizon 2020 research and innovation programme under grant agreement No 958218

The total heat flow, *Q*, which passes through each PnU configuration, is obtained by the simulation results. Hence, the equivalent U-value, U_{eq}, is calculated by the following equation:

$$U_{eq,PnU} = \frac{Q}{A_{PnU}(T_{in} - T_{out})}$$

For the geometries which include window or glass door, the equivalent U-value is calculated by the equation:

$$U_{eq,PnU} \cdot A_{PnU} = U_{eq,opWall} \cdot A_{opWall} + U_{Window} \cdot A_{Window}$$

Where U_{opWall} is the equivalent thermal transmittance of the opaque area of PnU, including the effect of all thermal bridges and A_{wall} the opaque area of SmartWall (area without the window opening), U_{win} and A_{wind} are the U-value and the window area (including the glass and the frame).

The hygrothermal behaviour of thermal bridges is assessed by means of the temperature factor, f_{Rsi}. The temperature factor at the internal surface, f_{Rsi} or f, is an indicator which is usually used for the thermal performance of thermal bridges. The f_{Rsi} expresses the relation of the thermal resistance of the envelope element (R_{tot}) to the thermal resistance of the element without the impact of the surface thermal resistance (R_{si}). Hence, it is defined as the difference between the internal surface temperature (T_{si}) and the outdoor temperature (T_{out}), divided by the difference between the indoor (T_{in}) and outdoor temperature. The temperature factor, f_{Rsi} (-), for a given surface resistance, R_{si}, is calculated by the following equation:

$$f_{R_{si}} = \frac{R_{tot} - R_{si}}{R_{tot}} = \frac{T_{si} - T_{out}}{T_{in} - T_{out}}$$

The temperature factor is also an indicator of the hygro-thermal performance of all types of thermal bridges. Mold growth is expected, when the relative humidity on a surface is higher than 80% for several days. The mold growth is avoided when the temperature factor is greater than a critical value depended on the building use and the consequent indoor relative humidity. The higher the desired indoor relative humidity, the higher the critical temperature factor will be in order to eliminate the likelihood of condensation and mold growth. For residential buildings, a typical value of the critical temperature factor is 0.7[10], however, national standards have set the lower limits for the temperature factor to be ranged between 0.65 to 0.75[11].

8.2 SmartWall

8.2.1 SmartWall version for the Voula (VVV) demo site

8.2.1.1 Geometries

There are four SmartWall types, depending on the presence of fan-coil and/or window:

- Type A – The module does not contain a fan-coil or window (Blank Type).
- Type B - The module contains a window, but it does not contain any fan-coil.
- Type C - The module contains a fan-coil but it does not contain any window.

[10] DIN 4108-2:2013, Thermal protection and energy economy in buildings - Part 2: Minimum requirements to thermal insulation.
[11] T. Kalamees, Critical values for the temperature factor to assess thermal bridges Proceedings of the Estonian Academy of Sciences, 12 (3-1) (2006) 219-229

This project has received funding from the European Union's Horizon 2020 research and innovation programme under grant agreement No 958218

- Type D - The module contains both a fan-coil and a window.

All types simulated with dimensions 1200 mm in length and 2500 mm in height and they are considered to be installed on the internal side of an existing wall. The SmartWall types are designed based on the ones that are going to be installed at VVV demo case. The materials of the SmartWall are anchored on two frames made by Hollow Rectangular Section (HRS) structural steel members with section 50x30mm and 1.8 mm thick. Spacers made by the heat breaker structure are placed in the fixing points to ensure movement treatment, except from the bottom side where the spacers are made from HRS frame, for statical reasons. The space between the frames (160 mm width) is filled with mineral wool. A gypsum board layer (12.5 mm thick) covers the internal side of SmartWall, while a mineral wool layer with aluminum foil (30 mm thick, as analysed in section 7.1.1) is placed on the opposite side that rests against the existing envelope. Moreover, in the cases where the fan-coil exists, a Vacuum Insulation Panel (VIP) layer, 20mm thick, is installed at the back side of the fan-coil. The rest area behind the fan-coil is air cavity. To simplify the models, the fan-coil and Toolbox is simulated as boxes with 2 mm thick metal case and an equivalent material based on the in-situ U-value measurements of the section 9.3.2.2).

The window frame is assumed to be made by aluminum, with U_f= 1.4 W/(m^{2}K), while the glassing system is assumed as double pane Argon filled with U_g= 1.2 W/(m^{2}K). The thermal transmittance of the overall window is equal to U_w= 1.29 W/(m^{2}K). The windows do not contain a blind box. All simulated geometries are illustrated in Figure 62.

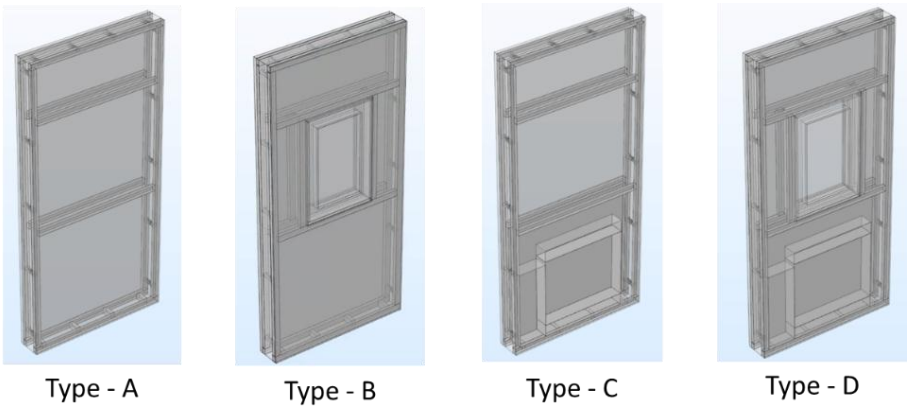

FIGURE 62: THE FOUR SIMULATED GEOMETRIES OF SMARTWALL – VVV VERSIONS.

Based on the above and the material properties of Table 36, the thermal transmittance of the blank type SmartWall, without consider any thermal bridge, $U_{clear,SW}$, is calculated according to ISO 6946[12] equal to $U_{clear,SW}$ =0.176 W/(m^{2}K).

8.2.1.2 Results

Table 43 summarizes the equivalent thermal transmittance (U_{eq}) and thermal resistance (R_{eq}) of the whole SmartWall (including the window, $U_{eq,SW}$ or $R_{eq,SW}$) and the opaque wall (excluding the window, $U_{eq,opWall}$ or $R_{eq,opWall}$). It is observed that the U-value of the opaque wall increased by:

- 0.05 W/(m^{2}K) due to the presence of metal frame,
- 0.05 W/(m^{2}K) due to the presence of window,

[12] ISO 6946:2017, Building components and building elements — Thermal resistance and thermal transmittance — Calculation methods.

This project has received funding from the European Union's Horizon 2020 research and innovation programme under grant agreement No 958218

- 0.03 W/(m^{2}K) due to the presence of fan-coil

The hygrothermal performance of thermal bridges is also presented in Table 43 by means of temperature factor, f. For each case, the temperature factor is higher than 0.7, indicating that there is not any moisture issue at the internal surface of the four types of SmartWall.

TABLE 43: THERMAL TRANSMITTANCE OF ALL TYPES OF SMARTWALL, INCLUDING THE EFFECT OF THERMAL BRIDGES.

SmartWall type	$U_{eq,SW}$ [W/(m^{2}K)]	$R_{eq,SW}$ [m^{2}K/W]	$U_{eq,opWall}$ [W/(m^{2}K)]	$R_{eq,opWall}$ [m^{2}K/W]	Increase of U-value		Temperature factor f [-]
					[W/(m^{2}K)]	[%]	
Type A	0.23	4.21	**0.23**	4.21	0.05	29%	0.87
Type B	0.46	2.02	**0.28**	3.42	0.10	58%	0.85 / 0.73 [a]
Type C	0.25	3.80	**0.25**	3.80	0.08	43%	0.89
Type D	0.48	1.92	**0.31**	3.09	0.13	74%	0.85 / 0.73[a]

[a] including the window area.

Figure 63 presents the simulated geometry of SmartWall - type A in COMSOL environment, the temperature and U-value contour at steady state conditions. It is obvious that this type does not contain severe thermal bridges creating an almost homogenous surface temperature. The presence of metal structure increases the equivalent U-value by 29% (from U_{clear}=0.18 W/(m^{2}K) to U_{eq}=0.23 W/(m^{2}K)) or 0.05 W/(m^{2}K). The use of HRS spacers at the bottom side of the SmartWall (this was selected for statical reasons) creates more severe thermal bridges than the use of heat breakers, since the U-value at the frame area of bottom side reaches up to 1 W/(m^{2}K), while the U-value at the rest frame area is up to 0.5 W/(m^{2}K).

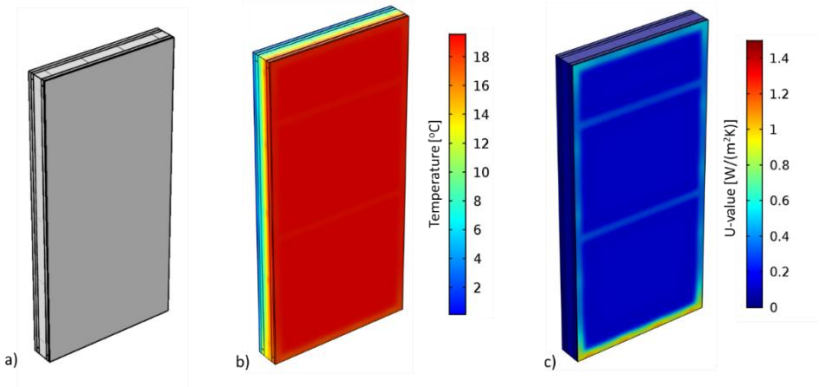

FIGURE 63: MODEL OF SMARTWALL TYPE A: A) GEOMETRY, B) TEMPERATURE AND C) U-VALUE CONTOUR.

Figure 64 presents the simulated geometry of type B, the temperature and the U-value contour at steady state conditions. It is obvious that the presence of window and metal structure create thermal bridges, increasing the wall U-value by 56% (from U_{clear}=0.18 W/(m^{2}K) to U_{eq}=0.28 W/(m^{2}K)).

This project has received funding from the European Union's Horizon 2020 research and innovation programme under grant agreement No 958218

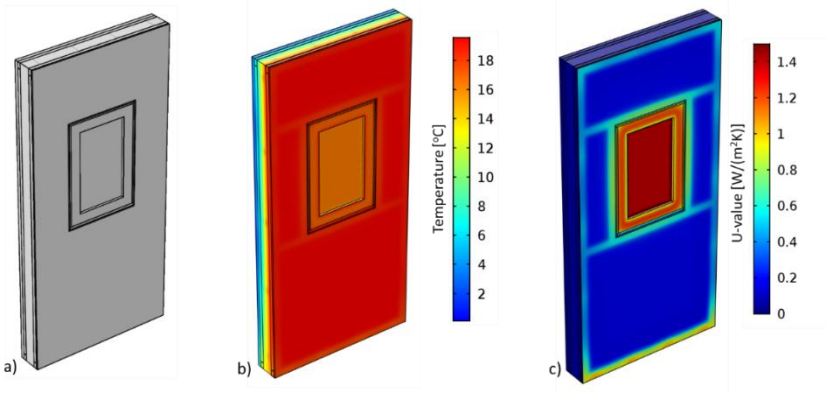

FIGURE 64: MODEL OF THE SMARTWALL TYPE B: A) GEOMETRY, B) TEMPERATURE AND C) U-VALUE CONTOUR.

Figure 65 presents the simulated geometry of type C (without the internal gypsum board to be visible the fan-coil and toolbox), the temperature and the U-value contour at steady state conditions. The presence of metal structure and fan-coil creates significant thermal bridges, increasing the wall U-value by 43% (from U_{clear}=0.18 W/(m^{2}K) to U_{eq}= 0.25 W/(m^{2}K)). It is shown that the presence of fan-coil increases the equivalent U-value by 10%, compared with the blank type SmartWall (type A).

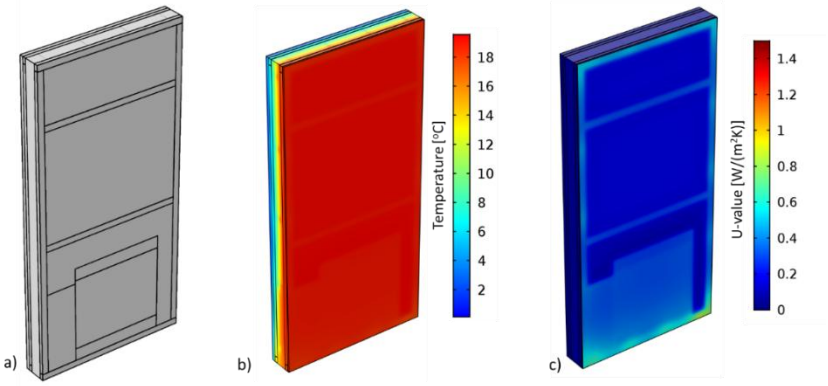

FIGURE 65: MODEL OF THE SMARTWALL TYPE C: A) GEOMETRY AND B) TEMPERATURE CONTOUR.

Figure 66 presents the simulated geometry of type D, the temperature and the U-value contour at steady state conditions. It is obvious that the presence of window, metal structure and fan-coil create thermal bridges, increasing the wall U-value by 72% (from U_{clear}=0.18 W/(m^{2}K) to U_{eq}= 0.30 W/(m^{2}K)).

This project has received funding from the European Union's Horizon 2020 research and innovation programme under grant agreement No 958218

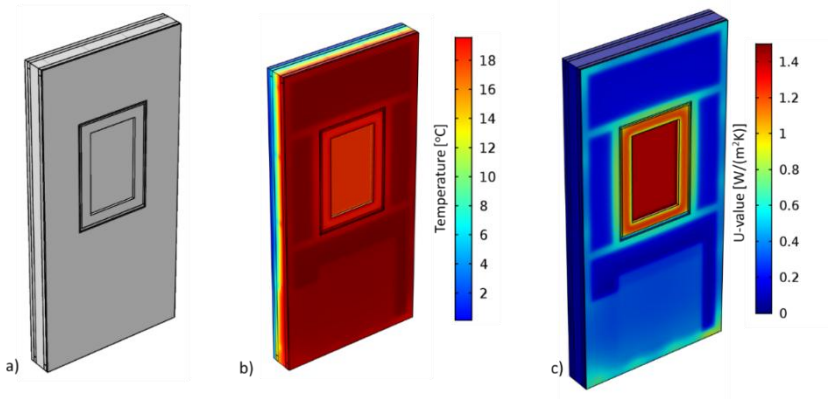

FIGURE 66: MODEL OF THE SMARTWALL TYPE D: A) GEOMETRY AND B) TEMPERATURE CONTOUR.

A parametric analysis was carried out in terms the use of different material and thickness of the insulation layer behind the fan-coil. The use of VIP and aerogel was investigated for thickness from 5 to 40 mm. It is reminded that the thickness of fan-coil is 116mm, so the space for insulation behind it is only 44mm. The thermal conductivity of VIP is assumed equal with 0.0075 W/(m·K), while the thermal conductivity of aerogel is assumed equal with 0.015 W/(m·K). Figure 67 illustrates the U-value of the opaque area of the SmartWall – Type D (the module that contains both a fan-coil and a window) for different insulation material and thickness. The 20mm thick VIP of the initial SmartWall design is thermally equivalent with the double thick (40mm) of aerogel. Also, the doubling of VIP thick (from 20 to 40 mm) results a reduction of U-value by 13%.

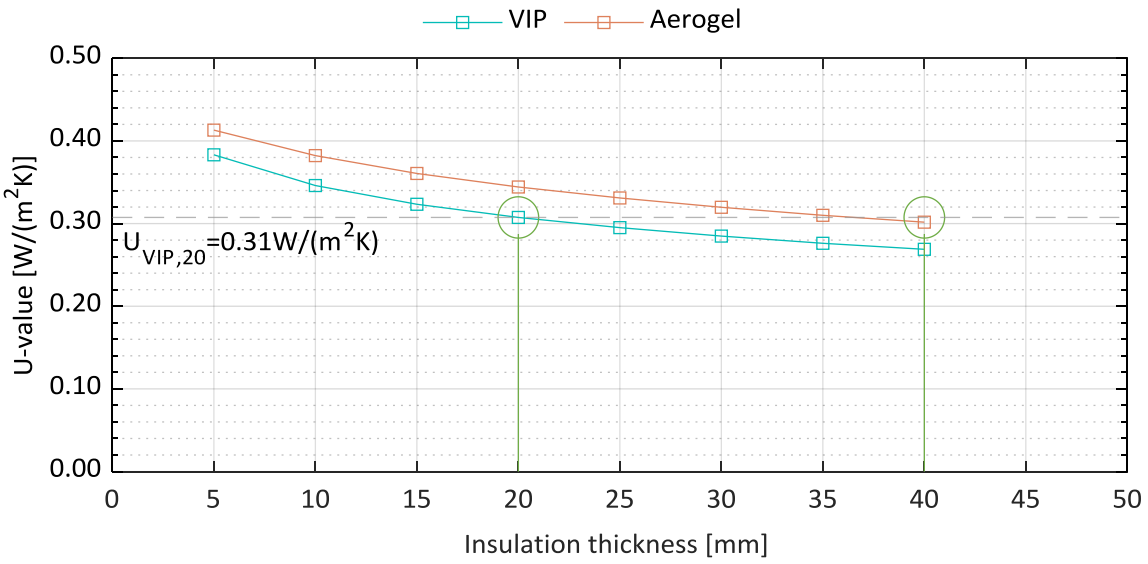

FIGURE 67: U-VALUES FOR DIFFERENT THICKNESSES OF VIP AND AEROGEL BEHIND THE FAN-COIL

This project has received funding from the European Union's Horizon 2020 research and innovation programme under grant agreement No 958218

8.2.2 SmartWall version for the Berlin demo site

8.2.2.1 Geometries

Based on the partitioning of walls at Berlin demo case, there are five SmartWall types, depending on the presence of fan-coil, window and/or ducting system:

- Type A - The module does not contain a fan-coil or window (Blank Type).
- Type B - The module contains a window, but it does not contain any fan-coil.
- Type C - The module contains a fan-coil but it does not contain any window.
- Type D - The module contains both a fan-coil and a window.
- Type E - The module contains both a fan-coil and a window, as well as ducting system.

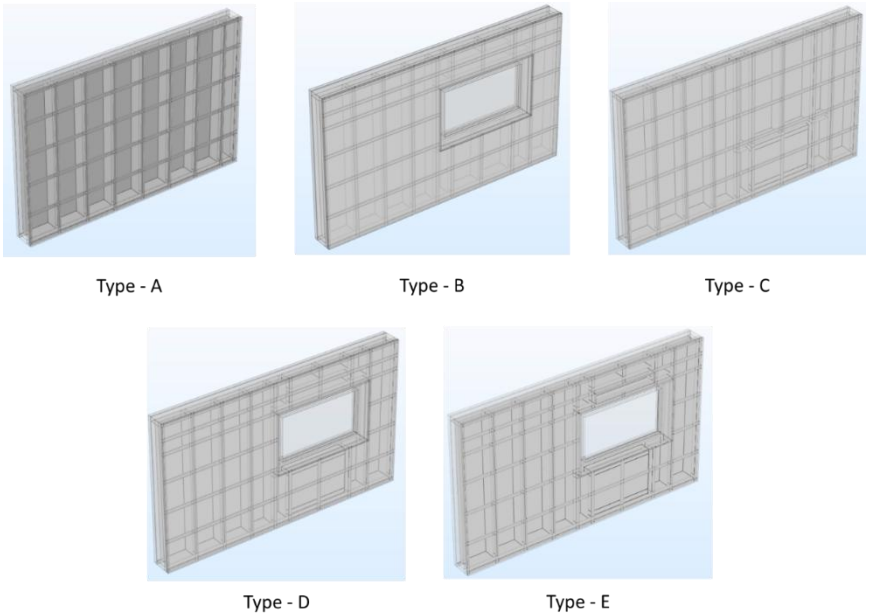

FIGURE 68: THE FOUR SIMULATED GEOMETRIES OF SMARTWALL – BERLIN VERSION.

All simulated geometries, illustrated in Figure 68, have with dimensions 4767 mm in length and 3113 mm in height (typical and representative dimensions for Berlin demo) and they are considered to be installed on the external side of an existing wall. Figure 69 illustrates the layer configuration of the Berlin version of SmartWall. The materials of the SmartWall are anchored on a timber frame with vertical studs with section 240 x 80mm and stud spacing equal to 625 mm. The gap inside the frame is filled with wood fibre blow in insulation (240mm thick). One layer of oriented strand board (OSB), 22 mm thick, and one layer of soft wood fibre insulation, 60 mm thick, are installed at the internal side of the frame (the side which is in touch with the existing wall). One layer of wood fibre board, 60 mm thick, is placed at the external side of frame. A ventilated timber frame made by timber batten and timber counter batten (20 x 60mm) is placed at the external side of the wood fibre board. A layer of weather board larch is anchored on the second timber frame finishing the external side of the SmartWall. Moreover, in the cases where the fan-coil exists, a Vacuum Insulation Panel (VIP) layer, 20mm thick, is installed at the back side of the fan-coil. The remaining area behind the fan-coil is air cavity. The window frame is assumed to be wood-aluminum, with U_f= 1.4 W/(m^{2}K), while the glassing system is assumed as triple pane Argon filled with U_g= 0.58 W/(m^{2}K). The thermal

This project has received funding from the European Union's Horizon 2020 research and innovation programme under grant agreement No 958218

transmittance of the overall window is equal to U_w= 0.89 W/(m^{2}K). The ducting system assumed to be a box with metal case and still air, without be operated.

Based on the above and the material properties of Table 37, the thermal transmittance of the blank type SmartWall, without consider any thermal bridge, $U_{clear,SW}$, is calculated according to ISO 6946[13] equal to $U_{clear,SW}$ =0.101 W/(m^{2}K).

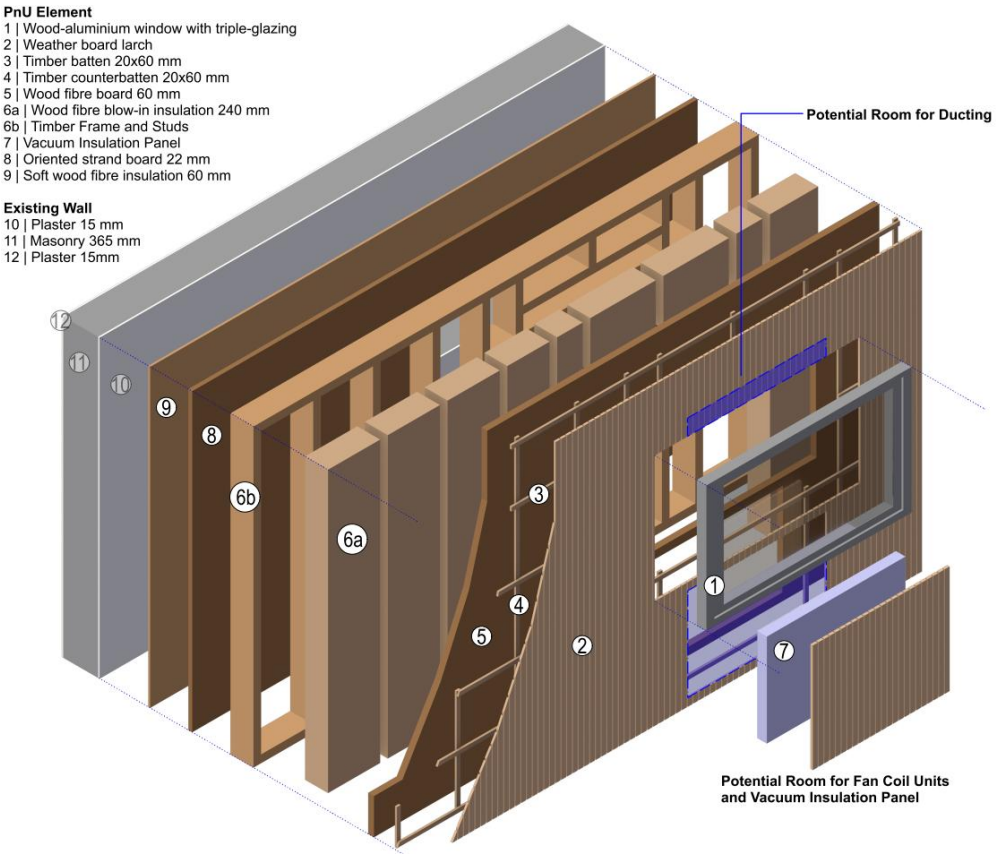

FIGURE 69: EXPLODED VIEW OF THE BERLIN VERSION OF SMARTWALL.

8.2.2.2 Results

Table 44 summarizes the equivalent thermal transmittance (U_{eq}) and thermal resistance (R_{eq}) of the whole SmartWall (including the window, $U_{eq,SW}$ or $R_{eq,SW}$) and the opaque wall (excluding the window, $U_{eq,opWall}$ or $R_{eq,opWall}$). It is observed that the U-value of the opaque wall increased by:

- 0.02 W/(m^{2}K) due to the presence of timber frame,
- 0.04 W/(m^{2}K) due to the presence of window,
- 0.01 W/(m^{2}K) due to the presence of fan-coil
- 0.06 W/(m^{2}K) due to the presence of ducting system

[13] ISO 6946:2017, Building components and building elements — Thermal resistance and thermal transmittance — Calculation methods.

This project has received funding from the European Union's Horizon 2020 research and innovation programme under grant agreement No 958218

The hygrothermal performance of thermal bridges is also presented in Table 44 by means of the temperature factor, f. For the cases without a window and/or ducting system, the temperature factor is high (0.97) indicating that there is not any moisture issue. However, the temperature factor for the types B and D is 0.80 for the wall area while the type E as long as the frame areas of types B and D present low values for the temperature factor (0.65 - 0.63). However, it should be mentioned that these values concern the internal surface of the SmartWall and not the internal surface of the whole renovated wall (including the existing wall). So, as the lowest values of the temperature factor are close to the standard limit (0.7), the temperature factor including the existing wall will be higher than this limit, indicating that there is a low possibility for moisture issues.

TABLE 44: THERMAL TRANSMITTANCE OF ALL TYPES OF SMARTWALL-BERLIN VERSION, INCLUDING THE EFFECT OF THERMAL BRIDGES.

SmartWall type	$U_{eq,SW}$ [W/(m²K)]	$R_{eq,SW}$ [m²K/W]	$U_{eq,opWall}$ [W/(m²K)]	$R_{eq,opWall}$ [m²K/W]	Increase of U-value		Temperature factor f [-]
					[W/(m²K)]	[%]	
Type A	0.12	8.07	**0.12**	8.07	20%	0.02	0.98
Type B	0.28	3.38	**0.16**	6.01	60%	0.06	0.80/ 0.65 [a]
Type C	0.13	7.74	**0.13**	7.74	25%	0.03	0.97
Type D	0.29	3.32	**0.17**	5.80	66%	0.07	0.80/ 0.65 [a]
Type E	0.34	2.77	**0.23**	4.15	130%	0.13	0.63

[a] including the window area.

Figure 70 shows the temperature and U-value contour at steady state conditions of the simulated geometry of SmartWall - type A, in COMSOL environment. It is obvious that this type does not contain severe thermal bridges creating an almost homogenous surface temperature, since the internal surface temperature of the stud area is ca. 0.2 K lower than the area between the studs. Also, the ventilated timber frame at the external side of the SmartWall (made by timber batten and timber counter batten) creates negligible thermal bridge. The presence of timber structure increases the equivalent U-value by 20% (from U_{clear}=0.10 W/(m²K) to U_{eq}=0.12 W/(m²K)) or 0.02 W/(m²K). The U-value between at the stud area reaches up to 0.26 W/(m²K), while it is 0.10 W/(m²K) between the studs.

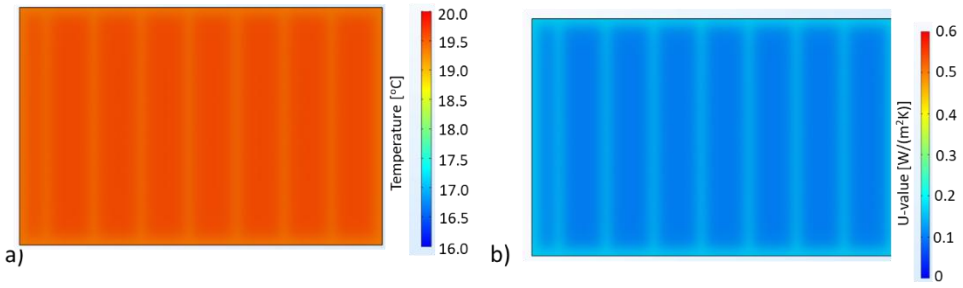

FIGURE 70: BERLIN VERSION OF SMARTWALL - TYPE A: A) TEMPERATURE AND B) U-VALUE CONTOUR.

Figure 71 shows the temperature and U-value contour at steady state conditions of the simulated geometry of SmartWall - type B. The presence of window and timber structure create thermal bridges, increasing the wall U-value by 60% or 0.06 W/(m²K) (from U_{clear}=0.10 W/(m²K) to U_{eq}=0.16 W/(m²K)). Removing the contribution of timber frame (0.02 W/(m²K)), it can be assumed that the presence of window increases the U-value by 0.04 W/(m²K).

This project has received funding from the European Union's Horizon 2020 research and innovation programme under grant agreement No 958218

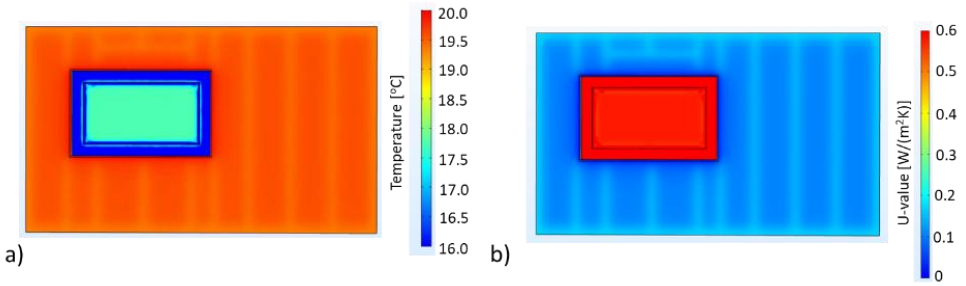

FIGURE 71: BERLIN VERSION OF SMARTWALL - TYPE B: A) TEMPERATURE AND B) U-VALUE CONTOUR.

Figure 72 presents the temperature and U-value contour at steady state conditions of the simulated geometry of SmartWall - type C. The presence of fan-coil and timber structure create thermal bridges, increasing the wall U-value by 25% or 0.03 W/(m^{2}K) (from U_{clear}=0.10 W/(m^{2}K) to U_{eq}=0.13 W/(m^{2}K)). Removing the contribution of timber frame (0.02 W/(m^{2}K)), it can be assumed that the presence of fan-coil increases the U-value by only 0.01 W/(m^{2}K).

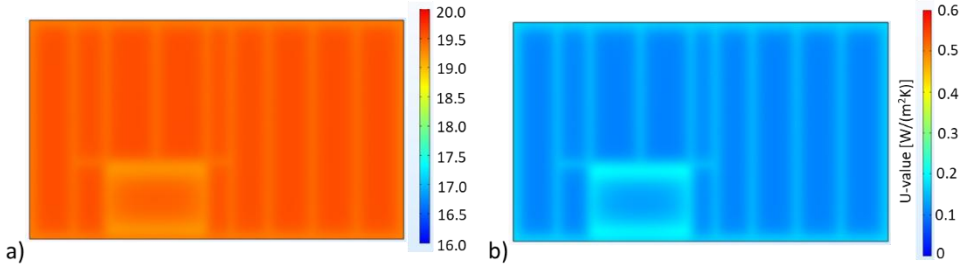

FIGURE 72: BERLIN VERSION OF SMARTWALL - TYPE C: A) TEMPERATURE AND B) U-VALUE CONTOUR.

Figure 73 illustrates the temperature and U-value contour at steady state conditions of the simulated geometry of SmartWall - type D. The presence of window, fan-coil and timber structure create thermal bridges, increasing the wall (opaque area) U-value by 66% or 0.07 W/(m^{2}K) (from U_{clear}=0.10 W/(m^{2}K) to U_{eq}=0.17 W/(m^{2}K)).

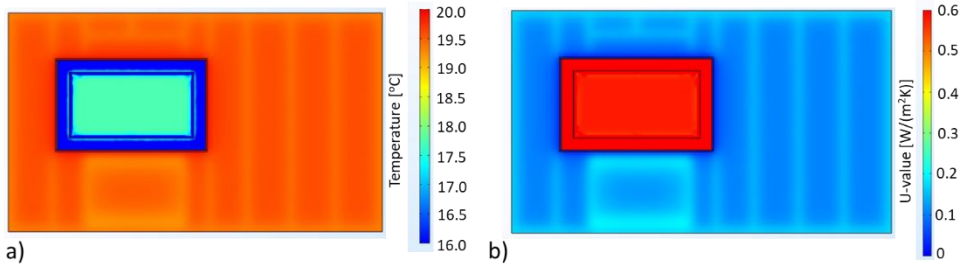

FIGURE 73: BERLIN VERSION OF SMARTWALL - TYPE D: A) TEMPERATURE AND B) U-VALUE CONTOUR.

Figure 74 shows the temperature and U-value contour at steady state conditions of the simulated geometry of SmartWall - type E. The presence of ducting system, window, fan-coil and timber structure create thermal bridges, increasing the wall U-value by 130% or 0.13 W/(m^{2}K) (from U_{clear}=0.10 W/(m^{2}K) to U_{eq}=0.23 W/(m^{2}K)). The ducting system creates significant thermal bridges, but when the system is operated, the temperature at this area will be significant higher eliminating

This project has received funding from the European Union's Horizon 2020 research and innovation programme under grant agreement No 958218

the impact of thermal bridges and the moisture issues. Removing the contribution of timber frame (0.02 W/(m^{2}K)), window (0.04 W/(m^{2}K)) and fan-coil (0.01 W/(m^{2}K)), it can be assumed that the presence of ducting system increases the U-value by only 0.06 W/(m^{2}K).

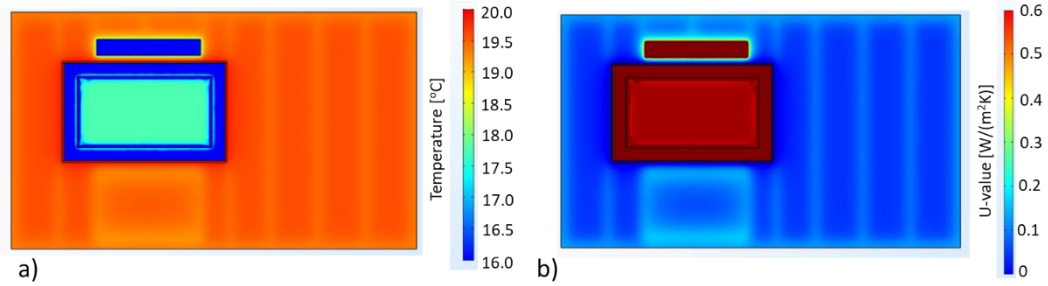

FIGURE 74: BERLIN VERSION OF SMARTWALL - TYPE E: A) TEMPERATURE AND B) U-VALUE CONTOUR.

8.3 eWHC/ConExWall

8.3.1 Geometry

The thermal and hygrothermal performance of eWHC/ConExWall PnU kit is investigated in a representative geometry, in accordance to the PnUs that are to be installed in the KASAVA demo case. The PnU geometry has dimensions 7.035 m length and 3.400 m height it is considered to be installed on the external side of an existing wall. The internal side of the ConExWall is a 20mm layer of wood fibre board with embodied heating pipes and a 60mm thick of Isover Orsik insulation (Isover Akustik TP1). Next, a layer of 50mm thick gypsum board (Farmacell) is anchored on a timber frame with vertical studs with section 180 x 80mm and stud spacing equal to 750 - 650 mm. The gap inside the frame is filled with ISOVER Akustik TP 1insulation (180mm thick), while a layer of hard wood insulation (STEICOprotect H) 50 mm thick is anchored on the external side of the frame. A 40mm thick ventilated timber frame is placed at the external side of the STEICOprotect layer, while a layer of 20mm thick wooden cladding (profiholz) is placed on the finishing layer of PnU. The anchoring system of the ConExWall consists of L-shaped (200 x 190 mm and 15mm thick) metal profiles with spacing 1.19 m that penetrates the PnU and anchored on the existing wall. The under-investigation PnU contains two windows (3.95 m^2 area each window) and two ventilation systems. The window frame is assumed to be wood-aluminum, with U_f= 1.4 W/(m^{2}K), while the glassing system is assumed as triple pane Argon filled with U_g= 0.58 W/(m^{2}K). The thermal transmittance of the overall window is equal to U_w= 0.74 W/(m^{2}K). The ventilated system assumed to be a box with metal case and still air, without be operated. For the thermal performance analysis of ConExWall, the vapor barriers are excluded. The eWHC geometry is constructed in COMSOL software, as depicted in Figure 75.

Based on the above and the material properties of Table 38, the thermal transmittance of the blank type SmartWall (for 180mm insulation thick), without consider any thermal bridge, $U_{clear,eWHC}$, is calculated according to ISO 6946[14] equal to $U_{clear,\ eWHC}$ =0.125 W/(m^{2}K). Assuming a 500mm thick of existing wall and thermal conductivity k=0.81 W/(m·K), the thermal transmittance of the renovated wall is $U_{clear,Wall\_eWHC}$ =0.116 W/(m^{2}K).

[14] ISO 6946:2017, Building components and building elements — Thermal resistance and thermal transmittance — Calculation methods.

This project has received funding from the European Union's Horizon 2020 research and innovation programme under grant agreement No 958218

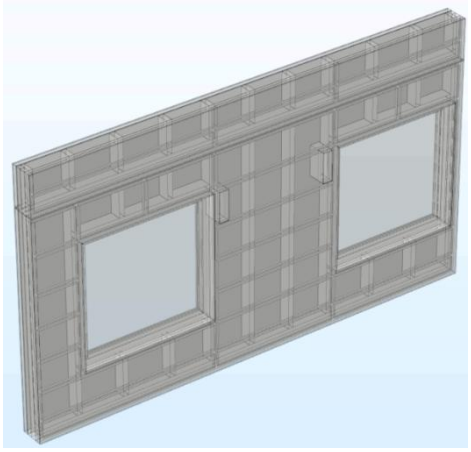

FIGURE 75: THE SIMULATED EWHC GEOMETRY IN COMSOL SOFTWARE.

8.3.2 Piping layer

For the thermal and hygrothermal analysis of ConExWall, the piping system considered to be in passive mode, meaning that the water temperature is changed depending on the boundary conditions. However, due to the complexity of the geometry, the heating pipes are impossible to be simulated along with the whole ConExWall geometry. For this reason, the contribution of heating pipes is calculated in the layer of wood fibre board. The layer is simulated with the heating pipes and an equivalent thermal conductivity is calculated taking into account the effect of water and piping system, according to the following equation:

$$k_{eq} = \frac{d_{layer}}{\frac{A \cdot (T_{in} - T_{out})}{Q} - \frac{1}{h_{in}} - \frac{1}{h_{out}}}$$

where d_{layer} equal with the layer of the soft heating board (20mm), Q the heat that penetrate the soft heating layer in [W], A the total area of the equivalent layer in [m^2] and T_{in}, T_{out}, h_{in} and h_{out} are the boundary conditions according to the Table 42.

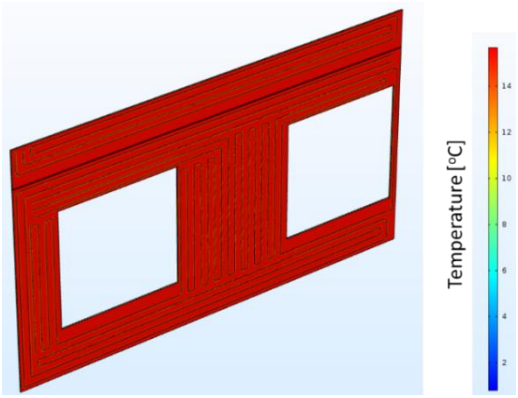

FIGURE 76: THE WOOD FIBRE BOARD EMBODIED WITH HEATING PIPES.

The wood fibre board was simulated with and without the embodied heating pipes. In the first case the average heat flow of the layer is 58.78 W/m^2, while in the second case (with the piping system) the average heat flow is increased by 4.83 W/m^2 (Table 45). This increase can be achieved if in the first case (layer without the heating pipes) the thermal conductivity is 0.053 W/(m·K) instead of 0.047 W/(m·K). So, the complex

This project has received funding from the European Union's Horizon 2020 research and innovation programme under grant agreement No 958218

geometry of the wood fibre board (k=0.047 W/m·K) with the water heating pipes can be replaced by another layer with thermal conductivity equal with 0.053 W/(m·K) without heating pipes.

TABLE 45: OUTCOMES OF THE ANALYSIS OF WOOD FIBRE BOARD WITH AND WITHOUT THE PIPING SYSTEM.

Geometry	Heat [W]	Thermal conductivity [W/(m·K)]
Wood fibre board without heating pipes	1187.85	0.047
Wood fibre board with heating pipes	1285.50	0.053

8.3.3 Results

Table 46 summarizes the equivalent thermal transmittance (U_{eq}) and thermal resistance (R_{eq}) of the whole ConExWall (including the window, $U_{eq,eWHC}$ or $R_{eq,eWHC}$) and the opaque wall (excluding the window, $U_{eq,opeWHC}$ or $R_{eq,opeWHC}$) for two different insulation thicknesses: 120 mm and 180 mm. It is observed that the presence of ventilation units, anchoring system, window and wooden frame almost double the U-value of the opaque wall. The wooden frame increases the U-value by ca. 0.02 W/(m^{2}K), while the anchoring system, the ventilation unit and the window further increase the U-value by 0.10 W/(m^{2}K).

The hygrothermal performance of thermal bridges is also presented in Table 46 by means of temperature factor, f. For both insulation thicknesses, the temperature factor is higher than 0.6, however when the existing wall is including the temperature factor is close to 0.7.

TABLE 46: THERMAL TRANSMITTANCE OF EWHC (WITHOUT THE EXISTING WALL) FOR TWO INSULATION THICKNESSES, INCLUDING THE EFFECT OF THERMAL BRIDGES.

Insulation thickness [mm]	$U_{clear,eWHC}$ [W/(m^{2}K)]	$U_{eq,opeWHC,noVent}$ [a] [W/(m^{2}K)]	$U_{eq,opeWHC}$ [b] [W/(m^{2}K)]	$U_{eq,eWHC}$ [c] [W/(m^{2}K)]	Temperature factor f [-]
120	0.153	0.17	0.27	0.40	0.60 / 0.67[d]
180	0.125	0.15	0.25	0.38	0.62 / 0.68[d]

[a] area away from windows, ventilation units and anchoring system.
[b] excluding windows.
[c] including windows.
[d] including the existing wall.

Figure 77 presents the temperature and the U-value contours of the internal side (surface that is in touch with the existing wall) of eWHC kit, for 180 mm insulation thickness. Except from the window area, whose U-value is much higher that the opaque wall, the ventilation units and the air gap in the hight of anchoring system (L-profiles) create significant thermal bridges providing temperature lower than 15°C. It is mentioned, that the temperature of the water inside the heating layer and the air temperature of the ventilation unit is free (assuming that the systems are not in operation mode - passive mode).

This project has received funding from the European Union's Horizon 2020 research and innovation programme under grant agreement No 958218

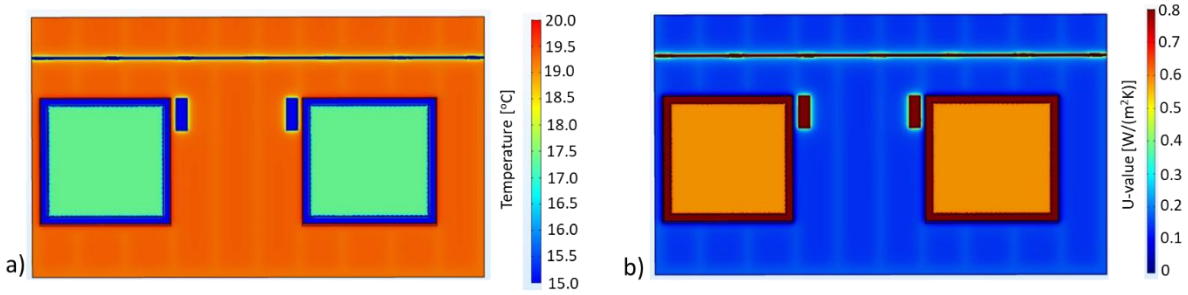

FIGURE 77: THE TEMPERATURE AND THE U-VALUE CONTOUR OF THE SIMULATED GEOMETRY AT THE INTERNAL SIDE.

Figure 78 presents the temperature contour at a cross section at the location of anchoring system (L-profiles) for 180 mm insulation thickness. The 15mm gap at the area of L-profile is usually air and this creates significant thermal bridge, as mentioned in Figure 77. If this gap is filled with insulation (such as PUR), this thermal bridge is eliminated, reducing the U-value of the renovated opaque wall (including the existing wall) by 0.02 W/(m^{2}K) (from 0.24 to 0.22 W/(m^{2}K)) or 8%. The installation of insulation at this gap also reduces the possibility of moisture issues in this area.

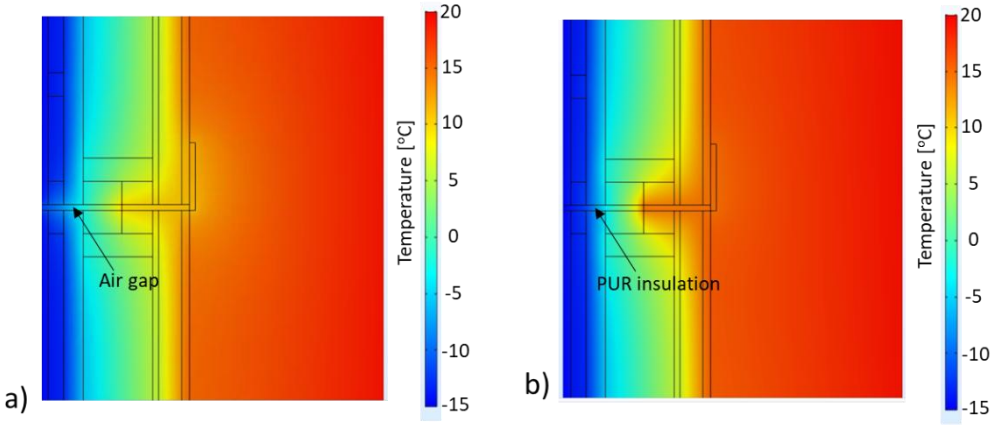

FIGURE 78: THE TEMPERATURE CONTOURS AT THE L-PROFILE AREA A) WITH AIR GAP AND B) WITH INSULATION.

8.4 eAHC/HybridWall

The aim of the simulations was to determine the effect of the AHU (Air Handling Unit) on the heat transfer coefficient (U-value) of the building envelope. When AHUs were installed at the level of the thermal insulation of the envelope, a reduction in thermal insulation parameters and a local decrease in the internal surface temperature of the wall could be expected.

8.4.1 Development of the model

Simulations were performed in ANSYS Fluent. A typical perimeter wall section of 2.9 m x 2 m (height x sparsity) was modelled. The model included the different layers of the structure (wall, thermal insulation layers, closed air cavity and possibly also AHU). As this was a ventilated insulation system with an air gap in front of the thermal insulation, the external cladding was not considered in the

This project has received funding from the European Union's Horizon 2020 research and innovation programme under grant agreement No 958218

model. The AHU has also been simplified for the model (removed fans, control system and heat exchangers). The geometry of the model can be seen in Figure 79.

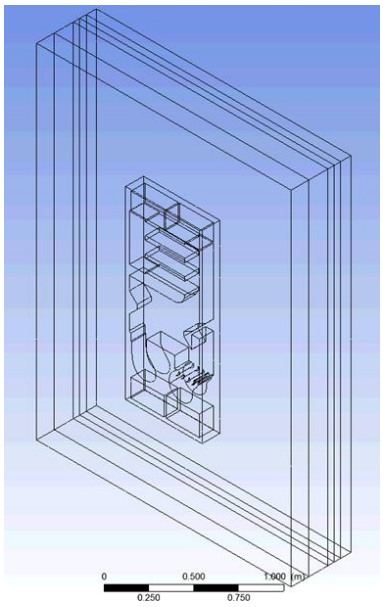

FIGURE 79: GEOMETRY OF THE MODEL.

The simulation was carried out in 3 variants:

- For the wall without AHU (reference variant)
- For the wall with AHU (in operation)
- For wall with AHU unit (off)

The dimensions of wall model are 2 metres (width) and 2.7 metres (height) - Aw = 5.4 m^2. The dimensions of the AHU are 0.6 metres (width) and 1.5 metres (height) – AREK = 0.9 m^2. The simulations were performed for an interior temperature of 22°C and an exterior temperature of 2°C. The anchoring system of the building envelope was not modelled and was accounted for in the final values by a surcharge U-value of 0.02 W/m^2K. Thermal resistance in AHU channels (AHU on) RAHU was assumed equal with 0.01 (m^2K)/W. The material properties and the boundary conditions are shown in previous sections in Table 39 and Table 42, respectively.

8.4.2 Results

Table 47 summarizes the simulated results of eAHC for the three variants. The results show that the wall with the AHU in operation has a lower heat transfer coefficient (0.188 W/m^2K) than the wall without the AHU (0.195 W/m^2K). Then, when the AHU is switched off, the parameters are worse (0.195 W/m^2K). The wall surface temperatures do not vary much and are in the range from 21.3 °C to 21.55 °C, indicating that the temperature factor is higher than 0.96 revealing that there is not any moisture issue at the internal surface of the wall.

This project has received funding from the European Union's Horizon 2020 research and innovation programme under grant agreement No 958218

TABLE 47: DETAILED SIMULATION RESULTS FOR EAHC.

Value	Insulated wall without AHU	AHU running	AHU stopped
Total heat flux [W]	18.9	18.1	22.8
Lowest Temperature at internal surface [°C]	21.55	21.41	21.30
Temperature difference [K]	20	20	20
Total area [m^2]	5.40	5.40	5.40
U-value [W/(m^2K)]	0.175	0.168	0.211
Correction factor for anchoring system of facade (U-value) [W/(m^2K)]	0.02	0.02	0.02
Overall U-value incl. anchors [W/(m^2K)]	0.195	0.188	0.231
Area of AHU [m^2]	0.9	0.9	0.9
U-value of AHU [W/(m^2K)]	-	-0.044	0.217
Heat flux through AHU [W]	-	-0.8	3.9
Relative thermal bridge of AHU [W/K]	-	-0.040	0.195

Figure 80 presents the temperature contour for the wall without AHU. The total heat flux value equals with 18.9 W, while the calculated U-value equals with 0.175 W/m^2K. The lowest surface temperature is 21.55°C, resulting a temperature factor equals with 0.98, meaning that there is not any possibility of moisture issue at the internal surface.

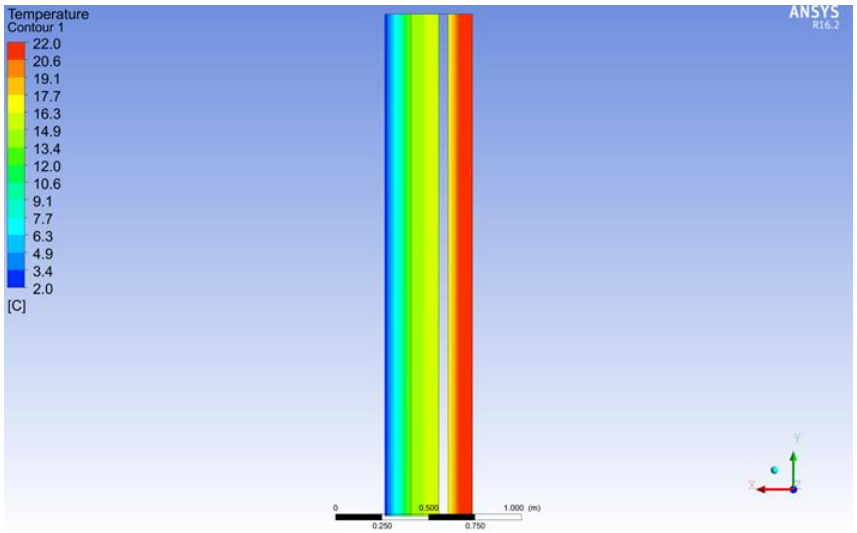

FIGURE 80: TEMPERATURE FIELD FOR THE WALL WITHOUT AHU.

Figure 81 presents the temperature contour for the wall with AHU in operation. The total heat flux value equals with 18.1 W, while the calculated U-value equals with 0.168 W/m^2K (reduced by 4% in comparison with the wall without AHU). The lowest surface temperature is 21.41 °C, resulting a

This project has received funding from the European Union's Horizon 2020 research and innovation programme under grant agreement No 958218

temperature factor equals with 0.97, meaning that there is not any possibility of moisture issue at the internal surface.

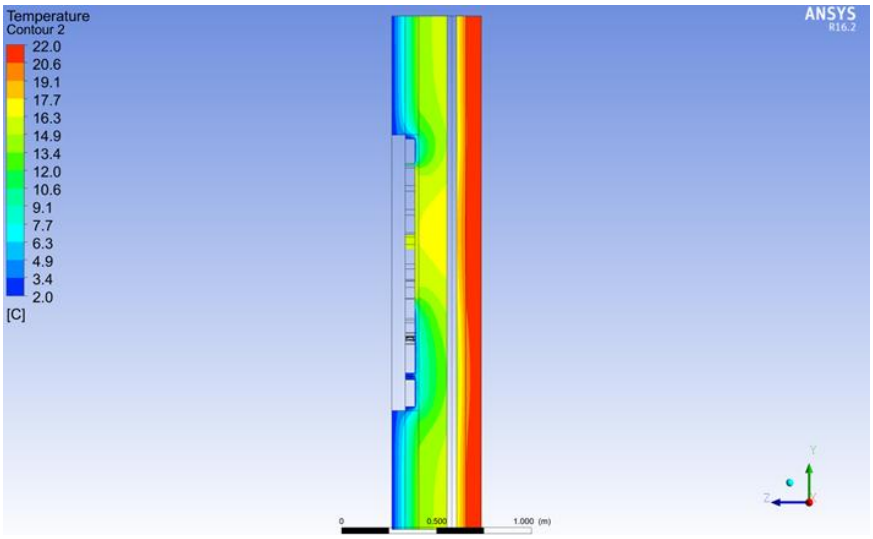

FIGURE 81: TEMPERATURE FIELD WHEN THE AHU IS SWITCHED ON

Figure 82 presents the temperature contour for the wall with AHU in switched-off mode. The total heat flux value equals with 22.8 W, while the calculated U-value equals with 0.211 W/m^{2}K (increased by 20% in comparison with the wall without AHU). The lowest surface temperature is 21.30 °C, resulting a temperature factor equals with 0.96, meaning that there is not any possibility of moisture issue at the internal surface.

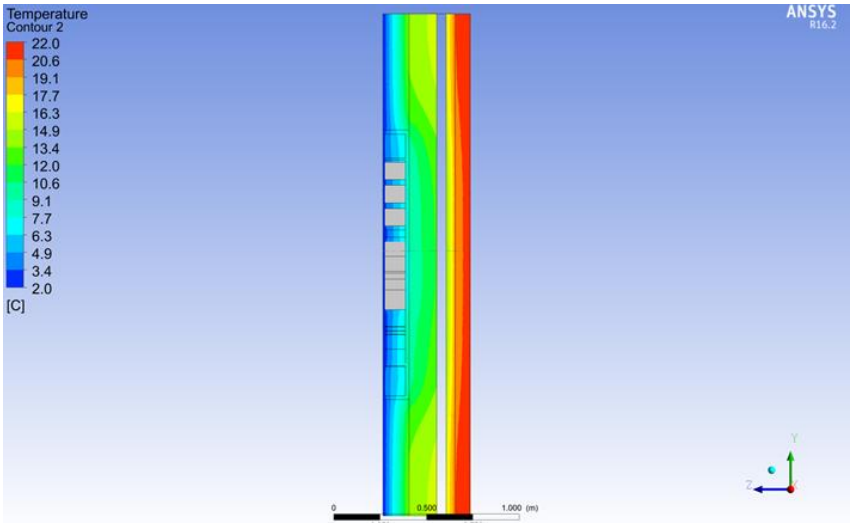

FIGURE 82: TEMPERATURE CONTOUR WHEN THE AHU IS SWITCHED OFF.

This project has received funding from the European Union's Horizon 2020 research and innovation programme under grant agreement No 958218

8.5 Smart Window

The thermal behaviour of the Basic window was modelled with the use of the THERM 7.8 software from Lawrence Berkeley National Laboratory (LBNL). The frame (Softline 82 MD^2 – 73mm) and sash (Perfectline 82 AD/MD^2 – 84mm) are made from PVC and include reinforcements from steel, while the gaskets are made from EPDM. The window comprises of triple glazing with a total thickness of 48 mm. The configuration of the glazing was presented in Table 40.

The spacers were modelled using the Two Box methodology. In this approach, the detailed edge seal is modelled as two boxes such that it results in the same heat flow as the actual edge construction. One 3 mm box with a thermal conductivity of 0.4 W/(m·K) replaces the polysulphide sealant and one 6.9 mm box with an equivalent thermal conductivity $\lambda_{eq,2B}$ replaces the spacer profile. Since there was no available information on the spacer, a warm edge spacer with $\lambda_{eq,2B}$ =0.31 W/(m·K) was assumed.

The boundary conditions of the model were set according to the corresponding European standards[15], as described in Table 42. The thermal transmittance of the frame U_f, the linear thermal transmittance Ψ and the total window thermal transmittance U_w were calculated according to the EN 10077 standards [16], and are presented in Table 13.

TABLE 48: THERMAL PROPERTIES OF THE FRAME AND THE WHOLE WINDOW FOR THE BASIC WINDOW

Thermal property	Value
U_f [W/(m^2K)]	1.14
Ψ[W/(m·K)]	0.030
U_w [W/(m^2K)]	0.90

The temperature contour for the frame cross-section is presented in Figure 83.

[15] EN ISO 10077-1:2017 – Thermal performance of windows, doors and shutters – Calculation of thermal transmittance – Part 1: General
[16] EN ISO 10077-2:2017 – Thermal performance of windows, doors and shutters – Calculation of thermal transmittance – Part 2: Numerical method for frames

This project has received funding from the European Union's Horizon 2020 research and innovation programme under grant agreement No 958218

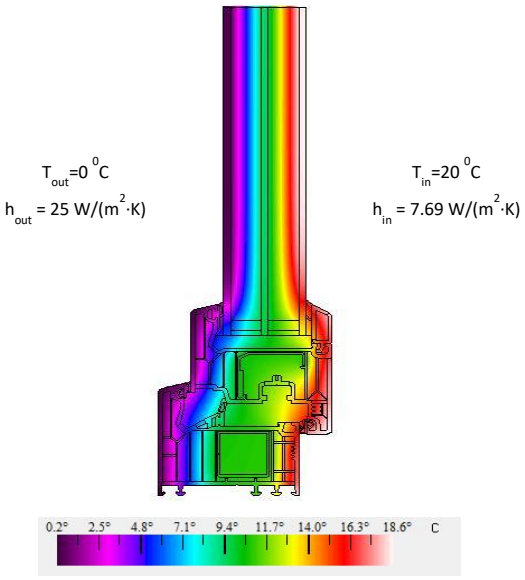

FIGURE 83: TEMPERATURE CONTOUR OF THE FRAME CROSS-SECTION FOR THE BASIC WINDOW.

This project has received funding from the European Union's Horizon 2020 research and innovation programme under grant agreement No 958218

9 Monitoring campaign at NTUA living-lab

A monitoring campaign was carried out for the in-situ measurement of the thermal/energy performance of the SmartWall and Smart Window prototypes installed in the Living Lab Pilot Building at the NTUA campus. The construction and the installation of two prototypes were performed in the frame of Task 4.4 “PnU kit prototypes” and further details are provided in D4.4.

9.1 Description of living-lab

A SmartWall and two Smart Window prototypes (one Basic window installed on the SmartWall and one Heat Harvesting Window - HHW) were constructed by AMS and BGTC, respectively, and installed at a pilot building in NTUA campus, called “living-lab”. The living-lab building is constructed by two shipping container and consists of three rooms; two South-oriented identical rooms located side by side and one larger room behind the previous two rooms. The total floor area of the living-lab is 60 m^2. The envelope of living lab is constructed by drywall materials consisting of 150mm graphite polystyrene and cement board from the external side of container’s wall (metal wall), as well as 50mm mineral wool, OSB and gypsum board at the internal side of container’s wall (Figure 84). The theoretical thermal transmittance (U-value) of the living-lab walls equals to 0.17 W/(m^2K), according to ISO 6946.

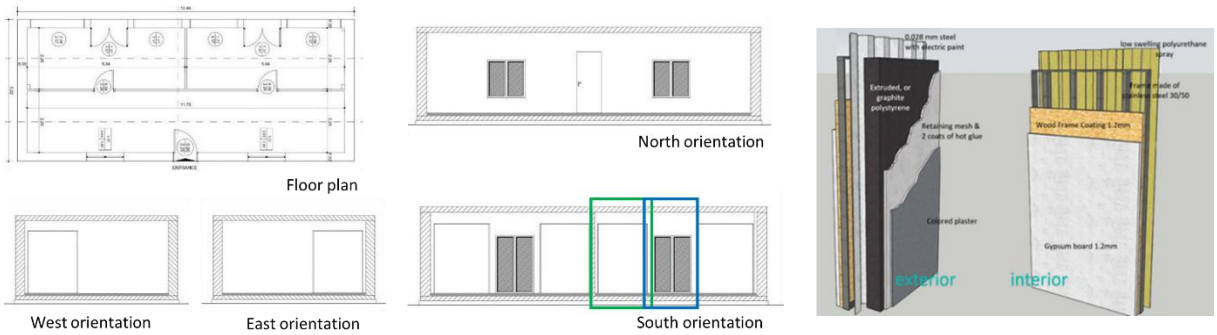

FIGURE 84: THE LIVING-LAB DESIGN.

Furthermore, the living-lab building accommodates six removable wall-panels (with rectangular frames), four of them placed on the southern façade, while the other two are placed with west and east orientation. This removable wall-panels system has been designed in such a manner, that any panel of similar dimensions could substitute the each one of the existing for demonstrating and testing purposes. The SmartWall and Smart Window prototypes selected to be installed at the south-east room (one of the two identical rooms), as depicted the green (for SmartWall) and blue rectangle (for Smart Window) in Figure 84 and the photo in Figure 85.

This project has received funding from the European Union’s Horizon 2020 research and innovation programme under grant agreement No 958218

FIGURE 85: THE INSTALED SMARTWALL AND SMART WINDOW PROTOTYPES AT NTUA LIVING-LAB.

9.2 Description of monitoring system

For the monitoring campaign of SmartWall and Smart Window prototypes, an experimental setup, comprised from a data acquisition system, heat flux sensors, temperature sensors and pyranometers, was used. The Data Acquisition System (DAS) was designed to collect and record the required temperature and heat flux measurements based on the Agilent 34972A data acquisition/logger switch unit (Figure 86a). The measurements were performed with a scan rate of 150 s and were then averaged to hourly or 10-minutes values for the calculations. For the heat flux measurements, heat flux plates of Hukseflux, type HFP01, were used for the measurement of opaque surfaces (SmartWall) and PHFS-01 FluxTeq were used for the U- and g- values of glazing systems. The HFP01 sensors (Figure 86b) have high sensitivity and are dedicated for heat flow measurements of building envelopes. The uncertainty of sensors is equal to 3%, by the guarded hot plate of National Physical Laboratory (NPL) of the UK (04/03/2017) according to ISO 8302 and ASTM C177[17]. The PHFS-01 FluxTeq sensor (Figure 86c) has minimal thickness while still maintaining excellent sensitivity. This sensor is recommended for permanent placement use such as long-term thermal monitoring of windows, walls, ducts, pipes, etc. For the temperature measurements Micro-BETAchip NTC thermistor (Figure 86d) probes (MCD 10k3MCD1) with a nominal resistance 10 kΩ at 25^{o}C, were used. Thermistors have higher accuracy in the small temperature ranges of building applications in comparison to thermocouples[18]. The absolute error of measurement is less than 0.5^{o}C [19]. For the radiation measurement two first class SMP6 Kipp & Zonen pyranometers (Figure 86e)

[17] Hukseflux Thermal Sensors, User Manual HFP01 & HFP03, manual version 1620, 2017.
[18] M.W. Ahmad, M. Mourshed, D. Mundow, M. Sisinni, Y. Rezgui, Building energy metering and environmental monitoring – A state-of-the-art review and directions for future research, Energy and Buildings, 120 (2016) 85-102.
[19] MICRO-BETACHIP (MCD), Thermistor Probe, Specifications 09/2015.

This project has received funding from the European Union's Horizon 2020 research and innovation programme under grant agreement No 958218

were used. This pyranometer has both digital and analogue outputs, low maintenance, extremely robust and reliable.

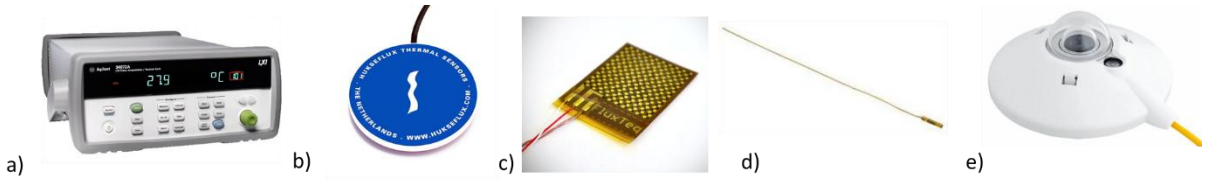

FIGURE 86: THE MEASURING EQUIPMENT: A) AGILENT 34972A DATA ACQUISITION/LOGGER, B) THE FHP01 SENSOR, C) THE PHFS-01 SENSOR, D) THE MICRO-BETACHIP NTC THERMISTOR AND E) THE SMP6 PYRANOMETER.

9.3 SmartWall prototype

9.3.1 Description and installation of SmartWall prototype

The aim of the installation of SmartWall prototype in living-lab is to face practical difficulties during the manufacturing and installation of PnU kit in real building envelope and to assess the thermal and energy performance as a renovation solution in existing building by means of in-situ monitoring techniques. The first aim was dealt with in the frame of the Task 4.4 and it is described in Deliverable 4.4 "PnU kit prototypes addressing the 3 demo building requirements", while the second aim was dealt with in the frame of Task 4.5. The energy assessment of SmartWall has to be done as a renovation solution in a poor-insulated existing wall. However, the living-lab walls are high insulated. For this reason, it was decided to remove a whole removable part of the living-lab in order to be replaced by an assembly that contains the SmartWall installed on a non-insulated wall simulating an existing wall where under realistic conditions SmartWall would be attached on it. A conventional brick wall would consist of brick 90mm – 50 mm air gap – brick 90 mm resulting a U-value equal with $U_{ex.wall}$=2.20 W/(m^{2}K)[20]. This wall is impossible to be built in the living-lab envelope. For this reason, an equivalent conventional wall was constructed by two cement boards and unventilated air layer yielding the same U-value with the conventional non-insulated wall. The SmartWall is installed at the internal side of the "existing wall" and a layer of EPS 20mm thick is placed among them simulating the mineral wool with aluminum foil that are going to be placed in real construction (see section 7.1.1). Following this approach, the installed SmartWall prototype consists of the SmartWall and the "badly insulated existing wall".

The dimensions of the SmartWall prototype are 1.760 m width and 2.550 m height. The installed SmartWall prototype is the most complicated type of SmartWall including a triple pane window with PVC frame (Basic Window) and external blinds, a slim type fan-coil, a toolbox and a PV panel placed on the top side of the external surface. Figure 87 illustrates the SmartWall prototype that was installed on the wall of NTUA living lab. Further information regarding the construction details of the SmartWall prototype is provided in D4.4.

[20] Hellenic building regulation (KENAK)

This project has received funding from the European Union's Horizon 2020 research and innovation programme under grant agreement No 958218

FIGURE 87: SMARTWALL PROTOTYPE 3D DESIGN (LEFT: INTERIOR SIDE, MIDDLE: EXTERIOR SIDE, RIGHT: PARTIALLY EXPLODED MODEL)

9.3.2 Experimental thermal performance of SmartWall prototype

9.3.2.1 Thermography

IR images were obtained in order to optically identify the thermal bridges of the SmartWall. The thermography test was carried out during the early morning hours in December, avoiding the solar radiation, following the ASTM C1060 standard[21]. An indoor/outdoor temperature difference higher than 10°C was achieved by means of activation of a heating source inside the building.

The IR camera (FLIR model 595) was used in order to obtain the required IR images of the internal wall surface for the calculation of the temperature profile. The thermal sensitivity of the IR camera is 0.1°C at 30°C with accuracy ±2°C. The IR images were obtained at a night during a winter day (December 2022), when the heating system of living lab (floor heating and fan-coil of SmartWall) was activated in order to create a high temperature difference between internal and external environment. The indoor temperature was 26°C while the external temperature was 13°C.

Figure 88 illustrates the IR image of SmartWall from the external side. The thermography image shows that the opaque surface of the SmartWall is almost homogenous. The thermal bridges due to metal structure are visible but they are not severe. On the other hand, the thermal bridges due to air leakage due to the removable walls of living lab are severe, but this are not created from the SmartWall prototype. From the internal side, the presence of metal structure creates a thermal bridge, but the temperature difference between the area of stud and the area away of stud is not higher than 1.2°C (Figure 88c).

[21] ASTM C1060-11a Standard, Standard Practice for Thermographic Inspection of Insulation Installations in Envelope Cavities of Frame Buildings.

This project has received funding from the European Union's Horizon 2020 research and innovation programme under grant agreement No 958218

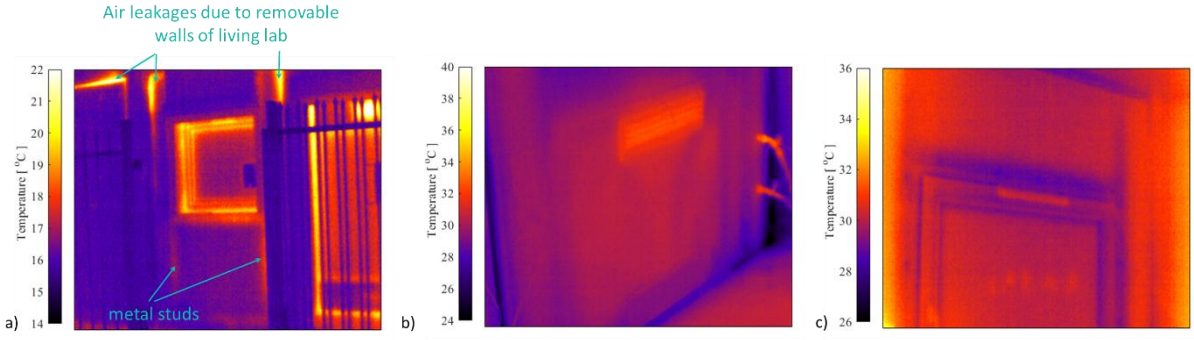

FIGURE 88: IR IMAGES: A) OUTSIDE SIDE OF SMARTWALL PROTOTYPE, B) FAN-COIL AND C) PV AREA AT THE INTERNAL SIDE AT THE.

9.3.2.2 In-situ U-value measurements

The thermal transmittance (U-value) and thermal resistance (R-value) of the SmartWall prototype was in-situ measured aiming to identify the real thermal performance of the SmartWall. The measurements were focused on two basic areas of SmartWall: the area above the window (PV area) and the area below the window (fan-coil area). The measurement of the real R- and U-value at these two areas reveals the real thermal performance of SmartWall (material properties, thermal bridging, etc) and validates the numerical models that are used for the thermal performance analysis of SmartWall (uncertainty of the equivalent thermal conductivity of fan-coil and Toolbox, see section 8.2.1.1).

The in-situ U- and R- value measurement of the SmartWall was performed according to ISO 9869 and the Average method[22]. The Average method assumes a one-dimensional quasi-steady state heat transfer model, which calculates the R-value of an assembly as the quotient of the mean indoor/outdoor surface temperature difference by the mean density of heat flow. The R-value is obtained by the following equation:

$$R = \frac{\sum_{j=1}^{N}(T_{si,j} - T_{se,j})}{\sum_{j=1}^{N} q_j}$$

where q [W/m^2] is the measured heat flux at the internal surface of the wall, T_{si} and T_{se} [^{o}C] are the internal and external surface temperatures, respectively, and the index j enumerates the individual measurements.

For the measurement of U-value the environmental (ambient) temperatures are used instead of the surface temperatures. So, the equation for the calculation of U-value is:

$$U = \frac{\sum_{j=1}^{N} q_j}{\sum_{j=1}^{N}(T_{i,j} - T_{e,j})}$$

where T_i and T_e [^{o}C] are the internal and external ambient temperatures, respectively.

According to ISO 9869, a unique R- and U-value result is obtained when the following criteria are fulfilled:

- The duration of data should be at least 3 days.

[22] ISO 9869-1:2014, Thermal insulation - Building elements - In-situ measurement of thermal resistance and thermal transmittance - Part 1: Heat flow meter method.

This project has received funding from the European Union's Horizon 2020 research and innovation programme under grant agreement No 958218

- The value calculated at the end of the data set should not deviate more than ±5% from the respective value obtained 24 hours before.
- The resulting value when applying the method to the first 2/3 of data should not deviate by more than ±5% from the respective value when analyzing the last 2/3 of data.
- The change in the stored heat in the wall should not be more than 5% of the heat passing through the wall over the measuring period.

The uncertainty of this method is between 14-28%.

Figure 89 illustrates a schematic diagram and a photo of the location of temperature and heat flux sensors. The heat flux sensors were installed at the internal surface of the SmartWall, one above the window ("PV area") and one under the window ("fan-coil area") avoiding, as possible, the thermal bridges due to the metal frame. Four temperature sensors (thermistors) were used for the measurement of internal and external surface temperature of PV and fan-coil area. For the U-value measurement, two shielded against solar/thermal radiation and ventilated thermistors were used for the measurement of the ambient internal and external temperature.

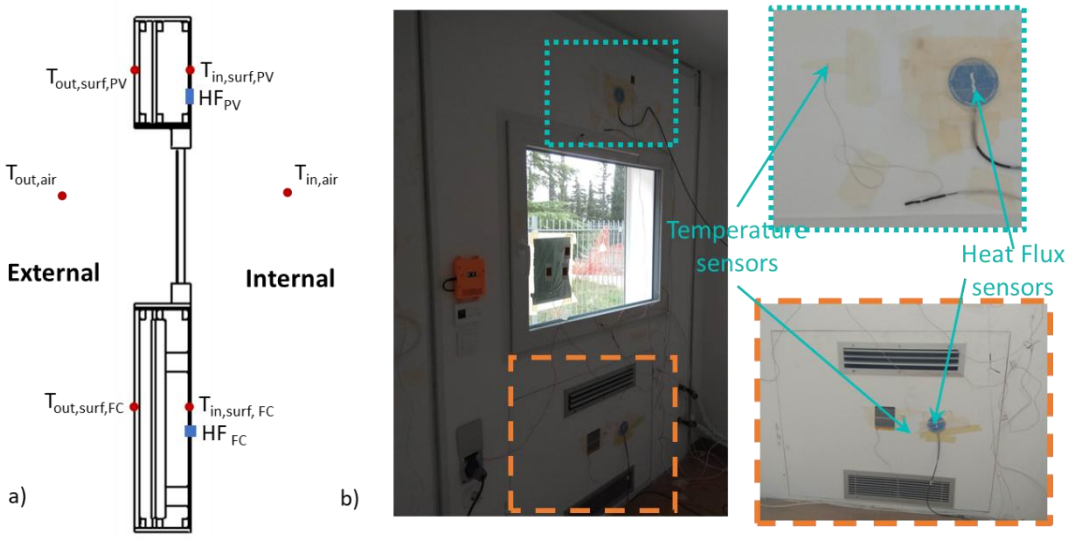

FIGURE 89: MEASURING SYSTEM: A) SCHEMATIC DIAGRAM OF THE LOCATION OF TEMPERATURE (RED CYCLE) AND HEAT FLUX (BLUE SQUARE) SENSORS B) ACTUAL VIEW OF INTERNAL SIDE OF SMARTWALL AND MEASURING SYSTEM.

The U- and R-value measurements were obtained during the periods when the floor heating system of living lab was activated, resulting a temperature difference higher than 10°C and the stable direction of the heat flow at the PV area of SmartWall. Table 50 presents the results of in-situ R- and U-value measurements, while Figure 90 and Figure 91 illustrates indicative convergence curves for R- and U-value measurements, respectively. The results show that the PV area, which acts as the behavior of the "blank type" of SmartWall (Type A), has a U-value equal to 0.21 W/(m^{2}K), while the fan-coil area (when it is not active) almost double its thermal transmittance (0.40 W/(m^{2}K)). However, this area, when the fan-coil is active, acts as an active layer providing negative thermal transmittance, meaning that this area creates heat losses during the cooling mode or heat gains during the heating mode. This is depicted in Figure 92, the activation of fan-coil to heating mode does not affect the heat flow at the PV area, while the direction of heat flow at the fan-coil area was changed, meaning that this area acts as heat source, when the fan-coil is operated and as heat losses (as typical wall) when the fan-coil is not operated. The U-value of fan-coil area at heating and cooling

This project has received funding from the European Union's Horizon 2020 research and innovation programme under grant agreement No 958218

mode is -0.17 W/(m^{2}K). The negative value of U-value means the heat source for heating period and heat loss for cooling period.

TABLE 49: RESULTS OF IN-SITU R- AND U- VALUE MEASUREMENT.

SmartWall area	Fan-Coil: No Active		Fan-Coil: Heating		Fan-Coil Cooling	
	R-value [(m^{2}K)/W]	U-value [W/(m^{2}K)]	R-value [(m^{2}K)/W]	U-value [W/(m^{2}K)]	R-value [(m^{2}K)/W]	U-value [W/(m^{2}K)]
PV area	4.41 ± 0.75	0.21 ± 0.03	4.37 ± 0.88	0.21 ± 0.04	4.16 ± 0.82	0.24 ± 0.04
Fan-coil area	2.75± 0.45	0.40 ± 0.06	-5.84 ± 1.20	-0.17 ± 0.04	-5.05 ± 1.02	-0.17 ± 0.04

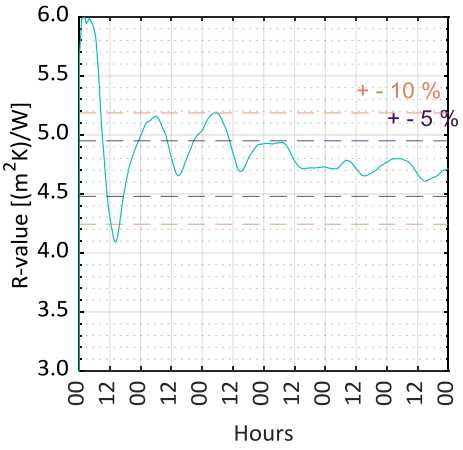

FIGURE 90: CONVERGENCE CURVE OF R-VALUE MEASUREMENT FOR PV AREA.

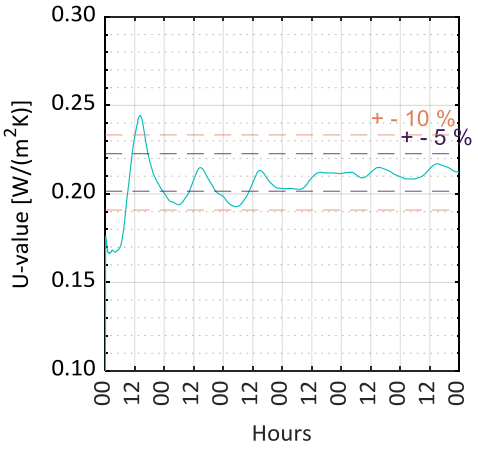

FIGURE 91: CONVERGENCE CURVE OF U-VALUE MEASUREMENT FOR PV AREA.

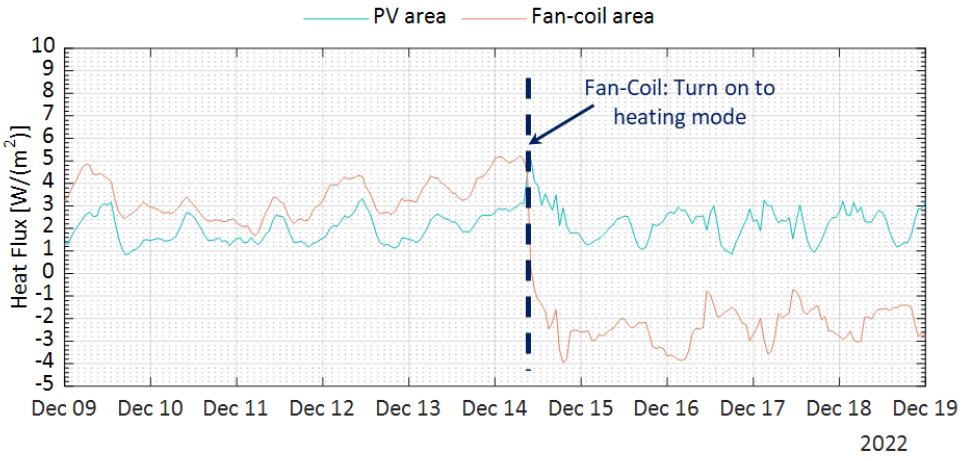

FIGURE 92: HEAT FLUX VALUES AT PV AND FAN-COIL AREA FOR ACTIVE AND NO ACTIVE HEATING SYSTEM.

This project has received funding from the European Union's Horizon 2020 research and innovation programme under grant agreement No 958218

9.3.2.3 PV placement

During the hot summer days, it was established that the surface external temperature of the SmartWall was extremely high, reaching even 55°C. This is observed due to the placement of PV panel which was in touch with the external SmartWall surface. The PV panel, due to its characteristics and black color, absorbed the solar radiation increasing the temperature of PV panel and accordingly the surface of SmartWall. The increase of external surface temperature of the wall resulted to the increase of heat flux. For the reduction of this heat flux (heat losses), (on 23th September) the PV panel was re-installed using spacers in order to create a ventilated area between the PV pane and the external surface of SmartWall.

As it is illustrated in Figure 93, the temperature of external surface of SmartWall in PV area (green line) is significantly reduced after the installation of spacers. The mean of the daily maximum temperature difference (which is observed at midday) between the air and the surface at the PV area was 13°C before the installation of spacers, while the installation of spacers reduces this difference to 7°C. This difference is more obvious comparing the temperature measurements of two similar days, Day 1: 14th September and Day 2: 12th October, when the air temperature and solar radiation have quite similar profile. The temperature at the PV area reaches up to 53°C at the Day 1, while this temperature drops by 13°C due to the ventilated area between the PV panel and wall surface (Day 2).

This project has received funding from the European Union's Horizon 2020 research and innovation programme under grant agreement No 958218

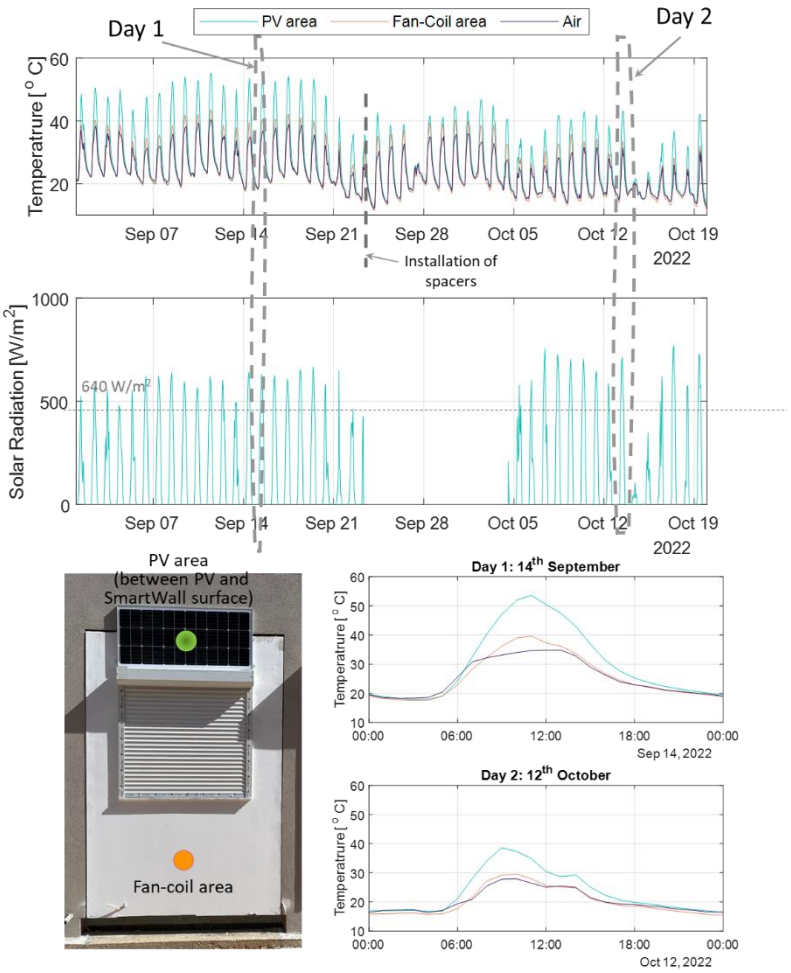

FIGURE 93: TEMPERATURE MEASUREMENTS AT THE PV AREA OF SMARTWALL PROTOTYPE.

9.3.3 Numerical thermal performance of SmartWall prototype

The numerical investigation of SmartWall prototype was carried out by means of COMSOL software. A fully detailed drawing of prototype was set up taking into account all construction details described in D4.4 (Figure 94). As the aim of the numerical analysis is the thermal performance of SmartWall focusing on the validation of model with the in-situ U-value measurements, the PV panel and the window blind box were received. Besides, the air cavity was considered as solid layer with equivalent thermal properties taking into account the heat transfer with convention, radiation and conduction, according to ISO 6946.

This project has received funding from the European Union's Horizon 2020 research and innovation programme under grant agreement No 958218

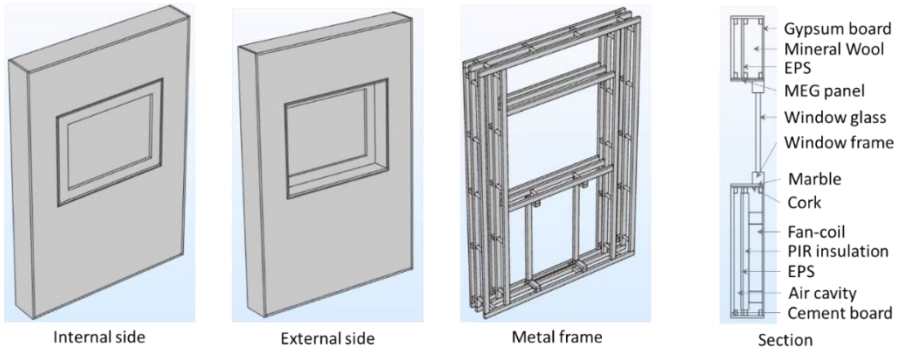

FIGURE 94: THE GEOMETRY OF SMARTWALL PROTOTYPE IN COMSOL.

The material thermal properties of the simulated geometry are presented in Table 50 and is based on D4.4 – Annex 11.3 (Bill of Quantities & technical data sheet). Based on ISO 6946, the U-value of the SmartWall prototype equals with 0.177 W/(m^{2}K), without taking into account any thermal bridge.

TABLE 50: THERMAL PROPERTIES OF SMARTWALL PROTOTYPE MATERIALS.

Material	Thickness [mm]	Thermal Conductivity [W/(m·K)]	Density [kg/m^3]	Specific Heat Capacity [J/(kg·K)]
Steel		60.5	7854	434
Air cavity	65	0.36[a]	1.1	1000
Gypsum board	12.5	0.20	680	980
Mineral Wool	160	0.045	28	1030
PIR insulation	50	0.022	50	1200
EPS	20	0.033	28	1450
MEG panel	20	0.25	1100	1000
Cement board	25	0.35	1150	1000
Marble sill	10	3.05	2657	508
Cork	10	0.040	115	1000
Fan-coil / Toolbox Case	2	40	2000	1500
Fan-coil / Toolbox Cavity		10-15	1380	1000
Window Glass Thermal transmittance - U_g	0.58[b] W/(m^{2}K) → k_g = 0.0232 W/(m^{2}K), d_g=40[mm]			
Window frame thermal transmittance - U_f	1.14[b] W/(m^{2}K) → k_g = 0.114 W/(m^{2}K), d_f=100[mm]			

[a] the air can be modelled as solid, taking into account the conduction, convection and radiation heat transfer, according to ISO 6946.
[b] the thermal transmittance of window glass and window frame was based on in-situ measurements, as described in section 9.4.

The geometry of SmartWall prototype (installed at the NTUA living-lab) is different with the SmartWall-Type 4 which is analyzed in section 8.2.1 and going to be installed at VVV demo case. The results regarding the thermal performance should not be confused.

The boundary conditions are summarized in Table 51.

This project has received funding from the European Union's Horizon 2020 research and innovation programme under grant agreement No 958218

TABLE 51: BOUNDARY CONDITIONS.

Boundary Condition	Value
Outdoor temperature	0°C
Indoor temperature	20°C
External heat transfer coefficient, h_{out}	25 W/(m^{2}K)
Internal heat transfer coefficient for walls, h_{in}	7.69 W/(m^{2}K)
Lateral surfaces	Adiabatic

Figure 95 illustrates the temperature contour of internal / external surface and a section at the middle width of SmartWall prototype. It is obvious that the metal frame of SmartWall and presence of fan-coil and Toolbox creates significant thermal bridges. The thermal resistance of the 50 mm RIR insulation behind the area of fan-coil and Toolbox equals with 2.27 (m^{2}K)/W, which is significantly lower (50%) than the thermal resistance of 160 mm mineral wool (4.57 (m^{2}K)/W). This difference results the low temperatures of the internal surface at the fan-coil area. Besides, even the presence of cork, the marble at the bottom of window creates high thermal bridge.

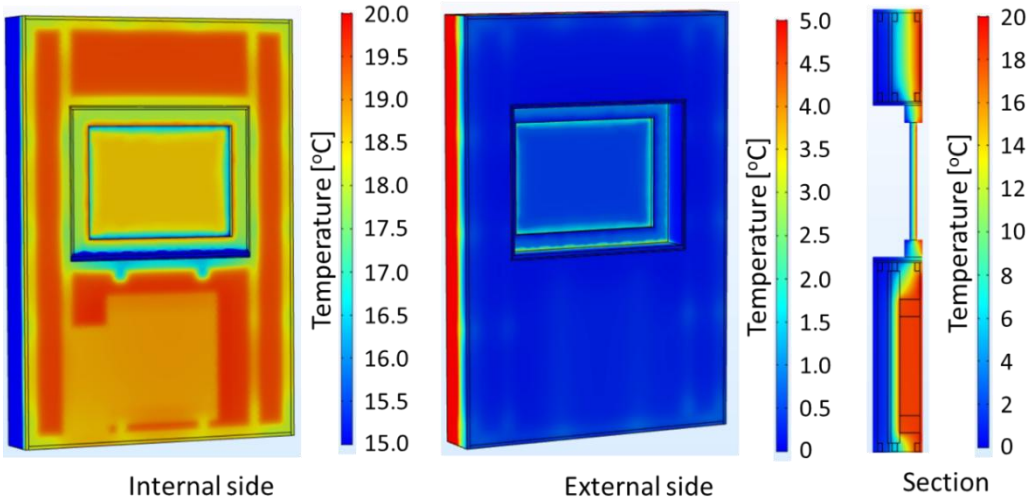

FIGURE 95: TEMPERATURE CONTOUR OF THE INTERNAL, EXTERNAL SURFACE AND A MIDDLE SECTION OF SMARTWALL PROTOTYPE.

As previous mentioned, the fan-coil and toolbox were simulated as boxes with metal case and an equivalent material inside them. The thermal properties of this equivalent material are obtained based on the in-situ thermal resistance (R-value) measurement of the SmartWall at the fan-coil area. The R-value is selected as an indicator that is independed of the environmental conditions (internal and external convection). Based on the results presented in section 9.3.2.2, the R-value at the fan-coil area is 2.75 (m^{2}K)/W.

Figure 96 presents the R-value of the fan-coil area of SmartWall as provided by COMSOL model for different properties of the equivalent material of fan-coil. The results show that the experimental R-value of fan-coil area is achieved when the equivalent material of fan-coil has thermal resistance equal to 0.1188 (m^{2}K)/W. This means that the thermal conductivity of this material is 0.94 W/(mK).

This project has received funding from the European Union's Horizon 2020 research and innovation programme under grant agreement No 958218

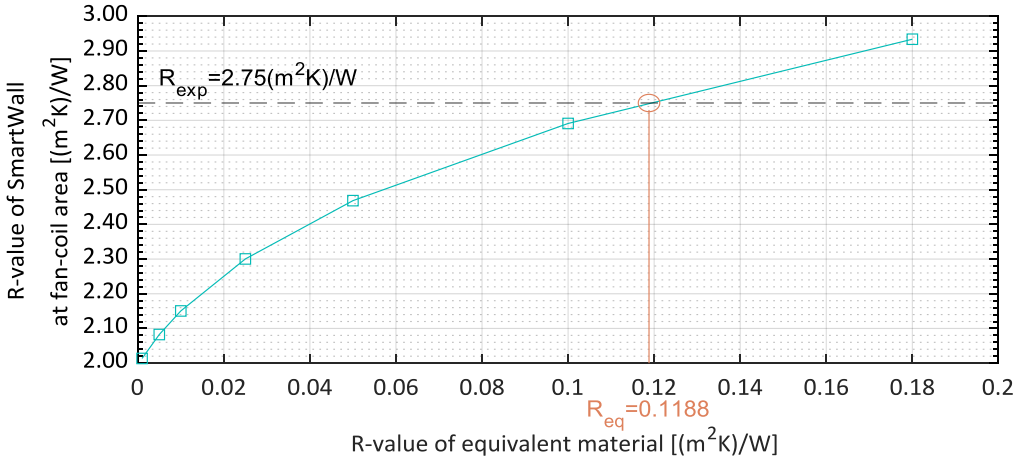

FIGURE 96: R-VALUE AT FAN-COIL AREA OF SMARTWALL UNDER DIFFERENT R-VALUE OF THE EQUIVALENT MATERIAL OF FAN-COIL.

Figure 97 presents the contour of U-value at the internal surface of SmartWall prototype, as calculated from COMSOL software. The U-values follow the trend of temperature contour indicating high U-values at the areas with thermal bridges. Specifically, the R-value at the area above the window, where there is not significant thermal bridge, equals with 4.33 (m^2K)/W (or U-value equals with 0.22 W/(m^2K)), while the R-value at the area of fan-coil, where the mineral wool insulation is replaced with the fan-coil and PIR insulation, equals with 2.75 (m^2K)/W (or U-value equals with 0.34 W/(m^2K)). The experimental value of R-value at the PV area was measured equal with 4.45 (m^2K)/W meaning that the difference between experimental and numerical value is only 3%.

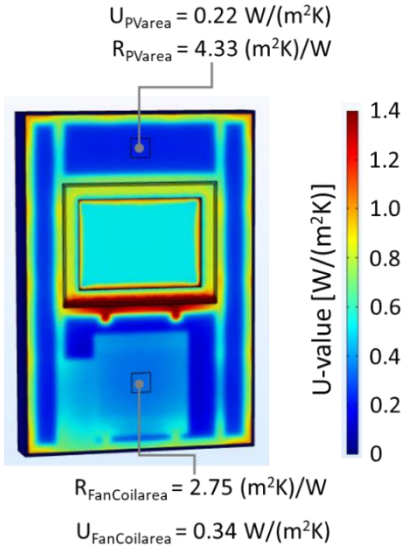

FIGURE 97: U-VALUE CONTOUR OF THE INTERNAL SURFACE OF SMARTWALL PROTOTYPE.

This project has received funding from the European Union's Horizon 2020 research and innovation programme under grant agreement No 958218

9.4 Smart Window prototypes

9.4.1 In-situ U-value measurements

The measurement of the U-value was conducted according to the average method described in ISO 9869-1[23]. For this purpose, it is necessary to measure the heat flow transmitted through the glass, as well as the air temperature on the exterior and the interior side. For the measurement of the R-value, it is additionally needed to measure the temperature of the glass surface on both the exterior and interior sides. Figure 98 presents the location of sensors at the two sides of Smart Window. PHFS-01 FluxTeq heat flow meters were placed on the interior surface of the glazing to measure the transmitted heat flow. The heat flow meters were shaded by an aluminium film attached directly on the opposite side of the glass (i.e. on the outer side of the outer pane) to shield the sensors from the effect of solar radiation. All temperatures were measured with the use of Micro-Betachip NTC thermistor probes (MCD 10k3MCD1).

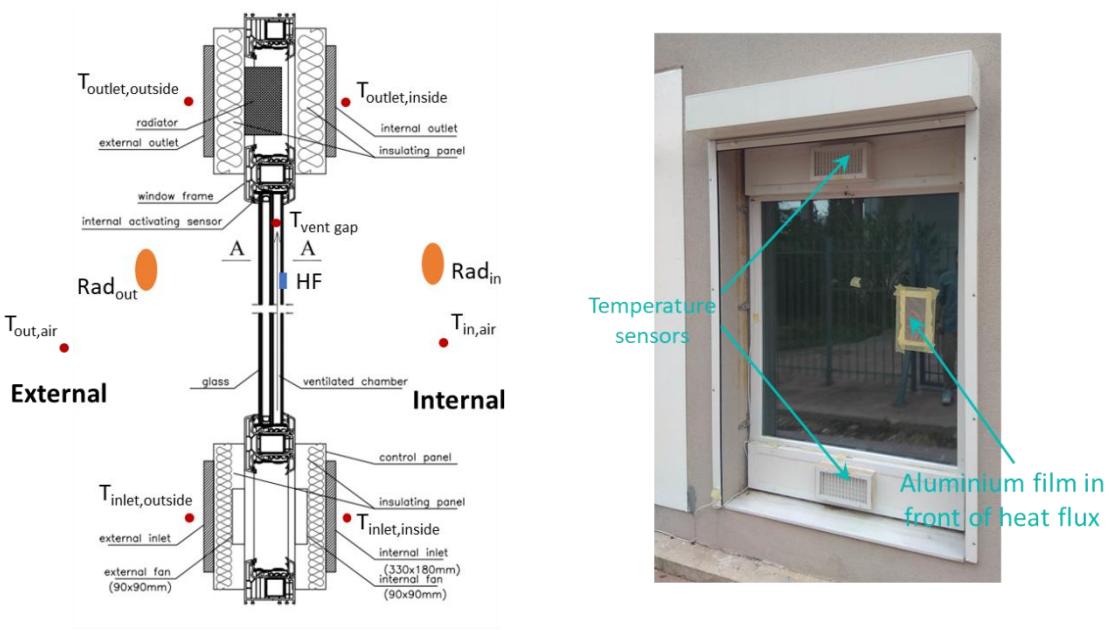

FIGURE 98: MEASURING SYSTEM: A) SCHEMATIC DIAGRAM OF THE LOCATION OF TEMPERATURE (RED CYCLE), HEAT FLUX (BLUE SQUARE) AND PYRANOMETER SENSORS (ORANGE ELLIPSE) B) ACTUAL VIEW OF EXTERNAL SIDE OF SMART WNDOW.

For the measurement of the U-value and R-value only night-time measurements are used, to avoid the effect of solar radiation. If the index j enumerates the individual measurements, then an estimate of the thermal transmittance (U-value) and the thermal resistance (R-value) are obtained as follows:

$$U = \frac{\sum_{j=1}^{n} q_j}{\sum_{j=1}^{n} (T_{i,j} - T_{e,j})}$$

$$R = \frac{\sum_{j=1}^{n} (T_{si,j} - T_{se,j})}{\sum_{j=1}^{n} q_j}$$

[23] ISO 9869-1:2014 – Thermal insulation – Building elements – In-situ measurement of thermal resistance and thermal transmittance – Part 1: Heat flow meter method

This project has received funding from the European Union's Horizon 2020 research and innovation programme under grant agreement No 958218

Where q_j is the heat flow through the glass, $T_{i,j}$ *and* $T_{e,j}$ the interior and exterior air temperatures and $T_{si,j}$ *and* $T_{se,j}$ the interior and exterior glass surface temperatures respectively. When the estimate is computed after each measurement, a convergence to an asymptotical value is observed.

The measured thermal transmittance (U-value) includes the heat transferred with conduction through the glazing system, as well as convection on the outer and inner glass surfaces. This measured (experimental) value corresponds to the actual convection conditions during the time of the measurements and, therefore, cannot be compared directly to the U-values calculated through software such as WINDOW, which use standardised values for convective heat transfer coefficients (e.g. EN 673[1] uses h_{se}=25 W/(m^{2}K) for external and h_{si}=7.69 W/(m^{2}K) for internal convection). As a result, to directly compare the measured with the calculated values presented in Table 41, it is necessary to "correct" the measured values in terms of convection, using the standardised convective heat transfer coefficients. This is done through the measured R-value, according to the equation:

$$U_{corr} = \frac{1}{\frac{1}{h_{se}} + R + \frac{1}{h_{si}}}$$

The measured and corrected U-values for the Heat Harvesting Window (HHW) and the Basic Windowl glazing are presented in Figure 99 and Figure 100. The results are summarized in Table 52 where the theoretical values correspond to the U-values calculated through WINDOW (see Table 41)

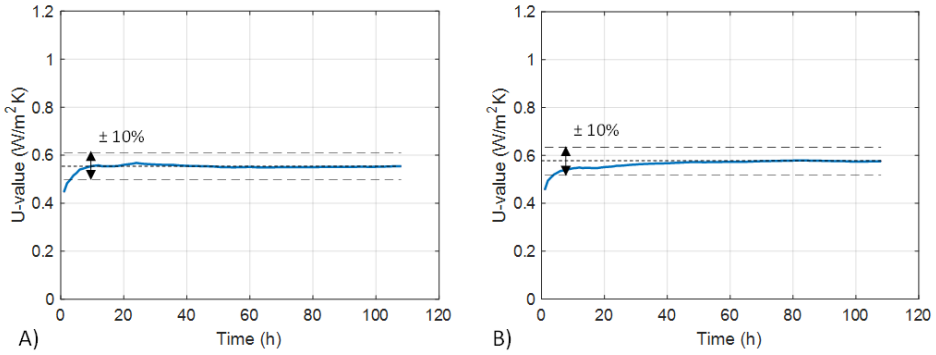

FIGURE 99: A) MEASURED (EXPERIMENTAL) AND B) CORRECTED U-VALUE FOR THE BASIC WINDOW.

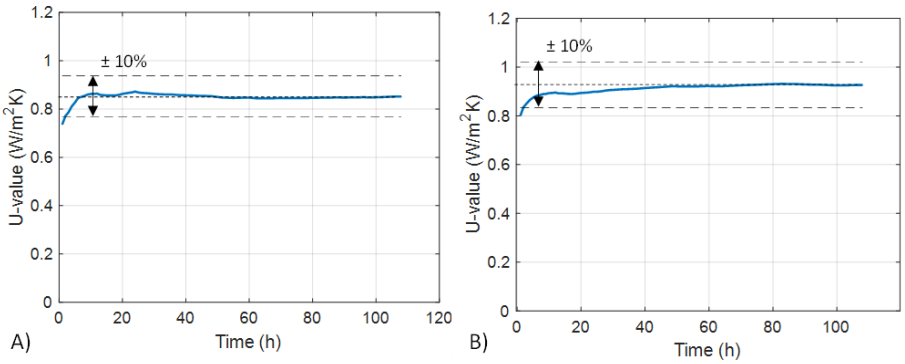

FIGURE 100: A) MEASURED (EXPERIMENTAL) AND B) CORRECTED U-VALUE FOR THE HEAT HARVESTING WINDOW (HHW).

This project has received funding from the European Union's Horizon 2020 research and innovation programme under grant agreement No 958218

TABLE 52: MEASURED (EXPERIMENTAL) AND CORRECTED U-VALUES FOR THE HHW AND THE BASIC WINDOW GLAZING.

	Theoretical U-value [W/(m^{2}K)]	Measured U-value [W/(m^{2}K)]	Corrected U-value for convection [W/(m^{2}K)]
Basic Window	0.58	0.55	0.57
HHW glazing (off-state)	0.75	0.85	0.93

According to the results presented in Table 52, the U-value of the SmartWall glazing (Basic Window) after the correction for convection is almost identical to the theoretical value (error of -1.7%) that was calculated by WINDOW. On the other hand, the U-value of the HHW glazing after the correction for convection is higher by 24% compared to the theoretical value. This difference can be attributed to the fact that commercial software, such as WINDOW, use standardized methodologies to calculate thermal properties which cannot take into account the effect of a non-sealed air gap. Therefore, even in its off-state, the insulating ability of the HHW glazing is significantly reduced compared to the corresponding insulated glazing unit.

It should be noted that only the U-value in the off-state of the HHW glazing could be determined, since the U-value measurements must be conducted during the night-time. In order for the HHW glazing to be in its on-state, the temperature in the air gap must reach 30°C, which is only possible during the day due to the effect of solar radiation. Therefore, the U-value in its on-state cannot be measured during the night-time measurements.

9.4.2 In-situ g-value measurements

For the g-value measurement, a method developed by F. Goia and V. Serra[24] was used which requires, additionally to the abovementioned measurements, the measurement of the global incident solar radiation on the glazing plane, as well as the global transmitted radiation through the glazing. Both of these were measured with two first class SMP6 Kipp & Zonen pyranometers, placed in a vertical position on the outside surface of the wall next to the glazing and right behind the glazing. The calculation of the g-value is carried out using only day-time measurements through linear regression according to the following equations:

$$g = \frac{\sum_{j=1}^{n}(E_{out,j} \cdot q_{g,j})}{\sum_{j=1}^{n} E_{out,j}^2}$$

$$q_{g,j} = E_{in,j} + q_{E,j}$$

$$q_{E,j} = q_j - q_{\Delta T,j}$$

$$q_{\Delta T,j} = U \cdot (\Delta T_j)$$

Where $E_{out,j}$ is the outdoor global radiation on vertical plane, $E_{in,j}$ is the indoor solar radiation on vertical plane behind the glazing and ΔT_j is the air temperature difference between the exterior and the interior side.

[24] F. Goia, V. Serra, Analysis of a non-calorimetric method for assessment of in-situ thermal transmittance and solar factor of glazed systems, Solar Energy, Vol. 166, 2018, pp. 458-471

This project has received funding from the European Union's Horizon 2020 research and innovation programme under grant agreement No 958218

The measured g-values are presented in Figure 101 and the results are summarized in Table 53, where the theoretical values presented correspond to the values calculated through WINDOW.

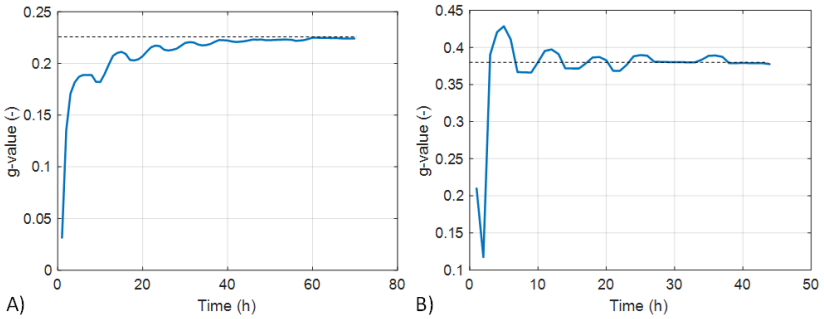

FIGURE 101: MEASURED G-VALUES OF A) HHW GLAZING AND B) BASIC WINDOWS' GLAZING.

TABLE 53: MEASURED G-VALUES FOR THE BASIC AND THE HEAT HARVESTING WINDOW GLAZING.

	Theoretical g-value [-]	Measured g-value [-]
Basic Window	0.53	0.38
HHW glazing (off-state)	0.25	0.23

As can be seen from Table 53, the measured g-value for the MHW glazing is by 8% lower compared to the g-value calculated by WINDOW. This error can be considered acceptable for the in-situ measurement methodology that was applied and, therefore, the measured g-value is fairly close to the theoretical value.

On the other hand, the measured g-value for the SmartWall glazing is much lower compared to the theoretical value (error of 28.3%). This error is a result of the configuration of the blind box on the exterior side of the SmartWall which behaves as an overhang and shades the interior pyranometer. Due to this effect the SmartWall glazing g-value could not be successfully measured in-situ.

The influence of the g-value of HHW is depicted in radiation measurements in Figure 102. The HHW reduces the external radiation (measured at vertical plane) by almost 80% reducing the solar gains during the summer months. The external radiation reaches up to 600 W/m^2, while the radiation that penetrates the HHW is only120 W/m^2.

This project has received funding from the European Union's Horizon 2020 research and innovation programme under grant agreement No 958218

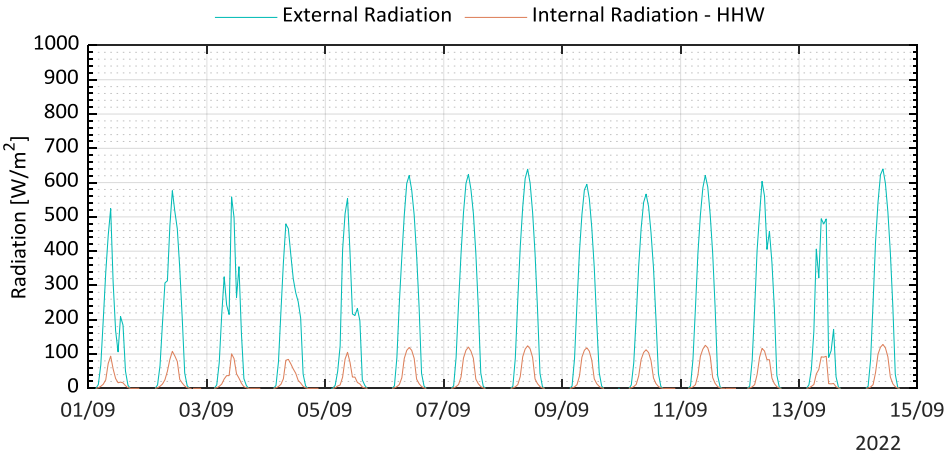

FIGURE 102: RADIATION MEASUREMENTS FOR HHW.

9.4.3 Monitoring of Heat Harvesting Window

The monitoring investigation of HHW focuses on the temperature measurements of air inlet and outlet during the operation of HHW. Figure 103 presents the monitoring measurements of HHW during the heating period. The setpoint of HHW is adjusted in such a way as to provide heating loads into the space. It is obvious that when the temperature in the ventilated gap of glazing exceeds 28°C, the air circulation between the inside inlet and inside outlet of HHW operates. The operation of HHW is revealed by the energy consumption measurement. When the HHW is not active (night hours and when the gap temperature is below 28°C) the electricity consumption is 4Wh, but when the HHW is active the electricity consumption increases and reaches up to 11 Wh. The contribution of HHW is reflected by the increase of air temperature by 1-3°C (between inside inlet and inside outlet), when the heat harvesting is active.

This project has received funding from the European Union's Horizon 2020 research and innovation programme under grant agreement No 958218

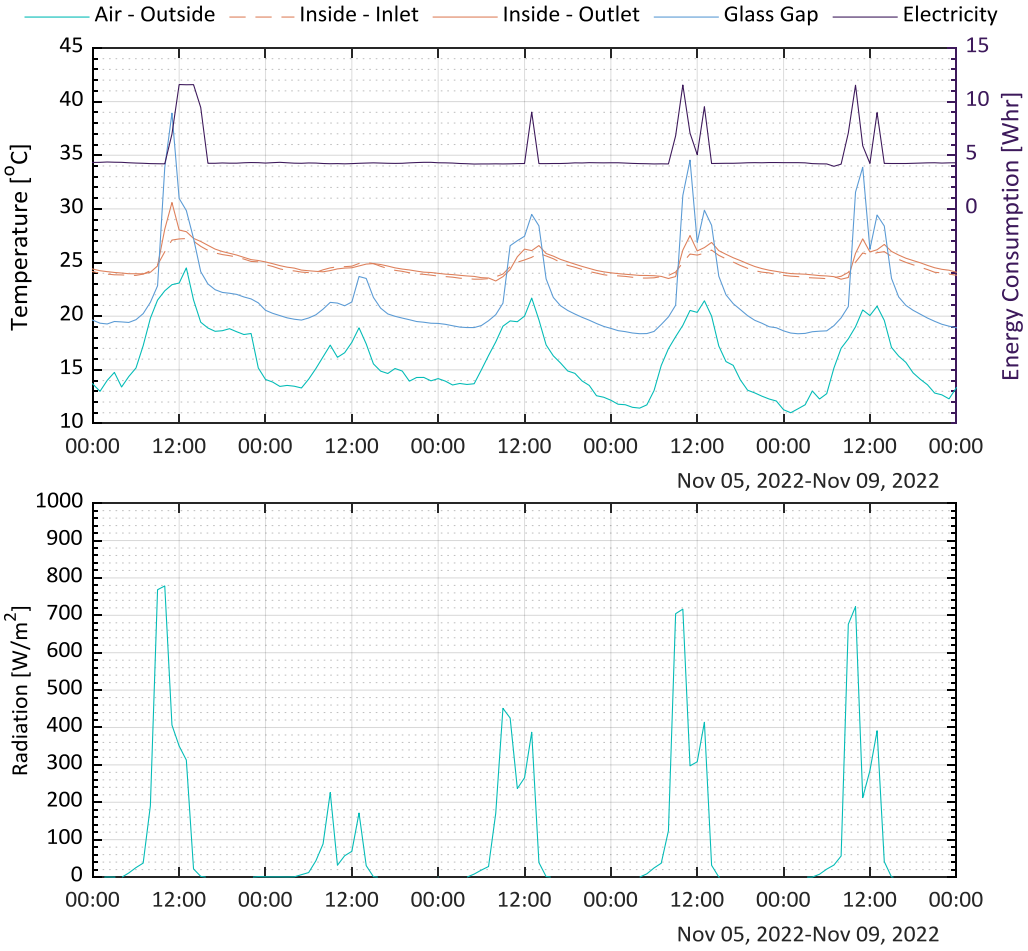

FIGURE 103: MONITORING MEASUREMENTS OF HHW FOR INDICATIVE DAYS DURING HEATING PERIOD.

This project has received funding from the European Union's Horizon 2020 research and innovation programme under grant agreement No 958218

10 Conclusions

The current deliverable (D4.5 - PnU kit prototype property and performance characterization) describes the activities performed in the frame of the Task 4.5 "PnU kit testing campaign" aiming to determine the PnU characteristics through a comprehensive testing campaign and to optimize the possible PnU weaknesses. The tests are divided into two sections:

- the execution of Factory Quality Procedures on manufacture's factories and
- the laboratory, medium and full-scale testing of the mechanical-structural, fire, acoustic, thermal and hygrothermal performance of indicative PnU kits.

The execution of **F.Q.Ps** at manufacturer's facilities brought to light the weaknesses during the manufacturing of PnU prototypes and indicated all needed remedial actions for each inspection test that should be done in order to eliminate possible defects. Additionally, the current Deliverable identified and recorded all the loop back actions between the remedial actions and manufacturing process, as imposed by the F.Q.P. developed and presented in previous PLURAL Deliverables. The inspection tasks of F.Q.P. contain visual, mechanical, operational tests during the manufacturing of PnU prototypes.

The **mechanical** performance analysis of the PLURAL PnUs assessed the mechanical properties of incorporated components, anchoring system, connections, etc in relation to seismic and self-weight, wind and snow loads. The SmartWall PnU kit, which will be installed in Greece (a highly seismic country), was experimentally investigated by means of shaking table tests, allowing for proper validation of the structural response under different earthquake tests[25]. No visible damage was observed in steel members, brick wall and SmartWall during triaxial shaking table tests. The videos of the experiments are available in the PLURAL website: https://www.plural-renovation.eu/. The final design of the SmartWall steel frame anchoring system was found adequate for the tested level of base motion. Besides, the mechanical performance analysis of eWHC/ConnExWall in terms of permanent, variable and accidental loads indicated the final design of anchoring system. In parallel, a ConnExWall prototype was subjected to laboratory tests in order to detect possible deformation during its installation. The tests were successful and no deformation of the facade could be detected. Additionally, the detailed analysis eAHC/HybridWall concluded to an optimized anchoring system by means of finite element simulation. The analysis focused on the basic components of anchoring system: connectors, lines, load lines, wind and load anchor.

The **fire** performance analysis focused on the SmartWall and Smart Window PnU kits, since the rest of the PnUs met in advance the local/national fire requirements, according to D1.3. Single Burning Item (SBI) tests, were carried out in the NTUA facilities. The two SmartWall prototypes (one "blank type" and one with fan-coil and Toolbox) were classified as B-s1, d0, while the Smart Window was classified as C-s3,d0.

The **acoustic** performance analysis focused on the eAHC/hybridWall PnU kit, as it is the only PnU that may generate noise (due to the air flow in the Air Handling Unit), while the other PnU kits either contain commercial and certified to noise elements and/or their acoustic performance has already been evaluated in the frame of the Task 4.1. The tests were carried out at CVUT facilities and two

[25] Peak ground acceleration (PGA) of 0.36g (highest seismic zone for Greece) and soil category B according to EC8 were chosen. The acceleration time histories used as base motion were modified from the Landers earthquake that occurred on June 28, 1992 near the town Landers of California, in order to be compatible with the RFRS.

This project has received funding from the European Union's Horizon 2020 research and innovation programme under grant agreement No 958218

prototypes were investigated. The acoustic analysis led to the development of the silencer box for the reduction of noise emitted to the duct system. The results showed that the tested volume flow rates, from 23.3 to 43.4 dB(A), while the night operation of the eAHC unit generates sound pressure level below the night noise limits

The **thermal** performance at material level of the PnUs identified all needed thermal properties of the incorporated materials and is currently used in the building and full kit simulation campaigns. For materials that their behavior was not obvious, addtional experimental tests were carried out, focusing on the measurement of thermal conductivity. The tables that summarize the material thermal properties are useful for the simulation tasks of other Work Packages.

The **building physics** of the PnU kits were investigated through the thermal and hygrothermal analysis of PnUs by means of commercial software. The investigation focused on the calculation of thermal transmittance (U-value), including the effect of all possible thermal bridges, and its hygrothermal performance indicating the possibility of moisture issues. During the analysis some measures for the reduction of thermal bridging and the optimization of thermal performance were proposed. An investigation of appropriate thickness of VIP or aerogel behind the fan-coil at SmartWall kits concludes that 20mm VIP or 40mm aerogel significantly reduces the thermal bridges. Besides, the use of PUR at the region of L-profiles (anchoring system) of ConnExWall can improve the U-value by 8%.

Finally, the performance **monitoring** of SmartWall and Smart Window prototypes established their thermal performance in real conditions. The two prototypes were installed at the NTUA living lab and were already monitored for six months. The experimental investigation of the two prototypes led to the identification of the real thermal characteristics of PnUs (U-values and g-values) and validated the numerical models that are used for all simulation tasks. Also, this monitoring campaign revealed the weakness of the PV installation on the SmartWall which can be improved with the use of appropriate spacers and the creation of a ventilated gap between the PV and SmartWall surface. Additionally, the behavior of SmartWall with activated fan-coil was indicated to be as an active layer at the area of fan-coil.

The above comprehensive testing campaign validated the performance of all PnU kits and gives confidence for their installation to the three demonstration sites of the project.

This project has received funding from the European Union's Horizon 2020 research and innovation programme under grant agreement No 958218

ANNEXES

This project has received funding from the European Union's Horizon 2020 research and innovation programme under grant agreement No 958218

11 Annex I – Investigation of SmartWall mechanical performance

11.1 Details of the experimental set-up and instrumentation

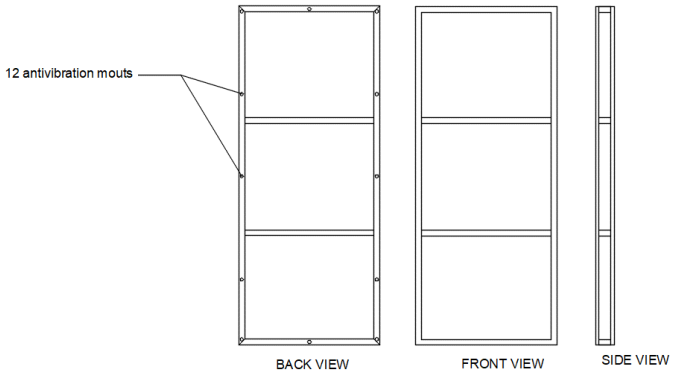

FIGURE 104: BACK-FRONT AND SIDE VIEW OF STEEL FRAME

FIGURE 105: ANTIVIBRATION MOUNT

FIGURE 106: FIXING SMARTWALL TO BRICK WALL- BASE SUPPORTS.

This project has received funding from the European Union's Horizon 2020 research and innovation programme under grant agreement No 958218

FIGURE 107: INSTRUMENTATION SET-UP: ACCELEROMETERS PLACED AT MEASUREMENT POINTS A1 AND A2 (SMARTWALL)

FIGURE 108: INSTRUMENTATION SET-UP: ACCELEROMETERS PLACED AT MEASUREMENT POINTS A3 AND A4 (SMARTWALL)

FIGURE 109: INSTRUMENTATION SET-UP: ACCELEROMETERS PLACED AT MEASUREMENT POINTS A5, A6 AND A7 (BRICK WALL)

This project has received funding from the European Union's Horizon 2020 research and innovation programme under grant agreement No 958218

11.2 Analysis of test data

11.2.1 Test response spectrum

In Figure 109 to Figure 114 (of Annex I), the comparison between the acceleration Test Response Spectrum (TRS) and Required Floor Response Spectrum and for damping 5% are presented for X, Y and Z global axes, for Test4, Test5, Test6, Test7 and Test8. The TRS were calculated using acceleration records at point A5XYZ at 24 divisions per octave resolution. The –10%/+50% Required Floor Response Spectrum for tested level are also shown in Figure 109 to Figure 114 (Annex I). Additionally, in the same figures, the TRS are presented up to 0.50sec period, the fundamental periods along each direction are depicted in vertical lines, while with a dark blue vertical line marks the value 1.40 times the highest period of the SmartWall. As shown in these figures, the Test Response Spectrum for 5% damping envelop the Required Floor Response Spectrum within a –10%/+50% tolerance band in the period range of 0 to 0.5sec along all axes.

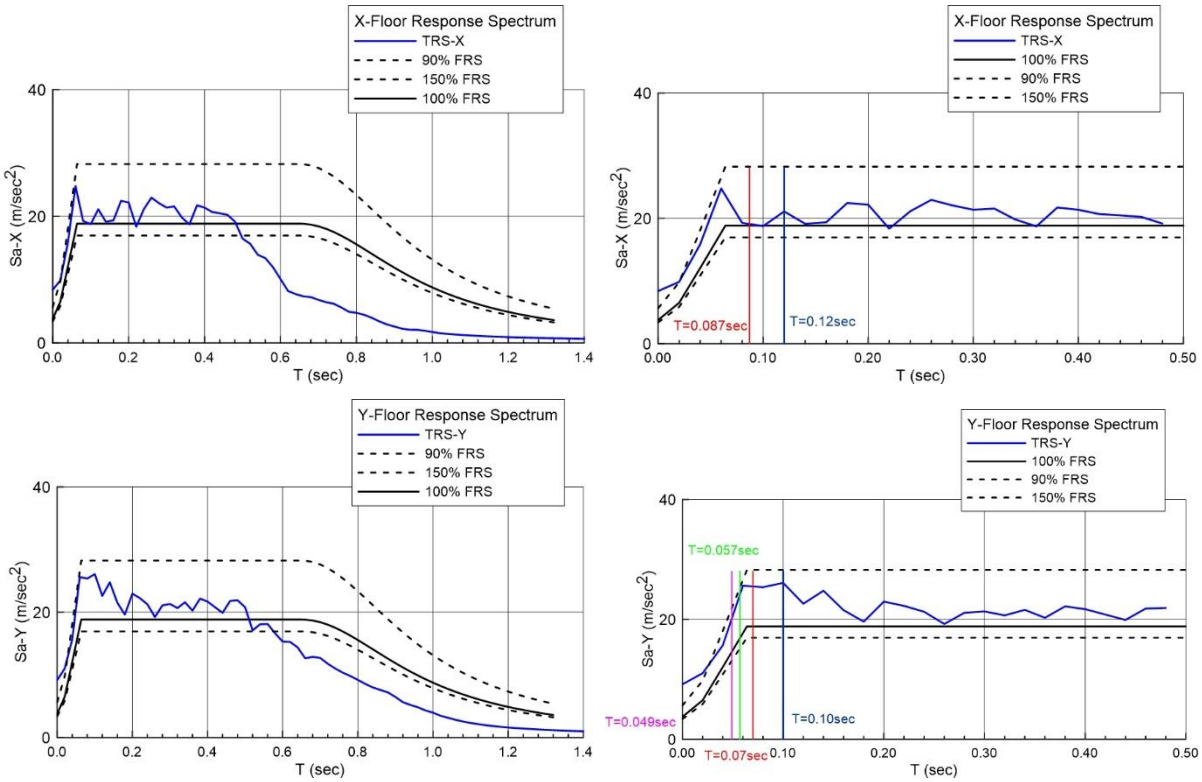

This project has received funding from the European Union's Horizon 2020 research and innovation programme under grant agreement No 958218

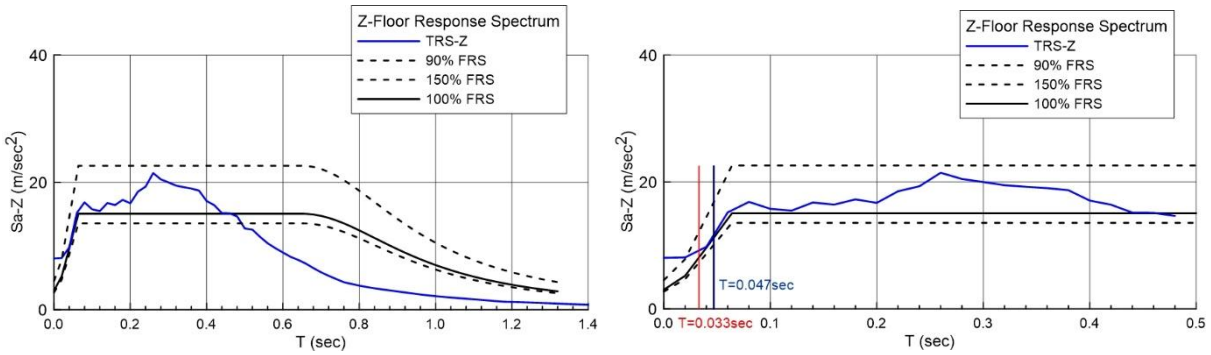

FIGURE 110: TEST 4- TRI-AXIAL XYZ: ACHIEVED TEST RESPONSE SPECTRUM (TRS) ALONG X, Y AND Z DIRECTION. COMPARISON TO REQUIRED FLOOR RESPONSE SPECTRUM, DAMPING 5%

This project has received funding from the European Union's Horizon 2020 research and innovation programme under grant agreement No 958218

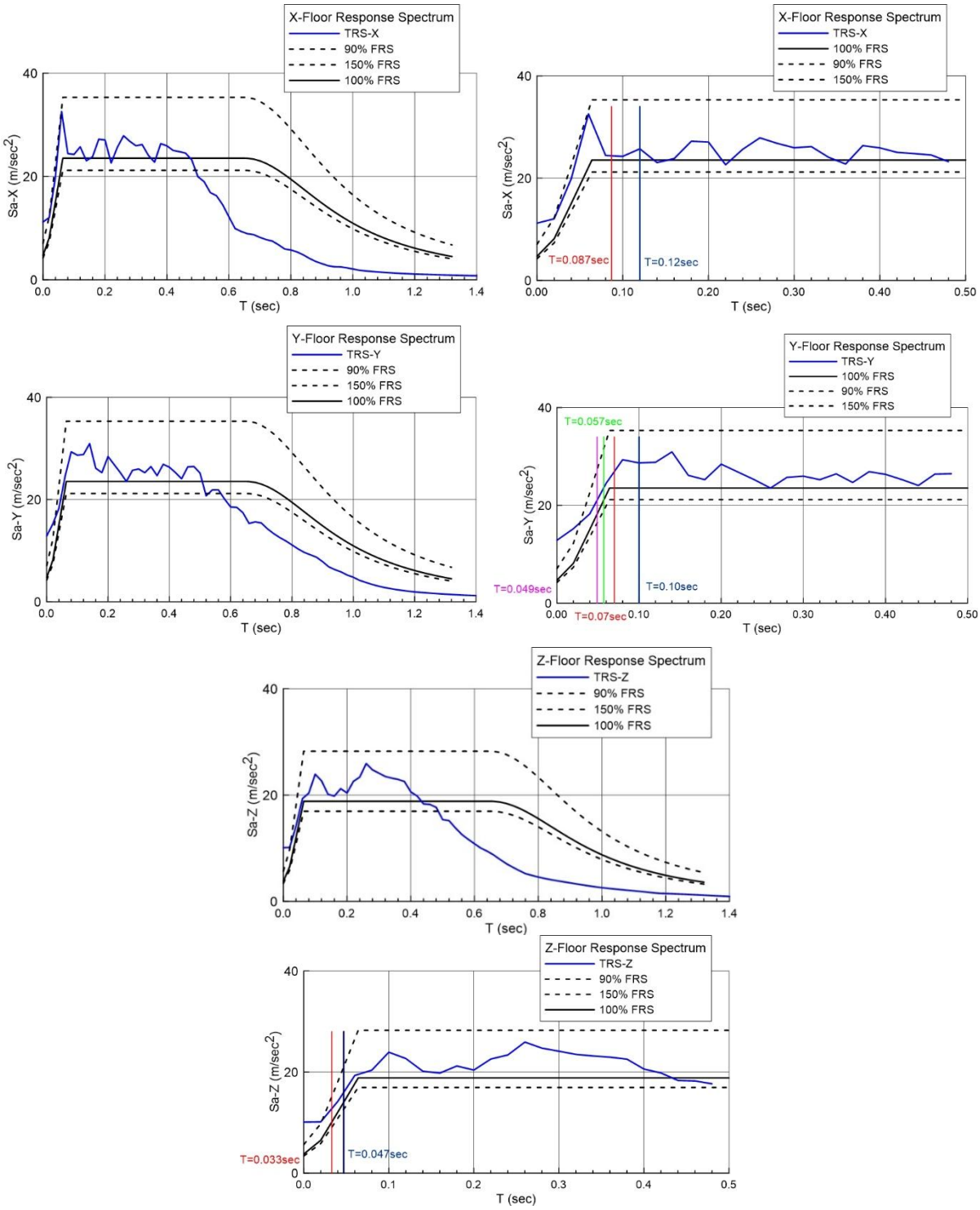

FIGURE 111: TEST 5- TRI-AXIAL XYZ: ACHIEVED TEST RESPONSE SPECTRUM (TRS) ALONG X, Y AND Z DIRECTION. COMPARISON TO REQUIRED FLOOR RESPONSE SPECTRUM, DAMPING 5%

This project has received funding from the European Union's Horizon 2020 research and innovation programme under grant agreement No 958218

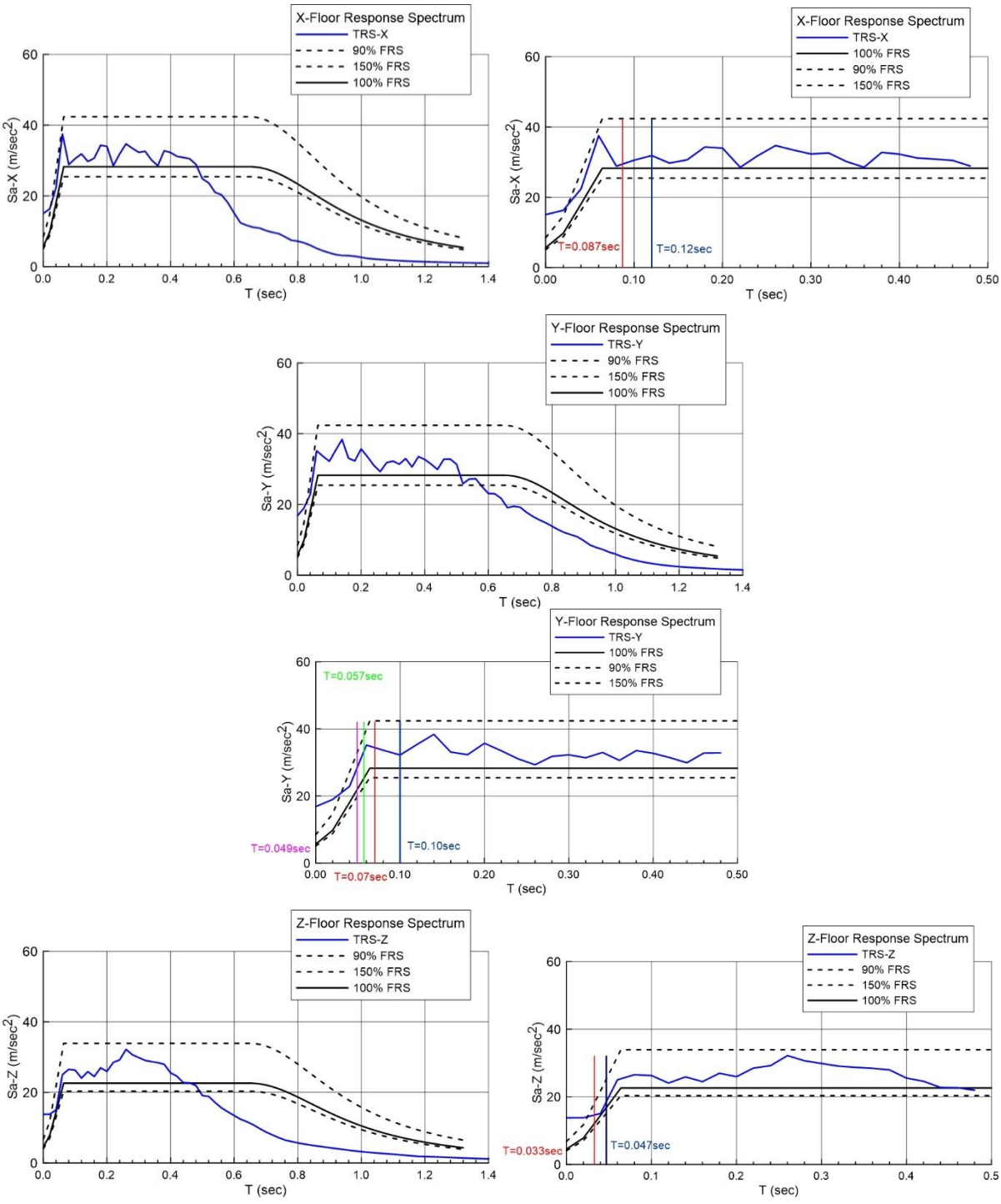

FIGURE 112: TEST 6- TRI-AXIAL XYZ: ACHIEVED TEST RESPONSE SPECTRUM (TRS) ALONG X, Y AND Z DIRECTION. COMPARISON TO REQUIRED FLOOR RESPONSE SPECTRUM, DAMPING 5%

This project has received funding from the European Union's Horizon 2020 research and innovation programme under grant agreement No 958218

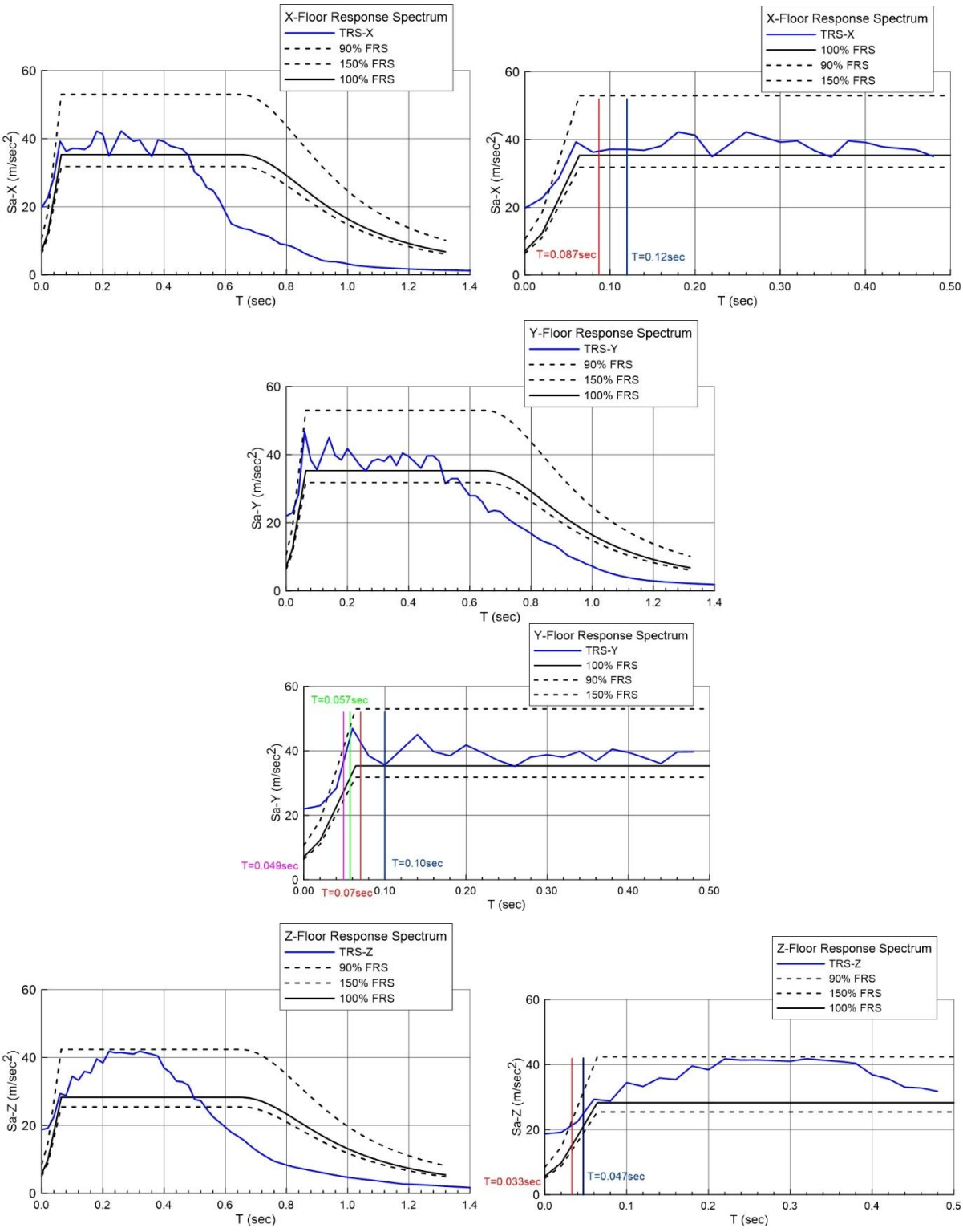

FIGURE 113: TEST 7- TRI-AXIAL XYZ: ACHIEVED TEST RESPONSE SPECTRUM (TRS) ALONG X, Y AND Z DIRECTION. COMPARISON TO REQUIRED FLOOR RESPONSE SPECTRUM, DAMPING 5%

This project has received funding from the European Union's Horizon 2020 research and innovation programme under grant agreement No 958218

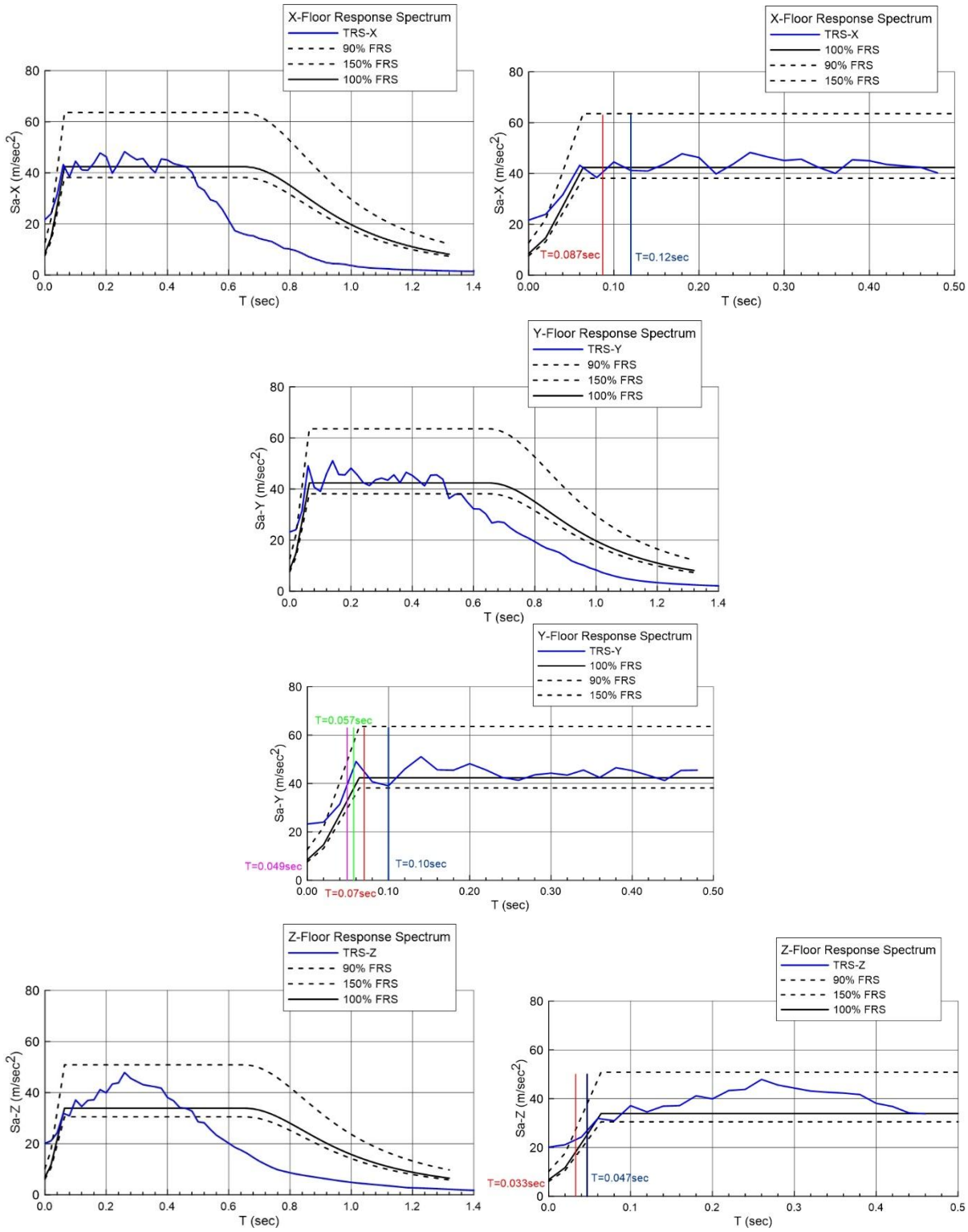

FIGURE 114: TEST 8- TRI-AXIAL XYZ: ACHIEVED TEST RESPONSE SPECTRUM (TRS) ALONG X, Y AND Z DIRECTION. COMPARISON TO REQUIRED FLOOR RESPONSE SPECTRUM, DAMPING 5%

This project has received funding from the European Union's Horizon 2020 research and innovation programme under grant agreement No 958218

11.2.2 Acceleration time histories

In Figure 115 to Figure 129, the time histories of the recorded accelerations at points A1XYZ to A7XYZ are shown for Test4, Test5, Test6, Test7 and Test8. In Table 54, the maximum absolute acceleration at each measurement point is given.

TABLE 54: MAXIMUM RECORDED ACCELERATION

Acceleration (m/sec^2)	Direction	Test 4	Test 5	Test 6	Test 7	Test 8
A1	X	15.00	17.30	19.16	24.20	27.83
	Y	25.37	38.24	35.14	58.95	62.80
	Z	10.54	13.55	14.84	22.24	23.65
A2	X	8.06	12.04	21.13	29.28	39.64
	Y	11.61	17.17	26.72	32.12	36.66
	Z	8.25	10.06	14.65	20.58	21.69
A3	X	25.42	29.31	36.43	39.12	36.15
	Y	14.33	22.61	30.97	37.69	36.83
	Z	9.36	12.42	14.22	22.57	23.59
A4	X	8.40	10.30	13.99	18.12	26.62
	Y	9.06	12.37	16.69	20.38	22.75
	Z	7.91	9.79	14.45	20.54	22.89
A5	X	8.40	11.19	15.06	19.77	21.66
	Y	9.18	12.87	16.83	21.97	23.23
	Z	8.04	10.10	13.78	18.74	20.13
A6	X	7.86	10.49	13.90	17.63	19.73
	Y	10.05	13.52	18.27	24.19	27.44
	Z	8.11	9.89	14.05	18.81	20.03
A7	X	7.65	9.99	13.07	16.35	19.13

This project has received funding from the European Union's Horizon 2020 research and innovation programme under grant agreement No 958218

	Y	7.47	9.66	13.04	15.29	17.34
	Z	8.48	10.23	14.31	19.09	20.14

This project has received funding from the European Union's Horizon 2020 research and innovation programme under grant agreement No 958218

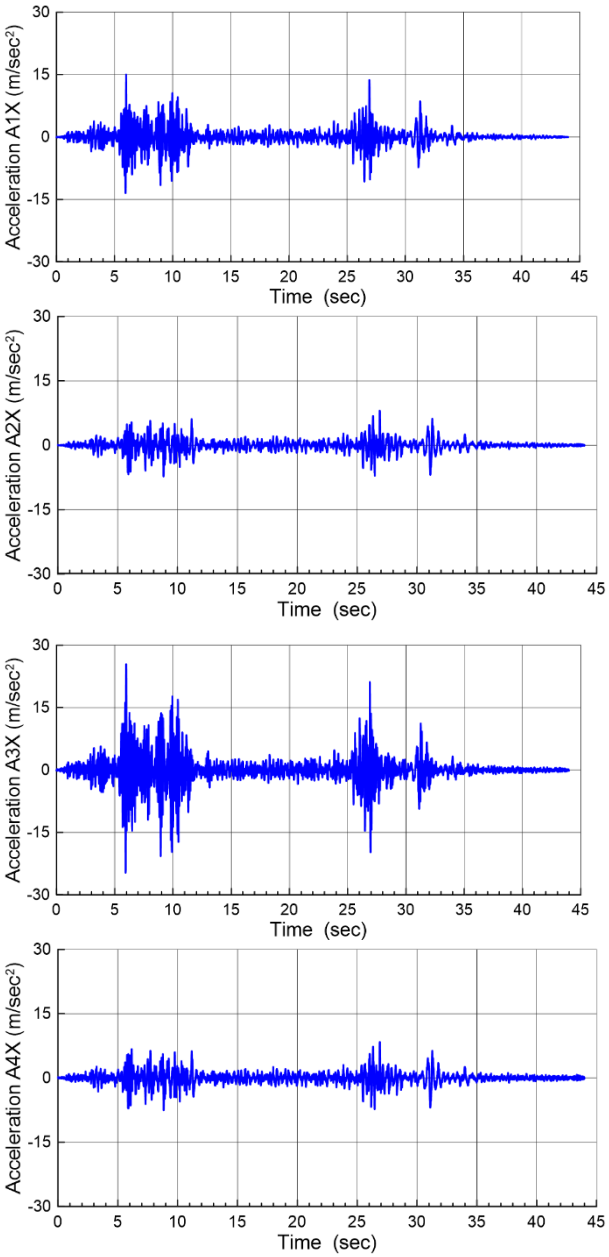

This project has received funding from the European Union's Horizon 2020 research and innovation programme under grant agreement No 958218

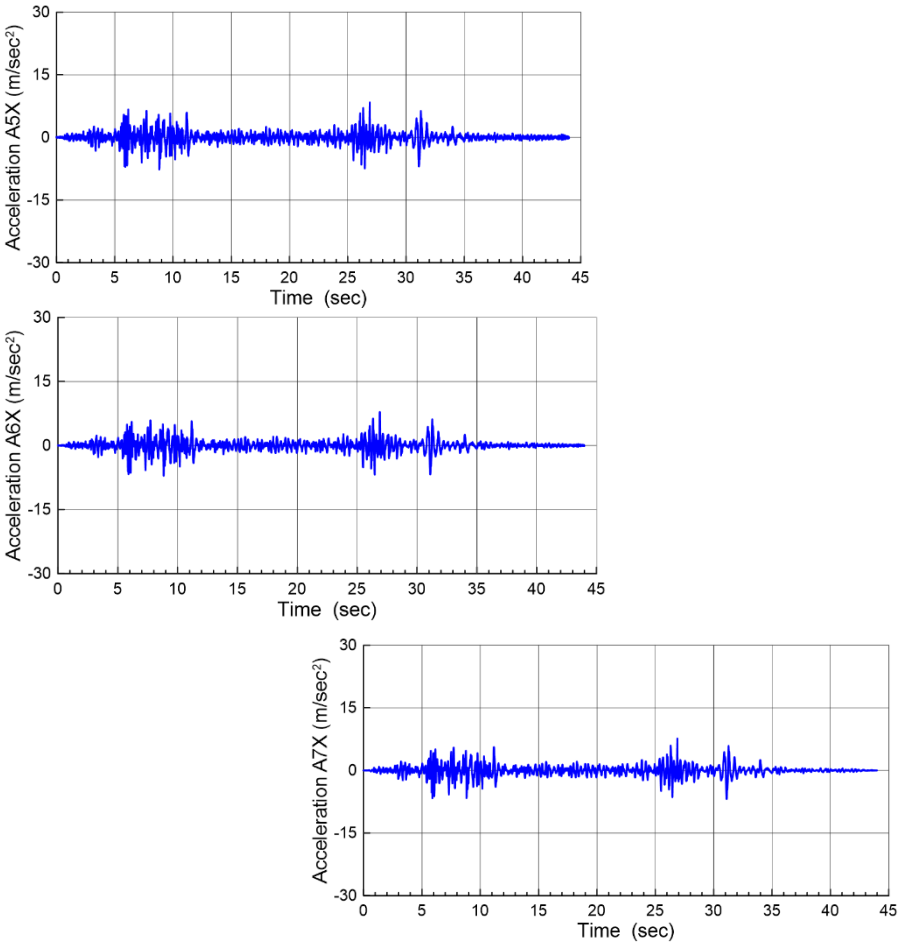

FIGURE 115: TEST 4: ACCELERATION TIME HISTORIES ALONG X DIRECTION AT MEASUREMENT POINTS A1 TO A7

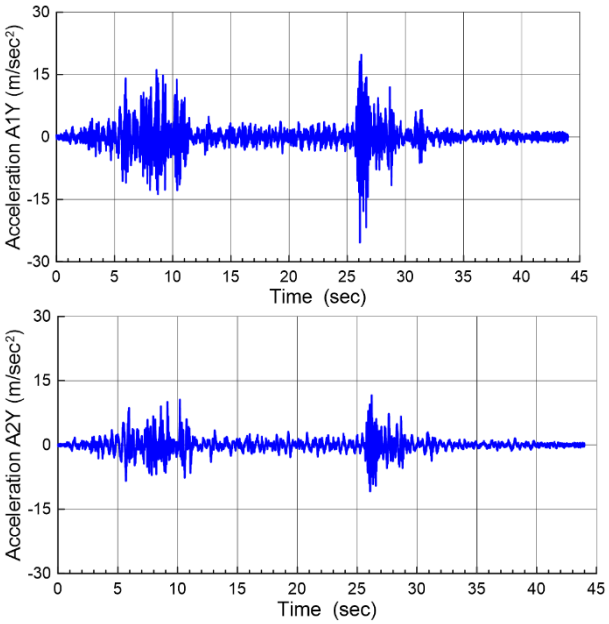

This project has received funding from the European Union's Horizon 2020 research and innovation programme under grant agreement No 958218

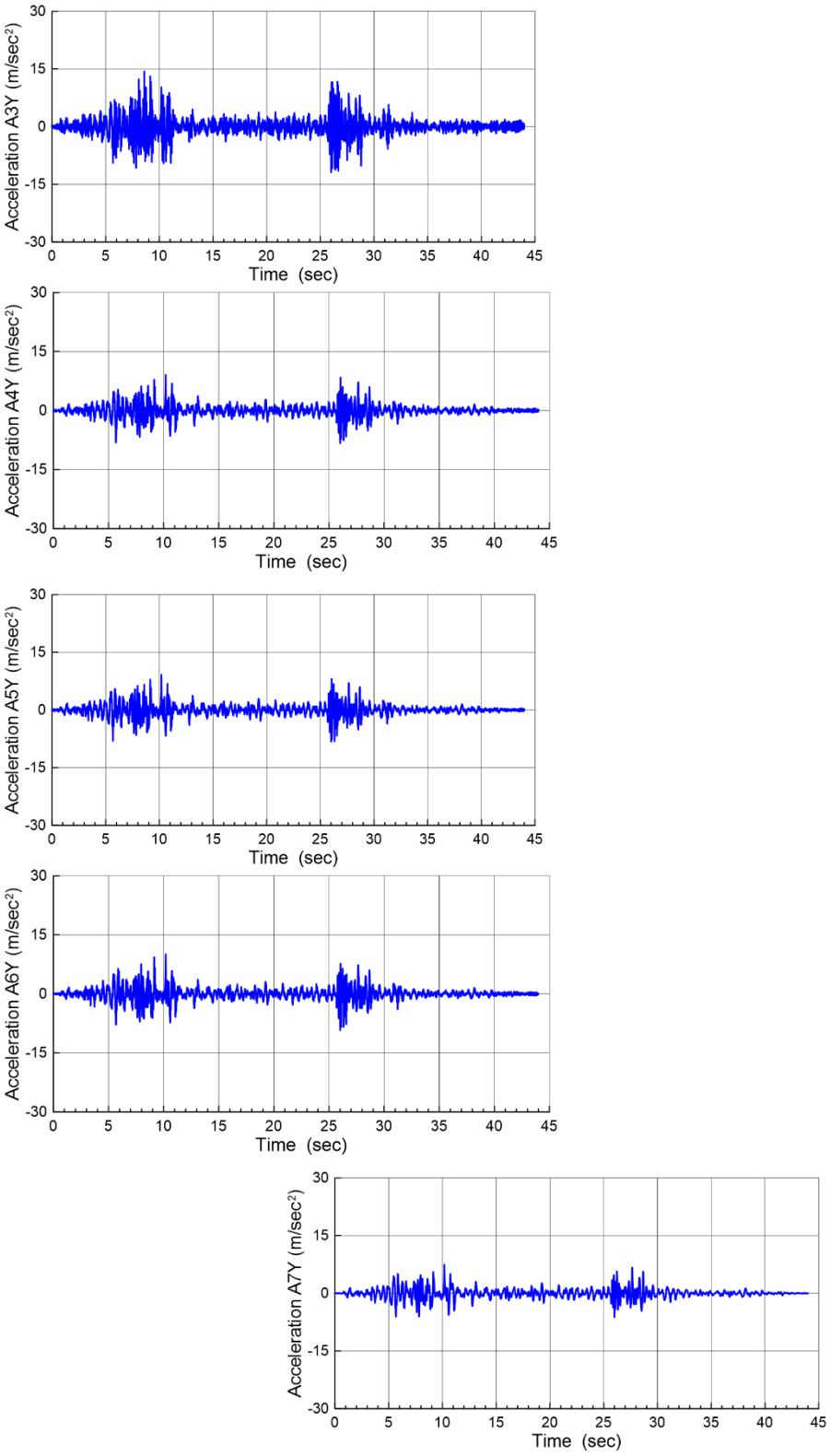

FIGURE 116: TEST 4: ACCELERATION TIME HISTORIES ALONG Y DIRECTION AT MEASUREMENT POINTS A1 TO A7

This project has received funding from the European Union's Horizon 2020 research and innovation programme under grant agreement No 958218

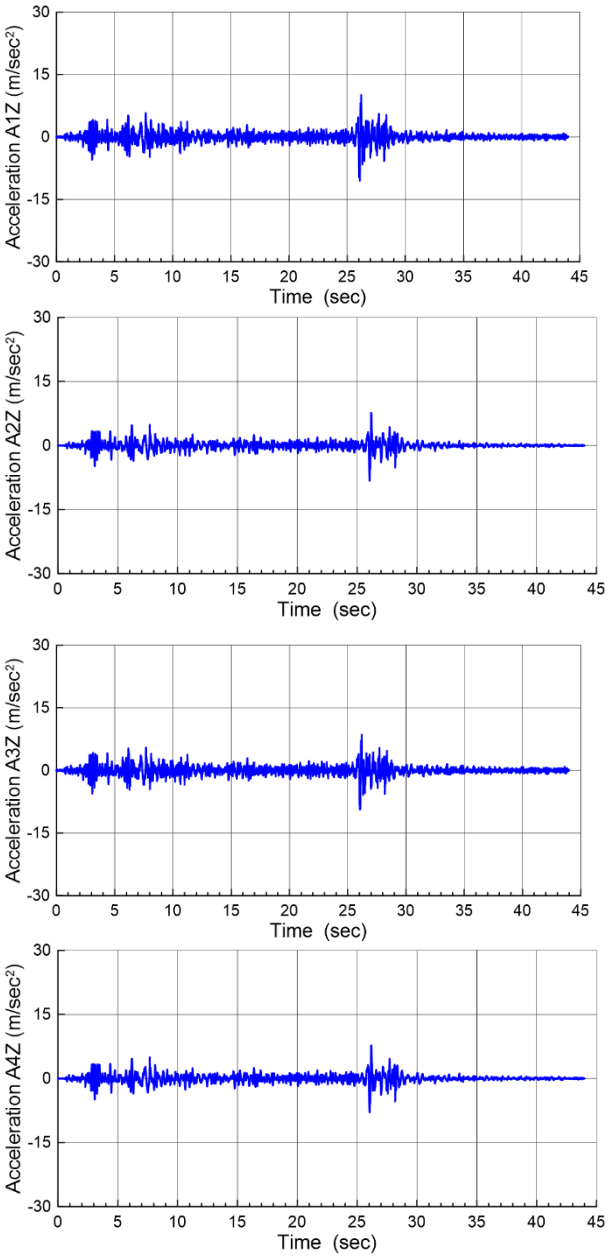

This project has received funding from the European Union's Horizon 2020 research and innovation programme under grant agreement No 958218

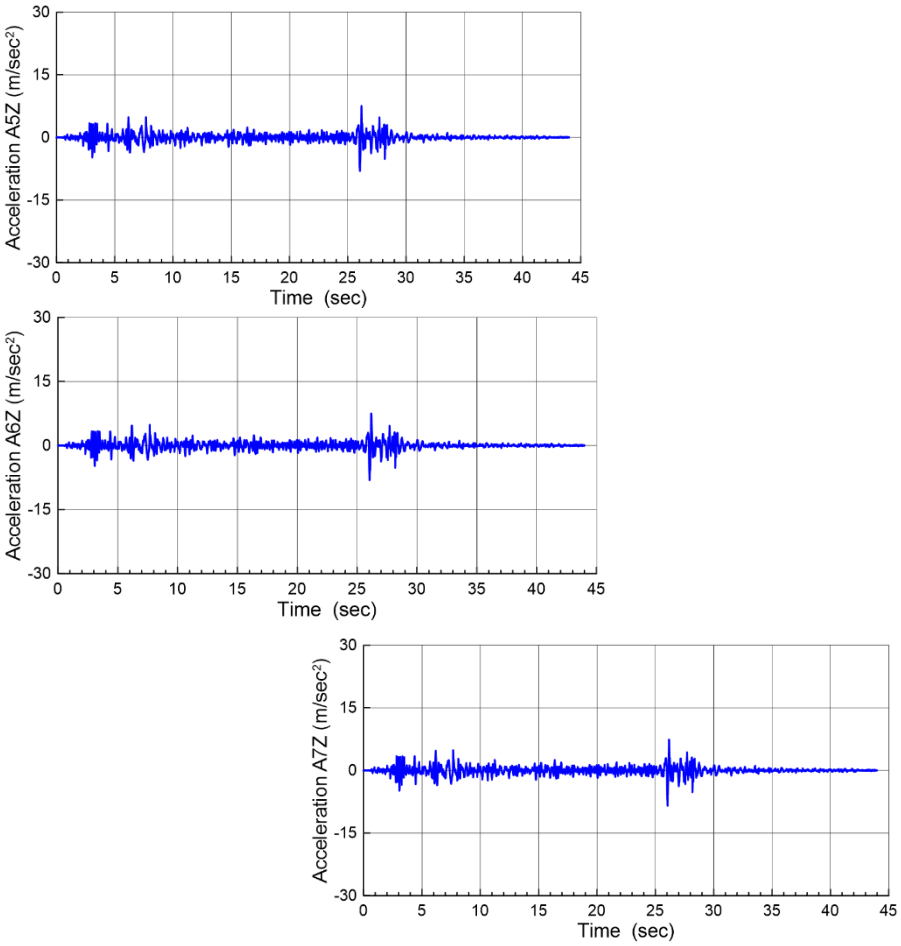

FIGURE 117: TEST 4: ACCELERATION TIME HISTORIES ALONG Z DIRECTION AT MEASUREMENT POINTS A1 TO A7

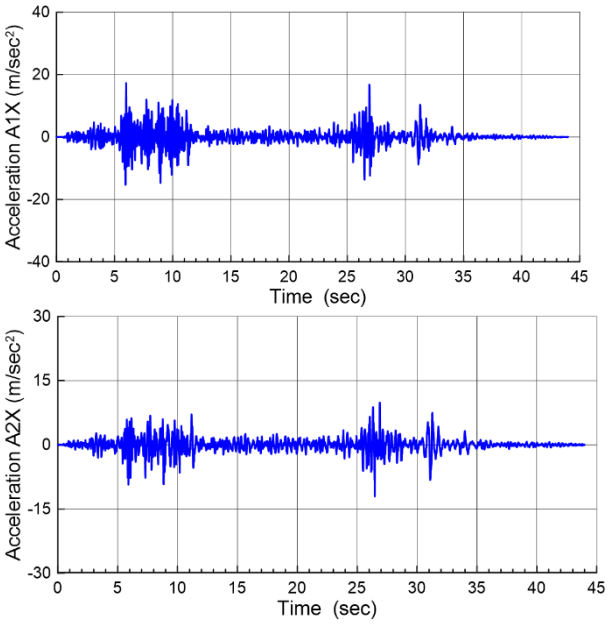

This project has received funding from the European Union's Horizon 2020 research and innovation programme under grant agreement No 958218

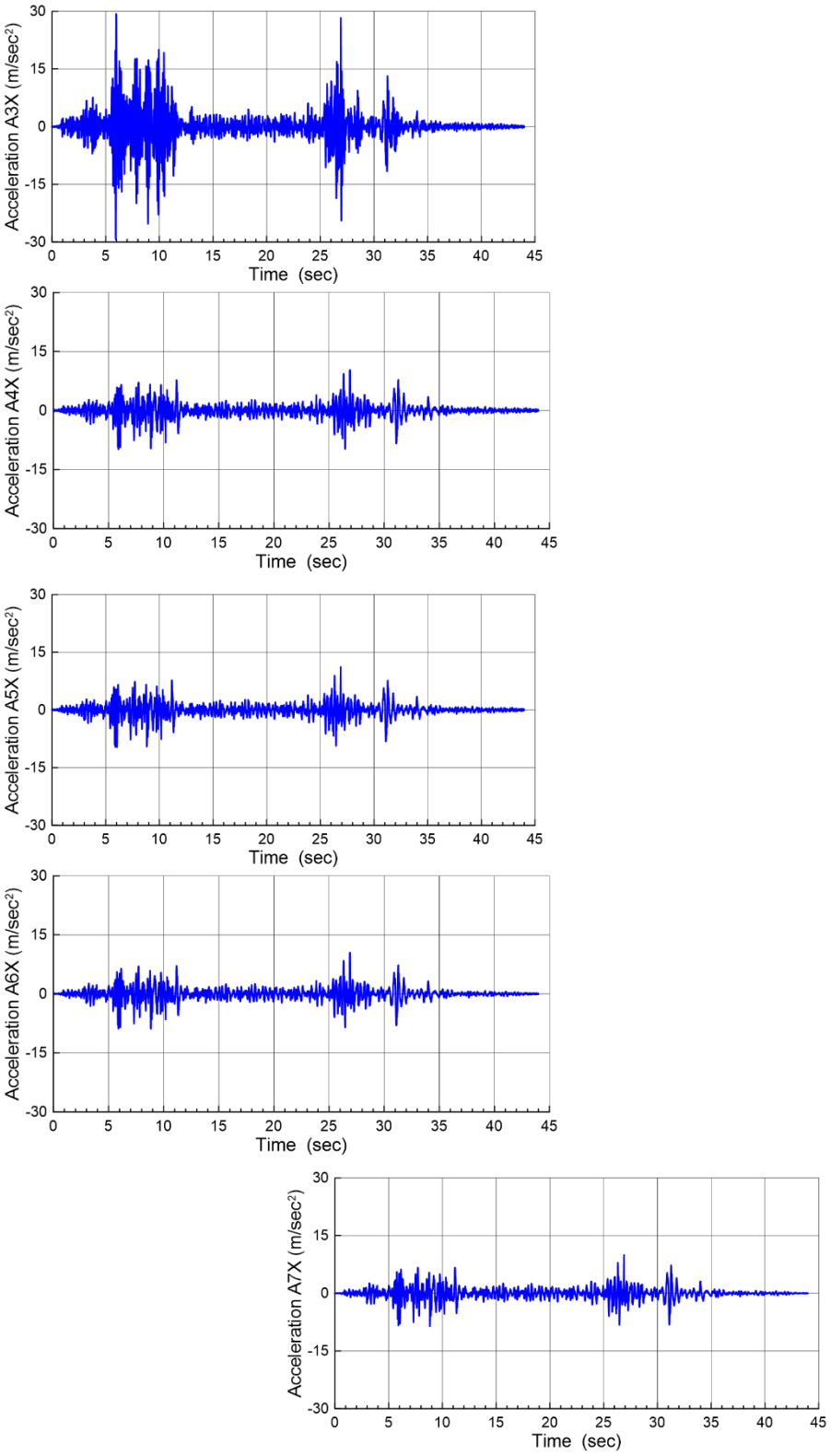

FIGURE 118: TEST 5: ACCELERATION TIME HISTORIES ALONG X DIRECTION AT MEASUREMENT POINTS A1 TO A7

This project has received funding from the European Union's Horizon 2020 research and innovation programme under grant agreement No 958218

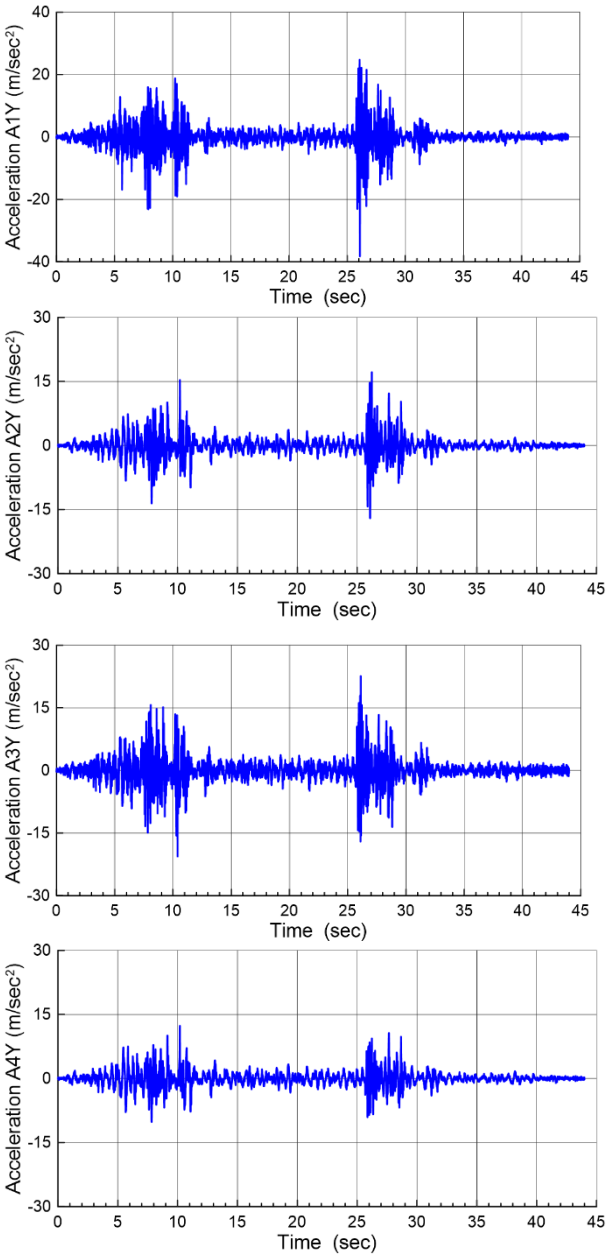

This project has received funding from the European Union's Horizon 2020 research and innovation programme under grant agreement No 958218

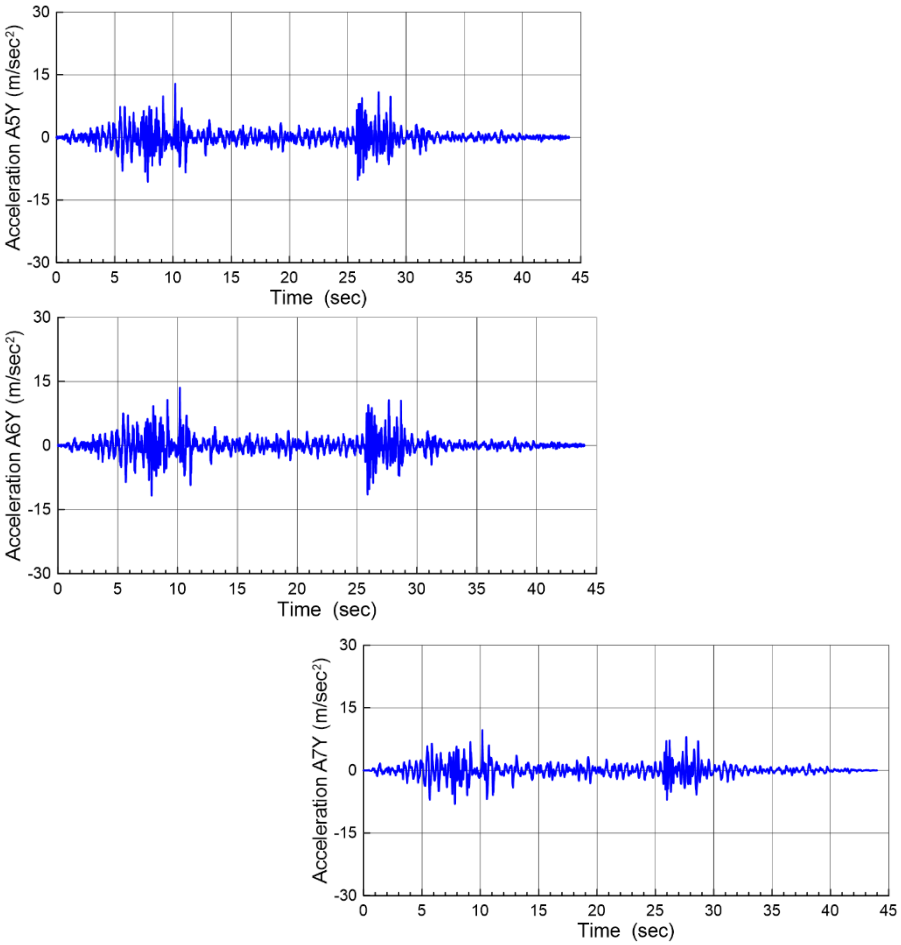

FIGURE 119: TEST 5: ACCELERATION TIME HISTORIES ALONG Y DIRECTION AT MEASUREMENT POINTS A1 TO A7

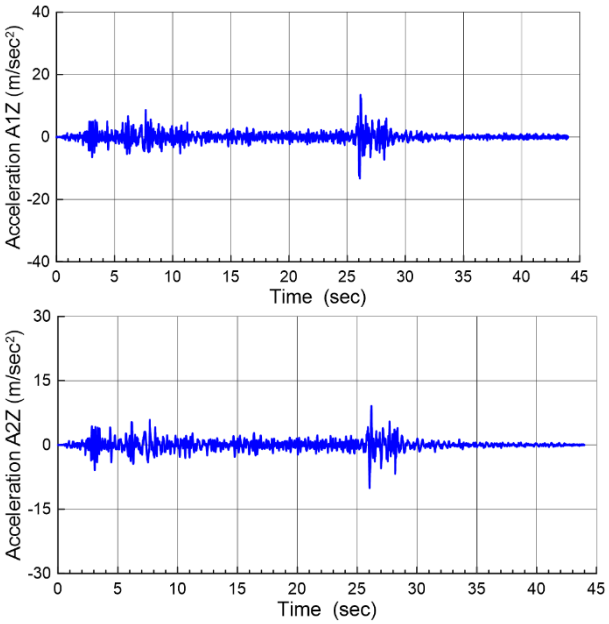

This project has received funding from the European Union's Horizon 2020 research and innovation programme under grant agreement No 958218

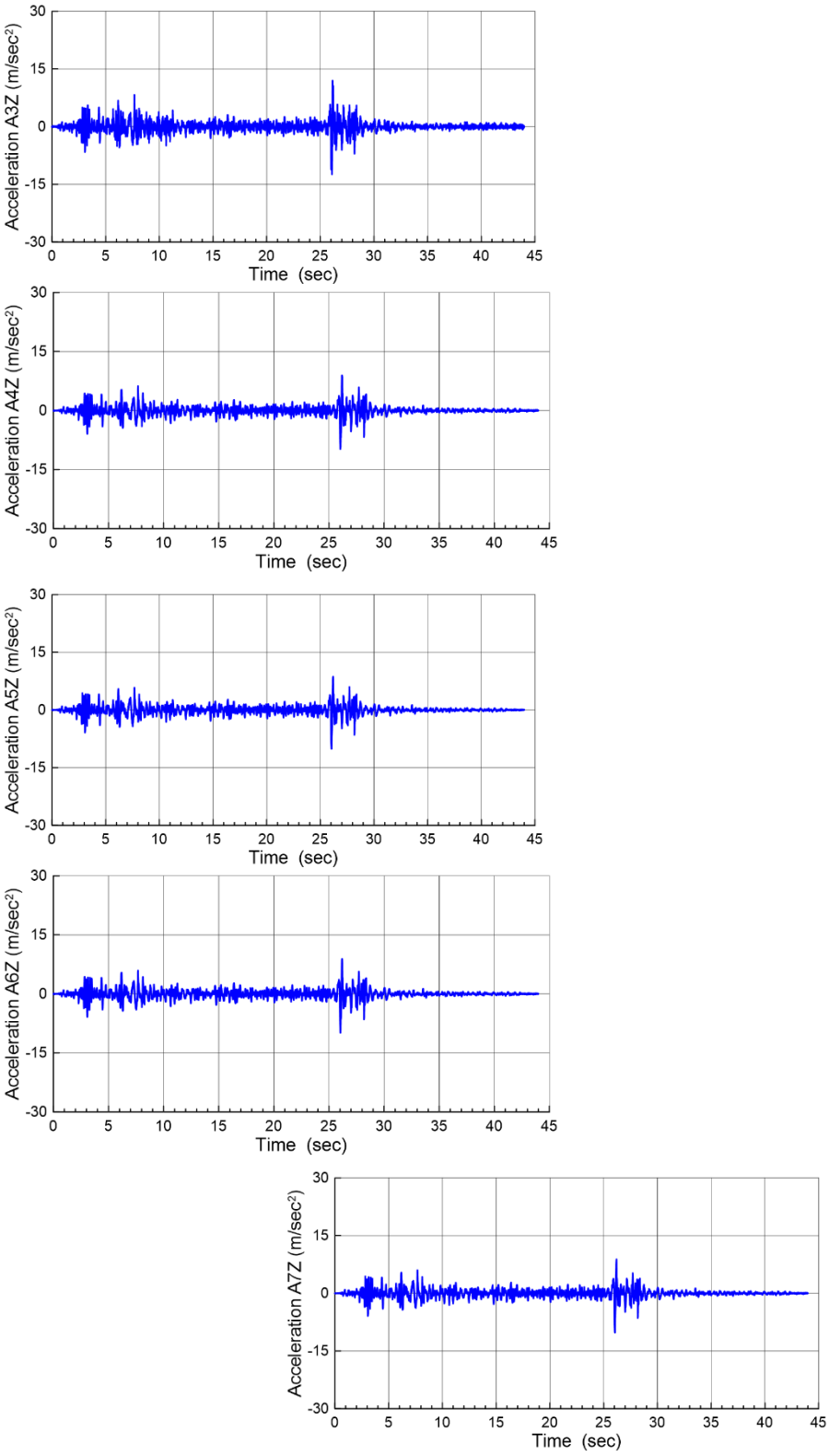

FIGURE 120: TEST 5: ACCELERATION TIME HISTORIES ALONG Z DIRECTION AT MEASUREMENT POINTS A1 TO A7

This project has received funding from the European Union's Horizon 2020 research and innovation programme under grant agreement No 958218

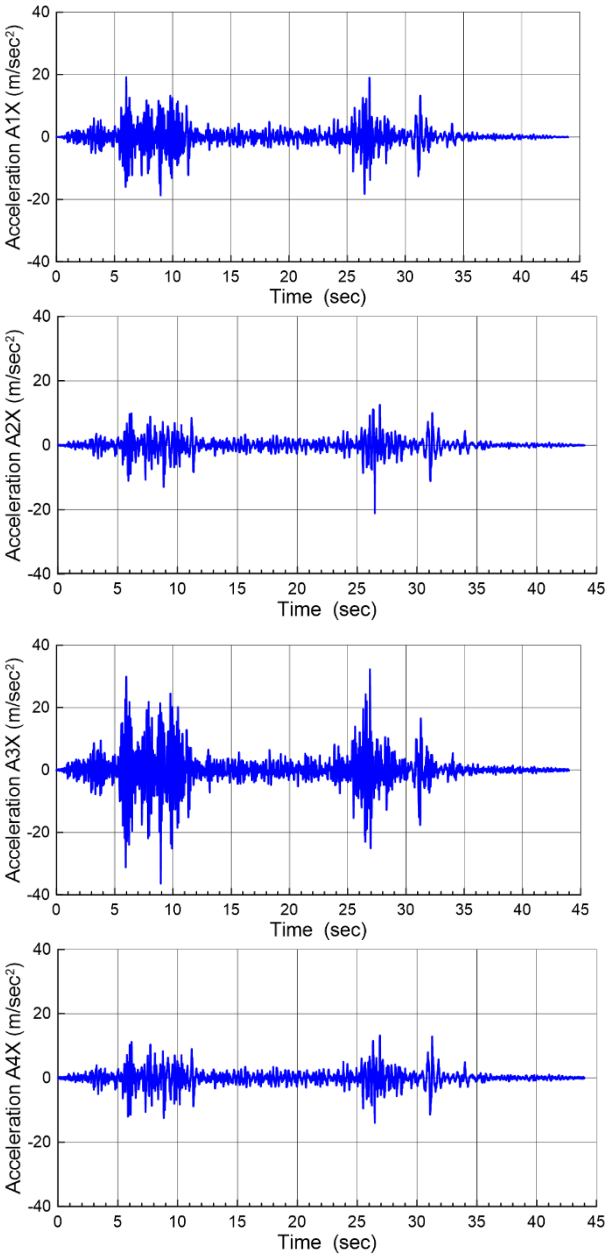

This project has received funding from the European Union's Horizon 2020 research and innovation programme under grant agreement No 958218

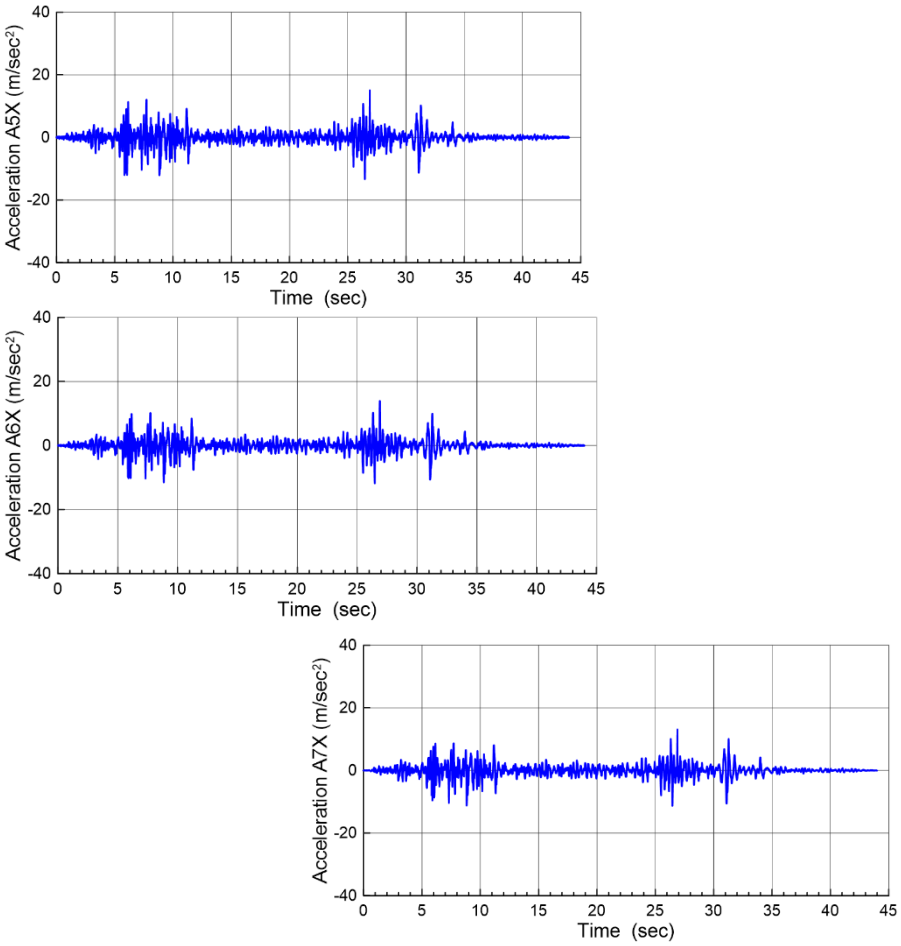

FIGURE 121: TEST 6: ACCELERATION TIME HISTORIES ALONG X DIRECTION AT MEASUREMENT POINTS A1 TO A7

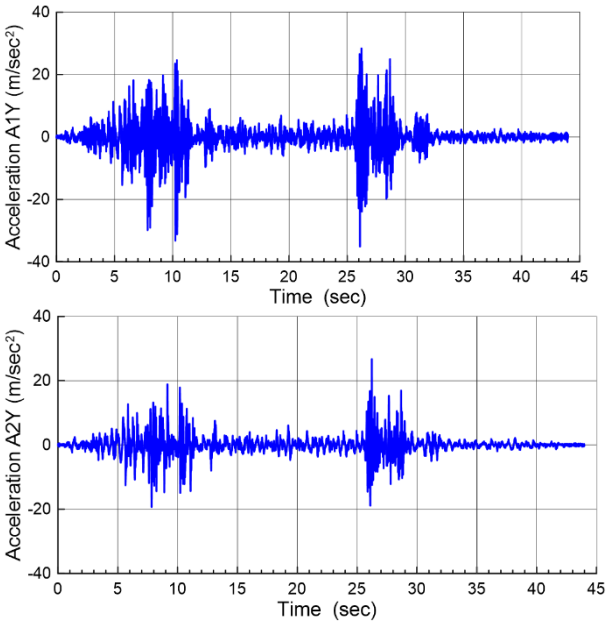

This project has received funding from the European Union's Horizon 2020 research and innovation programme under grant agreement No 958218

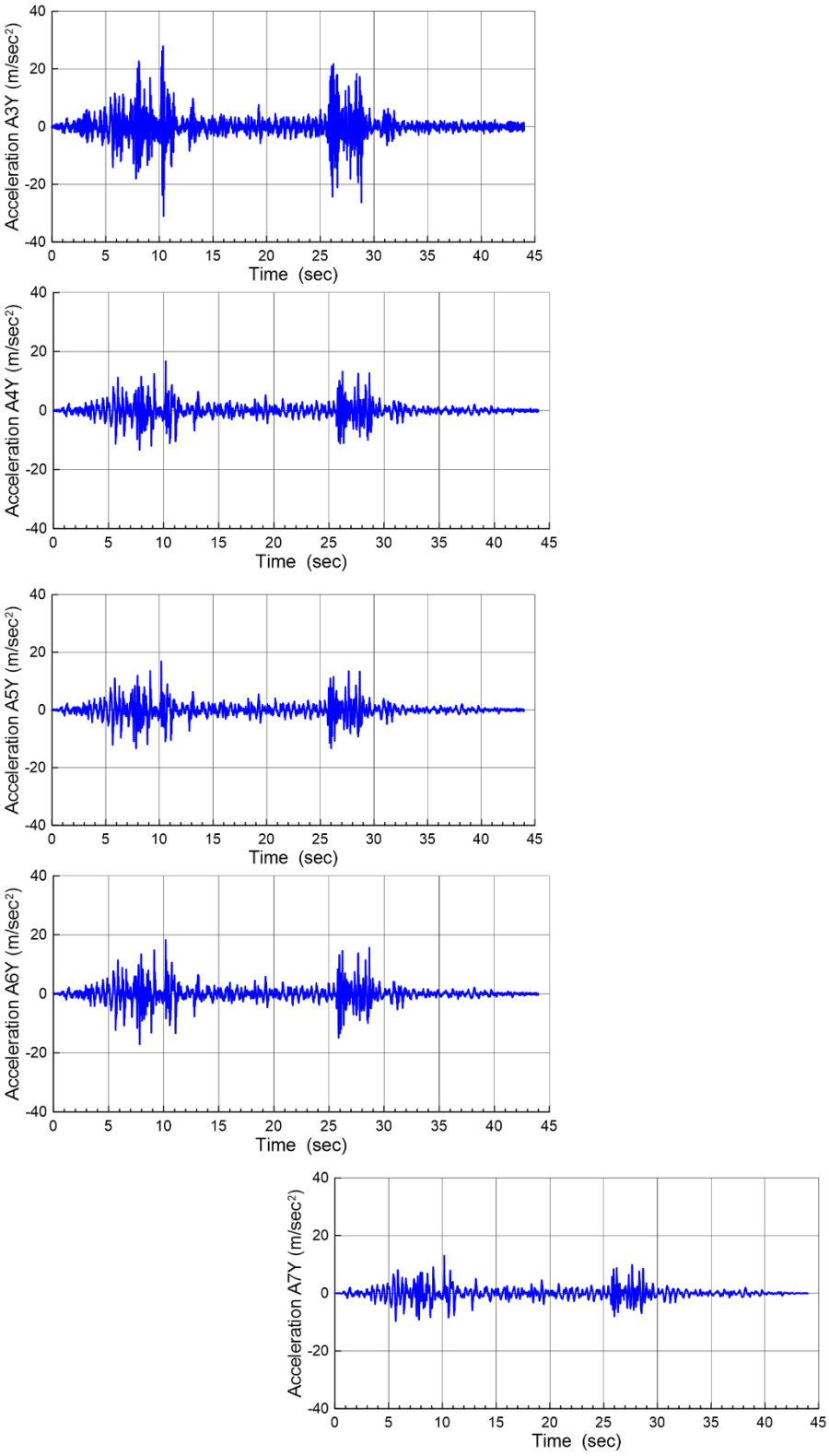

FIGURE 122: TEST 6: ACCELERATION TIME HISTORIES ALONG Y DIRECTION AT MEASUREMENT POINTS A1 TO A7

This project has received funding from the European Union's Horizon 2020 research and innovation programme under grant agreement No 958218

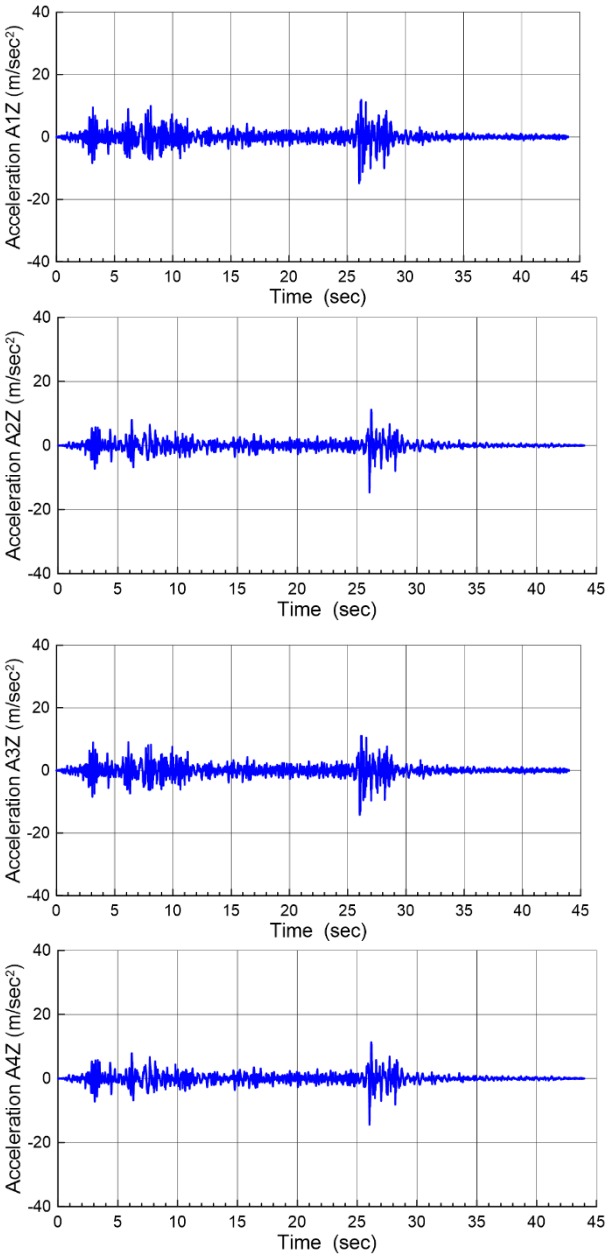

This project has received funding from the European Union's Horizon 2020 research and innovation programme under grant agreement No 958218

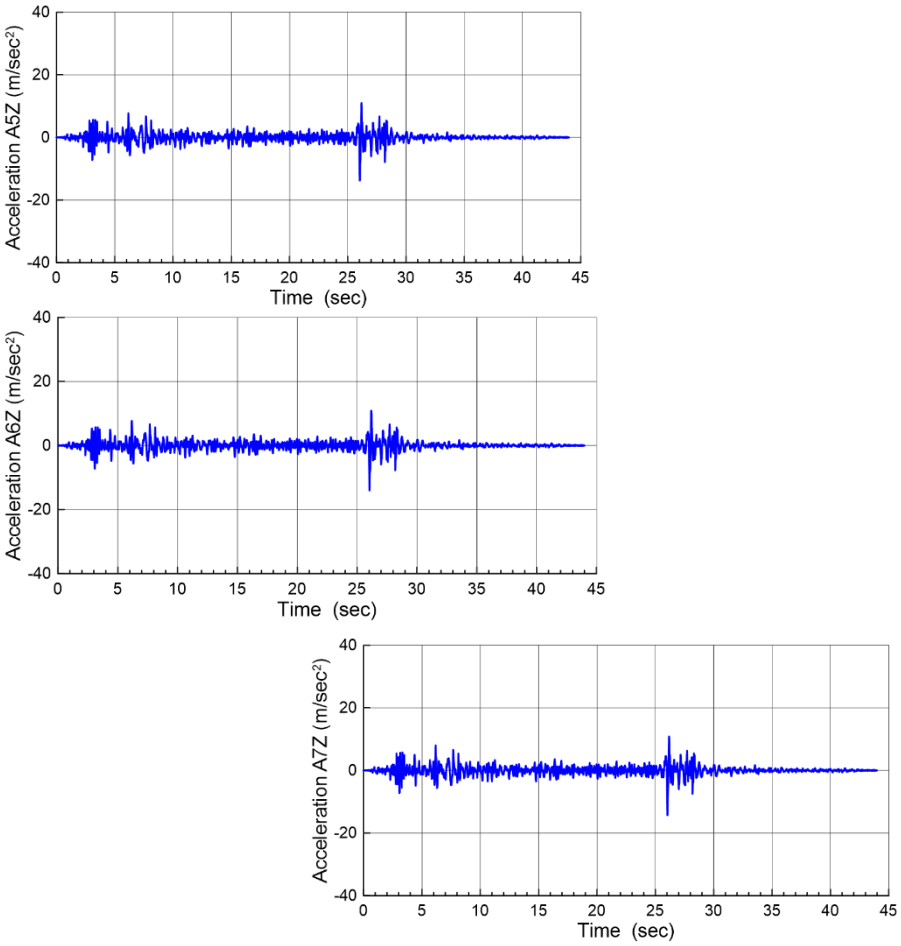

FIGURE 123: TEST 6: ACCELERATION TIME HISTORIES ALONG Z DIRECTION AT MEASUREMENT POINTS A1 TO A7

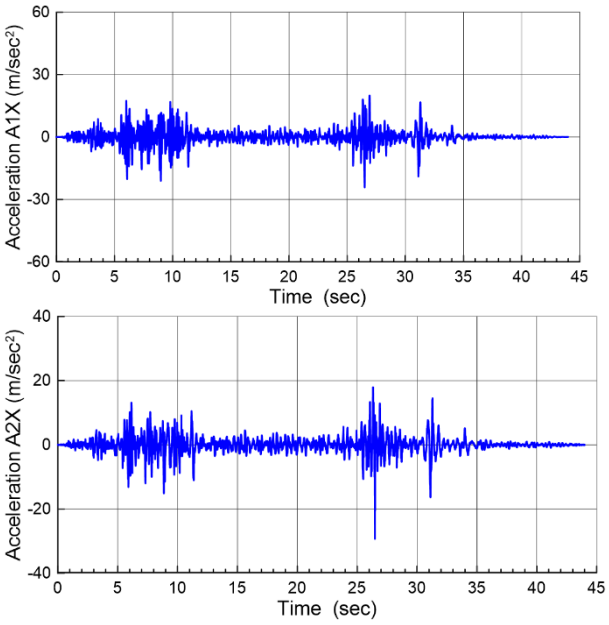

This project has received funding from the European Union's Horizon 2020 research and innovation programme under grant agreement No 958218

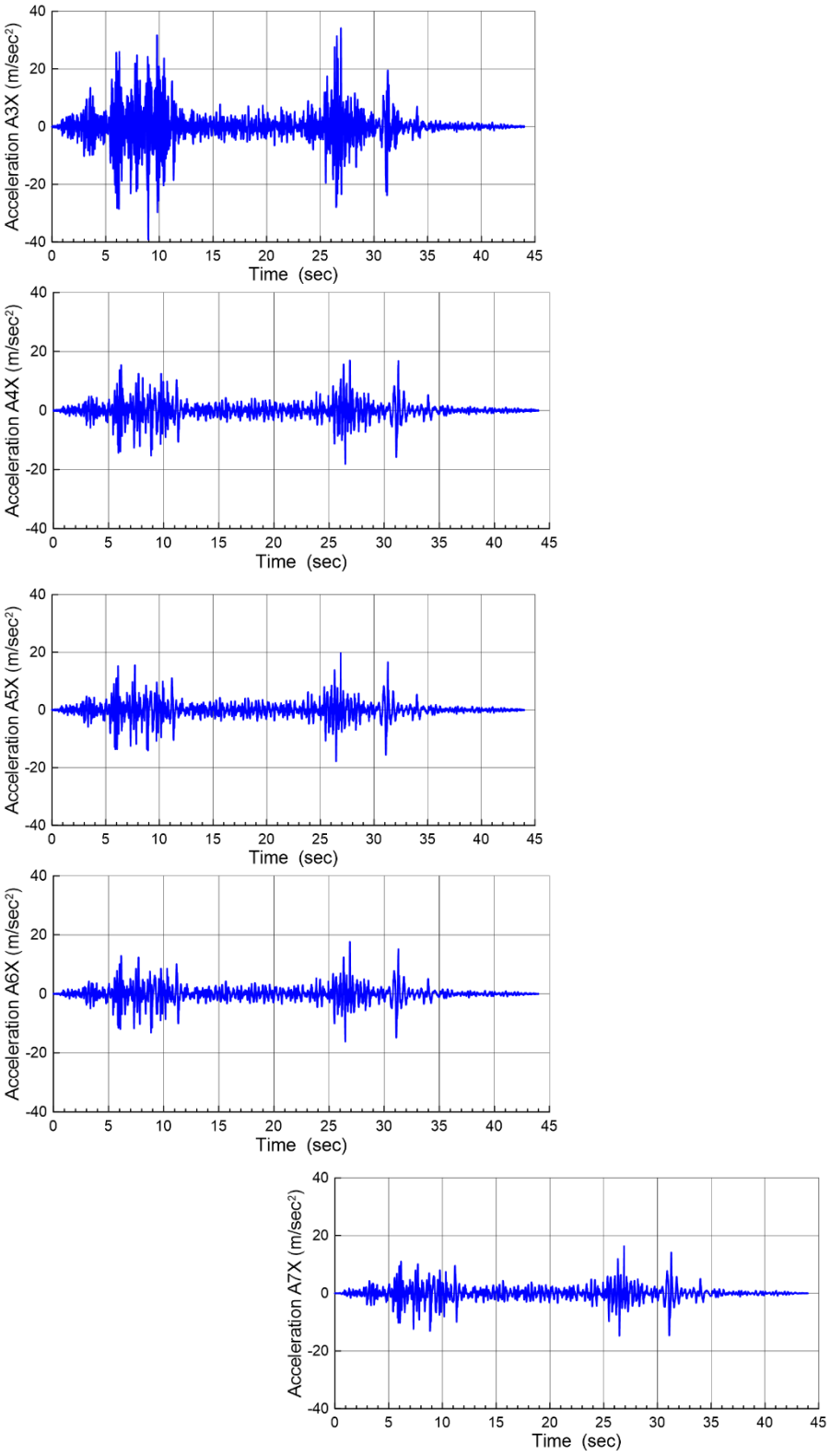

FIGURE 124: TEST 7: ACCELERATION TIME HISTORIES ALONG X DIRECTION AT MEASUREMENT POINTS A1 TO A7

This project has received funding from the European Union's Horizon 2020 research and innovation programme under grant agreement No 958218

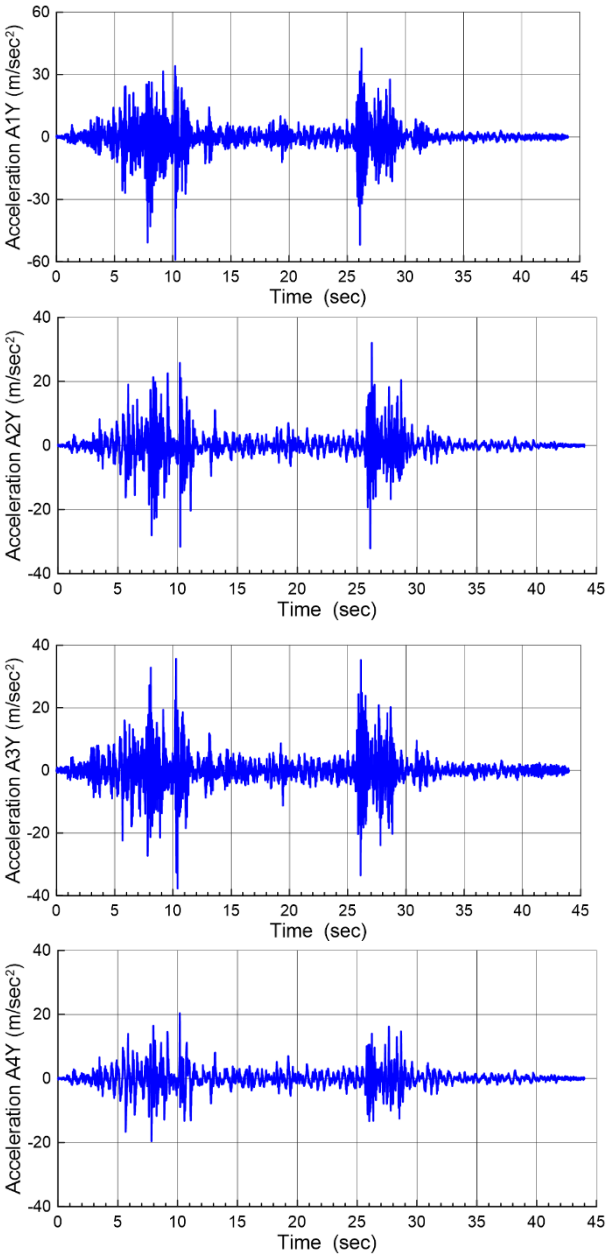

This project has received funding from the European Union's Horizon 2020 research and innovation programme under grant agreement No 958218

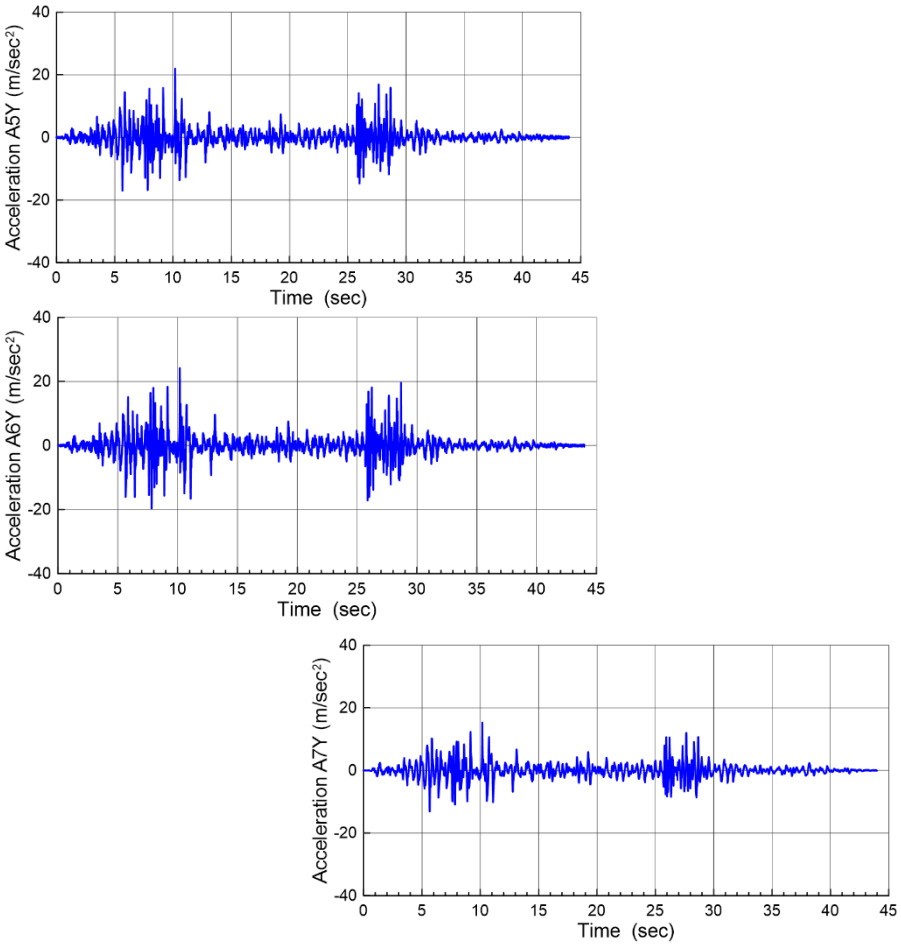

FIGURE 125: TEST 7: ACCELERATION TIME HISTORIES ALONG Y DIRECTION AT MEASUREMENT POINTS A1 TO A7

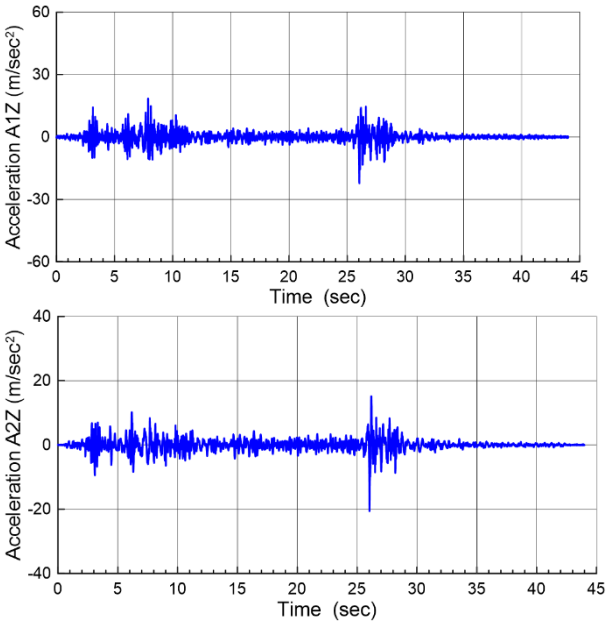

This project has received funding from the European Union's Horizon 2020 research and innovation programme under grant agreement No 958218

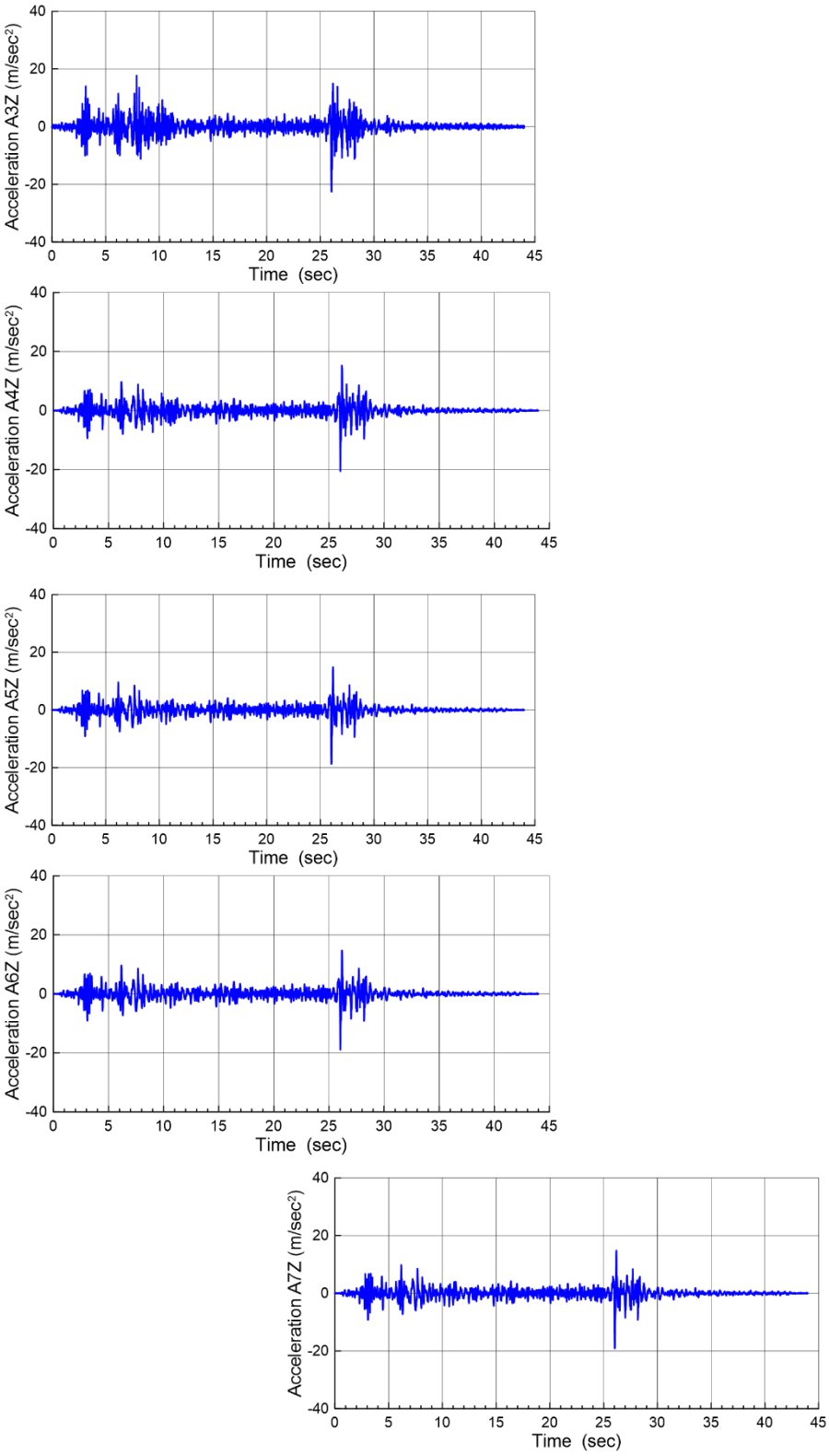

FIGURE 126: TEST 7: ACCELERATION TIME HISTORIES ALONG Z DIRECTION AT MEASUREMENT POINTS A1 TO A7

This project has received funding from the European Union's Horizon 2020 research and innovation programme under grant agreement No 958218

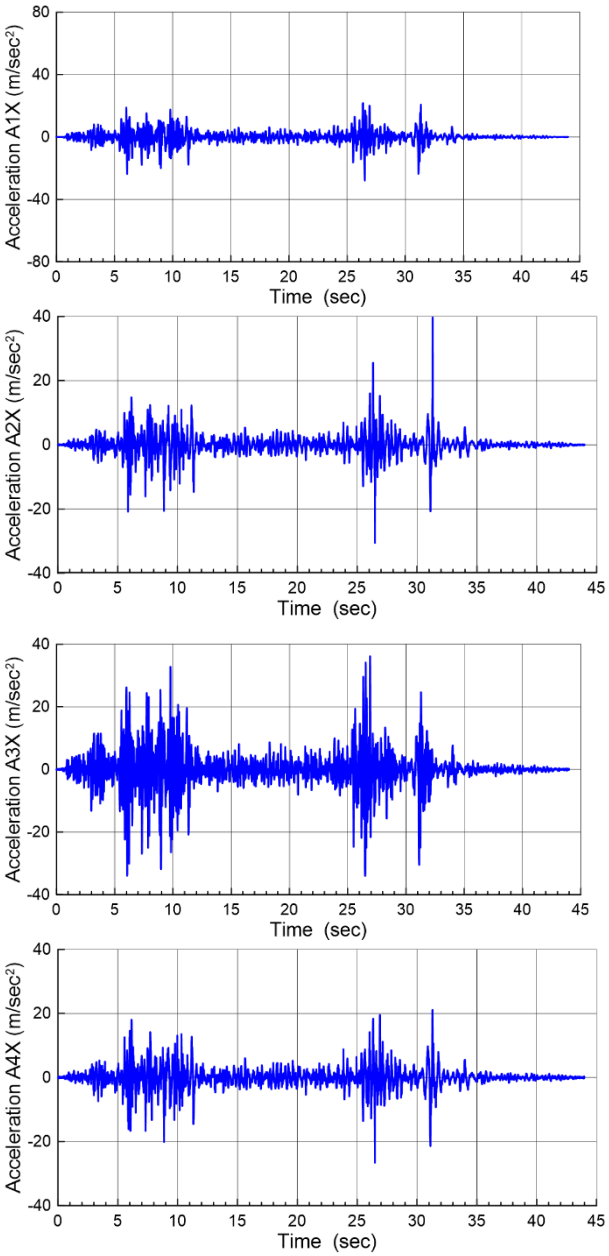

This project has received funding from the European Union's Horizon 2020 research and innovation programme under grant agreement No 958218

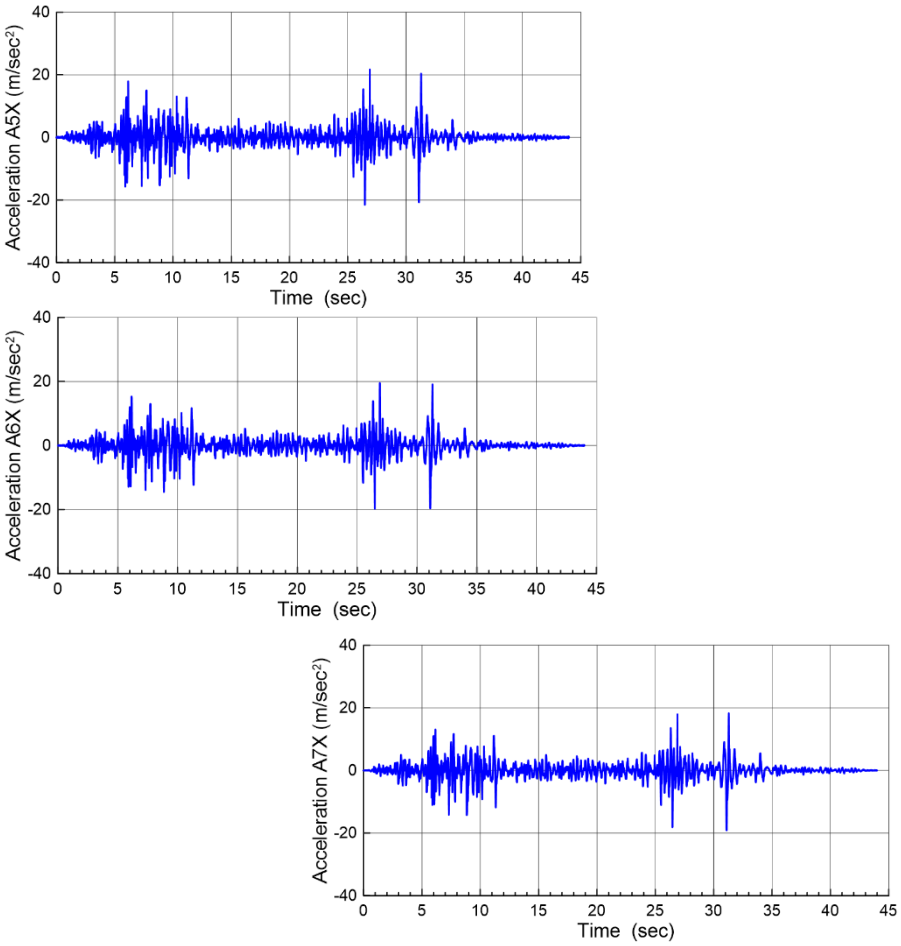

FIGURE 127: TEST 8: ACCELERATION TIME HISTORIES ALONG X DIRECTION AT MEASUREMENT POINTS A1 TO A7

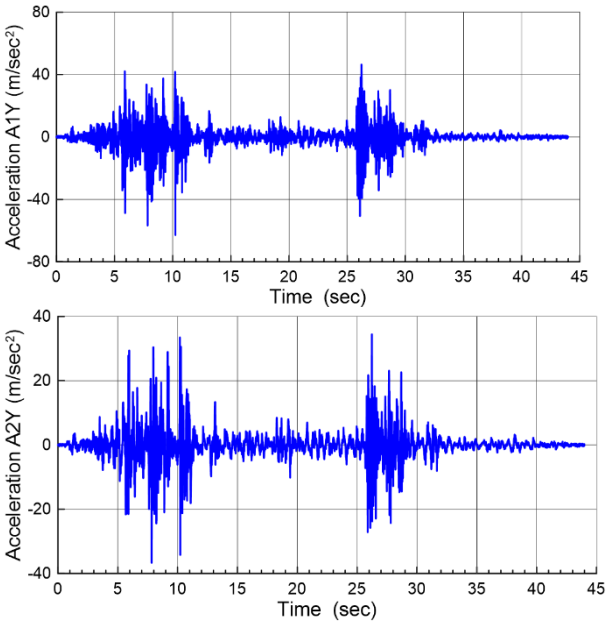

This project has received funding from the European Union's Horizon 2020 research and innovation programme under grant agreement No 958218

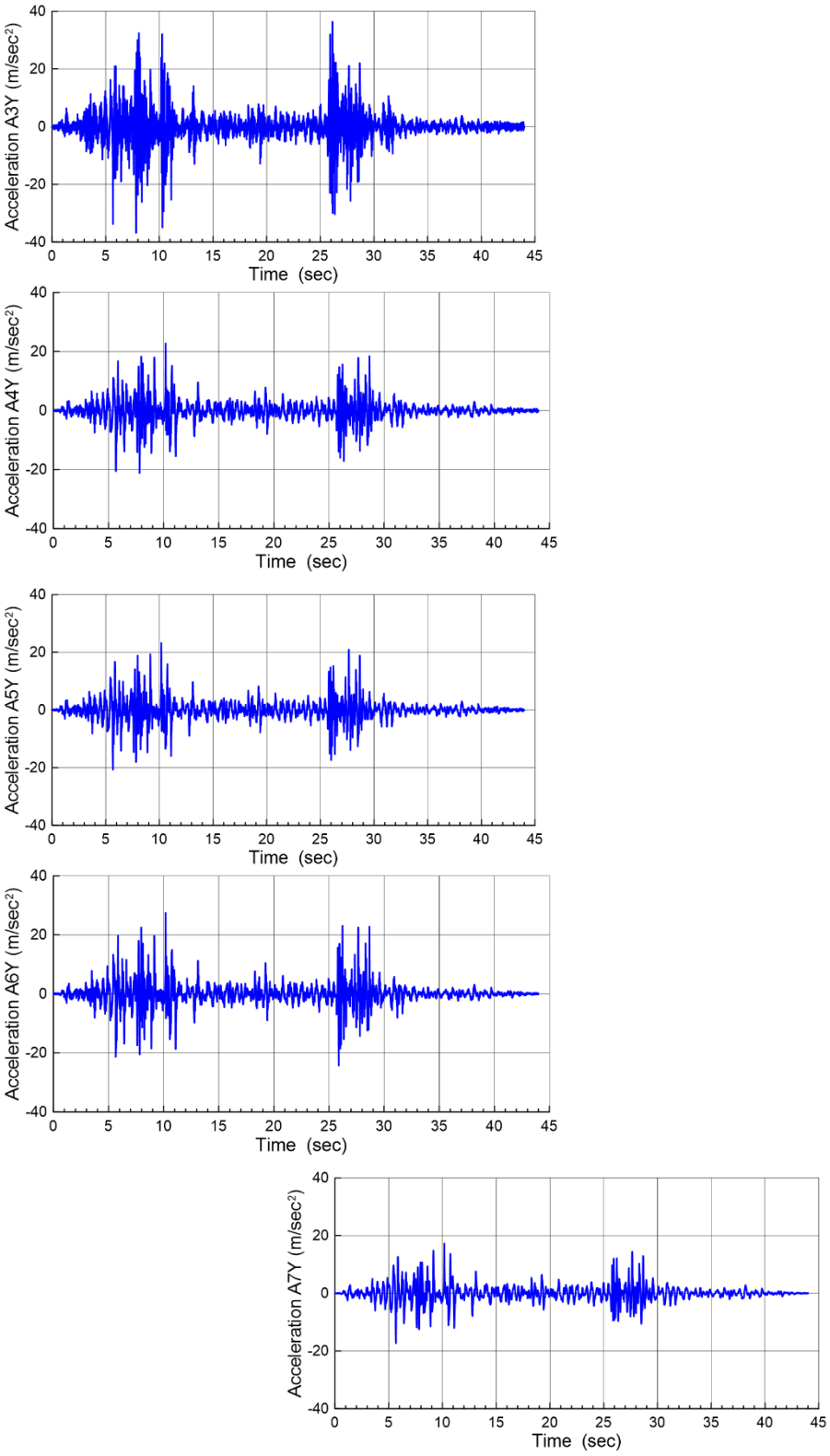

FIGURE 128: TEST 8: ACCELERATION TIME HISTORIES ALONG X DIRECTION AT MEASUREMENT POINTS A1 TO A7

This project has received funding from the European Union's Horizon 2020 research and innovation programme under grant agreement No 958218

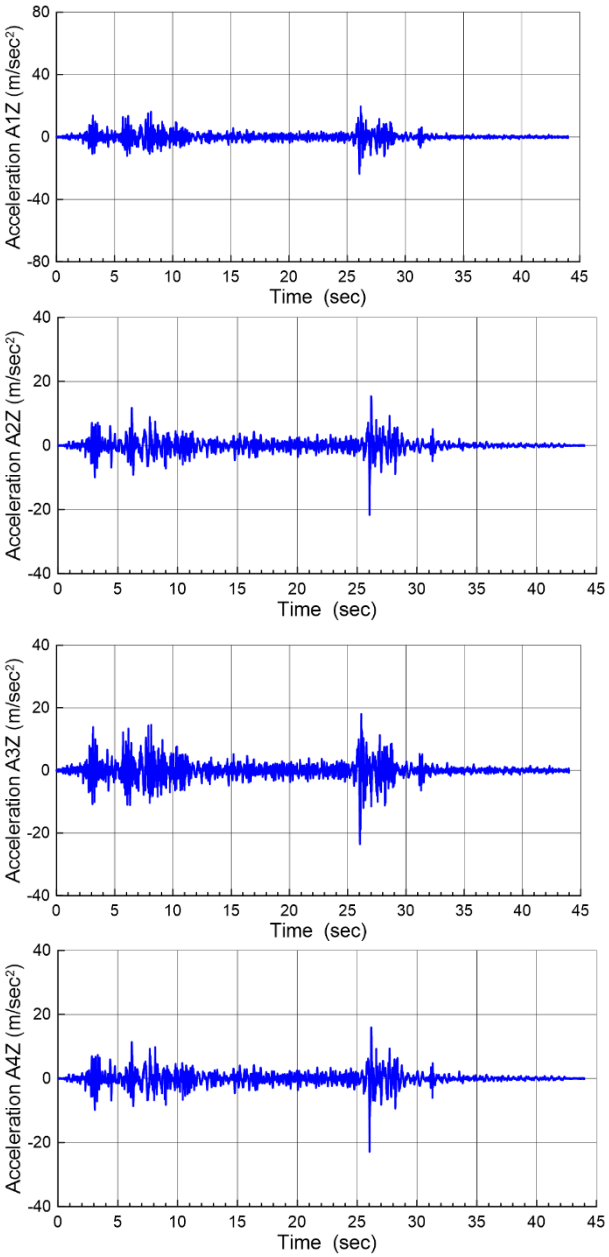

This project has received funding from the European Union's Horizon 2020 research and innovation programme under grant agreement No 958218

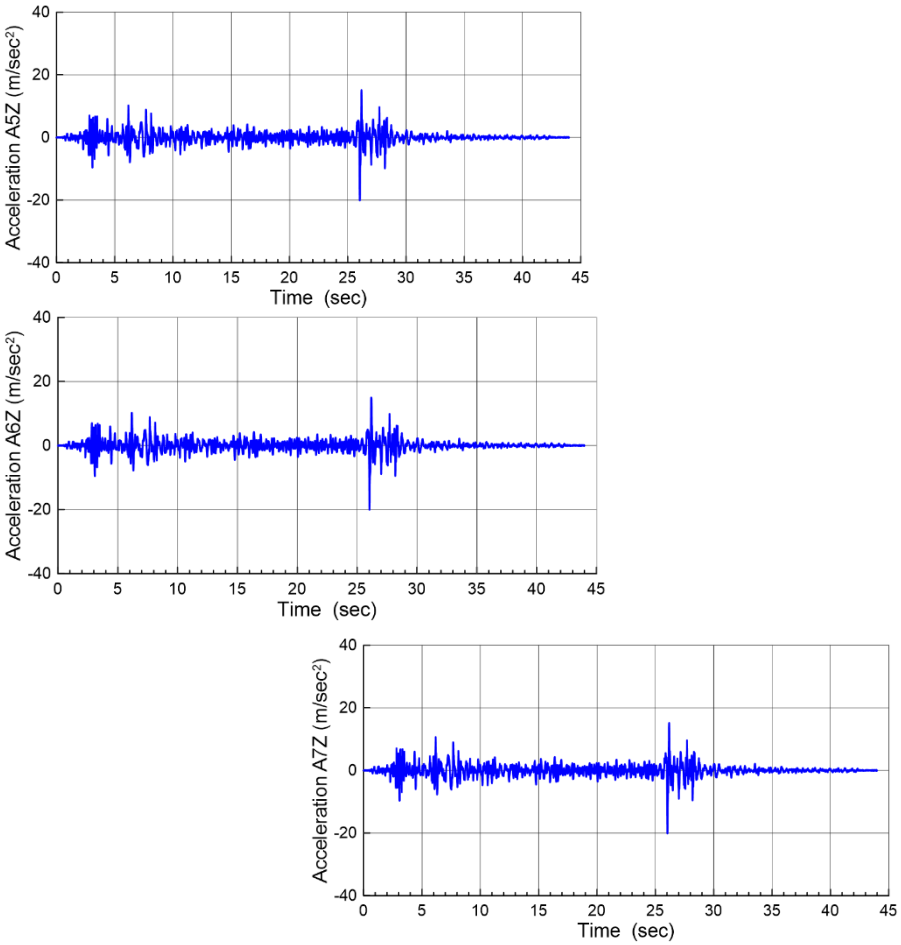

FIGURE 129: TEST 8: ACCELERATION TIME HISTORIES ALONG Z DIRECTION AT MEASUREMENT POINTS A1 TO A7

11.2.3 Observed damages

During testing, no visible damage was observed on the SmartWall, infill wall and steel frame.

11.3 Dynamic characteristics- after shaking table tests

After triaxial tests, logarithmic sine sweep was performed in order to check for any variation of the dynamic characteristics of the specimen. These tests were performed separately along X, Y and Z directions, with frequency range from 0.5 Hz to 35 Hz, at a rate of one octave per minute and an amplitude of excitation equals to 0.50 m/sec2 (0.05 g). In Figure 42, the natural frequencies and the damping coefficients, after seismic tests of the specimen are given. The Transfer functions (TRF) between base and recorded acceleration at points A1 to A6 are shown in Figure 130 and Figure 131, for sine sweep tests in X and Y direction. In Figure 132 and Figure 133, the transfer functions before and after seismic verification tests at points A1 to A6 are compared. Practical the frequencies and

This project has received funding from the European Union's Horizon 2020 research and innovation programme under grant agreement No 958218

damping ratios of SmartWall were the same as those measured prior seismic tests. Reduction of frequency and increase of damping ratio was found along X direction, for brick wall.

TABLE 55: DYNAMIC PROPERTIES AFTER SHAKING TABLE TESTS

Position	Direction	Fundamental frequency (Hz)	Period (sec)	Damping ratio (%)
A1 SmartWall Outer frame	X Y Z	11.33 13.28/16.87/19.35 -	0.088 0.075/0.057/0.052 -	4.04 2.70/1.50/5.00 -
A2 SmartWall Inner frame	X Y Z	23.83 13.28/16.21 -	0.042 0.075/0.062 -	4.04 2.70/1.50 -
A3 SmartWall Outer frame	X Y Z	11.33 13.28/ 16.21/19.82 28.34	0.088 0.075/0.062/0.050 0.035	4.04 2.70/1.50/5.00 4.02
A4 SmartWall Inner frame	X Y Z	24.27 13.13/16.11 -	0.041 0.076/0.062 -	10.02 2.70/1.50 -
A5 Brick wall	X Y Z	23.78 13.13/16.11 -	0.042 0.076/0.062 -	10.03 2.70/1.50 -
A6 Brick wall	X Y Z	23.78 13.13/16.11 -	0.042 0.076/0.062 -	10.03 2.70/1.50 -

This project has received funding from the European Union's Horizon 2020 research and innovation programme under grant agreement No 958218

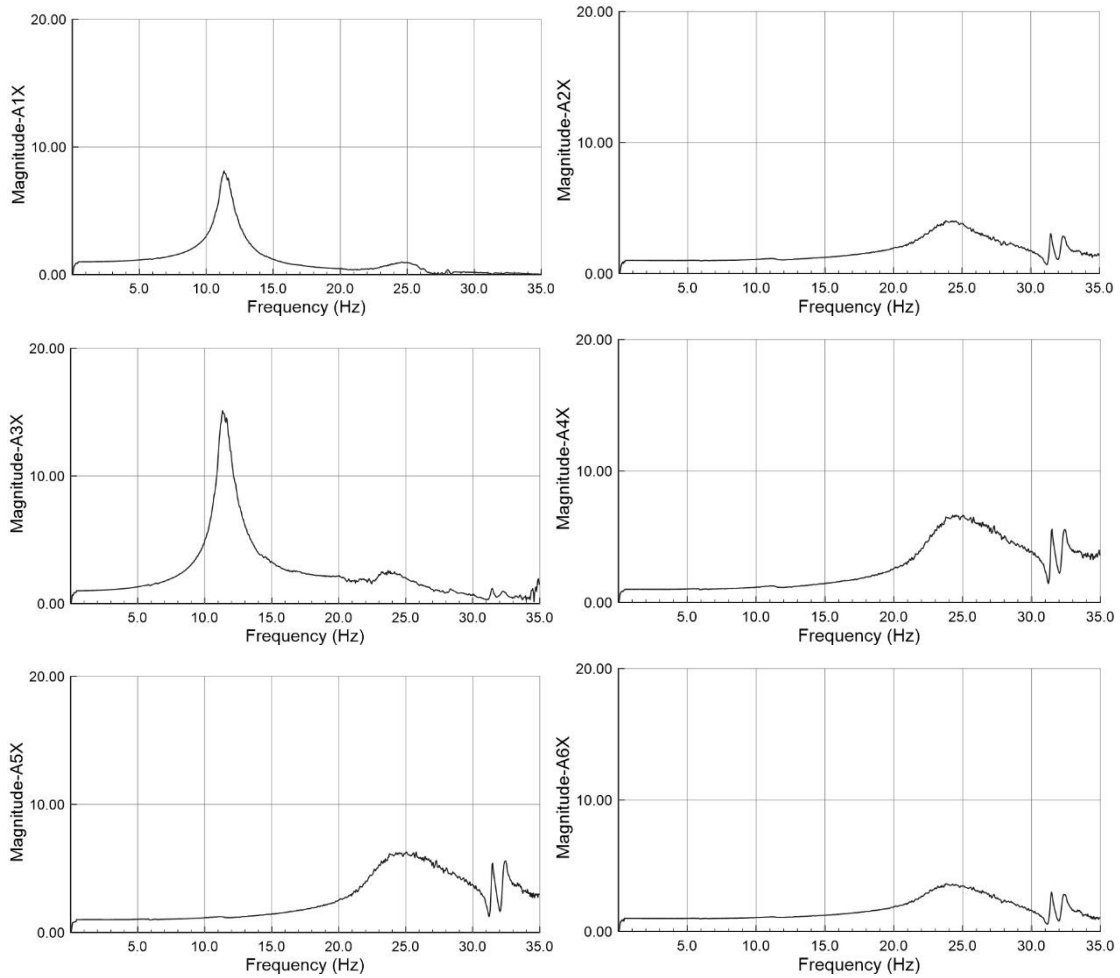

FIGURE 130: SINE SWEEP IN X DIRECTION AFTER SEISMIC TESTS: TRANSFER FUNCTION AT MEASUREMENT POINTS A1 TO A6

This project has received funding from the European Union's Horizon 2020 research and innovation programme under grant agreement No 958218

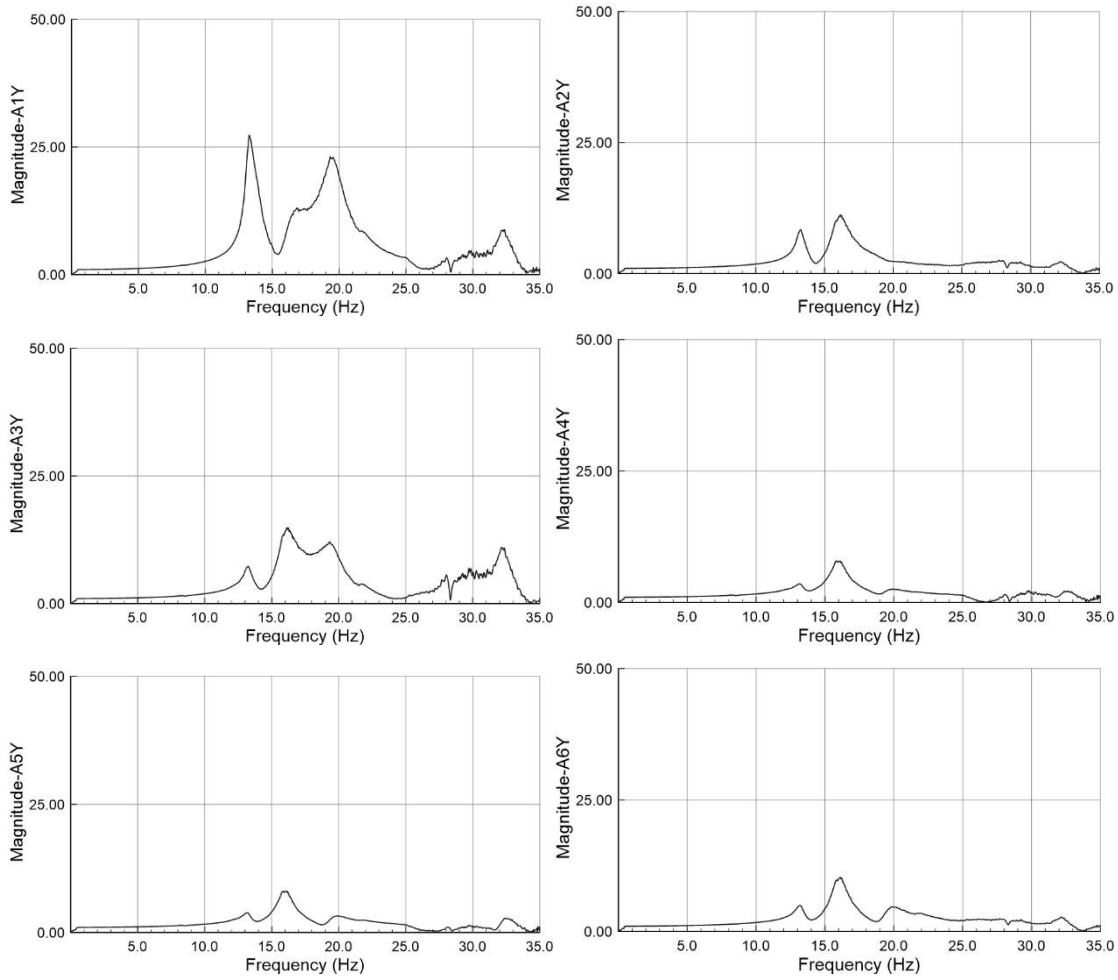

FIGURE 131: SINE SWEEP IN Y DIRECTION AFTER SEISMIC TESTS: TRANSFER FUNCTION AT MEASUREMENT POINTS A1 TO A6

This project has received funding from the European Union's Horizon 2020 research and innovation programme under grant agreement No 958218

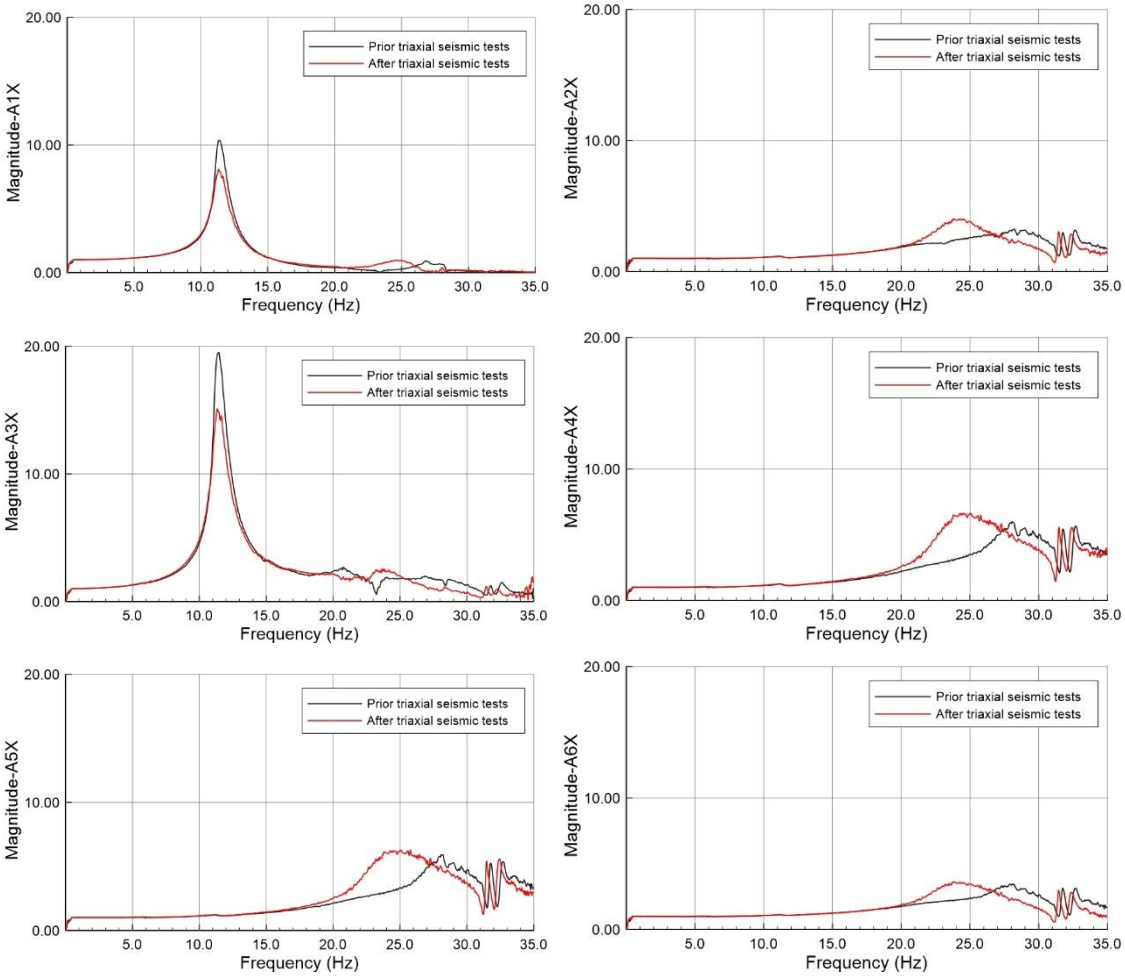

FIGURE 132: SINE SWEEP IN X DIRECTION PRIOR SEISMIC TESTS: TRANSFER FUNCTION PRIOR AND AFTER SEISMIC TESTS AT MEASUREMENT POINTS A1 TO A6

This project has received funding from the European Union's Horizon 2020 research and innovation programme under grant agreement No 958218

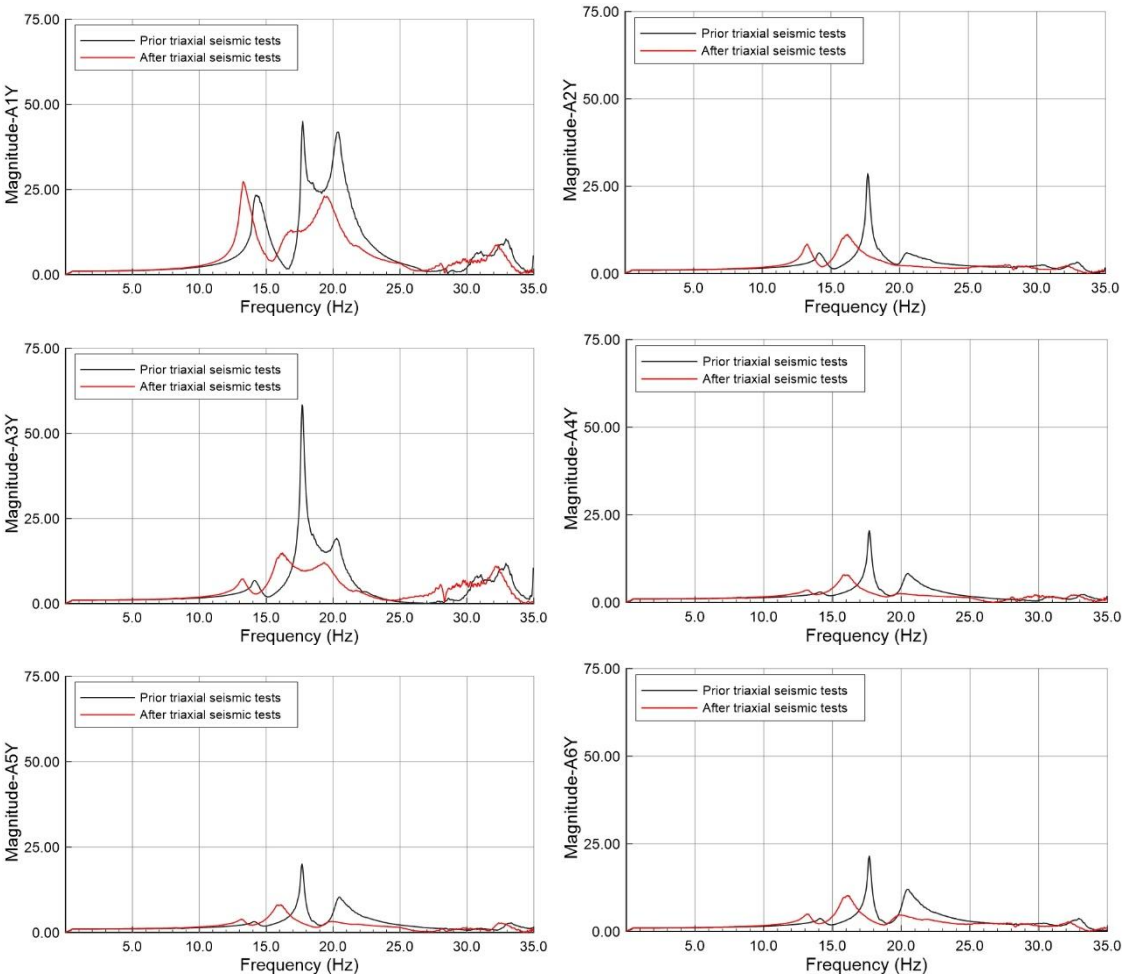

FIGURE 133: SINE SWEEP IN Y DIRECTION: TRANSFER FUNCTION PRIOR AND AFTER SEISMIC TESTS AT MEASUREMENT POINTS A1 TO A6

This project has received funding from the European Union's Horizon 2020 research and innovation programme under grant agreement No 958218

12 Annex II – Details for the mechanical investigation of eWHC / ConnExWall

The design values of actions (STR/GEO) are to be taken according to Table A1.2(B)(CZ)-1. For the determination of fundamental combination of actions, the less favourable of the twin expressions (6.10a), (6.10b) is to be applied. The application of a combination of actions according to the expressions (6.10a) and (6.10b) gives in common cases more uniform reliability level of structures for various ratios of characteristic values of variable loads and permanent loads.

Table A1.2(B)(CZ)-1 – Design values of actions (STR/GEO) (set B)

Persistent and transient design situations	Permanent actions		Leading variable action	Accompanying variable actions	
	Unfavourable	Favourable		Main (if any)	Others
Eq. (6.10a)	1,35 $G_{k,j,sup}$	1,00 $G_{k,j,inf}$		1,5$\psi_{0,1}Q_{k,1}$ (0 where favourable)	1,5 $\psi_{0,i}Q_{k,i}$ (0 where favourable)
Eq. (6.10b)	1,35 × 0,85 $G_{k,j,sup}$	1,00 $G_{k,j,inf}$	1,5 $Q_{k,1}$ (0 where favourable)		1,5 $\psi_{0,i}Q_{k,i}$ (0 where favourable)
See EN 1991 to EN 1999 for application of γ factors for imposed deformations. NOTE The characteristic values of all permanent actions from one source are multiplied by $\gamma_{G,sup}$ if the total resulting action effect is unfavourable and $\gamma_{G,inf}$ if the total resulting action effect is favourable. For example, all actions originating from the self-weight of the structure may be considered as coming from one source; this also applies if different materials are involved.					

NOTE 1 As an alternative, a combination of actions according to the expression (6.10) may be used. This combination may nevertheless lead to the less economical solution. If the expression (6.10) is used for the determination of design values of actions, the values of partial factors γ and reduction factors ψ are to be taken according to Table A1.2(B)(CZ)-2.

FIGURE 134: DESIGN VALUES OF ACTIONS, SET A

Table A1.2(B)(CZ)-2 – Design values of actions (STR/GEO) (set B)

Persistent and transient design situations	Permanent actions		Leading variable action	Accompanying variable actions	
	Unfavourable	Favourable		Main (if any)	Others
Eq. (6.10)	1,35 $G_{k,j,sup}$	1,00 $G_{k,j,inf}$	1,50 $Q_{k,1}$ (0 where favourable)		1,50 $\psi_{0,i}Q_{k,i}$ (0 where favourable)

The design values of actions (STR/GEO) are given in Table A1.2(C)(CZ). For determination of combination of actions the expression (6.10) is to be used.

Table A1.2(C) (CZ) – Design values of actions (STR/GEO) (set C)

Persistent and transient design situations	Permanent actions		Leading variable action	Accompanying variable actions	
	Unfavourable	Favourable		Main (if any)	Others
Eq. (6.10)	1,00$G_{k,j,sup}$	1,00$G_{k,j,inf}$	1,30 $Q_{k,1}$ (0 where favourable)		1,30 $\psi_{0,i}$ $Q_{k,i}$ (0 where favourable)

NOTE 2 For the determination of the design values of actions given in Tables A1.2(A)(CZ) to A1.2 (C)(CZ), the procedures provided in Annex B, Table B.3, may be used in specific cases.

NOTE 3 Where the maximum water level is known and the water action may be considered as permanent action, then the partial factor γ_G = 1 may be applied for the determination of the design value of water action.

NOTE 4 For the determination of the design values of actions in transient design situations, see also EN 1991-1-6.

FIGURE 135: DESIGN VALUES OF ACTIONS SET B, C

This project has received funding from the European Union's Horizon 2020 research and innovation programme under grant agreement No 958218

Design strategy

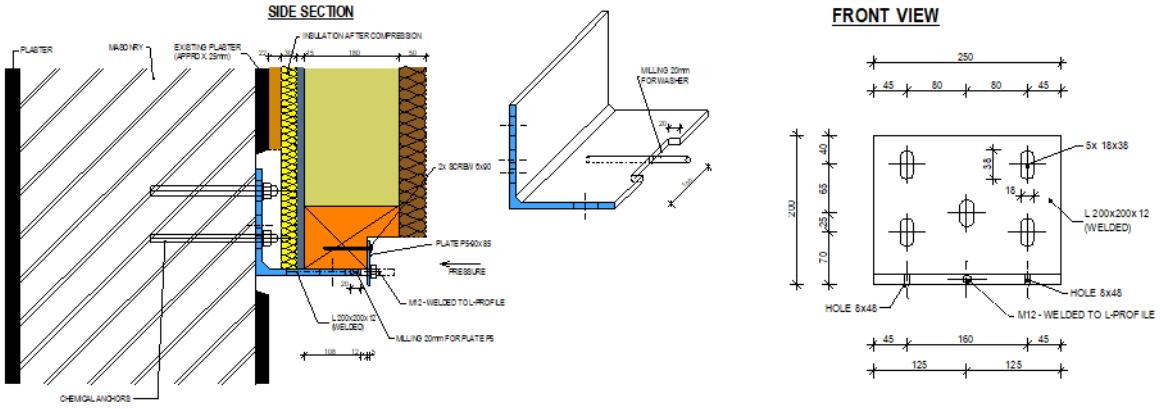

FIGURE 136: ANCHOR DESIGN.

Technická data pro použití HIT-HY 270 s kotevním šroubem HIT-V nebo pouzdrem HIT-IC

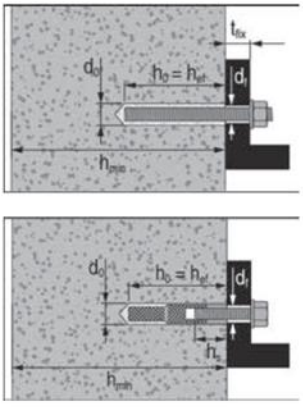

Plná pálená cihla[1] 290x140x65, f_b = 12 MPa, c ≥ c_{cr}		ETA-13/1036			
HIT-V šroub, HIT-IC pouzdro s vnitřním závitem		**M8**	**M10**	**M12**	**M16**
Průměr vrtání - HIT-V	d_0 [mm]	10[2]	12[2]	14[2]	18[2]
Průměr vrtání - HIT-IC	d_0 [mm]	14[2]	16[2]	18[2]	
Maximální průměr otvoru v kotevní desce	d_f [mm]	9	12	14	18
Efektivní kotevní hloubka - HIT-V	h_{ef} [mm]	50…300			
Efektivní kotevní hloubka - HIT-IC	h_{ef} [mm]	50…80			
Vzdálenost od okraje	c_{cr} [mm]	140 (b)[4]			
Osová vzdálenost	s_{cr} [mm]	290 vodorovně (l), 140 svisle (2x h+10)[4]			
Minimální vzdálenost od okraje	c_{min} [mm]	140 (b)[4]			
Minimální osová vzdálenost	s_{min} [mm]	140 (b) vodorovně, 65 (h) svisle4)			
Minimální tloušťka zdiva	h_{min} [mm]	h_{ef} + 30	h_{ef} + 30	h_{ef} + 30	h_{ef} + 36
Utahovací moment	T_{inst} [Nm]	5	8	10	10
Orientační spotřeba kotvící hmoty - HIT-V	[ml]	5…20	6…26	6…34	8…46
Návrhová únosnost v tahu, h_{ef} = 50mm - HIT-V, HIT-IC	N_{Rd} [kN]	0,8	0,8	0,8	0,8
Návrhová únosnost v tahu, h_{ef} = 80mm - HIT-V, HIT-IC	N_{Rd} [kN]	1,4 (1,6)[5]	1,4 (1,6)[5]	1,4 (1,6)[5]	1,4 (1,6)[5]
Návrhová únosnost v tahu, h_{ef} ≥ 100mm - HIT-V	N_{Rd} [kN]	2,4 (2,8)[5]	2,4 (2,8)[5]	2,4 (2,8)[5]	2,4 (2,8)[5]
Návrhová únosnost ve smyku, h_{ef} ≥ 50mm - HIT-V, HIT-IC	V_{Rd} [kN]	0,5	0,5	0,5	0,5

FIGURE 137: LOAD-BEARING CAPACITY OF CHEMICAL ANCHORS USED IN THE CZECH REPUBLIC – HILTI EXAMPLE

This project has received funding from the European Union's Horizon 2020 research and innovation programme under grant agreement No 958218

Chemický systém FIS V, FIS VW HIGH SPEED a FIS VS LOW SPEED s kotevním svorníkem FIS A[5]
Nejvyšší garantovaná zatížení jednotlivé kotvy[1),6)] ve zdivu z plných cihel při předsazené montáži.
Při návrhu je nutné zohlednit celé schválení ETA–10/0383.

							Zdivo z plných cihel			
Typ	Pevnost zdiva v tlaku f_b [N/mm²]	Objemová hmotnost zdiva ρ [kg/dm³]	Min. rozměr cihly[7)] (d x š x v) [mm]	Min. účinná kotevní hloubka[4)] h_{ef} [mm]	Min. tloušťka kotevního podkladu h_{min} [mm]	Max. utahovací moment $T_{inst\ max}$ [Nm]	Garantovaná tahová zatížení[3)] N_{perm} [kN]	Garantovaná smyková zatížení[3)] V_{perm} [kN]	Min. osová vzdálenost[2)] s_{min} [mm]	Min. vzdálenost od okraje[2)] c_{min} [mm]
Plná cihla Mz, 2DF dle EN 771-1										
M8	≥ 10	≥ 1,8	240x115x113	85	115	10	0,86	0,86	120	60
M10	≥ 10						0,86	1,00	120	60
M8	≥ 16						1,29	1,43	120	60
M10	≥ 16						1,29	1,57	120	60
Plná vápenopísková cihla dle EN 771										
M8/M10	≥ 10	≥ 2,0	250x240x240	85	240	10	2,29	1,29	80	60
M8/M10	≥ 20						2,57	1,86	80	60
M8/M10	≥ 28						2,57	2,57	80	60
Plné cihly z lehčeného betonu dle EN 771-3										
M8	≥ 4	≥ 1,6	250x240x239	50	240	4	0,57	0,86	250	130
M8	≥ 4			85			1,00	1,00	250	130
M10	≥ 4			85			1,14	1,00	250	130
M8	≥ 6			50			0,86	1,29	250	130
M8	≥ 6			85			1,43	1,29	250	130
M10	≥ 6			85			1,86	1,57	250	130
M12	≥ 6			110			2,14	1,86	250	130
M8	≥ 8			50			1,14	1,71	250	130
M8/M10	≥ 8			85			2,43	2,00	250	130
M12/M16	≥ 8			85			2,57	2,43	250	130

[1)] Nezbytné součinitele bezpečnosti pro odolnost materiálu a pro zatížení of γ_L = 1,4 jsou zohledněny.
[2)] Minimální přípustné osové vzdálenosti a vzdálenosti od okraje. Detaily zahrnující vzdálenosti od spár jsou uvedeny ve schválení.
[3)] Při kombinaci tahového, smykového a ohybového zatížení stejně jako při menších vzdálenostech osových a okrajových nahlédněte do schválení.
[6)] gvz, A4 a C.
[7)] Uvedené hodnoty zatížení platí pro suché zdivo a při teplotním zatížení do +50°C (resp. krátkodobě do +80 °C) a při čištění otvoru dle schválení. Uvedené typy dihel a jejich únosností jsou pouze malým výtahem ze schválení.

FIGURE 138: LOAD-BEARING CAPACITY OF CHEMICAL ANCHORS USED IN THE CZECH REPUBLIC – FISCHER EXAMPLE

Chemical anchors are considered for connecting a steel anchor to masonry. In each steel element there are 5 holes. It is assumed that 4 functional anchors can be installed in these five holes.

Self-weight, permanent loads

- Eurocode 1: Action on structures – Part 1-1: General actions – Densities, self-weight, imposed loads for buildings (ČSN EN 1991-1-1, 03/2004)
- National Annex - Eurocode 1: Action on structures – Part 1-1: General actions – Densities, self-weight, imposed loads for buildings (ČSN EN 1991-1-1 NA, ed.A, 06/2011)
- Self-weight of panels is estimated: gk= 1,0 kN/m^2
- Prestress axial loads is set by experiment: PSk= 0,9 kN/m^2

Wind load

- Eurocode 1: Actions on structures - Part 1-4: General actions - Wind loads (ČSN EN 1991-1-4, ed.2, 11/2020)
- National Annex - Eurocode 1: Actions on structures - Part 1-4: General actions - Wind loads (ČSN EN 1991-1-4, ed.A, 07/2013)

This project has received funding from the European Union's Horizon 2020 research and innovation programme under grant agreement No 958218

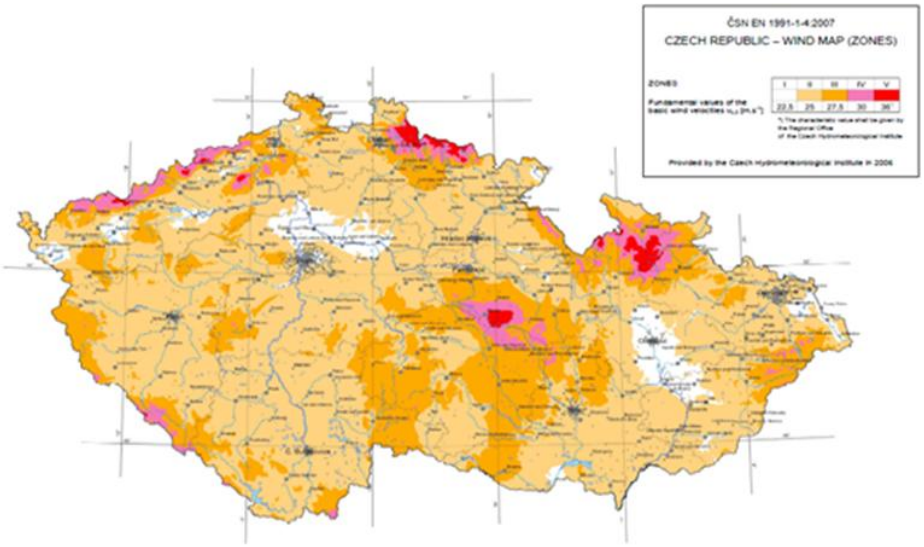

FIGURE 139: WIND MAP OF CZECH REPUBLIC.

For Kasava: $v_{b,0}$ = 25.0 m/s

Static calculation of the anchorage:

Loads on the panel:

Permanent loads:

Self-weight: gk= 1,0 kN/m^2; gd= 1,0*1,35= 1,350 kN/m2

Prestress axial loads: PSk= 0,9 kN/m2; PSd= 0,9*1,35= 1,215 kN/m2

Variable loads:

Wind loads are calculated in the following table.

This project has received funding from the European Union's Horizon 2020 research and innovation programme under grant agreement No 958218

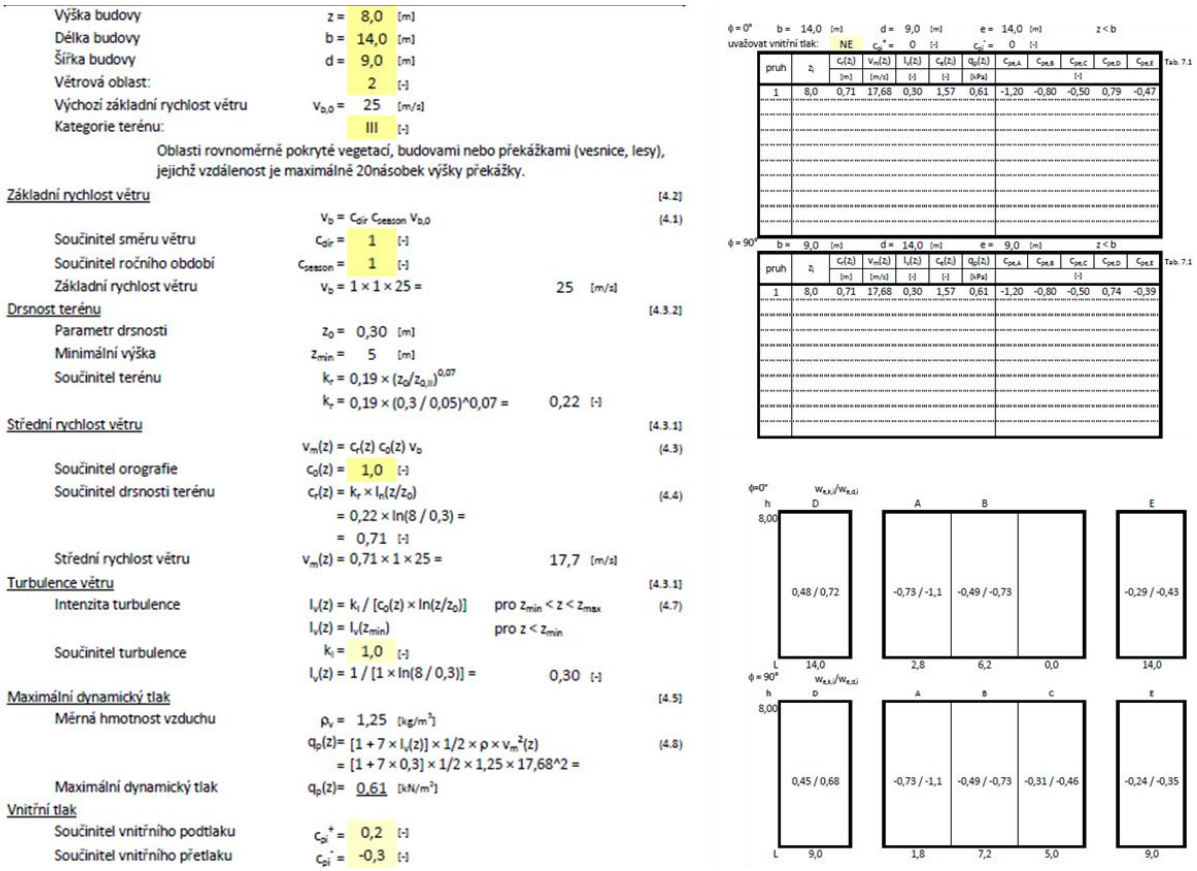

Výška budovy	z =	8,0	[m]
Délka budovy	b =	14,0	[m]
Šířka budovy	d =	9,0	[m]
Větrová oblast:		2	[-]
Výchozí základní rychlost větru	$v_{b,0}$ =	25	[m/s]
Kategorie terénu:		III	[-]

Oblasti rovnoměrně pokryté vegetací, budovami nebo překážkami (vesnice, lesy), jejichž vzdálenost je maximálně 20násobek výšky překážky.

Základní rychlost větru [4.2]

$v_b = c_{dir} c_{season} v_{b,0}$ (4.1)

Součinitel směru větru c_{dir} = 1 [-]

Součinitel ročního období c_{season} = 1 [-]

Základní rychlost větru $v_b = 1 \times 1 \times 25 =$ 25 [m/s]

Drsnost terénu [4.3.2]

Parametr drsnosti z_0 = 0,30 [m]

Minimální výška z_{min} = 5 [m]

Součinitel terénu $k_r = 0,19 \times (z_0/z_{0,II})^{0,07}$

$k_r = 0,19 \times (0,3 / 0,05)^{0,07} =$ 0,22 [-]

Střední rychlost větru [4.3.1]

$v_m(z) = c_r(z)\, c_0(z)\, v_b$ (4.3)

Součinitel orografie $c_0(z)$ = 1,0 [-]

Součinitel drsnosti terénu $c_r(z) = k_r \times \ln(z/z_0)$ (4.4)

$= 0,22 \times \ln(8 / 0,3) =$

$= 0,71$ [-]

Střední rychlost větru $v_m(z) = 0,71 \times 1 \times 25 =$ 17,7 [m/s]

Turbulence větru [4.3.1]

Intenzita turbulence $I_v(z) = k_I / [c_0(z) \times \ln(z/z_0)]$ pro $z_{min} < z < z_{max}$ (4.7)

$I_v(z) = I_v(z_{min})$ pro $z < z_{min}$

Součinitel turbulence k_I = 1,0 [-]

$I_v(z) = 1 / [1 \times \ln(8 / 0,3)] =$ 0,30 [-]

Maximální dynamický tlak [4.5]

Měrná hmotnost vzduchu ρ_v = 1,25 [kg/m³]

$q_p(z) = [1 + 7 \times I_v(z)] \times 1/2 \times \rho \times v_m^2(z)$ (4.8)

$= [1 + 7 \times 0,3] \times 1/2 \times 1,25 \times 17,68^2 =$

Maximální dynamický tlak $q_p(z)$ = 0,61 [kN/m²]

Vnitřní tlak

Součinitel vnitřního podtlaku c_{pi}^+ = 0,2 [-]

Součinitel vnitřního přetlaku c_{pi}^- = -0,3 [-]

$\phi = 0°$ b = 14,0 [m] d = 9,0 [m] e = 14,0 [m] z < b

uvažovat vnitřní tlak: NE c_{pi}^+ = 0 [-] c_{pi}^- = 0 [-]

pruh	z_j [m]	$c_r(z)$ [-]	$v_m(z)$ [m/s]	$I_v(z)$ [-]	$c_e(z)$ [-]	$q_p(z)$ [kPa]	$c_{pe,A}$ [-]	$c_{pe,B}$ [-]	$c_{pe,C}$ [-]	$c_{pe,D}$ [-]	$c_{pe,E}$ [-]	Tab. 7.1
1	8,0	0,71	17,68	0,30	1,57	0,61	-1,20	-0,80	-0,50	0,79	-0,47	

$\phi = 90°$ b = 9,0 [m] d = 14,0 [m] e = 9,0 [m] z < b

pruh	z_j [m]	$c_r(z)$ [-]	$v_m(z)$ [m/s]	$I_v(z)$ [-]	$c_e(z)$ [-]	$q_p(z)$ [kPa]	$c_{pe,A}$ [-]	$c_{pe,B}$ [-]	$c_{pe,C}$ [-]	$c_{pe,D}$ [-]	$c_{pe,E}$ [-]	Tab. 7.1
1	8,0	0,71	17,68	0,30	1,57	0,61	-1,20	-0,80	-0,50	0,74	-0,39	

FIGURE 140: WIND PRESSURE ON SURFACE.

Wind suction (zone B): $w_{e,k}$= -0,490 kN/m^2; $w_{e,d}$= 0,49*1,5= 0,735 kN/m^2

The most loaded row of anchors:

Vertical loading:

V_{Sd} = 2.7*1.0*1.35= 3.645 kN/m

Horizontal load:

$N_{Sd} = w_{e,d} + P_{Sd}$ = 1.7*0.490*1.5+1.7*0.9*1.35= 3.316 kN/m

Number of chemical anchors per meter (Fischer anchors M10):

$N_1 = (V_{Sd}/V_{Rd} + N_{Sd}/N_{Rd})$= (3.645/1.000+3.316/0.860)= 7.5

Number of chemical anchors per meter (Hilti HIT-HY 270 anchors M10):

$N_2 = (V_{Sd}/V_{Rd} + N_{Sd}/N_{Rd})$= (3.645/0.500+3.316/2.800)/1.2= 7.062

Estimated scheme of anchors:

This project has received funding from the European Union's Horizon 2020 research and innovation programme under grant agreement No 958218

This project has received funding from the European Union's Horizon 2020 research and innovation programme under grant agreement No 958218

13 Annex III – One third octave band of sound pressure level at a distance 1 m for eAHC unit

13.1 Results of sound pressure level for PROTOTYPE 1 and 2

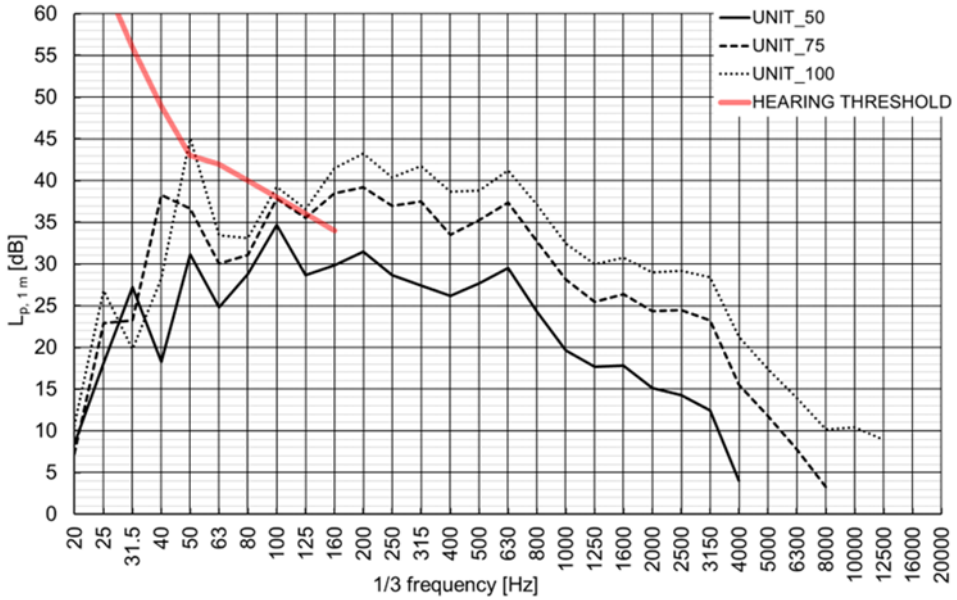

FIGURE 141: 1/3 SPECTRUM OF SOUND PRESSURE LEVEL AT A DISTANCE 1 M FROM UNIT FOR PROTOTYPE_1.

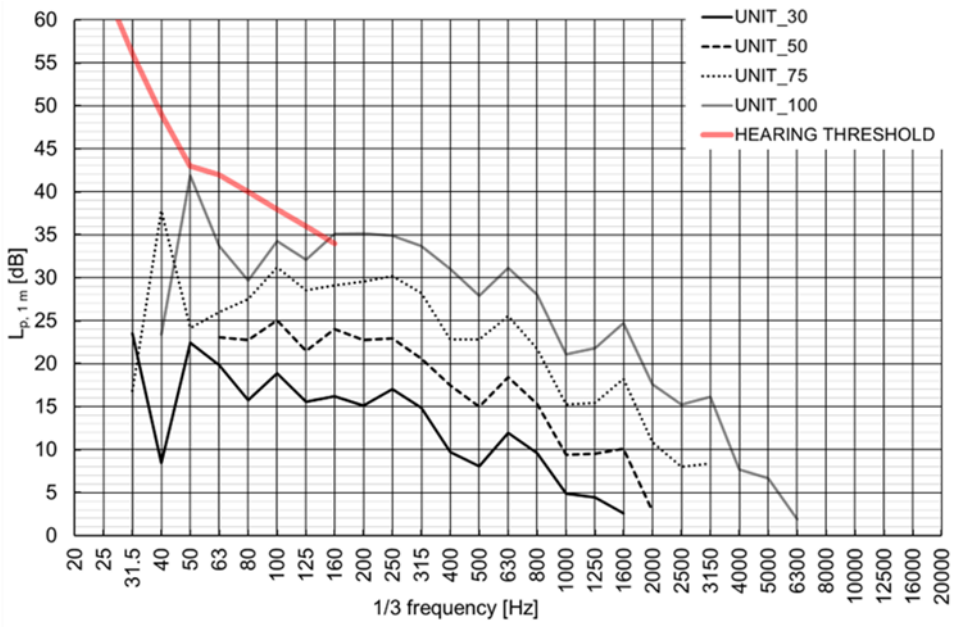

FIGURE 142: 1/3 SPECTRUM OF SOUND PRESSURE LEVEL AT A DISTANCE 1 M FROM UNIT FOR PROTOTYPE_2.

This project has received funding from the European Union's Horizon 2020 research and innovation programme under grant agreement No 958218

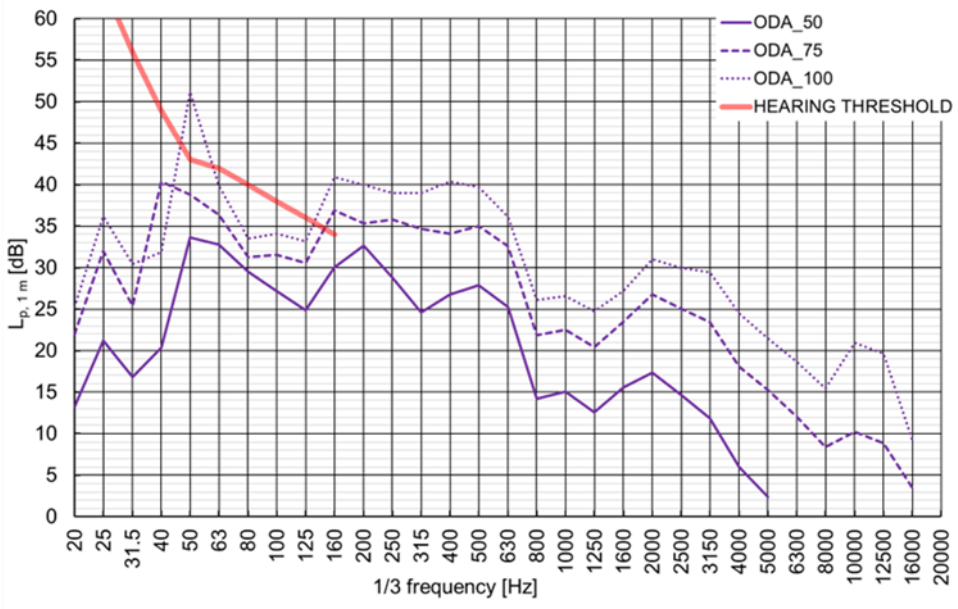

FIGURE 143: 1/3 SPECTRUM OF SOUND PRESSURE LEVEL AT A DISTANCE 1 M FROM ODA FOR PROTOTYPE_1.

FIGURE 144: 1/3 SPECTRUM OF SOUND PRESSURE LEVEL AT A DISTANCE 1 M FROM ODA FOR PROTOTYPE_2.

This project has received funding from the European Union's Horizon 2020 research and innovation programme under grant agreement No 958218

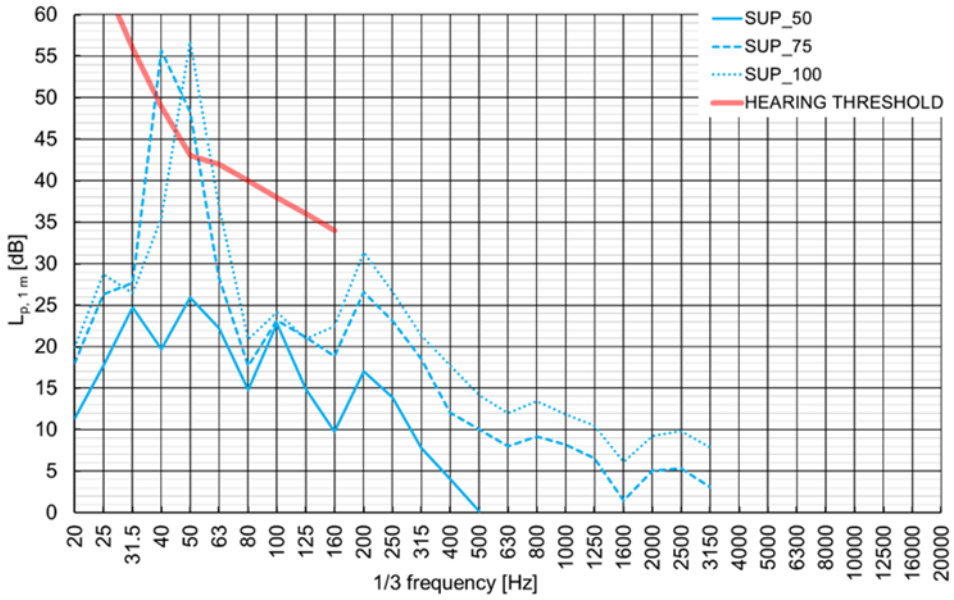

FIGURE 145: 1/3 SPECTRUM OF SOUND PRESSURE LEVEL AT A DISTANCE 1 M FROM SUP FOR PROTOTYPE_1.

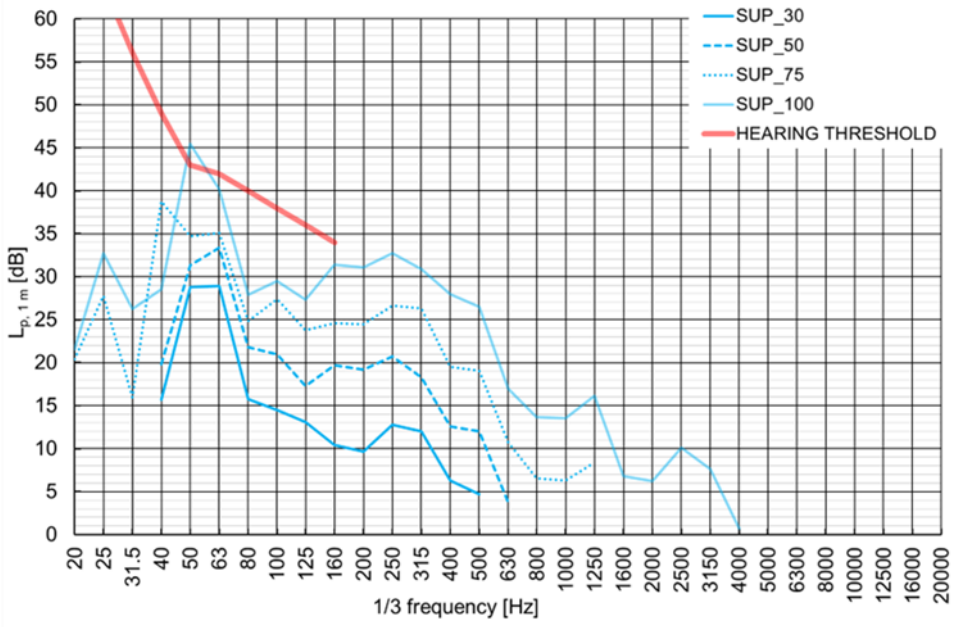

FIGURE 146: 1/3 SPECTRUM OF SOUND PRESSURE LEVEL AT A DISTANCE 1 M FROM SUP FOR PROTOTYPE_2.

This project has received funding from the European Union's Horizon 2020 research and innovation programme under grant agreement No 958218

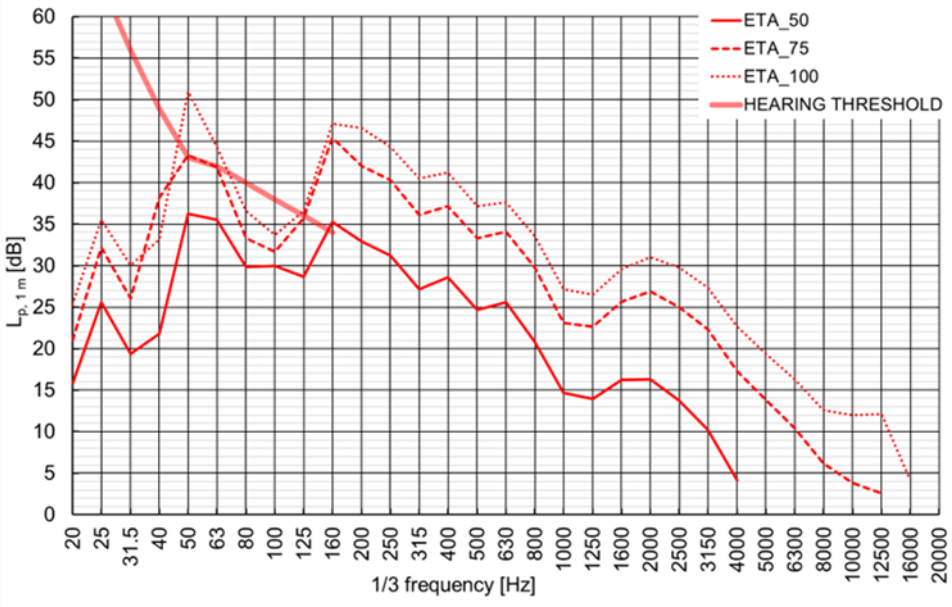

FIGURE 147: 1/3 SPECTRUM OF SOUND PRESSURE LEVEL AT A DISTANCE 1 M FROM ETA FOR PROTOTYPE_1.

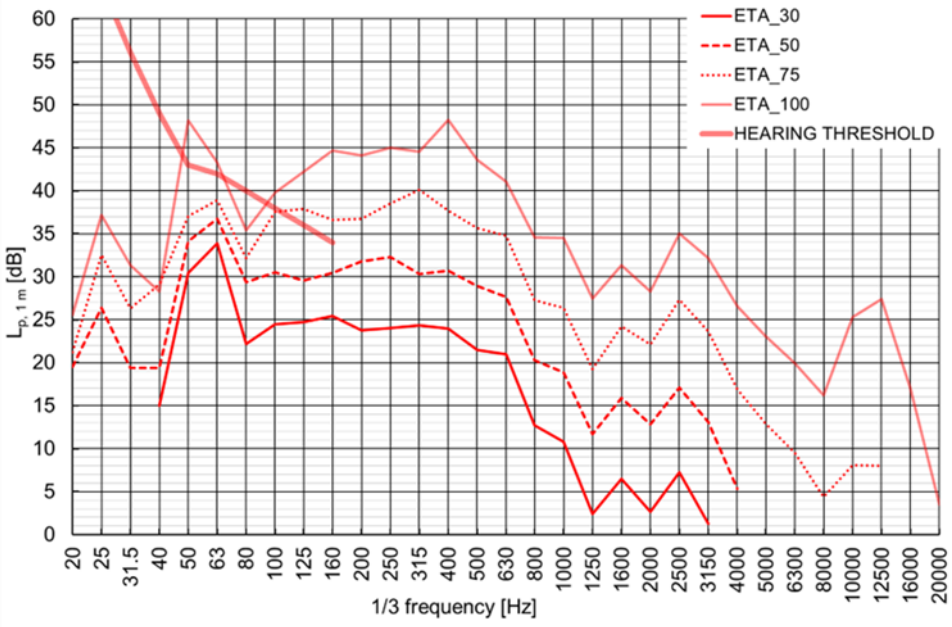

FIGURE 148: 1/3 SPECTRUM OF SOUND PRESSURE LEVEL AT A DISTANCE 1 M FROM ETA FOR PROTOTYPE_2.

This project has received funding from the European Union's Horizon 2020 research and innovation programme under grant agreement No 958218

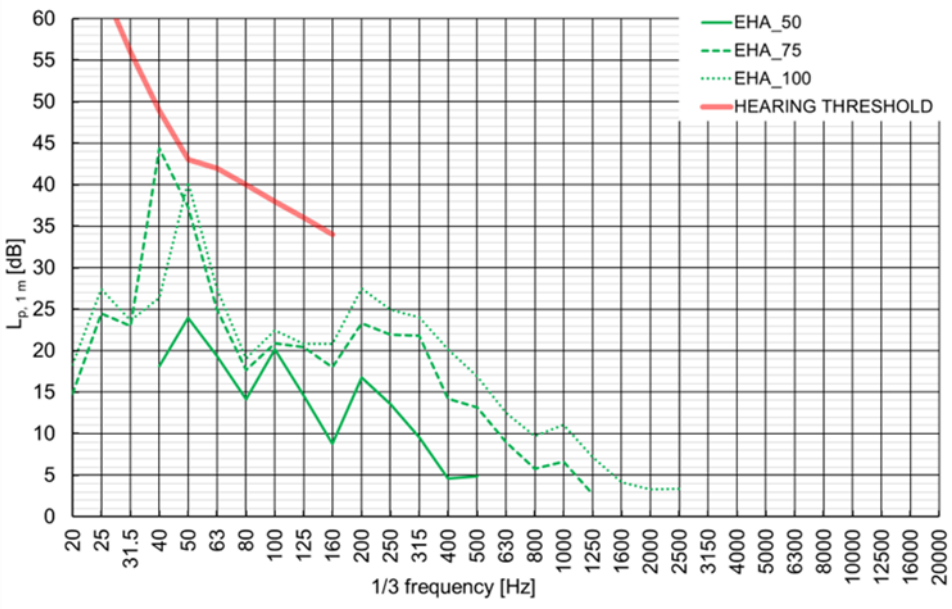

FIGURE 149: 1/3 SPECTRUM OF SOUND PRESSURE LEVEL AT A DISTANCE 1 M FROM EHA FOR PROTOTYPE_1.

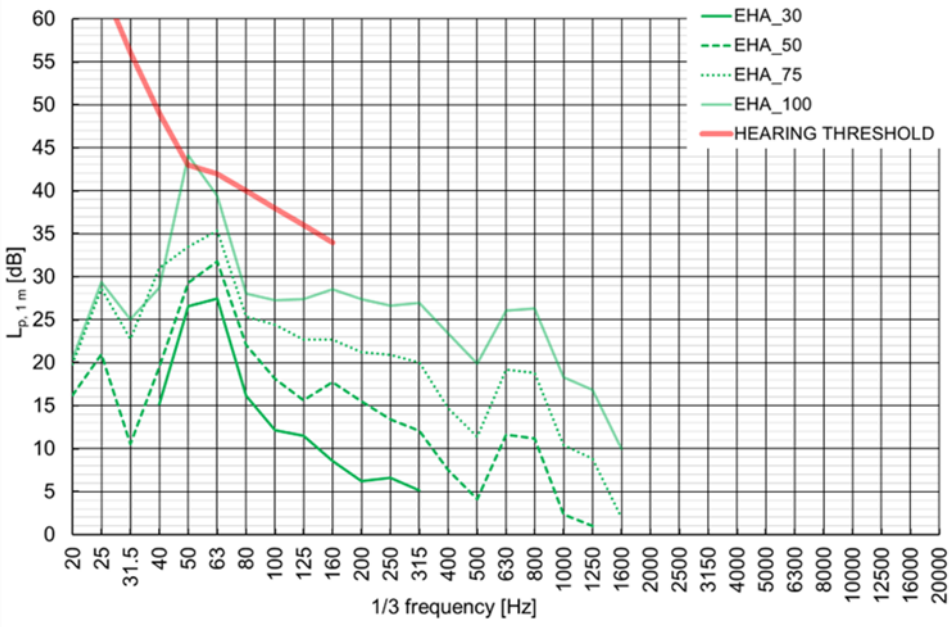

FIGURE 150: 1/3 SPECTRUM OF SOUND PRESSURE LEVEL AT A DISTANCE 1 M FROM EHA FOR PROTOTYPE_2.

This project has received funding from the European Union's Horizon 2020 research and innovation programme under grant agreement No 958218

13.2 Results of sound pressure level for PROTOTYPE 2 with different types of silencers

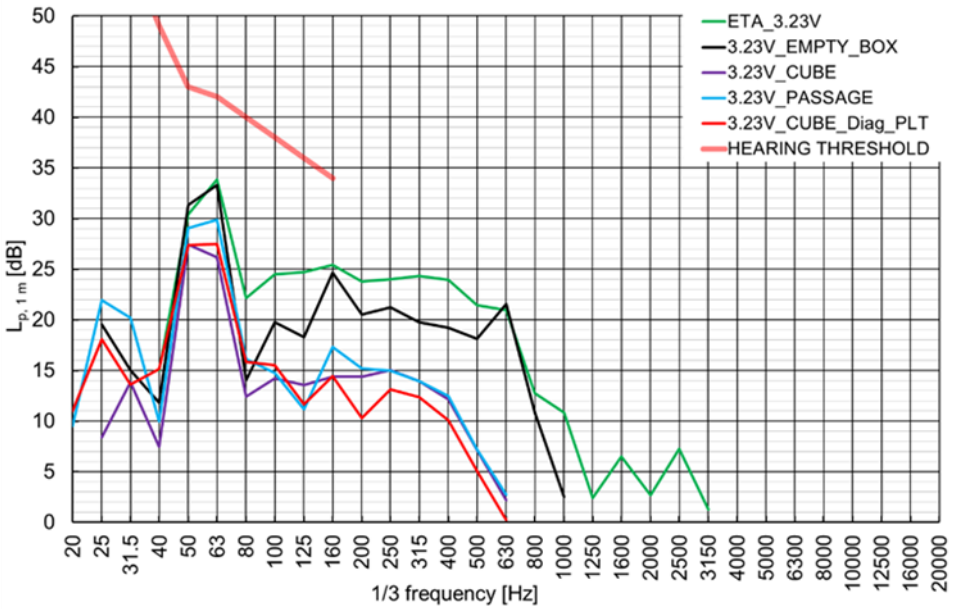

FIGURE 151: 1/3 SPECTRUM OF SOUND PRESSURE LEVEL AT A DISTANCE 1 M FROM ETA FOR PROTOTYPE_2 WITH DIFFERENT TYPE OF SILENCERS AND FOR CONSTANT VOLTAGE 3.23 V FOR EXTRACT AND 3.07 V FOR SUPPLY AIR.

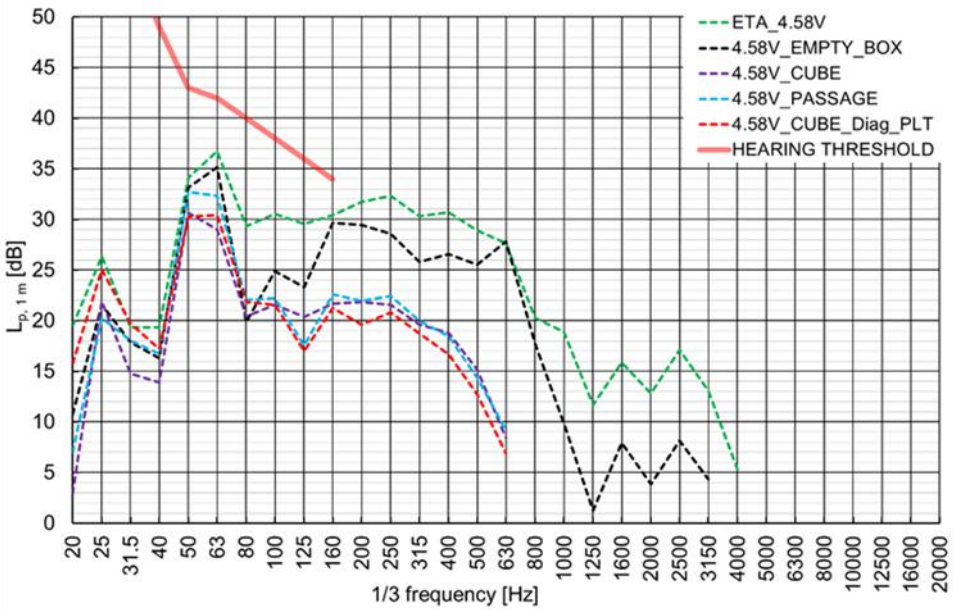

FIGURE 152: 1/3 SPECTRUM OF SOUND PRESSURE LEVEL AT A DISTANCE 1 M FROM ETA FOR PROTOTYPE_2 WITH DIFFERENT TYPE OF SILENCERS AND FOR CONSTANT VOLTAGE 4.58 V FOR EXTRACT AND 4.4 V FOR SUPPLY AIR.

This project has received funding from the European Union's Horizon 2020 research and innovation programme under grant agreement No 958218

FIGURE 153: 1/3 SPECTRUM OF SOUND PRESSURE LEVEL AT A DISTANCE 1 M FROM ETA FOR PROTOTYPE_2 WITH DIFFERENT TYPE OF SILENCERS AND FOR CONSTANT VOLTAGE 6.36 V FOR EXTRACT AND 5.98 V FOR SUPPLY AIR.

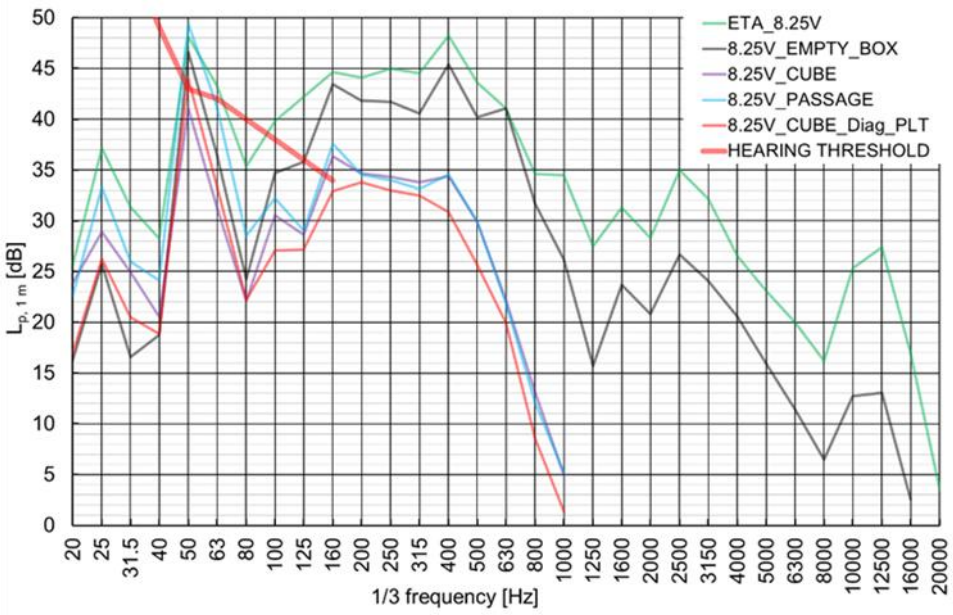

FIGURE 154: 1/3 SPECTRUM OF SOUND PRESSURE LEVEL AT A DISTANCE 1 M FROM ETA FOR PROTOTYPE_2 WITH DIFFERENT TYPE OF SILENCERS AND FOR CONSTANT VOLTAGE 8.25 V FOR EXTRACT AND 7.33 V FOR SUPPLY AIR.

This project has received funding from the European Union's Horizon 2020 research and innovation programme under grant agreement No 958218